ISSN 1007-9327 (print)
ISSN 2219-2840 (online)

World Journal of *Gastroenterology*

World J Gastroenterol 2023 May 21; 29(19): 2888-3047

Published by Baishideng Publishing Group Inc

World Journal of Gastroenterology

Contents

Weekly Volume 29 Number 19 May 21, 2023

Contents

Contents

ABOUT COVER

Editorial Board Member of *World Journal of Gastroenterology*, John K Triantafillidis, MD, PhD, FEBGH, Associate Professor of Medicine, Staff Physician, Iasi University of Medicine and Pharmacy, Romania, "Metropolitan General" Hospital, Holargos, Athens 15562, Greece. jktrian@gmail.com

AIMS AND SCOPE

The primary aim of *World Journal of Gastroenterology* (*WJG*, *World J Gastroenterol*) is to provide scholars and readers from various fields of gastroenterology and hepatology with a platform to publish high-quality basic and clinical research articles and communicate their research findings online. *WJG* mainly publishes articles reporting research results and findings obtained in the field of gastroenterology and hepatology and covering a wide range of topics including gastroenterology, hepatology, gastrointestinal endoscopy, gastrointestinal surgery, gastrointestinal oncology, and pediatric gastroenterology.

INDEXING/ABSTRACTING

The *WJG* is now abstracted and indexed in Science Citation Index Expanded (SCIE, also known as SciSearch®), Current Contents/Clinical Medicine, Journal Citation Reports, Index Medicus, MEDLINE, PubMed, PubMed Central, Scopus, Reference Citation Analysis, China National Knowledge Infrastructure, China Science and Technology Journal Database, and Superstar Journals Database. The 2022 edition of Journal Citation Reports® cites the 2021 impact factor (IF) for *WJG* as 5.374; IF without journal self cites: 5.187; 5-year IF: 5.715; Journal Citation Indicator: 0.84; Ranking: 31 among 93 journals in gastroenterology and hepatology; and Quartile category: Q2. The *WJG*'s CiteScore for 2021 is 8.1 and Scopus CiteScore rank 2021: Gastroenterology is 18/149.

RESPONSIBLE EDITORS FOR THIS ISSUE

Production Editor: *Yi-Xuan Cai*; **Production Department Director:** *Xiang Li*; **Editorial Office Director:** *Jia-Ru Fan*.

NAME OF JOURNAL
World Journal of Gastroenterology

ISSN
ISSN 1007-9327 (print) ISSN 2219-2840 (online)

LAUNCH DATE
October 1, 1995

FREQUENCY
Weekly

EDITORS-IN-CHIEF
Andrzej S Tarnawski

EDITORIAL BOARD MEMBERS
http://www.wjgnet.com/1007-9327/editorialboard.htm

PUBLICATION DATE
May 21, 2023

INSTRUCTIONS TO AUTHORS
https://www.wjgnet.com/bpg/gerinfo/204

GUIDELINES FOR ETHICS DOCUMENTS
https://www.wjgnet.com/bpg/GerInfo/287

GUIDELINES FOR NON-NATIVE SPEAKERS OF ENGLISH
https://www.wjgnet.com/bpg/gerinfo/240

PUBLICATION ETHICS
https://www.wjgnet.com/bpg/GerInfo/288

PUBLICATION MISCONDUCT
https://www.wjgnet.com/bpg/gerinfo/208

ARTICLE PROCESSING CHARGE
https://www.wjgnet.com/bpg/gerinfo/242

STEPS FOR SUBMITTING MANUSCRIPTS
https://www.wjgnet.com/bpg/GerInfo/239

ONLINE SUBMISSION
https://www.f6publishing.com

World Journal of Gastroenterology

Submit a Manuscript: https://www.f6publishing.com

World J Gastroenterol 2023 May 21; 29(19): 2888-2904

DOI: 10.3748/wjg.v29.i19.2888

ISSN 1007-9327 (print) ISSN 2219-2840 (online)

REVIEW

Radiomics in colorectal cancer patients

Riccardo Inchingolo, Cesare Maino, Roberto Cannella, Federica Vernuccio, Francesco Cortese, Michele Dezio, Antonio Rosario Pisani, Teresa Giandola, Marco Gatti, Valentina Giannini, Davide Ippolito, Riccardo Faletti

Specialty type: Radiology, nuclear medicine and medical imaging

Provenance and peer review: Invited article; Externally peer reviewed.

Peer-review model: Single blind

Peer-review report's scientific quality classification

Grade A (Excellent): 0
Grade B (Very good): 0
Grade C (Good): C, C
Grade D (Fair): 0
Grade E (Poor): 0

P-Reviewer: Tari DU, Italy; Yang L, China

Received: February 16, 2023
Peer-review started: February 16, 2023
First decision: March 24, 2023
Revised: April 7, 2023
Accepted: April 25, 2023
Article in press: April 25, 2023
Published online: May 21, 2023

Riccardo Inchingolo, Francesco Cortese, Michele Dezio, Unit of Interventional Radiology, F. Miulli Hospital, Acquaviva delle Fonti 70021, Italy

Cesare Maino, Teresa Giandola, Davide Ippolito, Department of Radiology, Fondazione IRCCS San Gerardo dei Tintori, Monza 20900, Italy

Roberto Cannella, Department of Biomedicine, Neuroscience and Advanced Diagnostics (BiND), University of Palermo, Palermo 90127, Italy

Federica Vernuccio, Institute of Radiology, University Hospital of Padova, Padova 35128, Italy

Antonio Rosario Pisani, Interdisciplinary Department of Medicine, Section of Nuclear Medicine, University of Bari "Aldo Moro", Bari 70121, Italy

Marco Gatti, Valentina Giannini, Riccardo Faletti, Department of Surgical Sciences, University of Turin, Turin 10126, Italy

Corresponding author: Riccardo Inchingolo, MD, Director, Doctor, Unit of Interventional Radiology, F. Miulli Hospital, Sp per Santeramo, Acquaviva delle Fonti 70021, Italy. riccardoin@hotmail.it

Abstract

The main therapeutic options for colorectal cancer are surgical resection and adjuvant chemotherapy in non-metastatic disease. However, the evaluation of the overall adjuvant chemotherapy benefit in patients with a high risk of recurrence is challenging. Radiological images can represent a source of data that can be analyzed by using automated computer-based techniques, working on numerical information coded within Digital Imaging and Communications in Medicine files: This image numerical analysis has been named "radiomics". Radiomics allows the extraction of quantitative features from radiological images, mainly invisible to the naked eye, that can be further analyzed by artificial intelligence algorithms. Radiomics is expanding in oncology to either understand tumor biology or for the development of imaging biomarkers for diagnosis, staging, and prognosis, prediction of treatment response and diseases monitoring and surveillance. Several efforts have been made to develop radiomics signatures for colorectal cancer patient using computed tomography (CT) images with different aims: The preoperative prediction of lymph node metastasis, detecting *BRAF* and *RAS* gene mutations. Moreover, the use of delta-radiomics allows the analysis of variations of the radiomics parameters extracted from CT scans performed at different timepoints. Most published studies concerning radiomics and magnetic resonance

imaging (MRI) mainly focused on the response of advanced tumors that under-went neoadjuvant therapy. Nodes status is the main determinant of adjuvant chemotherapy. Therefore, several radiomics model based on MRI, especially on T2-weighted images and ADC maps, for the preoperative prediction of nodes metastasis in rectal cancer has been developed. Current studies mostly focused on the applications of radiomics in positron emission tomogra-phy/CT for the prediction of survival after curative surgical resection and assessment of response following neoadjuvant chemoradiotherapy. Since colorectal liver metastases develop in about 25% of patients with colorectal carcinoma, the main diagnostic tasks of radiomics should be the detection of synchronous and metachronous lesions. Radiomics could be an additional tool in clinical setting, especially in identifying patients with high-risk disease. Nevertheless, radiomics has numerous shortcomings that make daily use extremely difficult. Further studies are needed to assess performance of radiomics in stratifying patients with high-risk disease.

Key Words: Colorectal cancer; Radiomics; Artificial intelligence; Liver metastases; Magnetic resonance imaging; Computed tomography; Positron emission tomography/computed tomography

Core Tip: Stratifying colorectal cancer patients with high-risk disease and the evaluation of the overall chemotherapy benefit are a clinical challenge. Radiomics through radiological images analysis using automated computer-based techniques allows the extraction of quantitative features from radiological images, mainly invisible to the naked eye, that can be further analyzed by artificial intelligence algorithms. Several efforts have been made to develop radiomics signatures for colorectal cancer patient using computed tomography (CT), magnetic resonance imaging, and positron emission tomography/CT, in particular to understand tumor biology, to develop imaging biomarkers for diagnosis, staging, and prognosis, to predict treatment response and to monitor disease.

Citation: Inchingolo R, Maino C, Cannella R, Vernuccio F, Cortese F, Dezio M, Pisani AR, Giandola T, Gatti M, Giannini V, Ippolito D, Faletti R. Radiomics in colorectal cancer patients. *World J Gastroenterol* 2023; 29(19): 2888-2904
URL: https://www.wjgnet.com/1007-9327/full/v29/i19/2888.htm
DOI: https://dx.doi.org/10.3748/wjg.v29.i19.2888

INTRODUCTION

Colorectal cancer is the fifth-most-common frequent in terms of incidence and mortality, with 1480000 new cases in 2020 worldwide[1]. The TNM staging process itself is widely based on radiological definition of boundaries of primary lesion, nodal and distant metastases. The main therapeutic options for colorectal cancer are surgical resection and adjuvant chemotherapy in non-metastatic patients; however, the evaluation of the overall adjuvant chemotherapy benefit in patients with a high risk of recurrence is a clinical challenge[2]. The decision is based on the TNM staging system[3], which represents the most important parameter: Colorectal cancer patients at stage III are globally recognized as patients who can benefit from chemotherapy, while for those at stage II with other clinical risk factors, the advantages of chemotherapy are still debated[2,4]. In presence of clinical risk factors, the final strategy is often decided by the oncologist or multidisciplinary teams.

Nowadays radiological images can represent a source of data that can be analyzed by using advanced computer-based techniques, working on numerical information coded within the Digital Imaging and Communications in Medicine files[5]: This image numerical analysis has been named "radiomics"[6]. Radiomics might be used as a non-invasive imaging biomarker and be able to provide a quantitative evaluation of medical images, with the chance to shift imaging from a qualitative to a quantitative approach[7,8]. To date, the radiomics approach has been extensively investigated in cancer patients with a specific focus on tumor diagnosis, staging, prognosis prediction, and long-term monitoring[7,9,10]. In this context, radiomics could play a pivotal role in colorectal cancer workup with the expectancy to help clinicians in identifying patients with high-risk disease.

RADIOMICS APPLIED TO CANCER-SUMMARY (PATHOLOGICAL CORRELATION, DIAGNOSIS, PROGNOSIS)

Since its advent in 2012[5], radiomics has been extensively applied in oncology studies and it has been demonstrated as a promising tool that can offer a risk-free and efficient method for diagnosis, classification, and prognosis prediction in oncology[11]. Radiomics, indeed, allows the extraction of quantitative features from radiological images, mainly invisible to the naked eye, that can be further analyzed by machine learning and artificial intelligence (AI) algorithms to produce signatures representing tumor phenotype.

The radiomics pipeline consists of different steps (Figure 1). First, multi-dimensional and multi-institutional data should be collected including high-quality medical images, clinical, and, eventually, molecular data. Once acquired, images should be pre-processed to improve image quality, harmonize raw data, and ensure generalizability across imaging protocols and patient populations, especially if multicentre datasets are acquired. This pre-processing step usually involves image co-registration, image denoising, signal intensity standardization, and/or normalization. Once the image datasets have been pre-processed, tumors should be segmented to extract regions of interest (ROIs) on which subsequent steps will be focused on. This task can be performed either manually, semi- or fully automatically. A big effort in the research field is addressed to the development of AI-based systems to automatically segment lesions and overcomes the most common limitations of manual segmentation. Afterward, from the segmented ROIs a large number of parameters (features) are extracted, including: (1) First-order features, from gray-level intensity histograms and lesion shape; (2) second-order features, related to the spatial relationship between pixels, calculated using different matrices, *e.g.*, gray-level co-occurrence, gray-level run-length, gray-level dependence, gray-level size zone, neighboring gray tone difference; and (3) transform-based features, *e.g.*, Wavelet, Gabor, Laws, Laplacian. However, since the number of extracted features could be much larger than the sample size of patients included in the algorithms' development, it is vital to reduce the number of features through a step called features selection. This step will strongly reduce the risk of overfitting[12], which occurs when the algorithm overadapts its performances based on data in the training set and consequently loses its generalizability. Besides, features selection will ensue to exclude features that are non-reproducible, redundant, and/or non-relevant for the task, and to reduce the computational cost, while improving the performance of the model[13]. Once the most performing features are selected, the radiomics signature is finally developed by using algorithms for classification, such as logistic regression[14,15], k-nearest neighbour[16], naïve Bayes classifier[17], support vector machines (SVM)[18,19], random forest (RF)[20,21], neural network [22,23] and deep learning[24,25]. In this step, is crucial to divide the image dataset into three subgroups: One for training, used to develop the algorithm, the second for testing, to fine-tune the model, and the last for validation, which aims to evaluate the performance on a different dataset. Training and testing could be performed also using a cross-validation approach, *i.e.*, in which different portions of the dataset are iteratively used to train and test the model. Conversely, the validation should be performed using patients that were never seen during the development of the algorithms. The validation step can be internal, when applied in a similar clinical setting and population to the training set, or preferably external, when applied in multiple clinical settings with varying disease prevalence[12,26].

Thanks to the vast number of images routinely used by radiologists and oncologists in their daily workload, radiomics is substantial in oncology to understand tumor biology or develop imaging biomarkers useful for diagnosis, staging, prediction of treatment response, disease monitoring and surveillance[27].

Understanding tumor biology through radiomics can be feasible because it allows the extraction of quantitative information about spatial and temporal heterogeneity in a non-invasively way and using routinely acquired images. This information can be consequently correlated with tumors' phenotype that can either reflects distinct traits (*e.g.*, internal necrosis and proliferation at the periphery) or mirrors genomic and molecular traits or be a signature or different outcomes. Moreover, texture features used in radiomics have been also demonstrated useful in reflecting key oncogenomics processes such as tumor angiogenesis[28], hypoxia[29], tumor invasion[30] and tumor proliferation[31].

The second scope of radiomics in the oncology field is to enhance precision medicine through the implementation of diagnostics and prognostic imaging biomarkers in a variety of solid tumors. Biomarkers for detection and diagnosis are those in a more advanced status since there are many studies that demonstrated their usefulness in discriminating between healthy, benign and malignant cancer in different sites[23,32-34]. However, the most promising applications in which radiomics could truly improve clinical practice are related to the prediction of treatment response and disease monitoring. Indeed, knowing, before or during therapy, which patients would respond might help choosing the best management possible. Moreover, after treatment, radiomics biomarkers may suggest more intense post-treatment surveillance due to a high risk of a tumor recurrence for a particular patient. In parallel to radiomics, it is worthwhile underling that a boost for the development of prognostic biomarkers for precision medicine could be provided by integrating radiomics features to additional layers of -omics information, *i.e.*, pathomics (features derived from digital pathological samples), and genomics. The motivation for this multi-omics approach to disease understanding is that the conventional markers

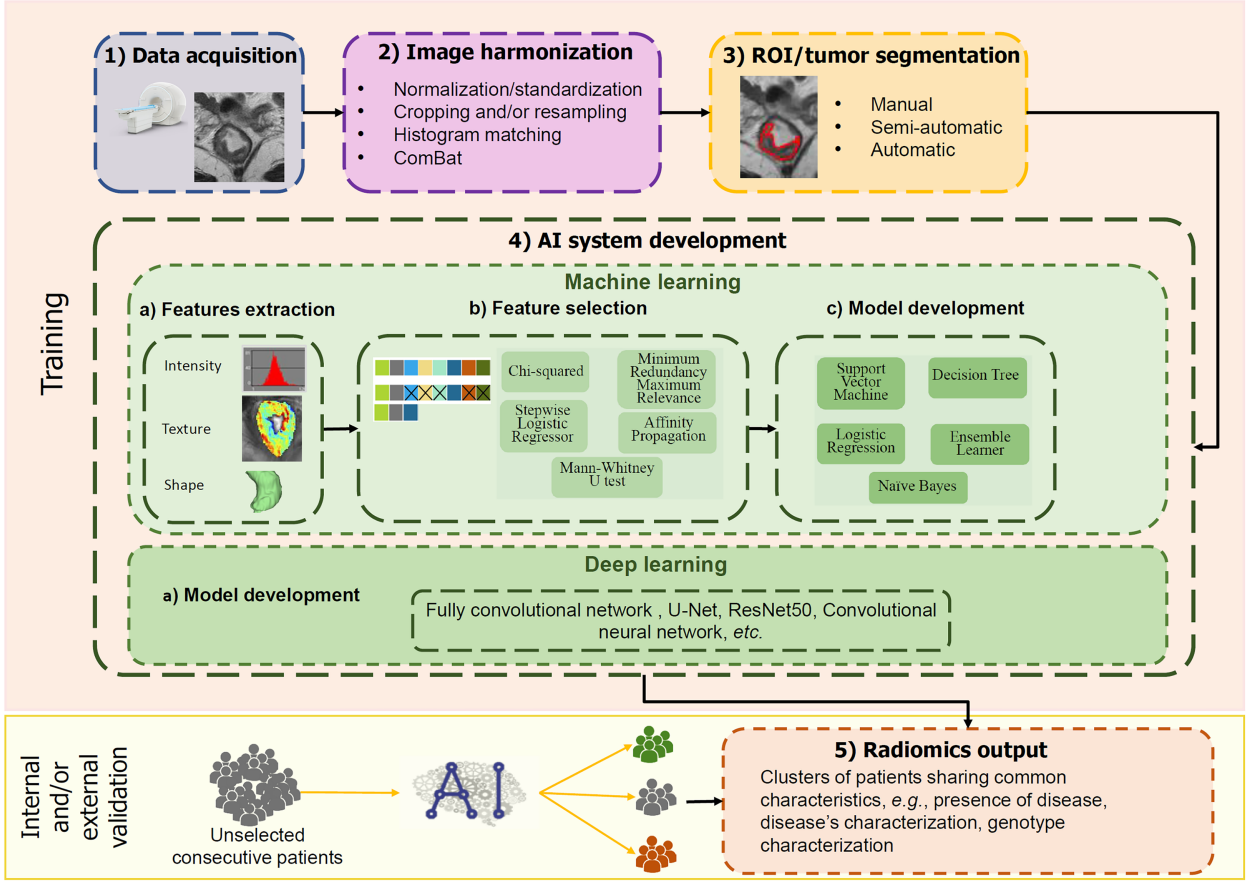

DOI: 10.3748/wjg.v29.i19.2888

Figure 1 Radiomics pipeline. ROI: Regions of interest.

discovery which molecularly dissect the disease part by part, if the sum of knowledge of parts will explain the operation of the whole, has mostly failed to understand the causes and cures for complex diseases. On the contrary, recent evidence suggests that patterns discovered from high dimensional, multi-modal data could improve estimation of disease aggressiveness and patient outcomes compared to single modality data.

COMPUTED TOMOGRAPHY

Tumor and nodes

Several efforts have been made to develop radiomics signatures for colorectal cancer patient using computed tomography (CT) images with different aims (Table 1). Li *et al*[35] developed and validated a clinical-radiomics nomogram for the preoperative prediction of nodes metastasis. They validated their algorithm on an internal dataset of 308 patients (136 with and 172 without lymph node metastases) and showed that the model which included clinical parameters, radiomics on both tumor and peripheral nodes was the one reaching the highest accuracy in predicting nodes metastases [area under the curve (AUC) = 0.7509; 95%CI: 0.6901-0.8071; accuracy: 73.70%; sensitivity: 60.29%; specificity: 84.30%; positive predictive value (PPV): 75.23%; and negative predictive value (NPV): 72.86% in the internal validation set]. If further validated, also on an external validation set, this model could be used as an individualized preoperative non-invasive tool, assisting in clinical treatment decision making and achieving precision treatment.

From another point of view, radiomics has also been proven effective in detecting *BRAF* and *RAS* (*KRAS* and *NRAS*) gene mutations, that are genomics signatures usually associated with shorter disease-free and overall survival. These mutations are determined through genetic molecular profiling by sampling the tumor, however biopsy carries several drawbacks, including the risk of adverse events, such as bleeding, physical and psychological discomfort[36].

For these reasons, radiomics could potentially be used to non-invasively predict RAS and BRAF mutation status in patients with colorectal cancer and to further guide treatments with surgery or chemotherapy[16,37]. Shi *et al*[16] validated a combined score that tracks *RAS* (*KRAS* and *NRAS*) and

Table 1 Summary of the most important published papers regarding the usefulness of radiomics in colorectal cancer patients using computed tomography imaging

Ref.	Imaging	Main aim	Patients (*n*)	Main findings
Li *et al*[35], 2020	CT	Prediction of nodes metastases	766	Overall diagnostic values: Sensitivity = 60.3%; specificity = 84.3%; PPV = 75.2%; NPV = 72.9%; AUC = 0.750
Shi *et al*[16], 2020	CT	Detect *RAS* and *BRAF* phenotypes	159	Combined score (semantic features and radiomics) AUC = 0.950; validation cohort AUC = 0.790
Giannini *et al* [41], 2020	CT	Predict response to treatment	38 (141 lesions)	Per-lesion diagnostic values: Sensitivity = 89%; specificity = 85%; PPV = 78%; NPV = 93%
Dercle *et al* [47], 2020	CT	Tumor response to anti-EGFR therapy	667	Sensitivity to therapy: AUCs 0.800 and 0.720 for FOLFIRI and FOLFIRI + cetuximab
Dohan *et al* [48], 2020	CT	Overall survival	491	SPECTRA score > 0.02 has a lower OS; SPECTRA Score at 2 mo has the same prognostic values as RECIST at 6 mo
Giannini *et al* [41], 2020	CT	Predict response to treatment	57 (242 lesions)	Per-lesion diagnostic values: Sensitivity = 99%; specificity = 94%; PPV = 95%; NPV = 99%; the radiomic approach can predict R- wrongly classified by RECIST as R^+
Taghavi *et al* [103], 2021	CT	Prediction of synchronous liver metastases	91	The radiomics model outperformed the clinical model: AUC = 0.93 *vs* 0.64
Rao *et al*[108], 2014	CT	Prediction of synchronous liver metastases	29	The mean entropy of the liver is significantly higher in metastatic patients (P = 0.02); Liver entropy can help the differential between metastatic and non-metastatic patients (AUC = 0.73-0.78)
Li *et al*[109], 2022	CT	Prediction of synchronous liver metastases	323	A combined clinical-radiomics model has a good AUC (= 0.79) in detecting liver metastases
Ng *et al*[111], 2013	CT	Prediction of overall survival	55	Entropy, uniformity, kurtosis, skewness, and standard deviation of the pixel distribution histogram can predict survival; each parameter can be considered an independent predictor of the overall survival state
Mühlberg *et al* [112], 2021	CT	Prediction of overall survival	103	Tumor burden score can discriminate patients with at least 1-year survival (AUC = 0.70); a machine-learning model better predict survival (AUC = 0.73)
Ravanelli *et al* [116], 2019	CT	Prediction of response and prognosis after chemotherapy	43	Uniformity is lower in responders (P < 0.001); uniformity is independently correlated with radiological response (OR = 20.00), overall survival (RR = 6.94) and progression-free survival (RR = 5.05)

PPV: Positive predictive value; NPV: Negative predictive value; AUC: Area under the curve; OS: Overall survival; SPECTRA: Survival PrEdiction in patients treated by FOLFIRI and bevacizumab for mCRC using contrast-enhanced computed tomography TextuRe Analysis; CT: Computed tomography.

BRAF mutant phenotypes in colorectal cancer from multicentre CT image data AUC of 0.79 on the validation cohort.

Recently, efforts have been made to translate radiomics signatures from a patient level to a lesion level, since it has been demonstrated that heterogeneous response, caused by the onset of new resistant tumor clones in some lesions, is a predictor of poor overall survival[38-40]. Differentiating which colorectal liver metastases (CRLM) responds and which lingers and eventually will progress in the same patient could pave the way to truly personalized treatment. Giannini *et al*[41] preliminary demonstrated the feasibility of using radiomics features from baseline CT to predict response of treatment after 3 mo. They validated the signature on an independent cohort of patients obtaining encouraging results especially in identifying patients with outlier lesions, *i.e.*, that do not respond in general condition were most lesions respond. In these cases, a target biopsy on non-responder lesions could have revealed a different genetic makeup or, in absence of extrahepatic lesions, suggested the local ablation of outlier metastases. More recently, another breakthrough has been made using the use of delta-radiomics, whose aim is to assess the treatment-induced change of radiomics features over time that could provide information about prognosis[42,43]. These variations can be measured in different ways, for example as the differences between features computed on the same tumour before and after treatment[44,45] or the net-change (*i.e.*, difference of radiomics features after treatment over the value before treatment)[46]. Other than providing additional information about tumour behaviour, delta-radiomics represents a very interesting approach since it could theoretically allow to adapt and modulate the ongoing treatment approach thanks to the predictive power of this technique[42].

Delta-radiomics has been already proven effective in predicting overall survival in patients with metastatic colorectal cancer[47,48]. Dercle *et al*[47] developed and validated on a multicentre dataset a delta-radiomics associated with tumor sensitivity to anti-EGFR therapy in colorectal cancer patients (AUC = 0.80). Similarly, Dohan *et al*[48] validated a delta-radiomics signature able to predict overall survival and identify good responders better than RECIST1.1 criteria in patients with metastatic colorectal cancer treated by FOLFIRI and bevacizumab as a first-line treatment. From a per-lesion point

of view, Giannini *et al*[45] validated a delta-radiomics signature able to predict long-term response (*i.e.*, more than 8 mo) of individual CRLM with an accuracy of 86% in the validation dataset. Of note, the delta-radiomics signature was able to reliably predict non-responder liver metastases wrongly classified as responder by lesion RECIST at the first time point. This per-lesion approach could strongly impact treatment, since according to the delta-radiomics signature it would be possible to pinpoint lesions with distinct biological and molecular features, thus enabling studies toward lesion-specific personalized treatment in liver-only metastatic colorectal cancer patients.

MAGNETIC RESONANCE IMAGING

Tumor evaluation

The application of radiomics and texture analysis by using magnetic resonance imaging (MRI) images has increased interest in recent years (Table 2), with a specific focus on liver pathology, renal carcinoma, prostate cancer, and, in slight minority of published studies, rectal cancer[49]. As mentioned above, the staging of rectal cancer is mainly based on MRI; however, radiological images analyzed by dedicated software can add important data useful for the best management of patients. In this setting, it is of utmost importance to underline the potentiality of radiomics as a non-invasive biomarker for predicting histopathological data, as demonstrated for different abdominal pathological conditions, related to the liver, pancreas, and colorectal[8]. Even if for many abdominal organs it can be difficult to obtain a useful histological sample, rectal cancer pathological data are easy to collect, considering that colonoscopy or sigmoidoscopy, depending on the location of the lesion, is the reference standard technique[50]. On these bases, most published studies when this search was performed mainly focused on the response of advanced tumors that underwent neoadjuvant therapy.

Recently, Chen *et al*[51], in a single-center prospective study, enrolled 137 patients who underwent neoadjuvant chemotherapy. The Authors demonstrated that the traditional clinical model reported an AUC of 67.6% and 70.1% in the training and validation cohort, respectively, quite similar to the selective clinical model (77.5% and 59.6%, respectively). On the other hand, when combining radiomics with clinical data the AUC raised to 94.9% and 84.4% in the training and validation cohort, respectively.

Similarly, Horvat *et al*[52], by enrolling 114 patients who underwent neoadjuvant chemotherapy, demonstrated that radiomics can help the radiologist determine the pathological complete response. The Authors found that combined clinical and radiomics models increased the agreement compared with radiologist interpretation and can help the less experienced radiologist in increasing diagnostic values, in particular specificity, PPV, and NPV.

Analogously, Dinapoli *et al*[53] analyzed the radiomics data of 221 patients from three different centers and demonstrated that this tool can help the prediction of pathological complete response before starting neoadjuvant chemotherapy. Moreover, the Authors performed an external validation, to test the obtained results, with good diagnostic values.

Even if few studies are published in the literature, to test the robustness of the radiomics approach in rectal cancer patients, Shahzadi *et al*[54], demonstrated that only one study can be used for external validation, underlying the overall lack of reproducibility and the need of further standardization before considered it a useful clinical tool. In this setting, future directions should be focused on multicentre studies with standardized MR protocols to validate and test the feasibility of the radiomics approach and its potential usefulness in current everyday clinical practice.

Node's evaluation

Nodes metastases is the main metastatic site of colorectal cancer and an important cause of post-operative recurrence and death[55]. Nodes status is a key factor in the TNM staging of colorectal cancer and the main determinant of adjuvant chemotherapy[56,57].

Preoperative knowledge of NS can provide valuable information for determining the need for adjuvant therapy and the adequacy of surgical resection, thus aiding in pre-treatment decision making [58].

In clinical practice, CT is the most used preoperative imaging method to detect metastatic lesions and perform tumor staging in patients with colorectal cancer. However, the limitation of CT examination is that it cannot discriminate between benign and malignant nodes[59].

MRI has the highest contrast resolution for soft tissues, allowing the best depiction of neoplastic lesions, their anatomical relationships, the depth of the rectal wall involvement, extramural venous invasion, circumferential resection margins, and the assessment of the N stage. For these reasons, MRI examination is considered the reference standard for locoregional staging and restaging in RC according to the main international guidelines[60-62].

Advances in pattern recognition tools and the increase in data set sizes have facilitated the development of radiomics, which may potentially improve predictive accuracy in oncology[63].

Therefore, in the last decade, several papers have been published, with different imaging techniques, reporting the potential role of radiomics in diagnosis, characterization, and evaluation of the tumor response to treatments[64-67] and nodal assessment[68-70].

Table 2 Summary of the most important published papers regarding the usefulness of radiomics in colorectal cancer patients using magnetic resonance imaging

Ref.	Imaging	Main aim	Patients (*n*)	Main findings
Horvat *et al* [52], 2022	MRI	Response to chemotherapy	114	Combined radiological-radiomics model increased agreement (κ = 0.82 *vs* κ = 0.25)
Dinapoli *et al* [53], 2018	MRI	Pathological complete response	221	Significant covariates, skewness, and entropy can predict pathological complete response, with AUCs = 0.730 and 0.750 for internal and external cohorts
Shahzadi *et al* [50], 2022	MRI	Response to chemotherapy	190	Radiomics combined with the T stage better predict response
Liu *et al*[23], 2021	MRI	Prediction of nodes metastases	186	Clinical-radiomics model improves performance: AUC = 0.827
Chen *et al*[72], 2022	MRI	Tumor differentiation and nodes metastases	37 (487 nodes)	Radiomics features of the primary tumor can predict tumor differentiation: AUC = 0.798
Liu *et al*[73], 2017	MRI	Tumor differentiation	68	Skewness and entropy are lower in pT1-2 in comparison with pT3-4 (P < 0.05)
Yang *et al*[74], 2019	MRI	Prediction of T and N stage	88	Skewness, kurtosis, and energy are higher in metastatic nodes in comparison with non-metastatic ones (P < 0.001)
Ma *et al*[75], 2019	MRI	Prediction of nodes metastases and N staging	152	SVM has higher diagnostic values for T and N stages (AUC = 0.862) in comparison with MLP and RF
Zhu *et al*[76], 2019	MRI	Prediction of nodes metastases	215	Radiomic model AUC = 0.818
Zhou *et al*[77], 2020	MRI	Prediction of nodes metastases	391	The combined model predicts nodes metastases: NPV = 93.7%, AUC = 0.818
Shu *et al*[34], 2019	MRI	Prediction of synchronous liver metastases	194	The Radiomics model combined clinical risk factors and LASSO features and showed a good predictive performance: AUC = 0.921
Liu *et al*[107], 2020	MRI	Prediction of synchronous liver metastases	127	A radiomic nomogram presents an accuracy of 81.6% in predicting liver metastases (AUC = 0.918)
Granata *et al* [115], 2022	MRI	Prediction of overall survival	90	Second-order features can predict infiltrative tumor growth, tumor budding, and mucinous type; a second-order feature can predict the risk of recurrence with an accuracy of 90%
Jalil *et al*[119], 2017	MRI	Prediction of prognosis after chemotherapy	56	MPP can predict overall survival (HR = 6.9) and disease-free survival (HR = 3.36); texture analysis can predict relapse-free survival on pre- and post-treatment analyses

AUC: Area under the curve; SVM: Support vector machine; MLP: Multilayer perceptron; RF: Random forest; NPV: Negative predictive value; HR: Hazard ratio; MPP: Mean positive pixel; MRI: Magnetic resonance imaging.

MRI can provide multiparameter images different from those obtained by CT, so it is of interest whether there exists an association between NS and multiregional radiomics features of multiparametric MR images in rectal cancer patients[71].

Liu *et al*[71] aimed to develop and validate a multiregional radiomics prediction model based on MRI and combine it with clinical-semantic data for the individualized preoperative prediction of lymph node metastasis in rectal cancer patients.

Similarly, the study of Chen *et al*[72] provides two non-invasive and quantitative methods, which respectively predict the tumor differentiation and regional nodes metastases for rectal cancer preoperatively. MRI images of both the primary tumor alongside the lymph nodes and specimens were performed with a node-to-node match and labeling. A prediction model was then successfully developed, which provided AUC values of 84.6% and 73.3% in the training and test cohort, respectively.

Liu *et al*[73] performed a histogram analysis on the ADC map of the whole tumor and reported that entropy was an independent predictor of nodal involvement. Recently, Yang *et al*[74] performed the same analysis on T2-weighted imaging of the whole tumor: They found that a lower skewness was an independent risk factor for lymph node metastases.

In a recent retrospective single-center study, radiomics features were extracted from preoperative high-resolution T2-weighted imaging of different histological RC and analyzed using different algorithms. The RF analysis showed a good diagnostic performance for the N-stage with an AUC of 74.6%. The prediction model was able to differentiate N0 from N1-N2 patients with a sensitivity of 79.0% and a specificity of 72.0%[75].

Zhu *et al*[76] compared the performance of two models based, respectively, on the radiomics signature of the primary tumor and of the lymph nodes, before and after chemoradiotherapy (CRT), for the prediction of nodal involvement in advanced rectal cancer. The authors concluded that the features

from the lymph node model perform better than the tumor features for the prediction of nodal involvement[76].

Similarly, Zhou *et al*[77] evaluated a multi-parametric MRI radiomics model for nodal assessment following CRT by combining the radiomic signature with an experienced radiologist's visual evaluation: stratified analyses indicated that the combined model could predict lymph node metastasis with a NPV of 100 and 87.8% after treatment[77].

Even if current literature is focusing on the importance and applicability of radiomics in rectal cancer, no significant studies have been published in the field of colorectal cancer, mainly because MR is not still validated as imaging technique for local staging and restaging of this kind of tumor.

PET/CT

18F-fluorodeoxyglucose positron emission tomography/computed tomography (18F-FDG PET/CT) is frequently employed in the staging and post-neoadjuvant assessment of patients with rectal cancer. PET/CT provides functional information of the primary tumor, nodes and distant metastases. In patients with colorectal cancer, the combination of texture parameters with the functional information obtained with PET/CT scan can further enhance the predictive power of PET/CT imaging[78]. Current studies mostly focused on the applications of radiomics in PET/CT for the prediction of survival after curative surgical resection and assessment of response following neoadjuvant chemoradiotherapy (Table 3).

For the prediction of prognosis in patients with colorectal cancer, Kang *et al*[79] showed that radiomics score from baseline PET scans was significantly associated with progression-free survival. Similarly, Lovinfosse *et al*[80] and Hotta *et al*[81] correlated the texture features in PET/CT with both progression-free survival and overall survival. Furthermore, a recent study provided a combined clinical-radiomics model with high predictive performance (C-index of 0.780) for recurrence-free survival in 196 patients with PET/CT[82].

Several studies explored the potential of radiomics for the prediction of response and survival after neoadjuvant chemoradiotherapy[83-89]. In an initial study of 27 patients with rectal cancer treated with neoadjuvant chemoradiotherapy, Bundschuh *et al*[83] calculated texture parameters (skewness and kurtosis) on PET/CT, which provided a good performance for late response prediction but no significant predictive capability for the assessment of early response. In a retrospective study performed by Bang *et al*[84], texture parameters extracted from PET images correlated with both tumor regression grading and disease-free survival in patients with rectal cancer undergoing neoadjuvant chemoradiotherapy. Giannini *et al*[85] combined radiomics features from PET and MRI to predict pathological complete response following neoadjuvant chemoradiotherapy with high accuracy (AUC of 0.86) in patients with rectal cancer. Similarly, Schurink *et al*[86] combined pretreatment tumor features on PET/CT and MRI to predict response to chemoradiotherapy in rectal cancer, with an AUC of 0.81. Shen *et al*[87] developed a RF model to predict pathological complete response after neoadjuvant chemoradiotherapy in 169 patients with rectal cancer, which demonstrated a sensitivity of 97.3% and a specificity of 81.8% for the identifications of cancers with complete response. Nevertheless, a study by Karahan Şen *et al*[88] found no superiority of texture features compared to metabolic tumor volume in predicting response to neoadjuvant chemoradiotherapy in patients with locally advanced rectal cancer.

For the prediction of lymph node metastasis, a retrospective study published by He and colleagues[90] analyzed the radiomics score and five machine-learning models to predict metastatic lymph nodes based on the radiomics features of 199 colorectal cancers, with an AUC of 0.747-0.581 in the test set. Additionally, the performance of PET/CT radiomics features for predicting perineural invasion has been explored in a recent retrospective study[91].

Finally, few other studies explored the correlation between radiomics signature extracted from PET/CT and rectal cancer genotypes, such as microsatellite instability status[92], RAS mutational status[93,94], TP53 and adenomatous polyposis coli mutations[94].

Despite the promising value of radiomics in PET/CT scans of rectal cancer, it should be noted that all current results are based on retrospective single-center studies with heterogeneity on the type of extracted features and analysis. Moreover, several current studies demonstrated insufficient quality according to the radiomics quality score assessment[95].

CRLM

CRLM develop in about 25% of patients with colorectal carcinoma, being more commonly synchronous (14%-17%) rather than metachronous (8%-15%)[96-99]. CT is most adopted to detect CRLM at preoperative staging due to its higher availability compared to MRI, while MRI is usually used in selected doubtful cases particularly in the challenging scenario of the "too small to characterize" hypoattenuating lesion. In addition, chemotherapy regimens may cause focal or diffuse hepatic changes at imaging that can profoundly alter visualization of hepatic metastases on CT, reducing its diagnostic accuracy and MRI proves to be helpful as problem-solving tool in some cases[100]. Therefore, the overall sensitivity, specificity and accuracy for the diagnosis of CRLM are lower for CT compared to

Table 3 Summary of the most important published papers regarding the usefulness of radiomics in colorectal cancer patients using positron emission tomography/computed tomography imaging

Ref.	Imaging	Main aim	Patients (*n*)	Main findings
Lovinfosse *et al* [80], 2018	PET/CT	Progression-free and overall survival	86	SUVmean, dissimilarity, and contrast from the neighborhood intensity-difference matrix are independently associated with overall survival
Hotta *et al*[81], 2021	PET/CT	Progression-free and overall survival	94	MTV, TLG, and GLCM entropy are associated with overall survival; SUVmax, MTV, TLG, and GLCM entropy are associated with progression-free survival
Bundschuh *et al* [83], 2014	PET/CT	Response after neoadjuvant chemotherapy	27	COV can assess histopathologic response during (sensitivity 68%, specificity 88%) and after (sensitivity 79%, specificity 88%) therapy
Bang *et al*[84], 2016	PET/CT	Response after neoadjuvant chemotherapy	74	MV is associated with 3-yr disease-free survival; Kurtosis and kurtosis gradient are associated with 3-yr disease-free survival
Giannini *et al* [85], 2019	PET/CT	Response after neoadjuvant chemotherapy	52	Second-order texture features (five from PET and one from MRI) can help distinguish responder and non-responder patients: Sensitivity = 86%; specificity = 83%; AUC = 0.860
Yuan *et al*[89], 2021	PET/CT	Response after neoadjuvant chemotherapy	66	A radiomics model can predict TRG 0 vs TRG 1-3: Sensitivity = 77.8%, specificity = 89.7%, AUC = 0.858
Schurink *et al* [86], 2021	PET/CT	Response after neoadjuvant chemotherapy	61	Combined baseline and global tumor features better predict response compared to baseline and local texture (AUC = 0.83 *vs* 0.79)
Shen *et al*[87], 2020	PET/CT	Predict pathological complete response	169	RF can predict complete response: Sensitivity = 81.8%; specificity = 97.3%; PPV = 81.8%; NPV = 97.3%; accuracy = 95.3%
He *et al*[90], 2021	PET/CT	Prediction of nodes metastases	199	Logist regression and XGBoost can accurately predict nodes metastases with AUC = 0.866 and 0.903, respectively
Ma *et al*[91], 2022	PET/CT	Prediction of perineural invasion and outcome	131	12 radiomics signatures are associated with peri-neural invasion; a radiomic score can differentiate between perineural positive and negative lesions: AUC = 0.900
Li *et al*[92], 2021	PET/CT	Prediction of microsatellite instability	173	2 radiomics features can predict microsatellite instability: Sensitivity = 83.3%; specificity = 76.3%; accuracy = 76.8%
Lovinfosse *et al* [93], 2016	PET/CT	Prediction of RAS status	151	SUVmax, SUV mean, skewness, SUV standard deviation, and SUV coefficient of variation are associated with RAF mutation (all $P < 0.001$)
Chen *et al*[94], 2019	PET/CT	Prediction of genetic mutations	74	MTV and SUV max are increased in mutated KRAS tumors (all $P < 0.001$); short-run low gray-level emphasis is associated with p53 mutations ($P = 0.001$); gray-level zone emphasis is associated with APC mutations ($P = 0.006$)

PET/CT: Positron emission tomography/computed tomography; PPV: Positive predictive value; NPV: Negative predictive value; AUC: Area under the curve; RF: Random forest; MTV: Metabolic tumor volume; TLG: Total lesion glycolysis; GLCM: Gray-level co-occurrence matrix; COV: Coefficient of variation; MV: Metabolic volume; OR: Odd ratio; MPP: Mean positive pixel.

MRI[100-102]. For this reason, at some center, abbreviated gadoxetate disodium MRI protocols are adopted rather than trusting CT only[103,104].

The adoption of radiomics has been proven successful in diagnostic, prognostic, and therapeutic stages[78].

Diagnosis and risk assessment

In term of diagnosis of synchronous classical logistic regression models (CLRM), it is relevant to highlight that even with MRI the sensitivity may be lower than 80%, particularly in patients with mucinous adenocarcinoma as primary tumor, prior local treatment in the liver or metastases smaller than 1 cm[102]. Therefore, the first main diagnostic task of radiomics should be the identification of CRLM before they can be seen by radiologist's naked eye (*i.e.*, detection of synchronous metastases). In a pilot study, Devoto *et al*[105] proved that radiomics can potentially predict the development of liver metastases on baseline liver CT, by demonstrating a higher heterogeneity of liver texture analysis in patients who developed liver metastases compared to patients who did not develop them. Other authors[34,106] investigated whether radiomics applied to T2-weighted images of the primary tumor on MRI could help in the preoperative prediction of CRLM: Shu *et al*[34] used a region of interest while Liu *et al*[107] used a volume of interest and both demonstrated that a radiomics nomogram constructed by combining radiomics and clinical data achieve AUC higher than 90% in the preoperative prediction of

CRLM.

The second main diagnostic task of radiomics should be preoperative identification of patients at risk of developing CLRM (*i.e.*, detection of metachronous metastases) based on micro-environmental changes in the apparently normal liver. Taghavi *et al*[106] and Rao *et al*[108] designed a prediction model based on liver CT radiomics for the detection of metachronous CRL, with the first study including more patients imaged at three centers and combining radiomics and clinical data achieving AUC of up to 86% in the validation cohort. Other studies tried to achieve the same goal by assessing the primary tumor on CT[109] or MRI[110]. Specifically, Li *et al*[109] obtained an AUC of 0.72 for the prediction of metachronous CLRM by combining clinical data and volumetric radiomics of the primary tumor on CT. In regard of MRI, a systematic review including 1497 patients estimated a pooled sensitivity and specificity of radiomics applied to rectal MRI of 0.76 and 0.85 respectively in predicting metachronous CLRM, and AUC of the included studies ranging from 0.83 to 0.87[110].

Prognosis

In terms of prognostic information, radiomics of CRLM has emerged as a promising tool to preoperatively predict patient survival at diagnosis and after therapy. Ng *et al*[111] suggested that tumors demonstrating less texture tumor heterogeneity using radiomic CT analysis may predict poorer survival at diagnosis[111]. Mühlberg *et al*[112] showed that CT-based geometric distribution and radiomics analysis of whole liver tumor burden from preoperative CT may help for prediction of 1-year survival. Radiomics of CRLM on CT seems also promising for differentiating desmoplastic from replacement histopathological growth patterns[113], and this differentiation may provide an earlier estimate of disease aggressiveness and prognosis as the desmoplastic histopathological growth pattern usually has longer overall survival[114]. As demonstrated by Granata *et al*[115] contrast MR-based radiomics and machine learning analysis may help in the preoperative prediction of the front of tumor growth (expansive or infiltrative), the tumor budding (absent, low grade or high grade) and tumor recurrence after surgery, all of which may affect patient outcome. Studies looking at survival after chemotherapy in patients with CRLMs obtained similar results regarding the role of texture homogeneity/heterogeneity in the prediction of prognosis[116,117]. As an example, Ravanelli *et al*[116] demonstrated that lower uniformity of CRLM on CT texture analysis was independently correlated with overall survival and progression free survival in patients treated with bevacizumab, but not in those treated with standard chemotherapy. Other radiomic features such as entropy, kurtosis, and skewness have been investigated so far on CT and MRI, all providing an additional piece of the puzzle and supporting the concept that the addition of texture analysis in the pre-treatment assessment may provide information on prognosis in patients with primary colorectal cancer and CLRM[118,119].

Treatment response

Finally, the correct assessment of response in the treatment of CLRM and the prompt prediction of early response is of utmost important in defining the success or failure of treatment interventions and in the selection of those patients requiring a change of the therapeutic regimen. Chemotherapy for CLRM in the modern era of oxaliplatin- and irinotecan-containing regimens (*e.g.*, FOLFOX, FOLFIRI, CAPOX/FOLFOXIRI, XELOX) has been implemented with the introduction of targeted biologics and immunotherapeutic agents (*e.g.*, bevacizumab, cetuximab, panitumumab, pembrolizumab), thus expanding the proportion of patients eligible for curative-intent surgery, but their use may lead to side effects or complications[120]. Prediction of tumor response before starting chemotherapy would allow to choose the best treatment, avoiding unnecessary adverse effects of the therapy. Radiomics of CLRM has been proven promising for predicting response to different chemotherapy regimens, but the predictive value of radiomics features seems to be treatment dependent[95]. As shown by two systematic reviews[95,121], most studies performed radiomics on CT rather than MRI. In patients treated with FOLFOX or FOLFIRI, low skewness and narrower standard deviation-both suggesting increased tumor homogeneity-were associated with a high response rate to chemotherapy[122]. Giannini *et al*[41] developed a radiomics signature to predict behaviour of individual CLRMs to targeted treatment in patients with HER2 amplification undergoing dual target therapy; in their model, the two most important radiomics features were difference in variance and homogeneity, thus again highlighting the role of texture analysis homogeneity of CLRM for assessing lesion diagnosis and outcome. Other studies investigated the role of radiomics in assessing tumor response after other targeted biologics and immunotherapeutic agents, such as regorafenib[117], and bevacizumab[116,48].

CONCLUSION

Nowadays much evidence has revealed that not all clinical risk features are equal, not all affect overall survival, and the decision to treat colorectal cancer with adjuvant chemotherapy should be assessed in multidisciplinary approach[123]. In this scenario, radiomics could play a pivotal role in colorectal cancer workup as an additional tool in clinical setting with the expectancy to help clinicians in identifying patients with high-risk disease. In particular, the main fields examined were the preoperative assess-

ment of the differentiation between low- and high-grade colorectal cancer, and the prediction of nodal metastases[124-131]. The results achieved good and consistent efficiency in identifying high-risk clinical factors, reinforcing the idea that radiomics could play a central role in colorectal cancer patient workup. Nevertheless, radiomics has numerous shortcomings that make daily use extremely difficult. Among these, the lack of standardization and validation, poor reproducibility, and missing prospective multicentric studies represent the main drawbacks that must be overcome to introduce the radiomics approach to the clinical routine[7]. Further studies are needed to assess the performance of radiomics in stratifying patients with high-risk disease in patients with non-metastatic colorectal cancer who could benefit from adjuvant chemotherapy.

FOOTNOTES

Author contributions: Inchingolo R, Maino C, Cannella R, Vernuccio F, Cortese F, Dezio M, Pisani AR, Giandola T, Gatti M, Giannini V, Ippolito D, and Faletti R equally contributed to this paper with conception and design of the study, literature review and analysis, drafting and critical revision and editing; and all authors gave final approval of the final version.

Conflict-of-interest statement: All the authors are aware of the content of the manuscript and have no conflict of interest.

Country/Territory of origin: Italy

ORCID number: Riccardo Inchingolo 0000-0002-0253-5936; Cesare Maino 0000-0002-5742-802X; Roberto Cannella 0000-0002-3808-0785; Federica Vernuccio 0000-0003-0350-1794; Francesco Cortese 0000-0002-2731-3766; Michele Dezio 0000-0001-6491-4969; Antonio Rosario Pisani 0000-0002-3335-9541; Teresa Giandola 0000-0001-8750-0531; Marco Gatti 0000-0001-8168-5280; Valentina Giannini 0000-0001-5052-8231; Davide Ippolito 0000-0002-2696-7047; Riccardo Faletti 0000-0002-8865-8637.

S-Editor: Chen YL
L-Editor: A
P-Editor: Yuan YY

REFERENCES

1 **Sung H**, Ferlay J, Siegel RL, Laversanne M, Soerjomataram I, Jemal A, Bray F. Global Cancer Statistics 2020: GLOBOCAN Estimates of Incidence and Mortality Worldwide for 36 Cancers in 185 Countries. *CA Cancer J Clin* 2021; **71**: 209-249 [PMID: 33538338 DOI: 10.3322/caac.21660]

2 **Argilés G**, Tabernero J, Labianca R, Hochhauser D, Salazar R, Iveson T, Laurent-Puig P, Quirke P, Yoshino T, Taieb J, Martinelli E, Arnold D; ESMO Guidelines Committee. Electronic address: clinicalguidelines@esmo.org. Localised colon cancer: ESMO Clinical Practice Guidelines for diagnosis, treatment and follow-up. *Ann Oncol* 2020; **31**: 1291-1305 [PMID: 32702383 DOI: 10.1016/j.annonc.2020.06.022]

3 **Weiser MR**. AJCC 8th Edition: Colorectal Cancer. *Ann Surg Oncol* 2018; **25**: 1454-1455 [PMID: 29616422 DOI: 10.1245/s10434-018-6462-1]

4 **Baxter NN**, Kennedy EB, Bergsland E, Berlin J, George TJ, Gill S, Gold PJ, Hantel A, Jones L, Lieu C, Mahmoud N, Morris AM, Ruiz-Garcia E, You YN, Meyerhardt JA. Adjuvant Therapy for Stage II Colon Cancer: ASCO Guideline Update. *J Clin Oncol* 2022; **40**: 892-910 [PMID: 34936379 DOI: 10.1200/JCO.21.02538]

5 **Lambin P**, Rios-Velazquez E, Leijenaar R, Carvalho S, van Stiphout RG, Granton P, Zegers CM, Gillies R, Boellard R, Dekker A, Aerts HJ. Radiomics: extracting more information from medical images using advanced feature analysis. *Eur J Cancer* 2012; **48**: 441-446 [PMID: 22257792 DOI: 10.1016/j.ejca.2011.11.036]

6 **Aerts HJ**, Velazquez ER, Leijenaar RT, Parmar C, Grossmann P, Carvalho S, Bussink J, Monshouwer R, Haibe-Kains B, Rietveld D, Hoebers F, Rietbergen MM, Leemans CR, Dekker A, Quackenbush J, Gillies RJ, Lambin P. Decoding tumour phenotype by noninvasive imaging using a quantitative radiomics approach. *Nat Commun* 2014; **5**: 4006 [PMID: 24892406 DOI: 10.1038/ncomms5006]

7 **Caruso D**, Polici M, Zerunian M, Pucciarelli F, Guido G, Polidori T, Landolfi F, Nicolai M, Lucertini E, Tarallo M, Bracci B, Nacci I, Rucci C, Iannicelli E, Laghi A. Radiomics in Oncology, Part 1: Technical Principles and Gastrointestinal Application in CT and MRI. *Cancers (Basel)* 2021; **13** [PMID: 34063937 DOI: 10.3390/cancers13112522]

8 **Lambin P**, Leijenaar RTH, Deist TM, Peerlings J, de Jong EEC, van Timmeren J, Sanduleanu S, Larue RTHM, Even AJG, Jochems A, van Wijk Y, Woodruff H, van Soest J, Lustberg T, Roelofs E, van Elmpt W, Dekker A, Mottaghy FM,

Wildberger JE, Walsh S. Radiomics: the bridge between medical imaging and personalized medicine. *Nat Rev Clin Oncol* 2017; **14**: 749-762 [PMID: 28975929 DOI: 10.1038/nrclinonc.2017.141]

9 **Caruso D**, Polici M, Zerunian M, Pucciarelli F, Guido G, Polidori T, Landolfi F, Nicolai M, Lucertini E, Tarallo M, Bracci B, Nacci I, Rucci C, Eid M, Iannicelli E, Laghi A. Radiomics in Oncology, Part 2: Thoracic, Genito-Urinary, Breast, Neurological, Hematologic and Musculoskeletal Applications. *Cancers (Basel)* 2021; **13** [PMID: 34072366 DOI: 10.3390/cancers13112681]

10 **Botta F**, Raimondi S, Rinaldi L, Bellerba F, Corso F, Bagnardi V, Origgi D, Minelli R, Pitoni G, Petrella F, Spaggiari L, Morganti AG, Del Grande F, Bellomi M, Rizzo S. Association of a CT-Based Clinical and Radiomics Score of Non-Small Cell Lung Cancer (NSCLC) with Lymph Node Status and Overall Survival. *Cancers (Basel)* 2020; **12** [PMID: 32486453 DOI: 10.3390/cancers12061432]

11 **Fan G**, Qin J, Liu H, Liao X. Commentary: Radiomics in oncology: A 10-year bibliometric analysis. *Front Oncol* 2022; **12**: 891056 [PMID: 35936758 DOI: 10.3389/fonc.2022.891056]

12 **van Timmeren JE**, Cester D, Tanadini-Lang S, Alkadhi H, Baessler B. Radiomics in medical imaging-"how-to" guide and critical reflection. *Insights Imaging* 2020; **11**: 91 [PMID: 32785796 DOI: 10.1186/s13244-020-00887-2]

13 **Defeudis A**, De Mattia C, Rizzetto F, Calderoni F, Mazzetti S, Torresin A, Vanzulli A, Regge D, Giannini V. Standardization of CT radiomics features for multi-center analysis: impact of software settings and parameters. *Phys Med Biol* 2020; **65**: 195012 [PMID: 32575082 DOI: 10.1088/1361-6560/ab9f61]

14 **Pan S**, Ding Z, Zhang L, Ruan M, Shan Y, Deng M, Pang P, Shen Q. A Nomogram Combined Radiomic and Semantic Features as Imaging Biomarker for Classification of Ovarian Cystadenomas. *Front Oncol* 2020; **10**: 895 [PMID: 32547958 DOI: 10.3389/fonc.2020.00895]

15 **Qi Y**, Zhang S, Wei J, Zhang G, Lei J, Yan W, Xiao Y, Yan S, Xue H, Feng F, Sun H, Tian J, Jin Z. Multiparametric MRI-Based Radiomics for Prostate Cancer Screening With PSA in 4-10 ng/mL to Reduce Unnecessary Biopsies. *J Magn Reson Imaging* 2020; **51**: 1890-1899 [PMID: 31808980 DOI: 10.1002/jmri.27008]

16 **Shi R**, Chen W, Yang B, Qu J, Cheng Y, Zhu Z, Gao Y, Wang Q, Liu Y, Li Z, Qu X. Prediction of KRAS, NRAS and BRAF status in colorectal cancer patients with liver metastasis using a deep artificial neural network based on radiomics and semantic features. *Am J Cancer Res* 2020; **10**: 4513-4526 [PMID: 33415015]

17 **Frøkjær JB**, Lisitskaya MV, Jørgensen AS, Østergaard LR, Hansen TM, Drewes AM, Olesen SS. Pancreatic magnetic resonance imaging texture analysis in chronic pancreatitis: a feasibility and validation study. *Abdom Radiol (NY)* 2020; **45**: 1497-1506 [PMID: 32266506 DOI: 10.1007/s00261-020-02512-8]

18 **Petkovska I**, Tixier F, Ortiz EJ, Golia Pernicka JS, Paroder V, Bates DD, Horvat N, Fuqua J, Schilsky J, Gollub MJ, Garcia-Aguilar J, Veeraraghavan H. Clinical utility of radiomics at baseline rectal MRI to predict complete response of rectal cancer after chemoradiation therapy. *Abdom Radiol (NY)* 2020; **45**: 3608-3617 [PMID: 32296896 DOI: 10.1007/s00261-020-02502-w]

19 **Wang JC**, Fu R, Tao XW, Mao YF, Wang F, Zhang ZC, Yu WW, Chen J, He J, Sun BC. A radiomics-based model on non-contrast CT for predicting cirrhosis: make the most of image data. *Biomark Res* 2020; **8**: 47 [PMID: 32963787 DOI: 10.1186/s40364-020-00219-y]

20 **Park S**, Chu LC, Hruban RH, Vogelstein B, Kinzler KW, Yuille AL, Fouladi DF, Shayesteh S, Ghandili S, Wolfgang CL, Burkhart R, He J, Fishman EK, Kawamoto S. Differentiating autoimmune pancreatitis from pancreatic ductal adenocarcinoma with CT radiomics features. *Diagn Interv Imaging* 2020; **101**: 555-564 [PMID: 32278586 DOI: 10.1016/j.diii.2020.03.002]

21 **Gu D**, Hu Y, Ding H, Wei J, Chen K, Liu H, Zeng M, Tian J. CT radiomics may predict the grade of pancreatic neuroendocrine tumors: a multicenter study. *Eur Radiol* 2019; **29**: 6880-6890 [PMID: 31227882 DOI: 10.1007/s00330-019-06176-x]

22 **Bagher-Ebadian H**, Janic B, Liu C, Pantelic M, Hearshen D, Elshaikh M, Movsas B, Chetty IJ, Wen N. Detection of Dominant Intra-prostatic Lesions in Patients With Prostate Cancer Using an Artificial Neural Network and MR Multi-modal Radiomics Analysis. *Front Oncol* 2019; **9**: 1313 [PMID: 31850209 DOI: 10.3389/fonc.2019.01313]

23 **Liu Y**, Fan H, Dong D, Liu P, He B, Meng L, Chen J, Chen C, Lang J, Tian J. Computed tomography-based radiomic model at node level for the prediction of normal-sized lymph node metastasis in cervical cancer. *Transl Oncol* 2021; **14**: 101113 [PMID: 33975178 DOI: 10.1016/j.tranon.2021.101113]

24 **Panic J**, Defeudis A, Mazzetti S, Rosati S, Giannetto G, Vassallo L, Regge D, Balestra G, Giannini V. A Convolutional Neural Network based system for Colorectal cancer segmentation on MRI images. *Annu Int Conf IEEE Eng Med Biol Soc* 2020; **2020**: 1675-1678 [PMID: 33018318 DOI: 10.1109/EMBC44109.2020.9175804]

25 **Barra D**, Nicoletti G, Defeudis A, Mazzetti S, Panic J, Gatti M, Faletti R, Russo F, Regge D, Giannini V. Deep learning model for automatic prostate segmentation on bicentric T2w images with and without endorectal coil. *Annu Int Conf IEEE Eng Med Biol Soc* 2021; **2021**: 3370-3373 [PMID: 34891962 DOI: 10.1109/EMBC46164.2021.9630792]

26 **Riley RD**, Snell KIE, Ensor J, Burke DL, Harrell FE Jr, Moons KGM, Collins GS. Minimum sample size for developing a multivariable prediction model: Part I - Continuous outcomes. *Stat Med* 2019; **38**: 1262-1275 [PMID: 30347470 DOI: 10.1002/sim.7993]

27 **Limkin EJ**, Sun R, Dercle L, Zacharaki EI, Robert C, Reuzé S, Schernberg A, Paragios N, Deutsch E, Ferté C. Promises and challenges for the implementation of computational medical imaging (radiomics) in oncology. *Ann Oncol* 2017; **28**: 1191-1206 [PMID: 28168275 DOI: 10.1093/annonc/mdx034]

28 **Ganeshan B**, Abaleke S, Young RC, Chatwin CR, Miles KA. Texture analysis of non-small cell lung cancer on unenhanced computed tomography: initial evidence for a relationship with tumour glucose metabolism and stage. *Cancer Imaging* 2010; **10**: 137-143 [PMID: 20605762 DOI: 10.1102/1470-7330.2010.0021]

29 **Gevaert O**, Xu J, Hoang CD, Leung AN, Xu Y, Quon A, Rubin DL, Napel S, Plevritis SK. Non-small cell lung cancer: identifying prognostic imaging biomarkers by leveraging public gene expression microarray data--methods and preliminary results. *Radiology* 2012; **264**: 387-396 [PMID: 22723499 DOI: 10.1148/radiol.12111607]

30 **Zhu Y**, Li H, Guo W, Drukker K, Lan L, Giger ML, Ji Y. Deciphering Genomic Underpinnings of Quantitative MRI-based Radiomic Phenotypes of Invasive Breast Carcinoma. *Sci Rep* 2015; **5**: 17787 [PMID: 26639025 DOI:

10.1038/srep17787]

31 **Segal E**, Sirlin CB, Ooi C, Adler AS, Gollub J, Chen X, Chan BK, Matcuk GR, Barry CT, Chang HY, Kuo MD. Decoding global gene expression programs in liver cancer by noninvasive imaging. *Nat Biotechnol* 2007; **25**: 675-680 [PMID: 17515910 DOI: 10.1038/nbt1306]

32 **Reginelli A**, Capasso R, Petrillo M, Rossi C, Faella P, Grassi R, Belfiore MP, Rossi G, Muto M, Muto P, Fiorello A, Serra N, Nizzoli R, De Filippo M, Cappabianca S, Carrafiello G, Brunese L, Rotondo A. Looking for Lepidic Component inside Invasive Adenocarcinomas Appearing as CT Solid Solitary Pulmonary Nodules (SPNs): CT Morpho-Densitometric Features and 18-FDG PET Findings. *Biomed Res Int* 2019; **2019**: 7683648 [PMID: 30733967 DOI: 10.1155/2019/7683648]

33 **Chiappa V**, Bogani G, Interlenghi M, Salvatore C, Bertolina F, Sarpietro G, Signorelli M, Castiglioni I, Raspagliesi F. The Adoption of Radiomics and machine learning improves the diagnostic processes of women with Ovarian MAsses (the AROMA pilot study). *J Ultrasound* 2021; **24**: 429-437 [PMID: 32696414 DOI: 10.1007/s40477-020-00503-5]

34 **Shu Z**, Fang S, Ding Z, Mao D, Cai R, Chen Y, Pang P, Gong X. MRI-based Radiomics nomogram to detect primary rectal cancer with synchronous liver metastases. *Sci Rep* 2019; **9**: 3374 [PMID: 30833648 DOI: 10.1038/s41598-019-39651-y]

35 **Li M**, Zhang J, Dan Y, Yao Y, Dai W, Cai G, Yang G, Tong T. A clinical-radiomics nomogram for the preoperative prediction of lymph node metastasis in colorectal cancer. *J Transl Med* 2020; **18**: 46 [PMID: 32000813 DOI: 10.1186/s12967-020-02215-0]

36 **Purnell SD**, Bloom JB, Valera V, Wood BJ, Turkbey B, Pinto PA. Targeted biopsy: benefits and limitations. *Curr Opin Urol* 2018; **28**: 219-226 [PMID: 29334506 DOI: 10.1097/MOU.0000000000000481]

37 **Negreros-Osuna AA**, Parakh A, Corcoran RB, Pourvaziri A, Kambadakone A, Ryan DP, Sahani DV. Radiomics Texture Features in Advanced Colorectal Cancer: Correlation with BRAF Mutation and 5-year Overall Survival. *Radiol Imaging Cancer* 2020; **2**: e190084 [PMID: 33778733 DOI: 10.1148/rycan.2020190084]

38 **van Kessel CS**, Samim M, Koopman M, van den Bosch MA, Borel Rinkes IH, Punt CJ, van Hillegersberg R. Radiological heterogeneity in response to chemotherapy is associated with poor survival in patients with colorectal liver metastases. *Eur J Cancer* 2013; **49**: 2486-2493 [PMID: 23692811 DOI: 10.1016/j.ejca.2013.03.027]

39 **Russo M**, Siravegna G, Blaszkowsky LS, Corti G, Crisafulli G, Ahronian LG, Mussolin B, Kwak EL, Buscarino M, Lazzari L, Valtorta E, Truini M, Jessop NA, Robinson HE, Hong TS, Mino-Kenudson M, Di Nicolantonio F, Thabet A, Sartore-Bianchi A, Siena S, Iafrate AJ, Bardelli A, Corcoran RB. Tumor Heterogeneity and Lesion-Specific Response to Targeted Therapy in Colorectal Cancer. *Cancer Discov* 2016; **6**: 147-153 [PMID: 26644315 DOI: 10.1158/2159-8290.CD-15-1283]

40 **Piotrowska Z**, Niederst MJ, Karlovich CA, Wakelee HA, Neal JW, Mino-Kenudson M, Fulton L, Hata AN, Lockerman EL, Kalsy A, Digumarthy S, Muzikansky A, Raponi M, Garcia AR, Mulvey HE, Parks MK, DiCecca RH, Dias-Santagata D, Iafrate AJ, Shaw AT, Allen AR, Engelman JA, Sequist LV. Heterogeneity Underlies the Emergence of EGFRT790 Wild-Type Clones Following Treatment of T790M-Positive Cancers with a Third-Generation EGFR Inhibitor. *Cancer Discov* 2015; **5**: 713-722 [PMID: 25934077 DOI: 10.1158/2159-8290.CD-15-0399]

41 **Giannini V**, Rosati S, Defeudis A, Balestra G, Vassallo L, Cappello G, Mazzetti S, De Mattia C, Rizzetto F, Torresin A, Sartore-Bianchi A, Siena S, Vanzulli A, Leone F, Zagonel V, Marsoni S, Regge D. Radiomics predicts response of individual HER2-amplified colorectal cancer liver metastases in patients treated with HER2-targeted therapy. *Int J Cancer* 2020; **147**: 3215-3223 [PMID: 32875550 DOI: 10.1002/ijc.33271]

42 **Nardone V**, Reginelli A, Grassi R, Boldrini L, Vacca G, D'Ippolito E, Annunziata S, Farchione A, Belfiore MP, Desideri I, Cappabianca S. Delta radiomics: a systematic review. *Radiol Med* 2021; **126**: 1571-1583 [PMID: 34865190 DOI: 10.1007/s11547-021-01436-7]

43 **Nasief H**, Zheng C, Schott D, Hall W, Tsai S, Erickson B, Allen Li X. A machine learning based delta-radiomics process for early prediction of treatment response of pancreatic cancer. *NPJ Precis Oncol* 2019; **3**: 25 [PMID: 31602401 DOI: 10.1038/s41698-019-0096-z]

44 **Jeon SH**, Song C, Chie EK, Kim B, Kim YH, Chang W, Lee YJ, Chung JH, Chung JB, Lee KW, Kang SB, Kim JS. Delta-radiomics signature predicts treatment outcomes after preoperative chemoradiotherapy and surgery in rectal cancer. *Radiat Oncol* 2019; **14**: 43 [PMID: 30866965 DOI: 10.1186/s13014-019-1246-8]

45 **Giannini V**, Pusceddu L, Defeudis A, Nicoletti G, Cappello G, Mazzetti S, Sartore-Bianchi A, Siena S, Vanzulli A, Rizzetto F, Fenocchio E, Lazzari L, Bardelli A, Marsoni S, Regge D. Delta-Radiomics Predicts Response to First-Line Oxaliplatin-Based Chemotherapy in Colorectal Cancer Patients with Liver Metastases. *Cancers (Basel)* 2022; **14** [PMID: 35008405 DOI: 10.3390/cancers14010241]

46 **Fave X**, Zhang L, Yang J, Mackin D, Balter P, Gomez D, Followill D, Jones AK, Stingo F, Liao Z, Mohan R, Court L. Delta-radiomics features for the prediction of patient outcomes in non-small cell lung cancer. *Sci Rep* 2017; **7**: 588 [PMID: 28373718 DOI: 10.1038/s41598-017-00665-z]

47 **Dercle L**, Lu L, Schwartz LH, Qian M, Tejpar S, Eggleton P, Zhao B, Piessevaux H. Radiomics Response Signature for Identification of Metastatic Colorectal Cancer Sensitive to Therapies Targeting EGFR Pathway. *J Natl Cancer Inst* 2020; **112**: 902-912 [PMID: 32016387 DOI: 10.1093/jnci/djaa017]

48 **Dohan A**, Gallix B, Guiu B, Le Malicot K, Reinhold C, Soyer P, Bennouna J, Ghiringhelli F, Barbier E, Boige V, Taieb J, Bouché O, François E, Phelip JM, Borel C, Faroux R, Seitz JF, Jacquot S, Ben Abdelghani M, Khemissa-Akouz F, Genet D, Jouve JL, Rinaldi Y, Desseigne F, Texereau P, Suc E, Lepage C, Aparicio T, Hoeffel C; PRODIGE 9 Investigators and PRODIGE 20 Investigators. Early evaluation using a radiomic signature of unresectable hepatic metastases to predict outcome in patients with colorectal cancer treated with FOLFIRI and bevacizumab. *Gut* 2020; **69**: 531-539 [PMID: 31101691 DOI: 10.1136/gutjnl-2018-316407]

49 **Thomas JV**, Abou Elkassem AM, Ganeshan B, Smith AD. MR Imaging Texture Analysis in the Abdomen and Pelvis. *Magn Reson Imaging Clin N Am* 2020; **28**: 447-456 [PMID: 32624161 DOI: 10.1016/j.mric.2020.03.009]

50 **Cunningham D**, Atkin W, Lenz HJ, Lynch HT, Minsky B, Nordlinger B, Starling N. Colorectal cancer. *Lancet* 2010; **375**: 1030-1047 [PMID: 20304247 DOI: 10.1016/S0140-6736(10)60353-4]

51 **Chen BY**, Xie H, Li Y, Jiang XH, Xiong L, Tang XF, Lin XF, Li L, Cai PQ. MRI-Based Radiomics Features to Predict Treatment Response to Neoadjuvant Chemotherapy in Locally Advanced Rectal Cancer: A Single Center, Prospective Study. *Front Oncol* 2022; **12**: 801743 [PMID: 35646677 DOI: 10.3389/fonc.2022.801743]

52 **Horvat N**, Veeraraghavan H, Nahas CSR, Bates DDB, Ferreira FR, Zheng J, Capanu M, Fuqua JL 3rd, Fernandes MC, Sosa RE, Jayaprakasam VS, Cerri GG, Nahas SC, Petkovska I. Combined artificial intelligence and radiologist model for predicting rectal cancer treatment response from magnetic resonance imaging: an external validation study. *Abdom Radiol (NY)* 2022; **47**: 2770-2782 [PMID: 35710951 DOI: 10.1007/s00261-022-03572-8]

53 **Dinapoli N**, Barbaro B, Gatta R, Chiloiro G, Casà C, Masciocchi C, Damiani A, Boldrini L, Gambacorta MA, Dezio M, Mattiucci GC, Balducci M, van Soest J, Dekker A, Lambin P, Fiorino C, Sini C, De Cobelli F, Di Muzio N, Gumina C, Passoni P, Manfredi R, Valentini V. Magnetic Resonance, Vendor-independent, Intensity Histogram Analysis Predicting Pathologic Complete Response After Radiochemotherapy of Rectal Cancer. *Int J Radiat Oncol Biol Phys* 2018; **102**: 765-774 [PMID: 29891200 DOI: 10.1016/j.ijrobp.2018.04.065]

54 **Shahzadi I**, Zwanenburg A, Lattermann A, Linge A, Baldus C, Peeken JC, Combs SE, Diefenhardt M, Rödel C, Kirste S, Grosu AL, Baumann M, Krause M, Troost EGC, Löck S. Analysis of MRI and CT-based radiomics features for personalized treatment in locally advanced rectal cancer and external validation of published radiomics models. *Sci Rep* 2022; **12**: 10192 [PMID: 35715462 DOI: 10.1038/s41598-022-13967-8]

55 **Xue H**, Du X, Xiao C, Yan Y, Zou Z, Xu Y. [Predictive value of lymph node ratio for postoperative distant metastasis of stage III colorectal cancer]. *Nan Fang Yi Ke Da Xue Xue Bao* 2014; **34**: 458-462 [PMID: 24752087]

56 **Watanabe T**, Muro K, Ajioka Y, Hashiguchi Y, Ito Y, Saito Y, Hamaguchi T, Ishida H, Ishiguro M, Ishihara S, Kanemitsu Y, Kawano H, Kinugasa Y, Kokudo N, Murofushi K, Nakajima T, Oka S, Sakai Y, Tsuji A, Uehara K, Ueno H, Yamazaki K, Yoshida M, Yoshino T, Boku N, Fujimori T, Itabashi M, Koinuma N, Morita T, Nishimura G, Sakata Y, Shimada Y, Takahashi K, Tanaka S, Tsuruta O, Yamaguchi T, Yamaguchi N, Tanaka T, Kotake K, Sugihara K; Japanese Society for Cancer of the Colon and Rectum. Japanese Society for Cancer of the Colon and Rectum (JSCCR) guidelines 2016 for the treatment of colorectal cancer. *Int J Clin Oncol* 2018; **23**: 1-34 [PMID: 28349281 DOI: 10.1007/s10147-017-1101-6.]

57 **Sabbagh C**, Mauvais F, Cosse C, Rebibo L, Joly JP, Dromer D, Aubert C, Carton S, Dron B, Dadamessi I, Maes B, Perrier G, Manaouil D, Fontaine JF, Gozy M, Panis X, Foncelle PH, de Fresnoy H, Leroux F, Vaneslander P, Ghighi C, Regimbeau JM; APCD-LNR-2011 study group. A lymph node ratio of 10% is predictive of survival in stage III colon cancer: a French regional study. *Int Surg* 2014; **99**: 344-353 [PMID: 25058763 DOI: 10.9738/INTSURG-D-13-00052.1]

58 **Huang YQ**, Liang CH, He L, Tian J, Liang CS, Chen X, Ma ZL, Liu ZY. Development and Validation of a Radiomics Nomogram for Preoperative Prediction of Lymph Node Metastasis in Colorectal Cancer. *J Clin Oncol* 2016; **34**: 2157-2164 [PMID: 27138577 DOI: 10.1200/JCO.2015.65.9128]

59 **Dighe S**, Purkayastha S, Swift I, Tekkis PP, Darzi A, A'Hern R, Brown G. Diagnostic precision of CT in local staging of colon cancers: a meta-analysis. *Clin Radiol* 2010; **65**: 708-719 [PMID: 20696298 DOI: 10.1016/j.crad.2010.01.024]

60 **Benson AB**, Venook AP, Al-Hawary MM, Arain MA, Chen YJ, Ciombor KK, Cohen S, Cooper HS, Deming D, Garrido-Laguna I, Grem JL, Gunn A, Hoffe S, Hubbard J, Hunt S, Kirilcuk N, Krishnamurthi S, Messersmith WA, Meyerhardt J, Miller ED, Mulcahy MF, Nurkin S, Overman MJ, Parikh A, Patel H, Pedersen K, Saltz L, Schneider C, Shibata D, Skibber JM, Sofocleous CT, Stoffel EM, Stotsky-Himelfarb E, Willett CG, Johnson-Chilla A, Gurski LA. NCCN Guidelines Insights: Rectal Cancer, Version 6.2020. *J Natl Compr Canc Netw* 2020; **18**: 806-815 [PMID: 32634771 DOI: 10.6004/jnccn.2020.0032]

61 **Nicholls RJ**, Zinicola R, Haboubi N. Extramural spread of rectal cancer and the AJCC Cancer Staging Manual 8th edition, 2017. *Ann Oncol* 2019; **30**: 1394-1395 [PMID: 31046085 DOI: 10.1093/annonc/mdz147]

62 **Glynne-Jones R**, Wyrwicz L, Tiret E, Brown G, Rödel C, Cervantes A, Arnold D; ESMO Guidelines Committee. Rectal cancer: ESMO Clinical Practice Guidelines for diagnosis, treatment and follow-up. *Ann Oncol* 2017; **28**: iv22-iv40 [PMID: 28881920 DOI: 10.1093/annonc/mdx224]

63 **Langs G**, Röhrich S, Hofmanninger J, Prayer F, Pan J, Herold C, Prosch H. Machine learning: from radiomics to discovery and routine. *Radiologe* 2018; **58**: 1-6 [PMID: 29922965 DOI: 10.1007/s00117-018-0407-3]

64 **Liu Z**, Wang S, Dong D, Wei J, Fang C, Zhou X, Sun K, Li L, Li B, Wang M, Tian J. The Applications of Radiomics in Precision Diagnosis and Treatment of Oncology: Opportunities and Challenges. *Theranostics* 2019; **9**: 1303-1322 [PMID: 30867832 DOI: 10.7150/thno.30309]

65 **Pinto Dos Santos D**, Dietzel M, Baessler B. A decade of radiomics research: are images really data or just patterns in the noise? *Eur Radiol* 2021; **31**: 1-4 [PMID: 32767103 DOI: 10.1007/s00330-020-07108-w]

66 **Kirienko M**, Ninatti G, Cozzi L, Voulaz E, Gennaro N, Barajon I, Ricci F, Carlo-Stella C, Zucali P, Sollini M, Balzarini L, Chiti A. Computed tomography (CT)-derived radiomic features differentiate prevascular mediastinum masses as thymic neoplasms *vs* lymphomas. *Radiol Med* 2020; **125**: 951-960 [PMID: 32306201 DOI: 10.1007/s11547-020-01188-w]

67 **Karmazanovsky G**, Gruzdev I, Tikhonova V, Kondratyev E, Revishvili A. Computed tomography-based radiomics approach in pancreatic tumors characterization. *Radiol Med* 2021 [PMID: 34386897 DOI: 10.1007/s11547-021-01405-0]

68 **Calabrese A**, Santucci D, Landi R, Beomonte Zobel B, Faiella E, de Felice C. Radiomics MRI for lymph node status prediction in breast cancer patients: the state of art. *J Cancer Res Clin Oncol* 2021; **147**: 1587-1597 [PMID: 33758997 DOI: 10.1007/s00432-021-03606-6]

69 **Benedetti G**, Mori M, Panzeri MM, Barbera M, Palumbo D, Sini C, Muffatti F, Andreasi V, Steidler S, Doglioni C, Partelli S, Manzoni M, Falconi M, Fiorino C, De Cobelli F. CT-derived radiomic features to discriminate histologic characteristics of pancreatic neuroendocrine tumors. *Radiol Med* 2021; **126**: 745-760 [PMID: 33523367 DOI: 10.1007/s11547-021-01333-z]

70 **Qin H**, Que Q, Lin P, Li X, Wang XR, He Y, Chen JQ, Yang H. Magnetic resonance imaging (MRI) radiomics of papillary thyroid cancer (PTC): a comparison of predictive performance of multiple classifiers modeling to identify cervical lymph node metastases before surgery. *Radiol Med* 2021; **126**: 1312-1327 [PMID: 34236572 DOI: 10.1007/s11547-021-01393-1]

71 **Liu X**, Yang Q, Zhang C, Sun J, He K, Xie Y, Zhang Y, Fu Y, Zhang H. Multiregional-Based Magnetic Resonance

Imaging Radiomics Combined With Clinical Data Improves Efficacy in Predicting Lymph Node Metastasis of Rectal Cancer. *Front Oncol* 2020; **10**: 585767 [PMID: 33680919 DOI: 10.3389/fonc.2020.585767]

72 **Chen P**, Wen D, Huang L, Ding J, Yang W, Sun J, Yang L, Zhou Z. Magnetic Resonance Imaging Radiomics-Based Model to Identify the Pathological Features and Lymph Node Metastasis in Rectal Cancer. May 3, 2022. [cited 1 March 2023]. Available from: https://www.medrxiv.org/content/10.1101/2022.05.02.22274247v1

73 **Liu L**, Liu Y, Xu L, Li Z, Lv H, Dong N, Li W, Yang Z, Wang Z, Jin E. Application of texture analysis based on apparent diffusion coefficient maps in discriminating different stages of rectal cancer. *J Magn Reson Imaging* 2017; **45**: 1798-1808 [PMID: 27654307 DOI: 10.1002/jmri.25460]

74 **Yang L**, Liu D, Fang X, Wang Z, Xing Y, Ma L, Wu B. Rectal cancer: can T2WI histogram of the primary tumor help predict the existence of lymph node metastasis? *Eur Radiol* 2019; **29**: 6469-6476 [PMID: 31278581 DOI: 10.1007/s00330-019-06328-z]

75 **Ma X**, Shen F, Jia Y, Xia Y, Li Q, Lu J. MRI-based radiomics of rectal cancer: preoperative assessment of the pathological features. *BMC Med Imaging* 2019; **19**: 86 [PMID: 31747902 DOI: 10.1186/s12880-019-0392-7]

76 **Zhu H**, Zhang X, Li X, Shi Y, Zhu H, Sun Y. Prediction of pathological nodal stage of locally advanced rectal cancer by collective features of multiple lymph nodes in magnetic resonance images before and after neoadjuvant chemoradiotherapy. *Chin J Cancer Res* 2019; **31**: 984-992 [PMID: 31949400 DOI: 10.21147/j.issn.1000-9604.2019.06.14]

77 **Zhou X**, Yi Y, Liu Z, Zhou Z, Lai B, Sun K, Li L, Huang L, Feng Y, Cao W, Tian J. Radiomics-Based Preoperative Prediction of Lymph Node Status Following Neoadjuvant Therapy in Locally Advanced Rectal Cancer. *Front Oncol* 2020; **10**: 604 [PMID: 32477930 DOI: 10.3389/fonc.2020.00604]

78 **Vernuccio F**, Cannella R, Comelli A, Salvaggio G, Lagalla R, Midiri M. [Radiomics and artificial intelligence: new frontiers in medicine]. *Recenti Prog Med* 2020; **111**: 130-135 [PMID: 32157259 DOI: 10.1701/3315.32853]

79 **Kang J**, Lee JH, Lee HS, Cho ES, Park EJ, Baik SH, Lee KY, Park C, Yeu Y, Clemenceau JR, Park S, Xu H, Hong C, Hwang TH. Radiomics Features of (18)F-Fluorodeoxyglucose Positron-Emission Tomography as a Novel Prognostic Signature in Colorectal Cancer. *Cancers (Basel)* 2021; **13** [PMID: 33494345 DOI: 10.3390/cancers13030392]

80 **Lovinfosse P**, Polus M, Van Daele D, Martinive P, Daenen F, Hatt M, Visvikis D, Koopmansch B, Lambert F, Coimbra C, Seidel L, Albert A, Delvenne P, Hustinx R. FDG PET/CT radiomics for predicting the outcome of locally advanced rectal cancer. *Eur J Nucl Med Mol Imaging* 2018; **45**: 365-375 [PMID: 29046927 DOI: 10.1007/s00259-017-3855-5]

81 **Hotta M**, Minamimoto R, Gohda Y, Miwa K, Otani K, Kiyomatsu T, Yano H. Prognostic value of (18)F-FDG PET/CT with texture analysis in patients with rectal cancer treated by surgery. *Ann Nucl Med* 2021; **35**: 843-852 [PMID: 33948903 DOI: 10.1007/s12149-021-01622-7]

82 **Lv L**, Xin B, Hao Y, Yang Z, Xu J, Wang L, Wang X, Song S, Guo X. Radiomic analysis for predicting prognosis of colorectal cancer from preoperative (18)F-FDG PET/CT. *J Transl Med* 2022; **20**: 66 [PMID: 35109864 DOI: 10.1186/s12967-022-03262-5]

83 **Bundschuh RA**, Dinges J, Neumann L, Seyfried M, Zsótér N, Papp L, Rosenberg R, Becker K, Astner ST, Henninger M, Herrmann K, Ziegler SI, Schwaiger M, Essler M. Textural Parameters of Tumor Heterogeneity in ¹F-FDG PET/CT for Therapy Response Assessment and Prognosis in Patients with Locally Advanced Rectal Cancer. *J Nucl Med* 2014; **55**: 891-897 [PMID: 24752672 DOI: 10.2967/jnumed.113.127340]

84 **Bang JI**, Ha S, Kang SB, Lee KW, Lee HS, Kim JS, Oh HK, Lee HY, Kim SE. Prediction of neoadjuvant radiation chemotherapy response and survival using pretreatment [(18)F]FDG PET/CT scans in locally advanced rectal cancer. *Eur J Nucl Med Mol Imaging* 2016; **43**: 422-431 [PMID: 26338180 DOI: 10.1007/s00259-015-3180-9]

85 **Giannini V**, Mazzetti S, Bertotto I, Chiarenza C, Cauda S, Delmastro E, Bracco C, Di Dia A, Leone F, Medico E, Pisacane A, Ribero D, Stasi M, Regge D. Predicting locally advanced rectal cancer response to neoadjuvant therapy with (18)F-FDG PET and MRI radiomics features. *Eur J Nucl Med Mol Imaging* 2019; **46**: 878-888 [PMID: 30637502 DOI: 10.1007/s00259-018-4250-6]

86 **Schurink NW**, van Kranen SR, Berbee M, van Elmpt W, Bakers FCH, Roberti S, van Griethuysen JJM, Min LA, Lahaye MJ, Maas M, Beets GL, Beets-Tan RGH, Lambregts DMJ. Studying local tumour heterogeneity on MRI and FDG-PET/CT to predict response to neoadjuvant chemoradiotherapy in rectal cancer. *Eur Radiol* 2021; **31**: 7031-7038 [PMID: 33569624 DOI: 10.1007/s00330-021-07724-0]

87 **Shen WC**, Chen SW, Wu KC, Lee PY, Feng CL, Hsieh TC, Yen KY, Kao CH. Predicting pathological complete response in rectal cancer after chemoradiotherapy with a random forest using (18)F-fluorodeoxyglucose positron emission tomography and computed tomography radiomics. *Ann Transl Med* 2020; **8**: 207 [PMID: 32309354 DOI: 10.21037/atm.2020.01.107]

88 **Karahan Şen NP**, Aksu A, Kaya GÇ. Value of volumetric and textural analysis in predicting the treatment response in patients with locally advanced rectal cancer. *Ann Nucl Med* 2020; **34**: 960-967 [PMID: 32951129 DOI: 10.1007/s12149-020-01527-x]

89 **Yuan Z**, Frazer M, Rishi A, Latifi K, Tomaszewski MR, Moros EG, Feygelman V, Felder S, Sanchez J, Dessureault S, Imanirad I, Kim RD, Harrison LB, Hoffe SE, Zhang GG, Frakes JM. Pretreatment CT and PET radiomics predicting rectal cancer patients in response to neoadjuvant chemoradiotherapy. *Rep Pract Oncol Radiother* 2021; **26**: 29-34 [PMID: 33948299 DOI: 10.5603/RPOR.a2021.0004]

90 **He J**, Wang Q, Zhang Y, Wu H, Zhou Y, Zhao S. Preoperative prediction of regional lymph node metastasis of colorectal cancer based on (18)F-FDG PET/CT and machine learning. *Ann Nucl Med* 2021; **35**: 617-627 [PMID: 33738763 DOI: 10.1007/s12149-021-01605-8]

91 **Ma J**, Guo D, Miao W, Wang Y, Yan L, Wu F, Zhang C, Zhang R, Zuo P, Yang G, Wang Z. The value of (18)F-FDG PET/CT-based radiomics in predicting perineural invasion and outcome in non-metastatic colorectal cancer. *Abdom Radiol (NY)* 2022; **47**: 1244-1254 [PMID: 35218381 DOI: 10.1007/s00261-022-03453-0]

92 **Li J**, Yang Z, Xin B, Hao Y, Wang L, Song S, Xu J, Wang X. Quantitative Prediction of Microsatellite Instability in Colorectal Cancer With Preoperative PET/CT-Based Radiomics. *Front Oncol* 2021; **11**: 702055 [PMID: 34367985 DOI: 10.3389/fonc.2021.702055]

93 **Lovinfosse P**, Koopmansch B, Lambert F, Jodogne S, Kustermans G, Hatt M, Visvikis D, Seidel L, Polus M, Albert A, Delvenne P, Hustinx R. (18)F-FDG PET/CT imaging in rectal cancer: relationship with the RAS mutational status. *Br J Radiol* 2016; **89**: 20160212 [PMID: 27146067 DOI: 10.1259/bjr.20160212]

94 **Chen SW**, Shen WC, Chen WT, Hsieh TC, Yen KY, Chang JG, Kao CH. Metabolic Imaging Phenotype Using Radiomics of [(18)F]FDG PET/CT Associated with Genetic Alterations of Colorectal Cancer. *Mol Imaging Biol* 2019; **21**: 183-190 [PMID: 29948642 DOI: 10.1007/s11307-018-1225-8]

95 **Staal FCR**, van der Reijd DJ, Taghavi M, Lambregts DMJ, Beets-Tan RGH, Maas M. Radiomics for the Prediction of Treatment Outcome and Survival in Patients With Colorectal Cancer: A Systematic Review. *Clin Colorectal Cancer* 2021; **20**: 52-71 [PMID: 33349519 DOI: 10.1016/j.clcc.2020.11.001]

96 **Engstrand J**, Nilsson H, Strömberg C, Jonas E, Freedman J. Colorectal cancer liver metastases - a population-based study on incidence, management and survival. *BMC Cancer* 2018; **18**: 78 [PMID: 29334918 DOI: 10.1186/s12885-017-3925-x]

97 **Hackl C**, Neumann P, Gerken M, Loss M, Klinkhammer-Schalke M, Schlitt HJ. Treatment of colorectal liver metastases in Germany: a ten-year population-based analysis of 5772 cases of primary colorectal adenocarcinoma. *BMC Cancer* 2014; **14**: 810 [PMID: 25369977 DOI: 10.1186/1471-2407-14-810]

98 **Manfredi S**, Lepage C, Hatem C, Coatmeur O, Faivre J, Bouvier AM. Epidemiology and management of liver metastases from colorectal cancer. *Ann Surg* 2006; **244**: 254-259 [PMID: 16858188 DOI: 10.1097/01.sla.0000217629.94941.cf]

99 **Scheele J**, Stangl R, Altendorf-Hofmann A. Hepatic metastases from colorectal carcinoma: impact of surgical resection on the natural history. *Br J Surg* 1990; **77**: 1241-1246 [PMID: 2253003 DOI: 10.1002/bjs.1800771115]

100 **Vernuccio F**, Dioguardi Burgio M, Barbiera F, Cusmà S, Badalamenti G, Midiri M, Vilgrain V, Brancatelli G. CT and MR imaging of chemotherapy-induced hepatopathy. *Abdom Radiol (NY)* 2019; **44**: 3312-3324 [PMID: 31435760 DOI: 10.1007/s00261-019-02193-y]

101 **Schulz A**, Viktil E, Godt JC, Johansen CK, Dormagen JB, Holtedahl JE, Labori KJ, Bach-Gansmo T, Kløw NE. Diagnostic performance of CT, MRI and PET/CT in patients with suspected colorectal liver metastases: the superiority of MRI. *Acta Radiol* 2016; **57**: 1040-1048 [PMID: 26622057 DOI: 10.1177/0284185115617349]

102 **Sivesgaard K**, Larsen LP, Sørensen M, Kramer S, Schlander S, Amanavicius N, Bharadwaz A, Tønner Nielsen D, Viborg Mortensen F, Morre Pedersen E. Diagnostic accuracy of CE-CT, MRI and FDG PET/CT for detecting colorectal cancer liver metastases in patients considered eligible for hepatic resection and/or local ablation. *Eur Radiol* 2018; **28**: 4735-4747 [PMID: 29736846 DOI: 10.1007/s00330-018-5469-0]

103 **Vernuccio F**, Cannella R, Bartolotta TV, Galia M, Tang A, Brancatelli G. Advances in liver US, CT, and MRI: moving toward the future. *Eur Radiol Exp* 2021; **5**: 52 [PMID: 34873633 DOI: 10.1186/s41747-021-00250-0]

104 **Canellas R**, Rosenkrantz AB, Taouli B, Sala E, Saini S, Pedrosa I, Wang ZJ, Sahani DV. Abbreviated MRI Protocols for the Abdomen. *Radiographics* 2019; **39**: 744-758 [PMID: 30901285 DOI: 10.1148/rg.2019180123]

105 **Devoto L**, Ganeshan B, Keller D, Groves A, Endozo R, Arulampalam T, Chand M. Using texture analysis in the development of a potential radiomic signature for early identification of hepatic metastasis in colorectal cancer. *Eur J Radiol Open* 2022; **9**: 100415 [PMID: 35340828 DOI: 10.1016/j.ejro.2022.100415]

106 **Taghavi M**, Trebeschi S, Simões R, Meek DB, Beckers RCJ, Lambregts DMJ, Verhoef C, Houwers JB, van der Heide UA, Beets-Tan RGH, Maas M. Machine learning-based analysis of CT radiomics model for prediction of colorectal metachronous liver metastases. *Abdom Radiol (NY)* 2021; **46**: 249-256 [PMID: 32583138 DOI: 10.1007/s00261-020-02624-1]

107 **Liu M**, Ma X, Shen F, Xia Y, Jia Y, Lu J. MRI-based radiomics nomogram to predict synchronous liver metastasis in primary rectal cancer patients. *Cancer Med* 2020; **9**: 5155-5163 [PMID: 32476295 DOI: 10.1002/cam4.3185]

108 **Rao SX**, Lambregts DM, Schnerr RS, van Ommen W, van Nijnatten TJ, Martens MH, Heijnen LA, Backes WH, Verhoef C, Zeng MS, Beets GL, Beets-Tan RG. Whole-liver CT texture analysis in colorectal cancer: Does the presence of liver metastases affect the texture of the remaining liver? *United European Gastroenterol J* 2014; **2**: 530-538 [PMID: 25452849 DOI: 10.1177/2050640614552463]

109 **Li Y**, Gong J, Shen X, Li M, Zhang H, Feng F, Tong T. Assessment of Primary Colorectal Cancer CT Radiomics to Predict Metachronous Liver Metastasis. *Front Oncol* 2022; **12**: 861892 [PMID: 35296011 DOI: 10.3389/fonc.2022.861892]

110 **Davey MS**, Davey MG, Ryan ÉJ, Hogan AM, Kerin MJ, Joyce M. The use of radiomic analysis of magnetic resonance imaging in predicting distant metastases of rectal carcinoma following surgical resection: A systematic review and meta-analysis. *Colorectal Dis* 2021; **23**: 3065-3072 [PMID: 34536962 DOI: 10.1111/codi.15919]

111 **Ng F**, Ganeshan B, Kozarski R, Miles KA, Goh V. Assessment of primary colorectal cancer heterogeneity by using whole-tumor texture analysis: contrast-enhanced CT texture as a biomarker of 5-year survival. *Radiology* 2013; **266**: 177-184 [PMID: 23151829 DOI: 10.1148/radiol.12120254]

112 **Mühlberg A**, Holch JW, Heinemann V, Huber T, Moltz J, Maurus S, Jäger N, Liu L, Froelich MF, Katzmann A, Gresser E, Taubmann O, Sühling M, Nörenberg D. The relevance of CT-based geometric and radiomics analysis of whole liver tumor burden to predict survival of patients with metastatic colorectal cancer. *Eur Radiol* 2021; **31**: 834-846 [PMID: 32851450 DOI: 10.1007/s00330-020-07192-y]

113 **Starmans MPA**, Buisman FE, Renckens M, Willemssen FEJA, van der Voort SR, Groot Koerkamp B, Grünhagen DJ, Niessen WJ, Vermeulen PB, Verhoef C, Visser JJ, Klein S. Distinguishing pure histopathological growth patterns of colorectal liver metastases on CT using deep learning and radiomics: a pilot study. *Clin Exp Metastasis* 2021; **38**: 483-494 [PMID: 34533669 DOI: 10.1007/s10585-021-10119-6]

114 **Galjart B**, Nierop PMH, van der Stok EP, van den Braak RRJC, Höppener DJ, Daelemans S, Dirix LY, Verhoef C, Vermeulen PB, Grünhagen DJ. Angiogenic desmoplastic histopathological growth pattern as a prognostic marker of good outcome in patients with colorectal liver metastases. *Angiogenesis* 2019; **22**: 355-368 [PMID: 30637550 DOI: 10.1007/s10456-019-09661-5]

115 **Granata V**, Fusco R, De Muzio F, Cutolo C, Setola SV, Dell' Aversana F, Ottaiano A, Avallone A, Nasti G, Grassi F, Pilone V, Miele V, Brunese L, Izzo F, Petrillo A. Contrast MR-Based Radiomics and Machine Learning Analysis to Assess Clinical Outcomes following Liver Resection in Colorectal Liver Metastases: A Preliminary Study. *Cancers*

(Basel) 2022; **14** [PMID: 35267418 DOI: 10.3390/cancers14051110]

116 **Ravanelli M**, Agazzi GM, Tononcelli E, Roca E, Cabassa P, Baiocchi G, Berruti A, Maroldi R, Farina D. Texture features of colorectal liver metastases on pretreatment contrast-enhanced CT may predict response and prognosis in patients treated with bevacizumab-containing chemotherapy: a pilot study including comparison with standard chemotherapy. *Radiol Med* 2019; **124**: 877-886 [PMID: 31172448 DOI: 10.1007/s11547-019-01046-4]

117 **Andersen IR**, Thorup K, Andersen MB, Olesen R, Mortensen FV, Nielsen DT, Rasmussen F. Texture in the monitoring of regorafenib therapy in patients with colorectal liver metastases. *Acta Radiol* 2019; **60**: 1084-1093 [PMID: 30612433 DOI: 10.1177/0284185118817940]

118 **Fiz F**, Viganò L, Gennaro N, Costa G, La Bella L, Boichuk A, Cavinato L, Sollini M, Politi LS, Chiti A, Torzilli G. Radiomics of Liver Metastases: A Systematic Review. *Cancers (Basel)* 2020; **12** [PMID: 33036490 DOI: 10.3390/cancers12102881]

119 **Jalil O**, Afaq A, Ganeshan B, Patel UB, Boone D, Endozo R, Groves A, Sizer B, Arulampalam T. Magnetic resonance based texture parameters as potential imaging biomarkers for predicting long-term survival in locally advanced rectal cancer treated by chemoradiotherapy. *Colorectal Dis* 2017; **19**: 349-362 [PMID: 27538267 DOI: 10.1111/codi.13496]

120 **Albano D**, Benenati M, Bruno A, Bruno F, Calandri M, Caruso D, Cozzi D, De Robertis R, Gentili F, Grazzini I, Micci G, Palmisano A, Pessina C, Scalise P, Vernuccio F, Barile A, Miele V, Grassi R, Messina C; Young SIRM Working Group. Imaging side effects and complications of chemotherapy and radiation therapy: a pictorial review from head to toe. *Insights Imaging* 2021; **12**: 76 [PMID: 34114094 DOI: 10.1186/s13244-021-01017-2]

121 **Wesdorp NJ**, van Goor VJ, Kemna R, Jansma EP, van Waesberghe JHTM, Swijnenburg RJ, Punt CJA, Huiskens J, Kazemier G. Advanced image analytics predicting clinical outcomes in patients with colorectal liver metastases: A systematic review of the literature. *Surg Oncol* 2021; **38**: 101578 [PMID: 33866191 DOI: 10.1016/j.suronc.2021.101578]

122 **Ahn SJ**, Kim JH, Park SJ, Han JK. Prediction of the therapeutic response after FOLFOX and FOLFIRI treatment for patients with liver metastasis from colorectal cancer using computerized CT texture analysis. *Eur J Radiol* 2016; **85**: 1867-1874 [PMID: 27666629 DOI: 10.1016/j.ejrad.2016.08.014]

123 **Babcock BD**, Aljehani MA, Jabo B, Choi AH, Morgan JW, Selleck MJ, Luca F, Raskin E, Reeves ME, Garberoglio CA, Lum SS, Senthil M. High-Risk Stage II Colon Cancer: Not All Risks Are Created Equal. *Ann Surg Oncol* 2018; **25**: 1980-1985 [PMID: 29675762 DOI: 10.1245/s10434-018-6484-8]

124 **Golia Pernicka JS**, Gagniere J, Chakraborty J, Yamashita R, Nardo L, Creasy JM, Petkovska I, Do RRK, Bates DDB, Paroder V, Gonen M, Weiser MR, Simpson AL, Gollub MJ. Radiomics-based prediction of microsatellite instability in colorectal cancer at initial computed tomography evaluation. *Abdom Radiol (NY)* 2019; **44**: 3755-3763 [PMID: 31250180 DOI: 10.1007/s00261-019-02117-w]

125 **Huang X**, Cheng Z, Huang Y, Liang C, He L, Ma Z, Chen X, Wu X, Li Y, Liu Z. CT-based Radiomics Signature to Discriminate High-grade From Low-grade Colorectal Adenocarcinoma. *Acad Radiol* 2018; **25**: 1285-1297 [PMID: 29503175 DOI: 10.1016/j.acra.2018.01.020]

126 **Altini C**, Maggialetti N, Branca A, Pisani AR, Rubini D, Sardaro A, Stabile Ianora AA, Rubini G. 18F-FDG PET/CT in peritoneal tumors: a pictorial review. *Clin Transl Imaging* 2023; **11**: 141-155

127 **Eresen A**, Li Y, Yang J, Shangguan J, Velichko Y, Yaghmai V, Benson AB 3rd, Zhang Z. Preoperative assessment of lymph node metastasis in Colon Cancer patients using machine learning: a pilot study. *Cancer Imaging* 2020; **20**: 30 [PMID: 32334635 DOI: 10.1186/s40644-020-00308-z]

128 **Caruso D**, Zerunian M, Ciolina M, de Santis D, Rengo M, Soomro MH, Giunta G, Conforto S, Schmid M, Neri E, Laghi A. Haralick's texture features for the prediction of response to therapy in colorectal cancer: a preliminary study. *Radiol Med* 2018; **123**: 161-167 [PMID: 29119525 DOI: 10.1007/s11547-017-0833-8]

129 **Coppola F**, Giannini V, Gabelloni M, Panic J, Defeudis A, Lo Monaco S, Cattabriga A, Cocozza MA, Pastore LV, Polici M, Caruso D, Laghi A, Regge D, Neri E, Golfieri R, Faggioni L. Radiomics and Magnetic Resonance Imaging of Rectal Cancer: From Engineering to Clinical Practice. *Diagnostics (Basel)* 2021; **11** [PMID: 33922483 DOI: 10.3390/diagnostics11050756]

130 **Alvarez-Jimenez C**, Antunes JT, Talasila N, Bera K, Brady JT, Gollamudi J, Marderstein E, Kalady MF, Purysko A, Willis JE, Stein S, Friedman K, Paspulati R, Delaney CP, Romero E, Madabhushi A, Viswanath SE. Radiomic Texture and Shape Descriptors of the Rectal Environment on Post-Chemoradiation T2-Weighted MRI are Associated with Pathologic Tumor Stage Regression in Rectal Cancers: A Retrospective, Multi-Institution Study. *Cancers (Basel)* 2020; **12** [PMID: 32722082 DOI: 10.3390/cancers12082027]

131 **Bordron A**, Rio E, Badic B, Miranda O, Pradier O, Hatt M, Visvikis D, Lucia F, Schick U, Bourbonne V. External Validation of a Radiomics Model for the Prediction of Complete Response to Neoadjuvant Chemoradiotherapy in Rectal Cancer. *Cancers (Basel)* 2022; **14** [PMID: 35205826 DOI: 10.3390/cancers14041079]

World Journal of Gastroenterology

Submit a Manuscript: https://www.f6publishing.com

World J Gastroenterol 2023 May 21; 29(19): 2905-2915

DOI: 10.3748/wjg.v29.i19.2905

ISSN 1007-9327 (print) ISSN 2219-2840 (online)

MINIREVIEWS

Branched chain amino acids in hepatic encephalopathy and sarcopenia in liver cirrhosis: Evidence and uncertainties

Giuseppe Marrone, Amato Serra, Luca Miele, Marco Biolato, Antonio Liguori, Antonio Grieco, Antonio Gasbarrini

Specialty type: Gastroenterology and hepatology

Provenance and peer review: Invited article; Externally peer reviewed.

Peer-review model: Single blind

Peer-review report's scientific quality classification

Grade A (Excellent): 0
Grade B (Very good): B, B
Grade C (Good): C
Grade D (Fair): 0
Grade E (Poor): 0

P-Reviewer: Fernandes SA, Brazil; Hong Xiang FK, Singapore; Long X, China

Received: December 28, 2022
Peer-review started: December 28, 2022
First decision: January 10, 2023
Revised: January 24, 2023
Accepted: April 20, 2023
Article in press: April 20, 2023
Published online: May 21, 2023

Giuseppe Marrone, Amato Serra, Luca Miele, Marco Biolato, Antonio Liguori, Antonio Grieco, Antonio Gasbarrini, Medical and Surgical Sciences, Fondazione Policlinico Universitario A. Gemelli-IRCCS, Università Cattolica del Sacro Cuore, Rome 00168, Italy

Corresponding author: Giuseppe Marrone, MD, PhD, Consultant Physician-Scientist, Medical and Surgical Sciences, Fondazione Policlinico Universitario A. Gemelli-IRCCS, Largo Agostino Gemelli 8, Rome 00168, Italy. giuseppe.marrone@policlinicogemelli.it

Abstract

Liver cirrhosis is commonly associated with nutritional alterations, reported in 20% of patients with compensated disease and over 60% of patients with decompensated cirrhosis. Nutritional disturbances are associated with a worse prognosis and increased risk of complication. Serum levels of branched-chain amino acids (BCAAs) are decreased in patients with liver cirrhosis. The imbalance of amino acids levels has been suggested to be associated with the development of complications, such as hepatic encephalopathy and sarcopenia, and to affect the clinical presentation and prognosis of these patients. Several studies investigated the efficacy of BCAAs supplementation as a therapeutic option in liver cirrhosis, but uncertainties remain about the real efficacy, the best route of administration, and dosage.

Key Words: Branched-chain amino acids; Hepatic encephalopathy; Sarcopenia; Liver cirrhosis

Core Tip: Nutritional perturbance is frequent in liver cirrhosis and has been correlated with the development of complications such as hepatic encephalopathy and sarcopenia. Branched-chain amino acids (BCAAs) have been implicated in the pathophysiology of these two complications and supplementation has been proposed as a therapeutic measure. In this review, we will examine the scientific evidence supporting the clinical use of BCAAs in cirrhotic subjects.

Citation: Marrone G, Serra A, Miele L, Biolato M, Liguori A, Grieco A, Gasbarrini A. Branched chain amino acids in hepatic encephalopathy and sarcopenia in liver cirrhosis: Evidence and uncertainties. *World J Gastroenterol* 2023; 29(19): 2905-2915
URL: https://www.wjgnet.com/1007-9327/full/v29/i19/2905.htm
DOI: https://dx.doi.org/10.3748/wjg.v29.i19.2905

INTRODUCTION

Liver cirrhosis is commonly associated with nutritional alterations, being reported in 20% of patients with compensated disease and over 60% of patients with decompensated cirrhosis[1]. In cirrhotic subjects, nutritional disturbances are associated with a worse prognosis and increased risk of complications such as hepatic encephalopathy (HE) and sarcopenia. On the other hand, serum levels of branched-chain amino acids (BCAAs) are decreased in patients with liver cirrhosis, and this has been associated with the development of complications[2]. Several studies investigated the efficacy of BCAAs supplementation in liver cirrhosis for the treatment and prevention of both HE and sarcopenia. The aim of this review is to analyze scientific evidence supporting the administration of BCAAs in patients with liver cirrhosis affected by HE and sarcopenia (Table 1).

HE

HE is one of the main complications of advanced cirrhosis. It consists of a wide spectrum of non-specific neurological or psychiatric abnormalities, ranging from subclinical alterations to coma, caused by liver failure and/or porto-systemic shunting. According to the West Haven classification HE is classified, as covert HE (CHE), including minimal HE (MHE) and grade 1 HE, and overt HE (OHE), including grade 2, grade 3, and grade 4 HE of the West Haven classification[3]. The prevalence of OHE in liver cirrhosis is 30%-40% at any time during the clinical course of the disease[4] while MHE or CHE occurs in 20%-80% of patients with cirrhosis[5]. HE is associated with a poor prognosis, and high socioeconomic costs and also carries a psychological burden on patients and families[6]. According to the American Association for the Study of Liver Diseases and the European Association for the Study of the Liver (EASL) Clinical Practice Guidelines, episodes of OHE should be actively treated[3]. The therapeutic approach encompasses the active treatment of precipitant factors (*e.g.*, infections, variceal bleeding), administration of non-absorbable disaccharides, such as lactulose, and non-absorbable antibiotics, such as rifaximin[7]. Secondary prophylaxis with oral rifaximin is recommended after an episode of OHE. In case of recurrent and intractable OHE associated with advanced liver disease, the patients should be evaluated for liver transplantation[3]. Other treatments such as metronidazole, neomycin, or intravenous administration of L-ornithine L-aspartate, have been proposed for the treatment of HE, but the evidence supporting their use is still limited or under debate[8]. According to EASL guidelines, despite their limited efficacy, the use of these medications is advocated as an additional treatment for patients -non-responsive to conventional therapies[3].

BCAAS AND HE

In recent years, growing interest in the role of BCAAs in liver cirrhosis has been observed in the scientific literature. A common feature in patients with liver cirrhosis is decreased BCAA plasmatic levels associated with the increase of aromatic amino acids (AAA), namely tyrosine and phenylalanine, thus leading to a low BCAA/AAA ratio, the so-called "Fisher ratio"[9]. This ratio is negatively correlated with the Child-Turcotte-Pugh score (CTP) and the severity of liver disease[10]. A low Fisher ratio is also associated with the development of HE and an excellent correlation has been found between this ratio and the grade of HE[11]. The role of BCAAs in the development of HE was first advocated in the "false neurotransmitters" hypothesis in the 80s[12]. Both AAA and BCAAs compete for the same transporter across blood-brain barrier. According to this hypothesis, the increased concentration of AAA in liver cirrhosis leads to an increased availability of aromatic neurotransmitters precursors, which cause a "false" dopaminergic transmission and inhibition of dopamine synthesis, resulting in neurodepression[13]. Other studies focused on the key role of increased ammonia levels in the development of HE, underling its neurotoxic role[14]. Despite this evidence, mechanisms involved in the pathogenesis of HE remain poorly understood.

The increase in blood ammonia is a consequence of impaired liver function and portosystemic shunts. Skeletal muscle is a key site of extrahepatic ammonia detoxification by the absorption of plasma ammonia and the conversion of α-ketoglutarate to glutamate, and then of glutamate to glutamine through glutamate dehydrogenase and glutamine synthetase enzymes, which remove two moles of

Table 1 Selected published studies on beneficial effects of branched chain amino acids in liver cirrhosis

Ref.	Study design	Participants	Intervention	Route	Treatment duration	Associated treatments	Outcomes	Results
Horst *et al* [16], 1984	Multicentric RCT	37 cirrhotic patients with OHE	BCAAs (20 g/d increased to 80 g/d) *vs* isonitrogenous diet (placebo)	Oral	4 wk	No	Mortality and hepatic enceph-alopathy assessed after 4 wk	HE recurrence (decreased). No differences in nitrogen balance
Muto *et al* [17], 2005	Multicentric RCT	646 patients with decompensated cirrhosis	BCAAs (12 g/d) *vs* standard diet (1.0-1.4 protein kg/d	Oral	2 yr	No	Mortality, development of liver cancer, rupture of esophageal varices, or progress of hepatic failure (event-free survival)	EFS (increased), health-related quality of life, mortality (decreased). No differences in improvement of HE
Les *et al*[18], 2011	Double-blind multicentric RCT	40 cirrhotic patients with previous episodes of minimal hepatic encephalopathy	BCAAs (30 g/d) *vs* isocaloric placebo (maltodextrin)	Oral	56 wk	No	Mortality and hepatic enceph-alopathy assessed after 56 wk	Improvement in MHE symptoms and muscle mass. No reduction of HE recurrence
Gluud *et al* [19], 2017	Meta-analysis of RCT	11 RCT; 14 RCT	BCAAs *vs* diets, antibiotics (neomycin) and non-absorbable disaccharides	Oral and IV	Variable	No	Effect on HE manifestations and prevention of HE episodes	Oral BCAAs improve HE manifestations and prevention of HE episodes. No effects for IV BCAA
Gluud *et al* [20], 2013	Systematic review with meta-analysis	8 RCT: 382 cirrhotic patients with recurrent MHE or OHE	BCAAs (0.25 g/kg body weight/day) *vs* no intervention/placebo/control supplements	Oral	Variable	No	Effect on HE manifestations, mortality, nutritionalstatus, and adverse events in patients with recurrent HE	Improvement in the recurrent HE manifestation (more evident in OHE than MHE). No differences in survival
Gluud *et al* [19], 2017	Cochrane systematic review	16 RCT: 827 cirrhotic patients with OHE or MHE	BCAAs *vs* placebo/no intervention/other (diet, lactulose, neomycicn)	Oral and IV	Variable	No	Beneficial or harmful effects of BCAA versus any control intervention in HE	Oral BCAAs improve HE manifestation (no effect *vs* lactulose or neomycicn). No effect on mortality
Park *et al* [21], 2017	Multicentric retrospective cohort study	307 cirrhotic patients with CTP 8-10	BCAAs (4.15 g/d or 8.3 g/d or 12.45 g/d) *vs* normal diet	Oral	24 wk	No	Changes in MELD score, CP score, incidence of cirrhosis-related complications and event-free survival over 2 yr	Improvement in MELD score, serum bilirubin and CTP score in 12.45/d BCAAs. No differences in HE manifestation
Tajiri *et al* [23], 2018	Retrospective observational study	53 cirrhotic patients with OHE	IV BCAAs and conventional therapies *vs* IV BCAAs and conventional therapies + IV L-carnitine	IV	Median 5 d (range 2-20 d)	L-carnitine conventional therapies (non-absorbable disaccharides and non-absorbable antibiotics)	Effect on HE manifestation, recurrence-free-survival and overall-survival	L-carnitine + BCAAS improve HE manifestation and reduce HE recurrence

BCAAs: Branched chain amino acids; RCT: Randomized control trial; OHE: Overt hepatic encephalopathy; HE: Hepatic encephalopathy; EFS: Early feeding skill; MELD: Model for end stage liver disease; CP: Child-pugh score; CTP: Child-Turcotte-Pugh score.

ammonia for each α-ketoglutarate molecule. Muscle uptake of plasma BCAAs increases with ammonia concentration in patients with liver cirrhosis, suggesting that BCAAs play an important role in ammonia detoxification in muscle and can contribute to preventing HE[13] (Figure 1).

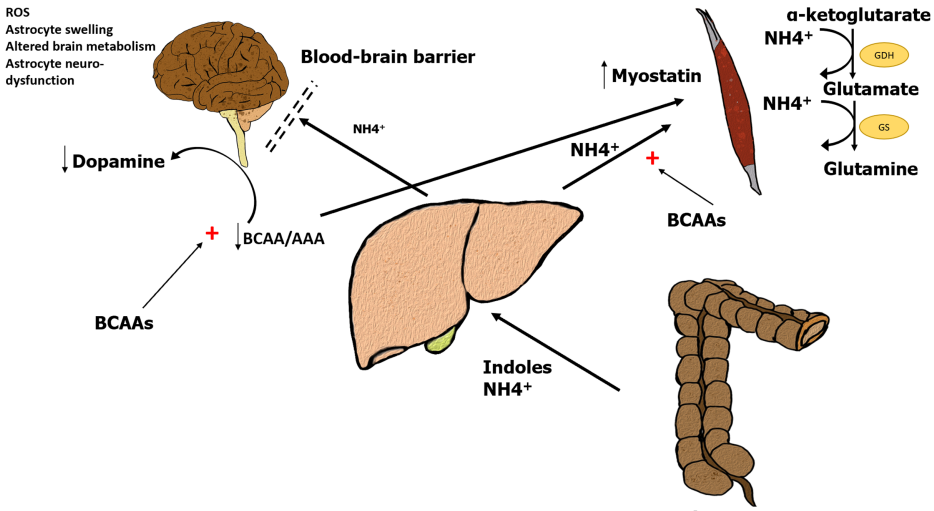

DOI: 10.3748/wjg.v29.i19.2905

Figure 1 Gut derived ammonia and other aromatic compounds pass into the systemic circulation due to reduced liver function and the presence of porto-systemic shunts. A low plasma branched chain amino acids (BCAA)/aromatic amino acids (AAA) ratio has been observed in liver cirrhosis. BCAA and AAA compete for the same transporter at blood-brain barrier. The increased availability of AAA causes an increase in aromatic neurotransmitter precursors resulting in a false dopaminergic transmission and a reduction in dopamine synthesis. At brain level, ammonia causes astrocyte metabolism changes including reactive oxygen species increase, altered glucose and protein metabolism and astrocyte swelling, resulting in altered neurotransmission. Muscle is a key site of ammonia detoxification by means of the sequential action of glutamate dehydrogenase and glutamine synthetase. Ammonia increases myostatin expression, thus resulting in reduced protein synthesis and inhibition of myogenesis. The administration of BCAAs can increase muscle ammonia uptake from blood and can interfere with amino acids pass throughout the blood brain barrier with beneficial effects on both hepatic encephalopathy and sarcopenia. BCAAs: Branched chain amino acids; AAA: Aromatic amino acids; NH4+: Ammonia; ROS: Reactive oxygen species; GDH: Glutamate dehydrogenase; GS: Glutamine synthetase.

EVIDENCE SUPPORTING THE THERAPEUTIC USE OF BCAAS IN HEPATIC ENCEPHALOPATHY

A possible therapeutic role of BCAAs supplementation in HE was first evaluated in animal models. In dogs with portocaval shunt, which developed HE, neurological manifestations induced by the simultaneous infusion of 1% tryptophan and 1% phenylalanine were prevented by the concomitant infusion of BCAAs (0.63% leucine + 0.4% isoleucine + 0.46% valine)[15]. Subsequently, several clinical studies evaluated the role of BCAAs in the treatment and prevention of HE in cirrhotic subjects. In the early 80s, a randomized study evaluated the effect of BCAAs in protein-intolerant cirrhotic. Enrolled subjects were fed with increasing amounts of either dietary protein or a BCAAs solution until they attained an intake of 80 g protein per day or until they developed stage 2 encephalopathy. Oral BCAAs supplements induced a positive nitrogen balance as an equivalent amount of dietary protein but decreased the risk of HE recurrence[16]. In 2005, a multicenter randomized controlled trial evaluated oral BCAAs (12 g/d for 2 years) compared with diet therapy with defined daily food intake (1.0-1.4 g protein kg/day) in patients with decompensated cirrhosis. The group who received BCCA showed an improvement in event-free survival and consequently, a reduction in mortality, but no statistically significant differences were found in HE[17]. Another randomized, double-blind, multicenter study evaluated subjects with cirrhosis with a previous episode of HE. The two groups of patients received a standard diet and a supplement of 30 g of BCAAs or maltodextrin over 56 wk. BCAAs supplementation was not associated with a reduction in HE recurrence but an improvement in MHE and muscle mass recovery were found in the BCAA-treated group[18]. A meta-analysis of randomized trials, performed by Gluud *et al*[19], confirmed that oral BCAAs administration has a beneficial effect on the clinical manifestation of HE, but no similar results were found for intravenous administration. Based on this evidence, the authors suggested using nonabsorbable disaccharides as the first-line treatment for HE, with a more beneficial effect through the addition of nonabsorbable antibiotics, while oral BCAAs may be considered as a second-line treatment. Another systematic review with meta-analysis evaluated the effects of oral BCAAs compared with placebo or control supplements in patients with HE. The administration of oral BCAAs was found to be associated with an improvement in HE recurrence {87 of 172 patients in the BCAAs group *vs* 56 of 210 in controls, risk ratio (RR) = 1.71 [95% confidence interval (CI): 1.17-2.51]}. The effect of oral BCAAs was higher in patients with OHE rather than in patients with MHE, but no difference in survival was found. These results strengthen the recommendation of oral BCAAs in patients who developed HE during enteral nutrition and in the case of recurrent HE. Most of the analyzed studies used the same dose of oral BCAAs (0.25 g/kg body weight/die) and no adverse events (including nausea and diarrhea) were reported[20]. A Cochrane systematic review, updated in 2017, evaluated the beneficial and harmful effects of BCAAs *vs* any control intervention for people with HE.

The study analyzed 16 randomized clinical trials, including 827 patients with OHE (12 trials) or MHE (4 trials). Control groups received placebo/no intervention in 2 trials, diets in 10 trials, lactulose in 2 trials, or neomycin in 2 trials. BCAAs were administrated orally in 8 trials and intravenous in 7 trials. No differences in mortality were found between BCAAs groups and control groups (RR = 0.88, 95%CI: 0.69-1.11). Reduced mortality was noted only when excluding trials in which control groups were treated with lactulose or neomycin (RR = 0.76, 95%CI: 0.63-0.92). The analysis also showed that BCAAs supplementation was associated with a beneficial effect on HE compared with controls (RR = 0.73, 95%CI: 0.61-0.88). Subgroup analyses showed that oral BCAAs but not intravenous BCAAs had a beneficial effect on overt encephalopathy. These differences were not found for MHE[21]. This systematic review supported the use of oral BCAAs in clinical practice but did not provide enough evidence to evaluate the benefit of BCAAs compared with other interventions. The most adequate dosage and duration of BCAAs supplementation is also a debated issue, since homeostasis of BCAAs in the body is extremely rapid, and circulating values quickly return to baseline after administration. A multicenter retrospective cohort study evaluated the effects of long-term BCAAs supplementation (at least 6 mo) compared with diet in patients with advanced liver disease (CTP 8-10) compared with no BCAAs enriched diet. Patients in the BCAAs group were divided into 3 subgroups according to the dose administrated: 4.15 g, 8.3 g, or 12.45 g/d. Statistical analysis revealed differences in the model for end-stage liver disease (MELD) score, serum albumin levels, and CTP score between the BCAAs group and control group at the baseline. Patients enrolled in the BCAAs group showed lower albumin levels and higher CTP scores, MELD scores, and HE grades (mostly grades 1-2). This was probably related to the propensity of physicians to prescribe BCAAs to patients with a worsened deterioration of hepatic function. Sub-group analysis showed a significant improvement in MELD score, serum bilirubin levels, and CTP score in patients who received the highest dose of BCAAs (12.45 g daily), whereas no significant differences were found in albumin levels. Conversely, only improvement in the serum bilirubin levels was observed in patients who received the lowest dose of BCAAs (4.15 g). This evidence provides a relationship between BCAAs dosage and its beneficial effect on prognostic scores in liver cirrhosis, suggesting high-dose BCAAs supplementation to achieve benefits. The study did not find significant differences in HE manifestations between the two groups. This was probably related to the shorter duration of BCAAs supplementation than in previous studies (about 30% of patients discontinued BCAAs within one year)[22].

A possible synergic role of L-carnitine and BCAAs on HE has been postulated. L-carnitine is a vitamin-like bio-factor that has been shown to induce ureagenesis, and improve energy metabolism leading to a reduction in blood and ammonia levels, thus protecting human astrocytes from ammonia-induced acute cytotoxicity[23]. A study on cirrhotic patients affected by OHE treated with intravenous BCAAs supplementation and conventional therapy (lactulose and non-absorbable antibiotics, showed that the addition of L-carnitine provided an improvement in blood ammonia concentration and Glasgow Coma Scale) with an improvement in HE recurrence. Despite the preliminary nature of the study, these results suggest a possible synergic role between L-carnitine and BCAAs in HE treatment [24].

SARCOPENIA IN LIVER CIRRHOSIS

Patients with chronic liver disease are at risk of malnutrition and sarcopenia[2]. The first definition of sarcopenia was proposed by Rosenberg[25], deriving from the Greek words "sarx" (muscle) and "penia" (reduction), to point out the decline in muscle mass and strength that occurs with healthy aging. The European Working Group on Sarcopenia in Older People in 2019 defined sarcopenia as a progressive and generalized skeletal muscle disorder that consists of decreased muscle quality or quantity and decreased physical function or muscle strength. Sarcopenia is distinguished as primary, or age-related in the absence of other evident specific cause, and secondary when the causal factor is a systemic, neoplastic, or inflammatory disease (*e.g.*, malignancy, inflammatory disease, or organ failure such as liver cirrhosis[26], affecting about 20%-60% of patients in the latter condition)[27]. In cirrhotic patients, the pathogenetic cascade is multifactorial: Since muscle mass is the result of protein anabolism and catabolism balance, reduced liver function, together with portosystemic shunts, causes decreased protein synthesis and ammonia detoxification, thus promoting sarcopenia and hyperammonemia. Hyperammonemia leads to increased muscle expression of the cytokine myostatin, a negative regulator of muscle growth by inhibition of myogenesis[28] (Figure 1). Other involved factors are BCAAs deficiency, which plays a key role in maintaining muscle mass and strength, and perturbation of sex hormone levels, with reduction of testosterone and concomitant increase in estrogen-to-androgen ratio. Hormonal changes suppress myoblast differentiation in skeletal muscle thus promoting sarcopenia[29]. Recently, changes in the intestinal microbiome (reduction of Methanobrevibacter, Prevotella e Akkermansia) and in the intestine-liver-muscle axis with increased bowel inflammation and bacterial translocation have been described in sarcopenic cirrhotic[30]. The role of gut microbiota is crucial for energy extraction from nutrients, in controlling low-grade systemic inflammation and bacterial infections, and has been involved in the genesis of HE, sarcopenia, and hepatocellular carcinoma (HCC) in liver cirrhosis[30-34].

BCAA IN THE TREATMENT OF SARCOPENIA

Despite growing interest in the clinical role of sarcopenia, few evidence-based therapeutic interventions are available to revert this condition in the context of liver cirrhosis. Current literature changed the old concept of protein restriction in patients with liver cirrhosis and daily recommended protein intake has been changed accordingly[35]. According to the European Society for Clinical Nutrition and Metabolism, high protein intake, variable from 1.2 g/kg/d protein in patients with compensated liver cirrhosis to 1.5 g/kg/d protein in patients with malnutrition and/or sarcopenia, is considered safe, well-tolerated, and recommended in liver cirrhosis. Another suggested dietary intervention is to shorten fasting periods by consuming three to five meals per day and taking a late evening snack. The aim of these suggestions is to reduce protein catabolism during overnight fasting and to reverse anabolic resistance and sarcopenia[1].

A nutritional interventional strategy aimed at increasing protein synthesis and preventing sarcopenia is BCAAs exogenous supplementation. BCAAs play a key role in protein synthesis and glucose metabolism. Leucine is involved in the activation of the intracellular mammalian target of rapamycin (mTOR) complex 1 pathway and inhibition of ubiquitin-proteasome signaling, thus resulting in increased protein synthesis, skeletal muscle hypertrophy, and reduced muscle turnover[36].

In experimental animal models of carbon tetrachloride-induced liver cirrhosis, muscle mass loss was described in association with decreased BCAAs and increased AAA plasma levels, while decreased α-ketoglutarate and ATP concentration in muscles was found[37]. A Japanese study evaluating cirrhotic subjects demonstrated a high prevalence of sarcopenia, low serum levels of BCAAs, and insulin-like growth factor 1. Patients with lower baseline levels of BCAAs had also a higher prevalence of CTP class B and C, lower albumin and zinc blood concentration, and lower body mass index (BMI), associated with risk of malnutrition, disease complication, and poor prognosis[38]. The presence of sarcopenia and low plasma levels of total BCAAs have also been associated with a significant reduction of survival in liver cirrhosis[39].

Several studies were performed to evaluate the effect of BCAAs administration to prevent sarcopenia and its complication in cirrhotic patients. In animal models, the administration of BCAAs reversed the metabolic alterations in skeletal muscles, promoting glucose uptake, which improves ATP production and muscle function[40,41]. In patients affected by alcoholic cirrhosis, skeletal muscle biopsy showed increased myostatin expression, dysfunctional mTOR pathway, and increased autophagic proteolysis when compared to well-matched healthy controls. These pathologic alterations were reversed after the administration of a single oral BCAAs mixture enriched with leucine. A monocentric prospective study on adult cirrhotics showed that oral BCAAs powder administration (13.5 g twice a day) for 24-wk was able to improve muscle strength with limited increase in muscle mass. It suggests that BCAAs supplementation alone could not be enough to achieve effective improvement of sarcopenia in cirrhotic patients and that aerobic and resistance exercise could also be necessary to induce protein synthesis response[42]. A prospective, randomized double-blind clinical trial in patients with liver cirrhosis and sarcopenia assessed by computed tomography (CT) scan, showed that BCAAs supplementation, in addition to a nutritional intervention and physical activity, could improve albumin levels and muscle mass. Administration of BCAAs also increased zinc levels after 12 wk of intervention[43]. Zinc is an essential nutrient for human health and its deficiency is often associated with malnutrition and chronic liver disease[44]. Improvement of hypoalbuminemia after BCAAs supplementation is correlated with improved glucose metabolism and a decrease in skeletal muscle fat infiltration, miming exercise training. In these patients, an improvement in liver-related event-free survival (including refractory pleural effusion, ascites, or both, varices rupture or treatment, and hepatocarcinogenesis) was observed and it might contribute to a better prognosis[45]. Today, in liver cirrhosis, an intervention program including physical exercise is considered useful to decelerate sarcopenia progression, but it can't completely prevent skeletal muscle atrophy[46]. The combination of BCAAs supplementation and walking exercise was found to be more effective than exercise alone in improving muscle mass and function and it should be considered a good therapeutic strategy in patients with overt sarcopenia and a prevention strategy in patients at risk of sarcopenia[47]. In a retrospective cohort study, patients with liver cirrhosis were classified into low, intermediate, and high-risk according to the presence of hypoalbuminemia and/or sarcopenia. The high-risk group, including patients with both sarcopenia ad hypoalbuminemia, had significantly lower overall survival than the low-risk group, including patients without both hypoalbuminemia and sarcopenia, regardless of HCC occurrence. The administration of BCAAs improved overall survival and prognosis in treated patients. The survival benefit of BCAAs supplementation was pronounced in the high and intermediate-risk groups[48]. Lastly, in cirrhotic patients, sarcopenia contributes to hyperammonemia due to the reduced capacity of sarcopenic muscle to detoxify circulating ammonia which increases the risk of HE. On the other hand, hyperammonemia through myostatin upregulation, mitochondrial dysfunction, and cellular stress response, induces further muscle depletion, generating a vicious circle. On these bases, nutritional interventions against sarcopenia, including BCAA supplementation, may have a beneficial effect also on HE[49,50].

β-HYDROXY-β-METHYLBUTYRATE SUPPLEMENTATION

A different strategy to counteract muscle mass loss, acting on BCAAs metabolism, is β-Hydroxy-β-methylbutyrate (HMB) supplementation. HMB is a natural derivative of the BCAA leucine, which has shown a positive effect on muscle mass and strength in malnourished subjects. Recently, the randomized, placebo-controlled, double-blind, parallel design strengthening health in the elderly through nutrition trial showed a significant improvement in weight, BMI, mid-arm circumference, and leg strength in elderly subjects receiving an HMB containing oral nutritional supplement along with dietary counseling over six months. Female treated subjects also showed a significant increase in handgrip strength and the whole population showed an improvement in nutritional parameters (including vitamin D levels, fat, protein, and carbohydrate intakes), but no significant difference was found in overall survival and hospital (re)admission rate[51].

A prospective non-randomized interventional cohort study evaluating the effectiveness of HMB supplements in the prehabilitation program of sarcopenic patients undergoing gastrointestinal surgery (HEROS trial, NCT05344313) is ongoing. The effect of HMB supplementation on muscle health and nutritional status has also been evaluated in liver cirrhosis. HMB supplementation in cirrhotic rats was able to increase plasma levels of BCAAs but showed detrimental effects on muscle and liver protein content and was associated with higher mortality and lower weight gain[52].

Despite some conflicting data in the experimental animal, recently, a small pilot randomized controlled clinical trial conducted in Italy demonstrated a significant improvement in muscle mass and performance in cirrhotic subjects receiving HMB supplements as well as dietary and lifestyle counseling. In the HMB-treated group a statistically significant improvement was found in muscle performance assessed through a six-minute walking test and chair stand test. HMB supplementation was also associated with a significant increase in muscle mass at the quadriceps level and with improvement in frailty (evaluated using liver frailty index[53])[54].

In a similar prospective randomized trial, HMB supplementation was evaluated in addition to standard BCAAs supplementation in two matched groups. Both HMB + BCAAs and BCAAs alone treatment have been associated with a significant longitudinal decrease in MELD score, an increase in BMI and fat mass but without significant changes in fat-free mass and handgrip strength. No significant differences were found between the two treated groups[55].

In both studies in cirrhotic subjects HMB supplements were well tolerated and no significant adverse events were reported. HMB supplementation represents an interesting therapeutic approach in the treatment of cirrhotic subjects with sarcopenia, but it is unclear whether it has additional positive effects compared to BCAAs supplementation. Adequately powered prospective studies are needed to assess efficacy, duration, and dose requirements.

THE ROLE OF ZINC IN HEPATIC ENCEPHALOPATHY AND SARCOPENIA

Another condition that can influence protein metabolism and nutritional status in cirrhosis, acting as a bridge between HE and sarcopenia, is zinc deficiency. Zinc is a trace element that is essential for the structure and function of various human proteins and enzymes[56]. Zinc deficiency has been described in cirrhotic subjects, resulting from multiple mechanisms including, among others, reduced dietary intake, reduced intestinal absorption, increased urinary excretion, reduced hepatic extraction, and hypoalbuminemia[57-60]. Ammonia metabolism in the liver requires urea cycle activity, which key enzyme, ornithine transcarbamylase, is a zinc enzyme. It has been reported that zinc supplementation in cirrhotic subjects results in an increase in urea cycle activity with an improvement, though not normalization, of the capacity for ammonia detoxification in the liver[61,62]. The reduction of ammonia detoxification in the liver, at least in part due to zinc deficiency, is associated with increased ammonia uptake in the muscle. In skeletal muscles, BCAAs serve as a glutamate source for glutamine-synthetase reaction to detoxify ammonia. It is therefore possible to link zinc deficiency with reduced plasma BCAAs levels in liver cirrhosis and with the above-described consequences of such condition on HE and sarcopenia [63]. Zinc deficiency has also been associated with taste alterations in elderly individuals and subjects with chronic diseases, including liver cirrhosis[64,65]. Taste alterations in cirrhosis go together with the reduction of appetite caused by abdominal distension due to ascites or osmotic laxatives and with reduced nutrient absorption due to portal hypertensive enteropathy and intestinal dysbiosis. All the described alterations contribute to the worsening of the nutritional status of patients with liver cirrhosis.

BCAAS AND LIVER FUNCTION

As reported above, some evidence exists regarding the effect of BCAA supplementation on overall liver function. Long-term BCAAs supplementation has been associated with improvement in MELD, CPT score, and bilirubin reduction in a retrospective Korean study, but no clear difference was reported in event-free survival[22]. A recent prospective study from the same research group confirmed the

improvement in prognostic scores in subjects receiving long-term BCAAs supplementation, but no differences in albumin and bilirubin levels were found. Interestingly, a significant increase in event-free survival, mainly regarding ascites and HE, was observed in the BCAAs-treated group, but no difference was noted regarding survival[66]. BCAAs supplementation has been investigated also in subjects undergoing treatment for HCC, showing some improvement in liver function after locoregional treatments. Three months of supplementation with a late evening snack enriched with a BCAAs mixture was associated with a rapid improvement in albumin and bilirubin levels and CPT score after radiofrequency ablation[67]. In subjects undergoing trans-arterial chemo-treatment for HCC, BCAAs supplementation was associated with an improvement in albumin but not in bilirubin values. Improved CPT score and survival were also observed in the BCAAs treated group but only in CPT class B patients[68].

CONCLUSION

Today it is widely accepted that low plasma levels of BCAAs levels play a key role in the development of cirrhosis complications such as sarcopenia and HE. The restoration of normal amino acid levels with BCAAs supplementation may improve the clinical course of HE and sarcopenia with few side effects. For these reasons, BCAAs administration should be considered in adult patients with advanced liver disease. BCAAs administration alone improves HE manifestation and reduces HE recurrence but has no significant improvement in mortality. Conversely, the use of BCAAs in addition to conventional therapies, such as non-absorbable disaccharides and non-absorbable antibiotics, shows benefits also in survival. In patients with sarcopenia, the administration of BCAAs improves muscle mass, muscle strength, and albumin levels with a consequent improvement in survival. All these beneficial effects are amplified when BCAAs are used in combination with physical exercise and nutritional intervention. These evidences supports the use of BCAAs supplements in clinical practice, especially in patients affected by concomitant HE and sarcopenia. BCAAs supplements should be used in combination with standard treatments. There is a need to identify patients at high risk of malnutrition and sarcopenia who could have an increased benefit from early nutritional intervention and BCAAs supplementation. According to the scientific literature, oral administration is more effective than intravenous administration and should be preferred. Early discontinuation of BCAAs administration is associated with reduced benefit so a long-term supplementation should be preferred. A minimum dose of 12 g/d of oral BCAAs is more effective than lower doses but further studies are needed to evaluate the most adequate dose and duration of BCAAs treatment.

FOOTNOTES

Author contributions: Marrone G and Serra A were responsible for the conception and writing of the paper; Miele L, Biolato M, and Liguori A reviewed the manuscript; Grieco A and Gasbarrini A performed final editing of the manuscript; and all the authors approved the final version of the manuscript.

Conflict-of-interest statement: All the authors report no relevant conflicts of interest for this article.

Country/Territory of origin: Italy

ORCID number: Giuseppe Marrone 0000-0002-9475-3948; Amato Serra 0000-0002-0191-6016; Luca Miele 0000-0003-3464-0068; Marco Biolato 0000-0002-5172-8208; Antonio Liguori 0000-0002-0801-7152; Antonio Grieco 0000-0002-0544-8993; Antonio Gasbarrini 0000-0003-4863-6924.

S-Editor: Wang JJ
L-Editor: A
P-Editor: Cai YX

REFERENCES

1 **Bischoff SC**, Bernal W, Dasarathy S, Merli M, Plank LD, Schütz T, Plauth M. ESPEN practical guideline: Clinical nutrition in liver disease. *Clin Nutr* 2020; **39**: 3533-3562 [PMID: 33213977 DOI: 10.1016/j.clnu.2020.09.001]

2 **Dasarathy S**, Merli M. Sarcopenia from mechanism to diagnosis and treatment in liver disease. *J Hepatol* 2016; **65**: 1232-

1244 [PMID: 27515775 DOI: 10.1016/j.jhep.2016.07.040]

3 **Vilstrup H**, Amodio P, Bajaj J, Cordoba J, Ferenci P, Mullen KD, Weissenborn K, Wong P. Hepatic encephalopathy in chronic liver disease: 2014 Practice Guideline by the American Association for the Study of Liver Diseases and the European Association for the Study of the Liver. *Hepatology* 2014; **60**: 715-735 [PMID: 25042402 DOI: 10.1002/hep.27210]

4 **Amodio P**, Del Piccolo F, Pettenò E, Mapelli D, Angeli P, Iemmolo R, Muraca M, Musto C, Gerunda G, Rizzo C, Merkel C, Gatta A. Prevalence and prognostic value of quantified electroencephalogram (EEG) alterations in cirrhotic patients. *J Hepatol* 2001; **35**: 37-45 [PMID: 11495040 DOI: 10.1016/S0168-8278(01)00129-5]

5 **Groeneweg M**, Moerland W, Quero JC, Hop WC, Krabbe PF, Schalm SW. Screening of subclinical hepatic encephalopathy. *J Hepatol* 2000; **32**: 748-753 [PMID: 10845661 DOI: 10.1016/S0168-8278(00)80243-3]

6 **Montagnese S**, Bajaj JS. Impact of Hepatic Encephalopathy in Cirrhosis on Quality-of-Life Issues. *Drugs* 2019; **79**: 11-16 [PMID: 30706419 DOI: 10.1007/s40265-018-1019-y]

7 **Bass NM**, Mullen KD, Sanyal A, Poordad F, Neff G, Leevy CB, Sigal S, Sheikh MY, Beavers K, Frederick T, Teperman L, Hillebrand D, Huang S, Merchant K, Shaw A, Bortey E, Forbes WP. Rifaximin treatment in hepatic encephalopathy. *N Engl J Med* 2010; **362**: 1071-1081 [PMID: 20335583 DOI: 10.1056/NEJMoa0907893]

8 **Rothenberg ME**, Keeffe EB. Antibiotics in the management of hepatic encephalopathy: an evidence-based review. *Rev Gastroenterol Disord* 2005; **5** Suppl 3: 26-35 [PMID: 17713457]

9 **Fischer JE**, Baldessarini RJ. False neurotransmitters and hepatic failure. *Lancet* 1971; **2**: 75-80 [PMID: 4103986 DOI: 10.1016/S0140-6736(71)92048-4]

10 **Dam G**, Sørensen M, Buhl M, Sandahl TD, Møller N, Ott P, Vilstrup H. Muscle metabolism and whole blood amino acid profile in patients with liver disease. *Scand J Clin Lab Invest* 2015; **75**: 674-680 [PMID: 26243157]

11 **Fischer JE**, Rosen HM, Ebeid AM, James JH, Keane JM, Soeters PB. The effect of normalization of plasma amino acids on hepatic encephalopathy in man. *Surgery* 1976; **80**: 77-91 [PMID: 818729]

12 **James JH**. Branched chain amino acids in heptatic encephalopathy. *Am J Surg* 2002; **183**: 424-429 [PMID: 11975931 DOI: 10.1016/S0002-9610(02)00808-5]

13 **Dam G**, Aamann L, Vistrup H, Gluud LL. The role of Branched Chain Amino Acids in the treatment of hepatic Encephalopathy. *J Clin Exp Hepatol* 2018; **8**: 448-451 [PMID: 30568347 DOI: 10.1016/j.jceh.2018.06.004]

14 **Norenberg MD**, Rama Rao KV, Jayakumar AR. Signaling factors in the mechanism of ammonia neurotoxicity. *Metab Brain Dis* 2009; **24**: 103-117 [PMID: 19104923 DOI: 10.1007/s11011-008-9113-6]

15 **Rossi-Fanelli F**, Freund H, Krause R, Smith AR, James JH, Castorina-Ziparo S, Fischer JE. Induction of coma in normal dogs by the infusion of aromatic amino acids and its prevention by the addition of branched-chain amino acids. *Gastroenterology* 1982; **83**: 664-671 [PMID: 7095369 DOI: 10.1016/S0016-5085(82)80204-7]

16 **Horst D**, Grace ND, Conn HO, Schiff E, Schenker S, Viteri A, Law D, Atterbury CE. Comparison of dietary protein with an oral, branched chain-enriched amino acid supplement in chronic portal-systemic encephalopathy: a randomized controlled trial. *Hepatology* 1984; **4**: 279-287 [PMID: 6706302 DOI: 10.1002/hep.1840040218]

17 **Muto Y**, Sato S, Watanabe A, Moriwaki H, Suzuki K, Kato A, Kato M, Nakamura T, Higuchi K, Nishiguchi S, Kumada H; Long-Term Survival Study Group. Effects of oral branched-chain amino acid granules on event-free survival in patients with liver cirrhosis. *Clin Gastroenterol Hepatol* 2005; **3**: 705-713 [PMID: 16206505 DOI: 10.1016/S1542-3565(05)00017-0]

18 **Les I**, Doval E, García-Martínez R, Planas M, Cárdenas G, Gómez P, Flavià M, Jacas C, Mínguez B, Vergara M, Soriano G, Vila C, Esteban R, Córdoba J. Effects of branched-chain amino acids supplementation in patients with cirrhosis and a previous episode of hepatic encephalopathy: a randomized study. *Am J Gastroenterol* 2011; **106**: 1081-1088 [PMID: 21326220 DOI: 10.1038/ajg.2011.9]

19 **Gluud LL**, Dam G, Borre M, Les I, Cordoba J, Marchesini G, Aagaard NK, Vilstrup H. Lactulose, rifaximin or branched chain amino acids for hepatic encephalopathy: what is the evidence? *Metab Brain Dis* 2013; **28**: 221-225 [PMID: 23275147 DOI: 10.1007/s11011-012-9372-0]

20 **Gluud LL**, Dam G, Borre M, Les I, Cordoba J, Marchesini G, Aagaard NK, Risum N, Vilstrup H. Oral branched-chain amino acids have a beneficial effect on manifestations of hepatic encephalopathy in a systematic review with meta-analyses of randomized controlled trials. *J Nutr* 2013; **143**: 1263-1268 [PMID: 23739310 DOI: 10.3945/jn.113.174375]

21 **Gluud LL**, Dam G, Les I, Marchesini G, Borre M, Aagaard NK, Vilstrup H. Branched-chain amino acids for people with hepatic encephalopathy. *Cochrane Database Syst Rev* 2017; **5**: CD001939 [PMID: 28518283 DOI: 10.1002/14651858.CD001939.pub4]

22 **Park JG**, Tak WY, Park SY, Kweon YO, Jang SY, Lee YR, Bae SH, Jang JY, Kim DY, Lee JS, Suk KT, Kim IH, Lee HJ, Chung WJ, Jang BK, Suh JI, Heo J, Lee WK. Effects of branched-chain amino acids (BCAAs) on the progression of advanced liver disease: A Korean nationwide, multicenter, retrospective, observational, cohort study. *Medicine (Baltimore)* 2017; **96**: e6580 [PMID: 28614215 DOI: 10.1097/MD.0000000000006580]

23 **Wang T**, Suzuki K, Kakisaka K, Onodera M, Sawara K, Takikawa Y. L-carnitine prevents ammonia-induced cytotoxicity and disturbances in intracellular amino acid levels in human astrocytes. *J Gastroenterol Hepatol* 2019; **34**: 1249-1255 [PMID: 30278111 DOI: 10.1111/jgh.14497]

24 **Tajiri K**, Futsukaichi Y, Kobayashi S, Yasumura S, Takahara T, Minemura M, Sugiyama T. L-Carnitine for the Treatment of Overt Hepatic Encephalopathy in Patients with Advanced Liver Cirrhosis. *J Nutr Sci Vitaminol (Tokyo)* 2018; **64**: 321-328 [PMID: 30381621 DOI: 10.3177/jnsv.64.321]

25 **Rosenberg IH**. Summary comments. *Am J Clin Nutr* 1989; **50**: 1231-1233 [DOI: 10.1093/ajcn/50.5.1231]

26 **Cruz-Jentoft AJ**, Bahat G, Bauer J, Boirie Y, Bruyère O, Cederholm T, Cooper C, Landi F, Rolland Y, Sayer AA, Schneider SM, Sieber CC, Topinkova E, Vandewoude M, Visser M, Zamboni M; Writing Group for the European Working Group on Sarcopenia in Older People 2 (EWGSOP2), and the Extended Group for EWGSOP2. Sarcopenia: revised European consensus on definition and diagnosis. *Age Ageing* 2019; **48**: 16-31 [PMID: 30312372 DOI: 10.1093/ageing/afy169]

27 **Meza-Junco J**, Montano-Loza AJ, Baracos VE, Prado CM, Bain VG, Beaumont C, Esfandiari N, Lieffers JR, Sawyer

MB. Sarcopenia as a prognostic index of nutritional status in concurrent cirrhosis and hepatocellular carcinoma. *J Clin Gastroenterol* 2013; **47**: 861-870 [PMID: 23751844 DOI: 10.1097/MCG.0b013e318293a825]

28 **Kumar A**, Davuluri G, Silva RNE, Engelen MPKJ, Ten Have GAM, Prayson R, Deutz NEP, Dasarathy S. Ammonia lowering reverses sarcopenia of cirrhosis by restoring skeletal muscle proteostasis. *Hepatology* 2017; **65**: 2045-2058 [PMID: 28195332 DOI: 10.1002/hep.29107]

29 **Kamimura H**, Sato T, Natsui K, Kobayashi T, Yoshida T, Kamimura K, Tsuchiya A, Murayama T, Yokoyama J, Kawai H, Takamura M, Terai S. Molecular Mechanisms and Treatment of Sarcopenia in Liver Disease: A Review of Current Knowledge. *Int J Mol Sci* 2021; **22** [PMID: 33572604 DOI: 10.3390/ijms22031425]

30 **Ponziani FR**, Picca A, Marzetti E, Calvani R, Conta G, Del Chierico F, Capuani G, Faccia M, Fianchi F, Funaro B, Josè Coelho-Junior H, Petito V, Rinninella E, Paroni Sterbini F, Reddel S, Vernocchi P, Cristina Mele M, Miccheli A, Putignani L, Sanguinetti M, Pompili M, Gasbarrini A; GuLiver study group. Characterization of the gut-liver-muscle axis in cirrhotic patients with sarcopenia. *Liver Int* 2021; **41**: 1320-1334 [PMID: 33713524 DOI: 10.1111/liv.14876]

31 **Patel VC**, Lee S, McPhail MJW, Da Silva K, Guilly S, Zamalloa A, Witherden E, Støy S, Manakkat Vijay GK, Pons N, Galleron N, Huang X, Gencer S, Coen M, Tranah TH, Wendon JA, Bruce KD, Le Chatelier E, Ehrlich SD, Edwards LA, Shoaie S, Shawcross DL. Rifaximin-α reduces gut-derived inflammation and mucin degradation in cirrhosis and encephalopathy: RIFSYS randomised controlled trial. *J Hepatol* 2022; **76**: 332-342 [PMID: 34571050 DOI: 10.1016/j.jhep.2021.09.010]

32 **Ponziani FR**, Bhoori S, Castelli C, Putignani L, Rivoltini L, Del Chierico F, Sanguinetti M, Morelli D, Paroni Sterbini F, Petito V, Reddel S, Calvani R, Camisaschi C, Picca A, Tuccitto A, Gasbarrini A, Pompili M, Mazzaferro V. Hepatocellular Carcinoma Is Associated With Gut Microbiota Profile and Inflammation in Nonalcoholic Fatty Liver Disease. *Hepatology* 2019; **69**: 107-120 [PMID: 29665135 DOI: 10.1002/hep.30036]

33 **Schneider KM**, Mohs A, Gui W, Galvez EJC, Candels LS, Hoenicke L, Muthukumarasamy U, Holland CH, Elfers C, Kilic K, Schneider CV, Schierwagen R, Strnad P, Wirtz TH, Marschall HU, Latz E, Lelouvier B, Saez-Rodriguez J, de Vos W, Strowig T, Trebicka J, Trautwein C. Imbalanced gut microbiota fuels hepatocellular carcinoma development by shaping the hepatic inflammatory microenvironment. *Nat Commun* 2022; **13**: 3964 [PMID: 35803930 DOI: 10.1038/s41467-022-31312-5]

34 **Gómez-Hurtado I**, Santacruz A, Peiró G, Zapater P, Gutiérrez A, Pérez-Mateo M, Sanz Y, Francés R. Gut microbiota dysbiosis is associated with inflammation and bacterial translocation in mice with CCl4-induced fibrosis. *PLoS One* 2011; **6**: e23037 [PMID: 21829583 DOI: 10.1371/journal.pone.0023037]

35 **European Association for the Study of the Liver**. European Association for the Study of the Liver. EASL Clinical Practice Guidelines on the management of hepatic encephalopathy. *J Hepatol* 2022; **77**: 807-824 [PMID: 35724930 DOI: 10.1016/j.jhep.2022.06.001]

36 **Hey P**, Gow P, Testro AG, Apostolov R, Chapman B, Sinclair M. Nutraceuticals for the treatment of sarcopenia in chronic liver disease. *Clin Nutr ESPEN* 2021; **41**: 13-22 [PMID: 33487256 DOI: 10.1016/j.clnesp.2020.11.015]

37 **Holeček M**, Vodeničarovová M. Muscle wasting and branched-chain amino acid, alpha-ketoglutarate, and ATP depletion in a rat model of liver cirrhosis. *Int J Exp Pathol* 2018; **99**: 274-281 [PMID: 30637824 DOI: 10.1111/iep.12299]

38 **Saeki C**, Kanai T, Nakano M, Oikawa T, Torisu Y, Saruta M, Tsubota A. Low Serum Branched-Chain Amino Acid and Insulin-Like Growth Factor-1 Levels Are Associated with Sarcopenia and Slow Gait Speed in Patients with Liver Cirrhosis. *J Clin Med* 2020; **9** [PMID: 33050430 DOI: 10.3390/jcm9103239]

39 **Sano A**, Tsuge S, Kakazu E, Iwata T, Ninomiya M, Tsuruoka M, Inoue J, Masamune A. Plasma free amino acids are associated with sarcopenia in the course of hepatocellular carcinoma recurrence. *Nutrition* 2021; **84**: 111007 [PMID: 33745507 DOI: 10.1016/j.nut.2020.111007]

40 **Nishitani S**, Takehana K, Fujitani S, Sonaka I. Branched-chain amino acids improve glucose metabolism in rats with liver cirrhosis. *Am J Physiol Gastrointest Liver Physiol* 2005; **288**: G1292-G1300 [PMID: 15591158 DOI: 10.1152/ajpgi.00510.2003]

41 **Tsien C**, Davuluri G, Singh D, Allawy A, Ten Have GA, Thapaliya S, Schulze JM, Barnes D, McCullough AJ, Engelen MP, Deutz NE, Dasarathy S. Metabolic and molecular responses to leucine-enriched branched chain amino acid supplementation in the skeletal muscle of alcoholic cirrhosis. *Hepatology* 2015; **61**: 2018-2029 [PMID: 25613922 DOI: 10.1002/hep.27717]

42 **Uojima H**, Sakurai S, Hidaka H, Kinbara T, Sung JH, Ichita C, Tokoro S, Masuda S, Sasaki A, Koizumi K, Egashira H, Kako M, Kobayashi S. Effect of branched-chain amino acid supplements on muscle strength and muscle mass in patients with liver cirrhosis. *Eur J Gastroenterol Hepatol* 2017; **29**: 1402-1407 [PMID: 28984678 DOI: 10.1097/MEG.0000000000000968]

43 **Hernández-Conde M**, Llop E, Gómez-Pimpollo L, Fernández Carrillo C, Rodríguez L, Van Den Brule E, Perelló C, López-Gómez M, Abad J, Martínez-Porras JL, Fernández-Puga N, Ferre C, Trapero M, Fraga E, Calleja JL. Adding Branched-Chain Amino Acids to an Enhanced Standard-of-Care Treatment Improves Muscle Mass of Cirrhotic Patients With Sarcopenia: A Placebo-Controlled Trial. *Am J Gastroenterol* 2021; **116**: 2241-2249 [PMID: 34074812 DOI: 10.14309/ajg.0000000000001301]

44 **Barbara M**, Mindikoglu AL. The role of zinc in the prevention and treatment of nonalcoholic fatty liver disease. *Metabol Open* 2021; **11**: 100105 [PMID: 34337376 DOI: 10.1016/j.metop.2021.100105]

45 **Kitajima Y**, Takahashi H, Akiyama T, Murayama K, Iwane S, Kuwashiro T, Tanaka K, Kawazoe S, Ono N, Eguchi T, Anzai K, Eguchi Y. Supplementation with branched-chain amino acids ameliorates hypoalbuminemia, prevents sarcopenia, and reduces fat accumulation in the skeletal muscles of patients with liver cirrhosis. *J Gastroenterol* 2018; **53**: 427-437 [PMID: 28741271 DOI: 10.1007/s00535-017-1370-x]

46 **Koya S**, Kawaguchi T, Hashida R, Goto E, Matsuse H, Saito H, Hirota K, Taira R, Matsushita Y, Imanaga M, Nagamatsu A, Shirono T, Shimose S, Iwamoto H, Niizeki T, Kuromatsu R, Miura H, Shiba N, Torimura T. Effects of in-hospital exercise on liver function, physical ability, and muscle mass during treatment of hepatoma in patients with chronic liver disease. *Hepatol Res* 2017; **47**: E22-E34 [PMID: 27062043 DOI: 10.1111/hepr.12718]

47 **Hiraoka A**, Michitaka K, Kiguchi D, Izumoto H, Ueki H, Kaneto M, Kitahata S, Aibiki T, Okudaira T, Tomida H,

Miyamoto Y, Yamago H, Suga Y, Iwasaki R, Mori K, Miyata H, Tsubouchi E, Kishida M, Ninomiya T, Kohgami S, Hirooka M, Tokumoto Y, Abe M, Matsuura B, Hiasa Y. Efficacy of branched-chain amino acid supplementation and walking exercise for preventing sarcopenia in patients with liver cirrhosis. *Eur J Gastroenterol Hepatol* 2017; **29**: 1416-1423 [PMID: 29016470 DOI: 10.1097/MEG.0000000000000986]

48 **Hanai T**, Nishimura K, Miwa T, Maeda T, Ogiso Y, Imai K, Suetsugu A, Takai K, Shimizu M. Usefulness of nutritional therapy recommended in the Japanese Society of Gastroenterology/Japan Society of Hepatology evidence-based clinical practice guidelines for liver cirrhosis 2020. *J Gastroenterol* 2021; **56**: 928-937 [PMID: 34533633 DOI: 10.1007/s00535-021-01821-z]

49 **Iqbal U**, Jadeja RN, Khara HS, Khurana S. A Comprehensive Review Evaluating the Impact of Protein Source (Vegetarian vs. Meat Based) in Hepatic Encephalopathy. *Nutrients* 2021; **13** [PMID: 33530344 DOI: 10.3390/nu13020370]

50 **Lattanzi B**, D'Ambrosio D, Merli M. Hepatic Encephalopathy and Sarcopenia: Two Faces of the Same Metabolic Alteration. *J Clin Exp Hepatol* 2019; **9**: 125-130 [PMID: 30765945 DOI: 10.1016/j.jceh.2018.04.007]

51 **Chew STH**, Tan NC, Cheong M, Oliver J, Baggs G, Choe Y, How CH, Chow WL, Tan CYL, Kwan SC, Husain FS, Low YL, Huynh DTT, Tey SL. Impact of specialized oral nutritional supplement on clinical, nutritional, and functional outcomes: A randomized, placebo-controlled trial in community-dwelling older adults at risk of malnutrition. *Clin Nutr* 2021; **40**: 1879-1892 [PMID: 33268143 DOI: 10.1016/j.clnu.2020.10.015]

52 **Holeček M**, Vodeničarovová M. Effects of beta-hydroxy-beta-methylbutyrate supplementation on skeletal muscle in healthy and cirrhotic rats. *Int J Exp Pathol* 2019; **100**: 175-183 [PMID: 31321841 DOI: 10.1111/iep.12322]

53 **Lai JC**, Covinsky KE, Dodge JL, Boscardin WJ, Segev DL, Roberts JP, Feng S. Development of a novel frailty index to predict mortality in patients with end-stage liver disease. *Hepatology* 2017; **66**: 564-574 [PMID: 28422306 DOI: 10.1002/hep.29219]

54 **Lattanzi B**, Bruni A, Di Cola S, Molfino A, De Santis A, Muscaritoli M, Merli M. The Effects of 12-Week Beta-Hydroxy-Beta-Methylbutyrate Supplementation in Patients with Liver Cirrhosis: Results from a Randomized Controlled Single-Blind Pilot Study. *Nutrients* 2021; **13** [PMID: 34371806 DOI: 10.3390/nu13072296]

55 **Espina S**, Sanz-Paris A, Gonzalez-Irazabal Y, Pérez-Matute P, Andrade F, Garcia-Rodriguez B, Carpéné C, Zakaroff A, Bernal-Monterde V, Fuentes-Olmo J, Arbones-Mainar JM. Randomized Clinical Trial: Effects of β-Hydroxy-β-Methylbutyrate (HMB)-Enriched vs. HMB-Free Oral Nutritional Supplementation in Malnourished Cirrhotic Patients. *Nutrients* 2022; **14** [PMID: 35684144 DOI: 10.3390/nu14112344]

56 **Leoni G**, Rosato A, Perozzi G, Murgia C. Zinc proteome interaction network as a model to identify nutrient-affected pathways in human pathologies. *Genes Nutr* 2014; **9**: 436 [PMID: 25367142 DOI: 10.1007/s12263-014-0436-0]

57 **Katayama K**. Zinc and protein metabolism in chronic liver diseases. *Nutr Res* 2020; **74**: 1-9 [PMID: 31891865 DOI: 10.1016/j.nutres.2019.11.009]

58 **Katayama K**, Kawaguchi T, Shiraishi K, Ito T, Suzuki K, Koreeda C, Ohtake T, Iwasa M, Tokumoto Y, Endo R, Kawamura N, Shiraki M, Hanai T, Habu D, Tsuruta S, Sakai H, Miwa Y, Kawada N, Kato A, Takei Y, Mine T, Kohgo Y, Seki T, Sata M, Ito Y, Fukui K, Nishiguchi S, Moriwaki H. The Prevalence and Implication of Zinc Deficiency in Patients With Chronic Liver Disease. *J Clin Med Res* 2018; **10**: 437-444 [PMID: 29581807 DOI: 10.14740/jocmr3374w]

59 **Cousins RJ**. Gastrointestinal factors influencing zinc absorption and homeostasis. *Int J Vitam Nutr Res* 2010; **80**: 243-248 [PMID: 21462106 DOI: 10.1024/0300-9831/a000030]

60 **Chiba M**, Katayama K, Takeda R, Morita R, Iwahashi K, Onishi Y, Kita H, Nishio A, Kanno T, Saito T, Maeda K, Naito M, Michida T, Ito T. Diuretics aggravate zinc deficiency in patients with liver cirrhosis by increasing zinc excretion in urine. *Hepatol Res* 2013; **43**: 365-373 [PMID: 22994500 DOI: 10.1111/j.1872-034X.2012.01093.x]

61 **Riggio O**, Merli M, Capocaccia L, Caschera M, Zullo A, Pinto G, Gaudio E, Franchitto A, Spagnoli R, D'Aquilino E. Zinc supplementation reduces blood ammonia and increases liver ornithine transcarbamylase activity in experimental cirrhosis. *Hepatology* 1992; **16**: 785-789 [PMID: 1505922 DOI: 10.1002/hep.1840160326]

62 **Katayama K**, Saito M, Kawaguchi T, Endo R, Sawara K, Nishiguchi S, Kato A, Kohgo H, Suzuki K, Sakaida I, Ueno Y, Habu D, Ito T, Moriwaki H. Effect of zinc on liver cirrhosis with hyperammonemia: a preliminary randomized, placebo-controlled double-blind trial. *Nutrition* 2014; **30**: 1409-1414 [PMID: 25280421 DOI: 10.1016/j.nut.2014.04.018]

63 **Holecek M**. Ammonia and amino acid profiles in liver cirrhosis: effects of variables leading to hepatic encephalopathy. *Nutrition* 2015; **31**: 14-20 [PMID: 25220875 DOI: 10.1016/j.nut.2014.03.016]

64 **Grüngreiff K**, Reinhold D, Wedemeyer H. The role of zinc in liver cirrhosis. *Ann Hepatol* 2016; **15**: 7-16 [PMID: 26626635 DOI: 10.5604/16652681.1184191]

65 **Stewart-Knox BJ**, Simpson EE, Parr H, Rae G, Polito A, Intorre F, Meunier N, Andriollo-Sanchez M, O'Connor JM, Coudray C, Strain JJ. Zinc status and taste acuity in older Europeans: the ZENITH study. *Eur J Clin Nutr* 2005; **59** Suppl 2: S31-S36 [PMID: 16254578 DOI: 10.1038/sj.ejcn.1602295]

66 **Park JG**, Tak WY, Park SY, Kweon YO, Chung WJ, Jang BK, Bae SH, Lee HJ, Jang JY, Suk KT, Oh MJ, Heo J, Woo HY, Jang SY, Lee YR, Lee JS, Kim DY, Kim SH, Suh JI, Kim IH, Kang MK, Lee WK. Effects of Branched-Chain Amino Acid (BCAA) Supplementation on the Progression of Advanced Liver Disease: A Korean Nationwide, Multicenter, Prospective, Observational, Cohort Study. *Nutrients* 2020; **12** [PMID: 32429077 DOI: 10.3390/nu12051429]

67 **Morihara D**, Iwata K, Hanano T, Kunimoto H, Kuno S, Fukunaga A, Yotsumoto K, Takata K, Tanaka T, Sakurai K, Iwashita H, Ueda S, Hirano G, Yokoyama K, Nakane H, Nishizawa S, Yoshikane M, Anan A, Takeyama Y, Kakumitsu S, Kitamura Y, Sakamoto M, Irie M, Shakado S, Sohda T, Watanabe H, Sakisaka S. Late-evening snack with branched-chain amino acids improves liver function after radiofrequency ablation for hepatocellular carcinoma. *Hepatol Res* 2012; **42**: 658-667 [PMID: 22380706 DOI: 10.1111/j.1872-034X.2012.00969.x]

68 **Kanekawa T**, Nagai H, Kanayama M, Sumino Y. Importance of branched-chain amino acids in patients with liver cirrhosis and advanced hepatocellular carcinoma receiving hepatic arterial infusion chemotherapy. *Cancer Chemother Pharmacol* 2014; **74**: 899-909 [PMID: 25138286 DOI: 10.1007/s00280-014-2564-z]

World Journal of Gastroenterology

Submit a Manuscript: https://www.f6publishing.com

World J Gastroenterol 2023 May 21; 29(19): 2916-2931

DOI: 10.3748/wjg.v29.i19.2916

ISSN 1007-9327 (print) ISSN 2219-2840 (online)

MINIREVIEWS

Assessment of delayed bleeding after endoscopic submucosal dissection of early-stage gastrointestinal tumors in patients receiving direct oral anticoagulants

Mitsushige Sugimoto, Masaki Murata, Takashi Kawai

Specialty type: Gastroenterology and hepatology

Provenance and peer review: Invited article; Externally peer reviewed.

Peer-review model: Single blind

Peer-review report's scientific quality classification

Grade A (Excellent): A
Grade B (Very good): B
Grade C (Good): 0
Grade D (Fair): 0
Grade E (Poor): 0

P-Reviewer: Gu ZC, China; Tharavej C, Thailand

Received: January 24, 2023
Peer-review started: January 24, 2023
First decision: March 21, 2023
Revised: April 3, 2023
Accepted: April 24, 2023
Article in press: April 24, 2023
Published online: May 21, 2023

Mitsushige Sugimoto, Takashi Kawai, Department of Gastroenterological Endoscopy, Tokyo Medical University Hospital, Tokyo 160-0023, Japan

Masaki Murata, Department of Gastroenterology, National Hospital Organization Kyoto Medical Center, Kyoto 612-8555, Japan

Corresponding author: Mitsushige Sugimoto, AGAF, MD, PhD, Professor, Department of Gastroenterological Endoscopy, Tokyo Medical University Hospital, 6-7-1, Nishishinjuku, Shinjuku-ku, Tokyo 160-0023, Japan. sugimo@tokyo-med.ac.jp

Abstract

Delayed bleeding is a major and serious adverse event of endoscopic submucosal dissection (ESD) for early-stage gastrointestinal tumors. The rate of post-ESD bleeding for gastric cancer is higher (around 5%-8%) than that for esophagus, duodenum and colon cancer (around 2%-4%). Although investigations into the risk factors for post-ESD bleeding have identified several procedure-, lesion-, physician- and patient-related factors, use of antithrombotic drugs, especially anticoagulants [direct oral anticoagulants (DOACs) and warfarin], is thought to be the biggest risk factor for post-ESD bleeding. In fact, the post-ESD bleeding rate in patients receiving DOACs is 8.7%-20.8%, which is higher than that in patients not receiving anticoagulants. However, because clinical guidelines for management of ESD in patients receiving DOACs differ among countries, it is necessary for endoscopists to identify ways to prevent post-ESD delayed bleeding in clinical practice. Given that the pharmacokinetics (*e.g.*, plasma DOAC level at both trough and T_{max}) and pharmacodynamics (*e.g.*, anti-factor Xa activity) of DOACs are related to risk of major bleeding, plasma DOAC level and anti-FXa activity may be useful parameters for monitoring the anti-coagulate effect and identifying DOAC patients at higher risk of post-ESD bleeding.

Key Words: Direct oral anticoagulants; Gastrointestinal tumors; Endoscopic submucosal dissection; Delayed bleeding; Adverse events; Anticoagulants

Core Tip: Recent international clinical guidelines for early-stage gastrointestinal tumors recommend endoscopic submucosal dissection (ESD) as the first-line treatment. Direct oral anticoagulants (DOACs) are a major risk factor for post-ESD bleeding and the pharmacokinetics and pharmacodynamics of DOACs may be related to risk of post-ESD bleeding. Therefore, one way to monitor the anticoagulant effect of DOACs in clinical practice may be to develop a system that effectively measures anti–FXa activity and plasma concentration. In the future, it may be useful to stratify risk of post-ESD delayed bleeding based on a scoring system that includes pharmacological parameters of DOACs.

Citation: Sugimoto M, Murata M, Kawai T. Assessment of delayed bleeding after endoscopic submucosal dissection of early-stage gastrointestinal tumors in patients receiving direct oral anticoagulants. *World J Gastroenterol* 2023; 29(19): 2916-2931
URL: https://www.wjgnet.com/1007-9327/full/v29/i19/2916.htm
DOI: https://dx.doi.org/10.3748/wjg.v29.i19.2916

INTRODUCTION

Endoscopic resection, a minimally invasive endoscopic non-surgical treatment, is now accepted as first-line management for most cases of early-stage esophageal cancer, gastric cancer and colorectal cancer or adenoma around the world[1]. Endoscopic resection mainly includes endoscopic mucosal resection (EMR) and endoscopic submucosal dissection (ESD). Indication for endoscopic resection for EMR and ESD is typically a local mucosal lesion with an extremely low risk of metastasis to lymph nodes (generally less than 1%), and lesions that can be resected *en-bloc*, irrespective of localization in the esophagus, stomach, duodenum or colon. Because ESD enables complete *en-bloc* resection and is associated with a lower recurrence rate than EMR[2,3], recent international clinical guidelines for early-stage gastrointestinal tumors recommend ESD as the first-line treatment over EMR and surgical resection[1,3-7]. To achieve good results and prognosis in ESD for early-stage gastrointestinal tumors, endoscopists and gastroenterologists require excellent skills and knowledge of the diagnosis, indications, actual procedures, and evaluation of curability, complications, long-term postoperative surveillance, and histopathology[3].

ESD often causes adverse events such as intra-operative and delayed bleeding from an artificial ulcer and perforation. The occurrence of such events has been linked to several procedure-, lesion-, physician- and patient-related factors[8-12]. Of the possible risk factors for post-ESD delayed bleeding, use of antithrombotic drugs, especially anticoagulants, is the biggest risk factor[13,14]. Although anticoagulants are mainly divided into warfarin and direct oral anticoagulants (DOACs), no parameters identified to date can be used to accurately monitor the anti-coagulate effect of DOACs in clinical practice or endoscopic/surgical procedures. Thus, it is important to clarify the association between post-ESD delayed bleeding for early-stage gastrointestinal tumors and DOACs, identify risk factors of post-ESD delayed bleeding in patients taking DOACs and methods to prevent bleeding in these patients.

Here, we review delayed bleeding after ESD for gastrointestinal tumors, risk factors for post-ESD bleeding, the pharmacological characteristics of DOACs, international clinical guidelines for endoscopic procedures in patients receiving DOACs, and post-ESD bleeding in patients receiving DOACs.

DELAYED BLEEDING AFTER ESD FOR GASTROINTESTINAL TUMORS

In Japan, upper and lower gastrointestinal tumors are detected in the early stages in many patients, mainly through the use of optimal screening methods, appropriate surveillance and the development of endoscopic diagnostic techniques for early detection and endoscopic equipment[15-17]. In general, evaluation of early-stage gastrointestinal tumors should be performed by expert endoscopists, using a high-definition endoscope by white-light imaging and advanced image-enhanced endoscopy[18]. The experience of the endoscopist may be related to the incidence of adverse events and effective prevention of procedure-related adverse events after ESD. Careful and appropriate coagulation for exposed blood vessels may reduce the gastrointestinal bleeding risk, especially in the stomach[7,19]. The rate of bleeding and its risk factors are known to differ among patients with esophagus, stomach, duodenum and colon cancer.

Esophageal squamous cell carcinoma

The recent development of high-vision endoscopes and techniques for endoscopic diagnosis, including narrow band imaging, has led to more frequent early detection of esophageal esophageal squamous cell carcinoma (SCC)[15,20]. Therefore, ESD is accepted as an effective procedure for detecting superficial

esophageal SCC. In Japan, the Esophageal Cancer Practice Guidelines 2017 weakly recommends endoscopic resection as first-line treatment for preoperatively diagnosed cT1a-MM/T1b-SM1 non-circumferential SCC[6]. In 2014, a meta-analysis of 15 studies with 776 patients with ESD-treated SCC reported pooled estimates of complete resection and *en bloc* resection rates of 89.4% [95%CI: 86.2%–91.9%] and 95.1% (92.6%–96.8%), respectively[21]. In addition, pooled estimates of adverse events such as post-ESD bleeding, perforation, and stenosis were 2.1% (95%CI: 1.2%–3.8%), 5.0% (3.5%–7.2%), and 11.6% (8.2%–16.2%), respectively[21].

Barrett's neoplasia and esophageal adenocarcinoma

The incidence of esophageal adenocarcinoma (EAC) located in Barrett's epithelium has been increasing, especially in Western countries, due to decreases in the *Helicobacter pylori (H. pylori)* infection rate and increases in reflux esophagitis[22]. The European Society of Gastrointestinal Endoscopy (ESGE) recommends using EMR for ≤ 20 mm visible lesions with low probability of submucosal invasion and for larger or multifocal benign dysplastic lesions. In Japan, ESD is strongly recommended over EMR for the radical treatment of superficial EAC with a low risk of metastasis[6]. A meta-analysis of 11 studies investigating the efficacy and safety of ESD for EAC (mean size: 27 mm) reported pooled estimates for *en bloc* resection and pooled R0 resection of 92.9% (95%CI: 90.3%-95.2%) and 74.5% (66.3%-81.9%), respectively[23]. Incidence of recurrence after curative resection was 0.17% (95%CI: 0%-0.3%) at a mean follow-up of 22.9 mo (17.5-28.3 mo)[23]. In adverse events, estimates for bleeding, perforation, and stricture were 1.7% (95%CI: 0.6%-3.4%), 1.5% (0.4%-3.0%) and 11.6% (0.9%-29.6%), respectively. Thus, the rate of post-ESD delayed bleeding in both esophageal SCC and EAC may not be very high (1.7%-2.1%).

Gastric cancer

In the ESGE, gastric cancers that are ≤ 30 mm, submucosal (sm1), and well-differentiated, or ≤ 20 mm, intramucosal, and poorly differentiated, and without ulcerative findings for both sets of criteria can be considered for ESD, although the decision should be individualized[4]. ESD for gastric cancer is associated with high rates of *en bloc* and R0 resection (> 90%), curative resection (75%–80%), low local recurrence (< 5%) and acceptable rates of adverse events (post-ESD bleeding 5%–10% and perforation < 3%)[24,25]. A recent meta-analysis of 22 studies in Western countries reported estimates for *en bloc* resection and R0 resection of 96% (95%CI: 93%-98%) and 84% (79%-89%), respectively[26]. Overall, adverse events occur in 9.5% of patients, including delayed bleeding (5.8%), perforation (3.4%), and stenosis (0.35%)[26]. The odds ratio (OR) indicates that there is no significant difference in risk of post-ESD bleeding between ESD and EMR (OR 1.26, 95%CI: 0.88-1.80)[27]. Another meta-analysis of 74 articles by Libânio *et al*[28] reported post-ESD bleeding rates ranging from 0.6% to 26.9% and a pooled bleeding rate of 5.1% (95%CI: 4.5%-5.7%), with significant heterogeneity across studies (I^2: 84.46, P < 0.001). However, bleeding rates were not significantly different among different study designs (5.9% in randomized clinical trials, 6.1% in prospective studies, and 4.9% in retrospective studies). The elderly Japanese population aged ≥ 85 years has increased from 1.4 to 4.8 million over the last two decades[29] and our investigation of a cohort of 10,320 patients showed that the incidence of bleeding in elderly patients aged > 80 years was 5.7% (95%CI: 4.6%-6.9%), which was significantly higher than in patients aged < 80 years (4.5%, 4.1%-5.0%)[30].

Duodenum

Because ESD for duodenal tumors is associated with high rates of post-ESD bleeding and perforation at both the early and late phases, the ESGE suggests reserving its use for selected cases and tumors in expert centers[4]. In particular, perforation rates are high, with an incidence > 10% in studies involving expert centers[31]. Further, distal location to the ampulla of Vater is a risk factor for delayed perforation [32]. A meta-analysis reported pooled rates of *en bloc* resection, need for surgical intervention, delayed bleeding, intraoperative and delayed perforation of 87%, 4%, 2%, 15% and 2%, respectively[33]. Meanwhile, a recent large retrospective Japanese study reported that the rate of post-ESD adverse events was significantly reduced in cases with complete closure of the mucosal defect compared to partial closure and no closure (1.7%, 25.0% and 15.6%, respectively, P < 0.01)[34].

Colon

In Japan, indications for ESD for colorectal tumors are lesions for which endoscopic *en bloc* resection is required, as follows: (1) Lesions for which *en bloc* resection with snare EMR is difficult to apply; (2) Mucosal tumors with submucosal fibrosis; (3) Sporadic localized tumors in conditions of chronic inflammation such as ulcerative colitis; and (4) Post-EMR local residual or recurrent early-stage cancers[5]. A recent systematic review of 109 studies on 19484 colorectal lesions resected by ESD reported rates of *en bloc* resection of 91%, R0 resection of 82.9%, and local recurrence of 2%. The study also reported a rate of post-ESD bleeding of 2.7% and perforation of 5.2%, and that 1.1% of all patients needed surgical treatment by severe adverse events[35].

Because the rate of post-ESD bleeding may be higher for gastric cancer (5%-8%) than that at other sites (around 2%-4%) due to direct exposure of artificial ulcers to gastric acid and bile, it is necessary for

endoscopists to be aware of and develop countermeasures for gastric ESD.

RISK FACTORS FOR POST-ESD GASTROINTESTINAL DELAYED BLEEDING

Risk factors for post-ESD bleeding are expected to differ among patients with esophagus, stomach, duodenum and colon cancer. Post-ESD bleeding has been shown to be associated with procedure-related factors (*e.g.*, type of knife, coagulation machine and endoscope, and coagulation mode), lesion-related factors (*e.g.*, gastrointestinal organ, large lesion size, location, presence within the ulcerated lesion, scarring, and fibrosis), physician-related factors (*e.g.*, experience with ESD) and patient-related factors [hemodialysis, drugs (antiplatelet drugs, anticoagulants, steroids, and non-steroidal anti-inflammatory drugs), hemostasis ability, and platelet count] (Figure 1)[8-12].

Libânio *et al*[28] showed in a meta-analysis of 74 articles that male sex (OR 1.25), cardiopathy (OR 1.54), antithrombotic drugs (OR 1.63), cirrhosis (OR 1.76), chronic kidney disease (CKD) (OR 3.38), tumor size > 20 mm (OR 2.70), resected specimen size > 30 mm (OR 2.85), localization in the lesser curvature (OR 1.74), flat/depressed morphology (OR 1.43), carcinoma histology (OR 1.46), and ulceration (OR 1.64) were significant risk factors for post-ESD bleeding of gastric cancer, whereas age, hypertension, submucosal invasion, fibrosis, and location (upper, middle, or lower third of stomach) were not. In terms of procedural factors, procedure duration > 60 min (OR, 2.05) and use of histamine-2 receptor antagonists instead of proton pump inhibitors (PPIs) (OR, 2.13) were associated with post-ESD bleeding, whereas endoscopist experience was not. Recently, Hatta *et al*[36] conducted a nationwide multicenter retrospective study focusing on post-ESD bleeding for gastric cancer and used the data to develop a model that applies 10 factors [warfarin, DOAC, hemodialysis, P2Y12 receptor antagonist, aspirin, tumor size > 30 mm, tumor location in the lower third, presence of multiple tumors and interruption of each kind of antithrombotic agent] to predict post-ESD bleeding (BEST-J score). According to the BEST-J score, rates of bleeding in patients categorized as low-risk, intermediate-risk, high-risk, and very high-risk were 2.8%, 6.1%, 11.4%, and 29.7%, respectively[36]. A validation study of the BEST-J score showed that the area under the curve for the BEST-J score at multicenter trials was 0.713 (95%CI: 0.625–0.802), which suggests that the BEST-J score may be useful for predicting post-ESD bleeding in not only expert centers but also general hospitals[37]. In addition, because the healing speed of post-ESD artificial ulcers is related to the post-ESD bleeding rate, factors that affect the healing speed of ulcers, namely *H. pylori* infection status, type of acid inhibitory drug (*e.g.*, PPIs and vonoprazan) and severity of gastric atrophy, may also be risk factors for post-ESD bleeding in gastric cancer[11,12,38]. In today's aging society, the number of patients taking anti-platelet drugs and anticoagulants for the prevention of cardio- and cerebrovascular diseases has risen. That a multicenter study reported a high incidence of post-ESD bleeding in Japanese aged > 80 years, especially in patients receiving hemodialysis and taking warfarin[30], indicates that careful management of ESD is required to prevent bleeding in patients aged > 80 years compared to younger patients.

Major risk factors for post-ESD bleeding for colorectal tumors are generally larger tumor size, location in the rectum or cecum, long procedure time, number of tumors, and taking anti-thrombotic drugs. Recently, Li *et al*[39] reported that post-ESD bleeding for colorectal tumors is observed in 4.7% of patients, and that hypertension (OR 2.829, 95%CI: 1.101-7.265) and using hot biopsy forceps for wound management (OR 2.873, 95%CI: 1.013-8.147) remain significant risk factors for bleeding after multivariate analysis. In another study, Seo *et al*[40] developed a risk-scoring model to predict bleeding after colorectal ESD following identification of the tumor location in the rectosigmoid colon (OR 6.49; 95%CI: 1.96-21.42), large tumor (> 30 mm) (2.10, 1.01-4.40), and use of antiplatelet agents except for aspirin alone (4.04, 1.44-11.30) as risk factors for bleeding[40]. When use of antiplatelet agents except for aspirin alone was scored as 1 point, tumor size > 30 mm as 1 point, and location in the rectosigmoid area as 2 points, the incidence of bleeding in low-risk (score 0-2) and high-risk groups (score 3-4) was 1.5% and 6.0%, respectively.

Thus, current evidence indicates that the use of antithrombotic drugs, especially anticoagulants (DOACs and warfarin) is the biggest risk factor for post-ESD bleeding[13,14].

PHARMACOLOGICAL CHARACTERISTICS OF DOACS

DOACs are currently the first-line drug for the pharmacological prevention of systemic embolism or stroke in atrial fibrillation patients. They are categorized into two main classes: Direct thrombin inhibitors (*i.e.*, dabigatran) and activated coagulation factor X (FXa) inhibitors (*i.e.*, apixaban, edoxaban, rivaroxaban, and betrixaban). Compared with anticoagulation with vitamin K antagonists (*i.e.*, warfarin) or low-molecular-weight heparins, DOACs are new agents that demonstrate superiority or noninferiority to prior standards of care in reducing the risk of thromboembolic complications and major and minor bleeding risk, have fewer monitoring requirements and less frequent follow-up need; and have more immediate drug onset and offset effects and fewer drug and food interactions[41-44]. However, an advantage of using vitamin K antagonist therapy is that a therapeutic international

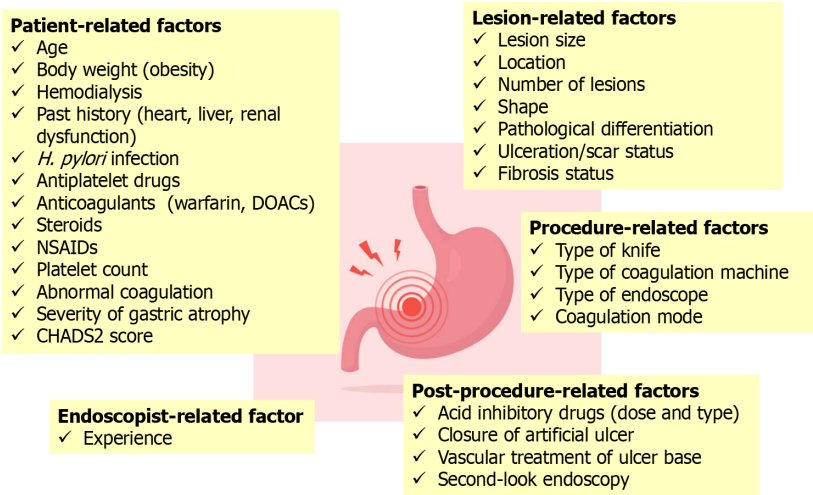

DOI: 10.3748/wjg.v29.i19.2916

Figure 1 Post-endoscopic submucosal dissection bleeding-related factors. DOACs: Direct oral anticoagulants; NSAIDs: Non-steroidal anti-inflammatory drugs; CHADS: Congestive heart failure, Hypertension, Age > 75 years, Diabetes mellitus, and Stroke.

normalized ratio range of 2.0-3.0 has been established and is recommended to prevent embolic complications in non-valvular atrial fibrillation in the treatment of deep vein thrombosis and pulmonary embolism. In contrast, a disadvantage of DOACs is that their anticoagulant effects in patients are unclear because there are no Food and Drug Administration (FDA)-approved methods to measure correctly the anticoagulant effect of DOACs. Although qualitative coagulation assays (*e.g.*, thrombin time, activated partial thromboplastin time, and prothrombin time) can be selected as first-line tests, they do not accurately measure the anticoagulant effect of DOACs (Table 1). Quantitative measures for direct assessment of anticoagulant effects do exist, including anti–FXa activity, plasma drug concentration (standard method in preclinical/clinical research and the most accurate method), dilute thrombin time, and ecarin thrombin time[45,46]. In fact, plotting anti–FXa activity against plasma levels of apixaban and rivaroxaban has been confirmed to show a direct linear relationship for both compounds[47].

Pharmacokinetic characteristics such as oral bioavailability, plasma protein binding and relative involvement of renal and non-renal elimination differ substantially among DOACs (Table 2). Pharmacokinetics is influenced by the type of DOAC, dose, renal function, liver function, age, sex, body weight, drug metabolic enzyme gene polymorphisms and drug-drug interactions, but not ethnicity, geographic region, aspirin use, or clopidogrel use[48]. DOACs are relatively safe and effective in patients with moderate CKD [creatinine clearance (Ccr) 30–50 mL/min]. Rivaroxaban, dabigatran and edoxaban will require dose adjustment for renal impairment and patients with severe renal dysfunction (Ccr < 30 mL/min) are recommended to avoid their use[49]. Regulatory agencies such as the FDA and European Medicines Agency have provided guidelines for performing dose adjustments according to the DOAC dose based on Ccr and anticoagulant indications[50]. The International Society on Thrombosis and Hemostasis suggests that use of DOACs are safe in patients of body mass index ≤ 40 kg/m^2 (body weight ≤ 120 kg) at standard doses but does not recommend them for patients of body weight > 120 kg [51]. Compared to warfarin, DOACs are more effective and safer in patients with low body weight (< 50 kg)[52].

DOACs are metabolized by either cytochrome P450 (CYP) metabolic enzymes in the liver or permeability glycoprotein transporters; thus, agents that induce or inhibit CYP metabolic enzymes or glycoprotein transporters can lead to major drug-drug interactions and place the patient at undue risk for adverse events. In fact, concomitant use of apixaban, rivaroxaban, or dabigatran with clarithromycin, a potent inhibitor of CYP3A4, and ATP-binding cassette multidrug transporters increases serum levels of DOACs by 20% to 100% and prolongs coagulation time[53,54]. The pharmacokinetics of DOACs also depend on genetic variations, such as *ABCB1* (ATP-binding cassette multidrug transporters, MDR1) (1236C>T, 2677G>T/A, and 3435C>T), *ABCG2* (421C>A), and *CYP3A5* polymorphisms (6986A>G)[55]. The plasma trough C/D ratio of apixaban is significantly higher in patients with the ABCG2 421A/A genotype and CYP3A5 6986 G allele carriers than in patients with the ABCG2 421C/C genotype and CYP3A5 6986 A/A genotype[55]. Given that CYP3A5 6986A>G and ABCG2 421C>A polymorphisms have allele frequencies of 65%-85%[56] and 29%-36%[57], respectively, in Asians, ABCB1, ABCG2, and CYP3A5 genotypes play pivotal roles in the interindividual variability of apixaban concentrations in Japanese patients.

Although the pharmacodynamic parameters of DOACs differ significantly among individuals and anticoagulant effects also vary widely among patients receiving DOACs, the lack of approved methods to monitor the anticoagulant effect of DOACs makes it unclear whether the effect is adequate in patients

Table 1 Possible methods for monitoring the anticoagulant ability of direct oral anticoagulants[49,71,87]

	Qualitative methods			Quantitative methods					Other	
	aPTT	TT	PT	Anti-FIIa levels	Anti-Fxa levels	Plasma level	dTT	ECT/ECA	CBC	CMP
Dabigatran	[2]	[2]	[2]	[1]		[1]	[2]	[2]	[2]	[2]
Apixaban			[2]		[1]	[1]			[2]	[2]
Edoxaban			[2]		[1]	[1]			[2]	[2]
Rivaroxaban			[2]		[1]	[1]			[2]	[2]

[1]Possible excellent markers.
[2]Possible sensitive markers.
APTT: Activated partial thromboplastin time; CBC: Complete blood count; CMP: Comprehensive metabolic panel; dTT: Dilute thrombin time; ECA: Ecarin chromogenic assay: ECT: Ecarin clotting time; FXa: Activated factor X; PT: Prothrombin time; TT: Thrombin time.

receiving DOAC. Compared with vitamin K antagonist therapy (therapeutic international normalized ratio range: 2.0-3.0), a disadvantage of DOACs is that the dosage of DOAC cannot be controlled according to anticoagulant effect. Therefore, the trough and time to reach maximum plasma concentration (T_{max}) and anti-FXa activity of DOAC-metabolizing enzyme polymorphisms may be useful parameters for accurately monitoring the anti-coagulate effects of DOACs and selecting patients at higher risk of major bleeding. Developing a system that easily measures the anti–FXa activity and plasma level could be an important way to monitor the anticoagulant effect of DOACs in clinical practice.

PHARMACOKINETICS OF DOACS AND MAJOR BLEEDING

Clinical trials have investigated the efficacy of dabigatran (RE-LY trial[58]), apixaban (ARISTOTLE trial [41]), edoxaban (ENGAGE AF TIMI48 trial[59]) and rivaroxaban (ROCKET AF trial[60]) for the prevention of stroke and embolism. According to these trials, adverse events of major bleeding and gastrointestinal bleeding occur at rates of 3.11% and 1.51% for dabigatran 150 mg given twice daily (bid), 2.13% and 0.76% at apixaban 5 mg bid, 2.75% and 1.51% at edoxaban 60 mg given once daily (oid) and 3.6% and 3.2% at rivaroxaban 20 mg oid (Table 3), respectively.

Because the anti-coagulate effects of DOACs are linked to plasma levels of DOAC and anti-FXa activity at trough and T_{max}[48,61,62], these pharmacokinetic and pharmacodynamic parameters are also expected to be related to risk of major bleeding, such as intracerebral and gastrointestinal bleeding. Using multiple logistic regression, Reilly *et al*[48] showed that major bleeding risk increased with dabigatran exposure ($P < 0.0001$), age ($P < 0.0001$), aspirin use ($P < 0.0003$), and diabetes ($P = 0.018$) as significant covariates. Further, patients with major bleeding had higher trough levels (55%) and post-dose levels (36%) than non-bleeding patients[48]. Reilly *et al*[48] also reported a median trough level of 116 ng/mL in 323 major bleeding patients compared with 75.3 ng/mL in 5899 no bleeding patients[48]. Additionally, a Cox regression analysis of time to first major bleeding with trough level, age, and CHADS2 score as covariates showed that, compared with the median trough level of 88 ng/mL, the rate of major bleeding doubled at a level of 210 ng/mL after adjustment for age and CHADS2 score. Moreover, Sakaguchi *et al*[63] showed that, in rivaroxaban-treated patients with major bleeding in Japan, major bleeding is independently predicted to be higher peak rivaroxaban levels and higher anti-FXa activity. Additionally, Sin *et al's* prospective study[64] of rivaroxaban-treated patients with atrial fibrillation with differing severity of CKD (Stage 1–3) showed that trough levels of rivaroxaban were higher in those with bleeding (59.9 ± 35.6 ng/mL) than in those without (41.1 ± 29.2 ng/mL; $P < 0.05$). Therefore, although plasma level and anti–FXa activity may be useful parameters for selecting patients receiving DOACs at higher risk of major bleeding, there is no evidence that patients with higher plasma levels and anti–FXa activity have higher risk of post-ESD bleeding.

A retrospective analysis of 5041 patients demonstrated that concomitant dabigatran–PPI treatment is linked to a significant reduction in bleeding risk compared with dabigatran alone without a PPI[65]. Although dabigatran is an orally administered prodrug, it is rapidly absorbed and converted to its active form, dabigatran. Thus, a potential mechanism for PPI–dabigatran interaction may be reduced dabigatran absorption and availability, which is most probably mediated *via* the effects of PPI on gastric pH, given the poor solubility of dabigatran at pH > 4[66]. Therefore, interactions between PPIs and dabigatran may lead to decreases in dabigatran levels[67].

In terms of gastrointestinal bleeding, unlike warfarin, DOACs remain in the gastrointestinal tract without being absorbed into the blood. Therefore, DOACs may directly inhibit the hemostatic

Table 2 Pharmacological characteristics of direct oral anticoagulant[71,87]

	Dabigatran	Apixaban	Edoxaban	Rivaroxaban
Target factor	Thrombin (Factor IIa)	Factor Xa	Factor Xa	Factor Xa
Half-time (h)	10.7-11.8	6.12-8.11	6.21-6.70	5.7-12.6
Time to peak effect (h)	4	3.0-3.5	1-1.5	1.4-3.3
Distribution volume (L)	50-70	21	107	50
Renal excretion (%)	85	27	35.4-50	50
Fecal excretion (%)	6	25	62.2	50
Hepatic metabolism	No	CYP3A4/5	CYP3A4	CYP3A4 and CYP2J2
Transporter	P-gP	P-gP/BCRP	P-gP	P-gP/BCRP
Protein binding (%)	28.2-31.5	87	40.0-58.9	92-95
Dialyzable	Yes	No	No	No
Prodrug	Yes	No	No	No
Bioavailability (%)	6.5	50	61.8	66-112
Dose for AF (in Japan)	150 mg	5 mg	60 mg	15 mg
Dosing time	Twice daily	Twice daily	Once daily	Once daily
Reversal agent	Idarucizumab	Andexanet alfa	Andexanet alfa	Andexanet alfa
FDA-approved indications	Nonvalvular AF, VTE (T, SP, P)	Nonvalvular AF, VTE (T, SP, P)	Nonvalvular AF, VTE (T)	Nonvalvular AF, VTE (T, SP, P)
Japanese insurance system-approved indications	Nonvalvular AF (P)	Nonvalvular AF (P), VTE (T, SP)	Nonvalvular AF (P), VTE (T, SP)	Nonvalvular AF (P), VTE (T, SP)
Non-pharmacologic interactions	Age, reduced GFR	Age, reduced body weight, reduced GFR, probable severe liver damage	Reduced GFR, probable severe liver damage	Age, reduced GFR, probable severe liver damage
Drug interactions	Dose reduction: Concomitant P-gp inhibitor, gastric acid inhibitory drug	Avoid: Concomitant P-gp and CYP3A4 inhibitors	Avoid: Concomitant rifampin	Avoid: Rivaroxaban with concomitant dual P-gp and CYP3A4 inhibitors
Contraindications	Ccr: < 30mL/min	Nonvalvular AF: Ccr: < 15mL/min, VTE: Ccr: < 30mL/min	Nonvalvular AF: Ccr: < 15mL/min, VTE: Ccr: < 30mL/min	Nonvalvular AF: Ccr: < 15mL/min, VTE: Ccr: < 30mL/min

AF: Atrial fibrillation; P: Prophylaxis; SP: Secondary prevention; T: Treatment; VTE: Venous thromboembolism; FDA: Food and Drug Administration; Ccr: Creatinine clearance.

mechanism in the gastrointestinal tract, thereby aggravating bleeding[68].

CLINICAL GUIDELINES: MANAGEMENT FOR PATIENTS TAKING DOACS IN ENDOSCOPIC PROCEDURES WITH HIGHER RISK FOR BLEEDING (ESD)

During gastrointestinal endoscopy and endoscopic treatment of patients receiving antithrombotic therapy, it is necessary to balance the risk of major and minor bleeding with the risk of thromboembolism resulting from withdrawal of antithrombotic therapy. Therefore, it is important to determine a management strategy (with withdrawal or not) that is optimized for individual patients based on consultation between the endoscopist and physician prescribing the antithrombotic drugs. The risk of thromboembolism is closely related to the underlying disease requiring anticoagulants, and the absolute risk of thromboembolism increases by more than 1% when anticoagulants are withdrawn for more than 4 d[69].

In 2012 the Japan Gastroenterological Endoscopy Society published "Guidelines for gastroenterological endoscopy in patients undergoing antithrombotic treatment" concerning thromboembolism associated with antithrombotic therapy withdrawal and bleeding[70]. The guidelines were updated with a 2017 appendix on anticoagulants in 2017[71]. Although the 2012 version recommends replacing DOACs with heparin during ESD in patients with high risk for post-procedure bleeding as an adverse

Table 3 Comparison of clinical trials on patients receiving direct oral anticoagulant: Major bleeding

	Dabigatran	Apixaban	Edoxaban	Rivaroxaban
Trial name	RE-LY[4]	ARISTOTLE[5]	ENGAGE AF TIMI48[6]	ROCKET AF[7]/J-ROCKET AF
Number of patients	18113	18201	21105	14264
Method	PROBE	RCT	RCT	RCT
Primary endpoints	Stroke or systemic embolism	Ischemic or hemorrhagic stroke or systemic embolism	Stroke or systemic embolism	Stroke or systemic embolism
Period (years)	2.0	1.8	2.8	1.9
$CHADS_2$ score (mean)	2.2	2.1	2.8	3.48 (J-ROCKET: 3.25)
Dosing dose	150 mg/10 mg bid	5 mg bid	60 mg/30 mg qd	20 mg od (J-ROCKET: 15 mg od)
Evaluation				
Thrombus/embolism (*vs* warfarin)	110 mg: Non-inferior, 150 mg: Superior	Superior	60 mg: Similar, 30 mg: Similar	On treatment: Superior, Intention-to-treat: Non-inferior
Outcomes: Stroke or systemic embolism	War: 1.69%/yr, D (110): 1.51%/yr, D (150): 1.11%/yr	War: 1.50%/yr, A: 1.27%/yr	War: 1.81%/yr, E (30): 2.06%/yr, E (60): 1.57%/yr	War: 2.2%/yr, R: 1.7%/yr
Major bleeding (*vs* warfarin)	110 mg: Superior, 150 mg: Similar	Superior	Superior	Similar
Bleeding rate	War: 3.36%/yr, D (110): 2.71%/yr, D (150): 3.11%/yr	War: 3.09%/yr, A: 2.13%/yr	War: 3.43%/yr, E (30): 1.61%/yr, E (60): 2.75%/yr	War: 3.4%/yr, R: 3.6%/yr
Intracranial bleeding	War: 0.74%/yr, D (110): 0.23%/yr, D (150): 0.30%/yr	War: 2.27%/yr, A: 1.79%/yr	War: 0.85%/yr, E (30): 0.26%/yr, E (60): 0.39%/yr	War: 0.7%/yr, R: 0.5%/yr
Gastrointestinal bleeding	War: 1.02%/yr, D (110): 1.12%/yr, D (150): 1.51%/yr	War: 0.86%/yr, A: 0.76%/yr	War: 1.23%/yr, E (30): 0.82%/yr, E (60): 1.51%/yr	War: 2.2%/yr, R: 3.2%/yr1
Minor bleeding (*vs* warfarin)	War: 16.37%/yr, D (110): 13.16%/yr, D (150): 14.84%/yr	War: 6.01%/yr, A: 4.07%/yr	War: 4.89%/yr, E (30): 3.52%/yr, E (60): 4.12%/yr	War: 11.4%/yr, R: 11.8%/yr
Mortality rate	War: 4.13%/yr, D (110): 3.75%/yr, D (150): 3.64%/yr	War: 3.94%/yr, A: 3.52%/yr	War: 4.35%/yr, E (30): 3.80%/yr, E (60): 3.99%/yr	War: 2.2%/yr, R: 1.9%/yr

A: Apixaban; D: Dabigatran; E: Edoxaban; R: Rivaroxaban; war: Warfarin; RCT: Randomized clinical trial; CHADS: Congestive heart failure, Hypertension, Age > 75 years, Diabetes mellitus, and Stroke; PROBE: Prospective randomized open blinded-endpoint.

event, the 2017 version recommends that patients receiving DOACs should continue to take the DOAC orally until the day before ESD and discontinue it on the morning of ESD (Table 4)[71]. Because the anticoagulant effects last 36–48 h for rivaroxaban and edoxaban given oid and 24–36 h for apixaban given bid, and the disappearance of anti-FXa activity and anticoagulant effects increase the risk of thrombosis, DOACs may be resumed the morning after ESD (up to 36 and 48 h when given bid and oid). In addition, when performing ESD, patients receiving concomitant DOAC and antiplatelet agents should be handled with care depending on the individual's condition and needs, while ESD can be performed on patients receiving antiplatelet monotherapy with aspirin or cilostazol[71].

In contrast to the Japanese guidelines, the updated guidelines by the British Society of Gastroenterology and ESGE suggest that patients receiving low-risk procedures for bleeding withdraw from the morning dose of DOAC on the morning of ESD, and recommend that the last dose of DOAC be taken 3 d before ESD for high-risk endoscopic procedures (strong recommendation and low-quality evidence) (Table 4)[72]. For patients receiving dabigatran with a Ccr 30–50 mL/min, this updated version recommends that the last dose be taken 5 d prior to the procedure (strong recommendation and low-quality evidence)[72].

The American Society for Gastrointestinal Endoscopy (ASGE) published a guideline on how to manage patients receiving antithrombotic agents for endoscopy in 2016[73]. This guideline suggests that patients undergoing low-risk procedures should continue taking DOACs (Table 4)[73] and that the resumption of DOACs after ESD be delayed until adequate hemostasis is ensured. If DOACs cannot be resumed within 12 to 24 h post-ESD, thromboprophylaxis should be considered to decrease thromboembolism risk in those with high risk for thromboembolism. However, this version of the ASGE guideline recommends that patients at high risk for thromboembolic events withdraw DOACs and receive bridge therapy to adequately manage patients taking DOACs when ESD is performed (Table 4).

Table 4 Summary of international guidelines concerning withdrawal of direct oral anticoagulants during gastroenterological endoscopy

Ref.	Country	Standard endoscopy	Biopsy	Low risk of bleeding	High risk of bleeding, including ESD
[71]	Japan	[1]	[2]Avoid peak plasma level	[2]Avoid peak plasma level	[3](1) Withdraw on the day of treatment; and (2) Heparin replacement
[72]	Europe	[1]	[3]Withdraw on the day of treatment	[3]Withdraw on the day of treatment	[3](1) Withdraw 3 d before treatment; (2) Withdraw 5 d before treatment for dabigatran patients at Ccr 30–50 mL/min; and (3) No heparin bridging
[73]	United States	[1]	[1]	[1]	[3](1) Withdraw; and (2) Bridge therapy required for patients at high risk for thromboembolic events
[74]	Korea	[1]	[1]	[1]	[3]Withdraw 2 d before treatment
[75]	Asia-Pacific	[1]	[1]	[1]	[3]Withdraw 2 d before treatment

[1]Withdrawal is not required.
[2]Withdrawal is not required but possible.
[3]Withdrawal is required.
ESD: Endoscopic submucosal dissection; Ccr: Creatinine clearance.

In contrast, the Korean clinical practice guideline does not recommend withdrawal of DOACs before low-risk procedures (weak recommendation and low-quality evidence) but suggests withdrawing DOACs > 48 h before high-risk procedures (weak recommendation and low-quality evidence) (Table 4)[74]. The recommendation to withdraw DOACs > 48 h before ESD is based on the fact that the half-life of DOACs is about 12 h and predictions that DOAC levels and anti-FXa activity will be almost undetectable after 48 h[74].

The Asian Pacific Association of Gastroenterology and Asian Pacific Society for Digestive Endoscopy guidelines recommend withholding DOACs at least 48 h before the procedure in DOAC patients receiving gastrointestinal ESD (strong recommendation and low-quality evidence) and do not recommend bridging anticoagulation (strong recommendation and low-quality evidence) (Table 4)[75]. In addition, these guidelines provide recommendations related to the timing of DOAC discontinuation before high-risk procedures according to Ccr[76]. In these guidelines, EMR for large colon polyp (≥ 2 cm) and ESD procedures, which have a higher risk of gastrointestinal bleeding compared with other high-risk endoscopic procedures, are categorized as ultra-high-risk endoscopic procedures[74,75].

Thus, as summarized in Table 4, guidelines for the management of patients undergoing ESD for early-stage gastrointestinal tumors who receive DOACs differ by country. Although subtle differences in the management of DOACs with ESD are important in clinical practice, we consider that these differences are dependent on the year in which the guidelines were published, the different dosage of DOAC in each country, the different numbers of concomitant antithrombotic drugs, and differences in the rate of genetic variations (*e.g.*, CYP3A4/5, ABCG2, and ABCB1 polymorphism).

GASTROINTESTINAL BLEEDING AFTER ESD IN PATIENTS RECEIVING DOACS

Post-ESD bleeding in patients receiving DOACs remains an unpreventable adverse event. Although the combination of heparin-bridging therapy and discontinuation of DOACs is one approach used to prevent thrombosis[70,71], heparin-bridging therapy with discontinuation of any anticoagulants causes an increased risk of delayed bleeding after surgical treatment, interventional procedures and ESD (gastric ESD: 10.8%-61.5%)[77-80] and does not reduce the risk of perioperative arterial thromboembolism[77-79]. In fact, a meta-analysis focused on heparin-bridging therapy with discontinuation of any anticoagulants for ESD found an increased risk of post-ESD bleeding without any benefit for thrombosis [81]. Another meta-analysis reported an increase in thrombosis in patients receiving heparin-bridging therapy with discontinuation of anticoagulants compared with those who discontinued anticoagulation without heparin bridging[82]. In Japan, although the updated guideline recommends discontinuing DOACs on the morning of ESD, most studies conducted on ESD for patients receiving DOACs have been retrospective and enrolled small numbers of patients (Table 5).

However, one study examined a large national database including 16977 patients receiving anticoagulation therapy who underwent high-risk endoscopic procedures. It showed that although warfarin led to a significantly higher post-procedure bleeding rate than DOACs (12.0% *vs* 9.9%, $P = 0.002$), the post-procedure bleeding rate was not significantly different in either upper or lower gastrointestinal ESD between patients receiving DOACs and warfarin[83]. In sub-analyses of procedure types in propensity-matched patients, the gastrointestinal bleeding rate in the DOAC group was 39.6% in

Table 5 Delayed bleeding after endoscopic submucosal dissection in patients receiving direct oral anticoagulants

Ref.	Year	Country	Type	Organ	DOAC patients	Bleeding rate	Non-DOAC patients	Bleeding rate
Nagata *et al*[83]	2018	Japan	Retrospective	Upper GI	275	39.6%	301 (warfarin)	45.8%
Horie *et al*[85]	2022	Japan	Retrospective	Esophagus	16[1]	13%	869[2]	0.3%[1]
Yoshio *et al*[88]	2017	Japan	Retrospective	Stomach	24	20.8%	73 (warfarin)	24.6%
Sanomura *et al*[89]	2018	Japan	Retrospective	Stomach	21	19.0%	40 (warfarin)	17.5%
Saito *et al*[90]	2020	Japan	Retrospective	Stomach	77	19.5%	66 (warfarin)	22.7%
Hatta *et al*[36]	2021	Japan	Retrospective	Stomach	253	17.0%	10,067	4.4%[1]
Tomida *et al*[84]	2021	Japan	Retrospective	Stomach	261	14%	467 (warfarin)	18%
Choi *et al*[91]	2021	Korea	Retrospective	Stomach	23	8.7%	1499	3.0%
Kagawa *et al*[37]	2022	Japan	Retrospective	Stomach	39	15.4%	752	4.3%[1]
Nagata *et al*[83]	2018	Japan	Retrospective	Lower GI	121	13.2%	111 (warfarin)	25.9%
Yamashita *et al*[92]	2018	Japan	Retrospective	Colon	9	22.0%	19 (warfarin)	26.3%
Ogiyama *et al*[93]	2020	Japan	Retrospective	Colon	43	23.3%	44 (warfarin)	11.4%
Harada *et al*[94]	2020	Japan	Retrospective	Colon	25	16.0%	26 (warfarin)	7.7%

[1]Included 2 endoscopic mucosal resection patients.
[2]Included no antithrombotic drug patients.
DOAC: Direct oral anticoagulants.

patients who received upper gastrointestinal ESD and 13.2% in those who received lower gastrointestinal ESD[83].

In a recent retrospective Japanese study of 261 patients with early-stage gastric cancer receiving DOACs, post-ESD bleeding occurred in 14% of patients, which is comparable to that in patients receiving warfarin (18%)[84]. Multivariate analysis demonstrated that age ≥ 65 (OR 2.96, 95%CI: 1.13-7.73), male sex (OR 2.12; 95%CI: 1.01–4.45), receiving multiple antithrombotic agents (OR 2.70, 95%CI: 1.74-4.21) and lesion size ≥ 20 mm (OR 1.67, 95%CI: 1.08-2.59) were independent risk factors for post-ESD bleeding in patients taking anticoagulants, and that cessation of anticoagulants without heparin-bridging therapy was associated with a low risk of bleeding (OR 0.32; 95%CI: 0.14–0.76). However, the multivariate analysis identified no significant independent increased risk factors for post-ESD bleeding and demonstrated that dabigatran was associated with a significantly lower risk of bleeding (OR 0.04, 95%CI: 0.16-0.97)[84]. Further, in a nationwide multicenter retrospective study of 10320 patients, multivariate analysis conducted by Hatta *et al*[36] showed that taking anticoagulants was an independent risk factor for post-ESD bleeding (OR 8.16; 95%CI: 4.74-14.04). Although the number of patients registered in each of these previous studies is relatively small (n = 21-261), both reported post-ESD bleeding in 8.7%-20.8% of gastric cancer patients receiving DOACs, considered to be equivalent to that in patients receiving warfarin (17.5%-22.7%) and higher than that in patients not receiving anticoagulants (Table 5).

Few studies have been conducted on esophageal, duodenal and colorectal ESD in patients receiving DOACs. Horie *et al*[85] reported that the post-endoscopic resection bleeding rate in esophageal cancer patients receiving DOACs (14 patients received ESD and 2 patients received EMR) was significantly higher than that in those not receiving antithrombotic drugs [13% (95%CI: 1.6%–38%) *vs* 0.3% (95%CI: 0.1%–1%), P = 0.003]. Moreover, the post-ESD bleeding rate in colorectal tumor patients receiving DOACs was 16.0%-23.3%, which is equivalent to that in those receiving warfarin (7.7%-26.3%) (Table 5).

Thus, despite the small number of DOAC patients who received ESD in previous studies, the post-ESD delayed bleeding rate appears to vary among different organs in patients not receiving DOACs, but not in patients receiving DOACs.

FUTURE OF ESD FOR PATIENTS RECEIVING DOACS

There is no doubt that patients receiving DOACs are at higher risk of post-ESD bleeding than patients not taking DOACs or receiving antithrombotic drugs. As mentioned above, although examining plasma DOAC level and anti-Xa activity in relation to CYP metabolic enzymes or glycoprotein transporter gene polymorphisms may serve as predictive markers for selecting DOAC patients with higher risk of post-ESD delayed bleeding, no studies have been conducted with such considerations. Although scoring

systems such as the BEST-J score are being developed to assess the risk of post-ESD delayed bleeding by stratifying multiple possible risk factors in clinical practice, we propose the need for a new scoring system that considers pharmacological parameters of DOACs, namely plasma DOAC level and anti-Xa activity.

DOACs is current recommended for not only patients with nonvalvular atrial fibrillation and venous thrombosis (VTE), but also those with cancer due to prevention of VTE by clinical guidelines[86]. Treatment or prophylaxis of VTE for patients with cancer must always balance the risk of incidence or recurrent VTE with the increased risk of major bleeding and take into consideration the consequences of these outcomes (including mortality, financial cost, quality of life)[86]. Developing a system that easily measures the anti–FXa activity and plasma level could be an important way to monitor the anticoagulant effect of DOACs and may help physicians to treat DOAC patients receiving ESD, endoscopic treatment, and surgical treatment and with cancer in clinical practice.

CONCLUSION

Post-ESD delayed bleeding for gastrointestinal tumors is a major adverse event, with an incidence of around 5%-8% for gastric cancer and 2%-4% for esophageal, duodenum and colorectal tumors. Of the many risk factors for bleeding, taking anticoagulants, including DOACs, is currently the biggest. In fact, the post-ESD bleeding rate in DOAC patients is 13% in esophageal cancer, 8.7%-20.8% in gastric cancer and 7.7%-26.3% in colorectal cancer. Compared with warfarin, the anticoagulant effects of which can be monitored using prothrombin time and international normalized ratio tests, there is currently no established method for monitoring the effects of DOACs. Thus, it is important to develop simple and accurate methods to evaluate the pharmacokinetics (*e.g.*, plasma DOAC level at trough and T_{max}) and pharmacodynamics (*e.g.*, anti-factor Xa activity) of DOACs. In the future, a scoring system that includes pharmacological parameters of DOACs may be useful for stratifying risk of post-ESD delayed bleeding in clinical practice.

FOOTNOTES

Author contributions: Sugimoto M wrote the paper; Sugimoto M, Murata M and Kawai T collected the data.

Supported by the Grant-in-Aid for Scientific Research in Japan, No. 21K07949.

Conflict-of-interest statement: All the authors report no relevant conflicts of interest for this article.

Country/Territory of origin: Japan

ORCID number: Mitsushige Sugimoto 0000-0002-9194-7392; Masaki Murata 0000-0002-4951-0584; Takashi Kawai 0000-0002-5320-8134.

S-Editor: Li L
L-Editor: A
P-Editor: Zhao S

REFERENCES

1 **Gotoda T**, Yamamoto H, Soetikno RM. Endoscopic submucosal dissection of early gastric cancer. *J Gastroenterol* 2006; **41**: 929-942 [PMID: 17096062 DOI: 10.1007/s00535-006-1954-3]

2 **Tanabe S**, Ishido K, Higuchi K, Sasaki T, Katada C, Azuma M, Naruke A, Kim M, Koizumi W. Long-term outcomes of endoscopic submucosal dissection for early gastric cancer: a retrospective comparison with conventional endoscopic resection in a single center. *Gastric Cancer* 2014; **17**: 130-136 [PMID: 23576197 DOI: 10.1007/s10120-013-0241-2]

3 **Ono H**, Yao K, Fujishiro M, Oda I, Nimura S, Yahagi N, Iishi H, Oka M, Ajioka Y, Ichinose M, Matsui T. Guidelines for endoscopic submucosal dissection and endoscopic mucosal resection for early gastric cancer. *Dig Endosc* 2016; **28**: 3-15 [PMID: 26234303 DOI: 10.1111/den.12518]

4 **Pimentel-Nunes P**, Libânio D, Bastiaansen BAJ, Bhandari P, Bisschops R, Bourke MJ, Esposito G, Lemmers A, Maselli R, Messmann H, Pech O, Pioche M, Vieth M, Weusten BLAM, van Hooft JE, Deprez PH, Dinis-Ribeiro M. Endoscopic

submucosal dissection for superficial gastrointestinal lesions: European Society of Gastrointestinal Endoscopy (ESGE) Guideline - Update 2022. *Endoscopy* 2022; **54**: 591-622 [PMID: 35523224 DOI: 10.1055/a-1811-7025]

5 **Tanaka S**, Kashida H, Saito Y, Yahagi N, Yamano H, Saito S, Hisabe T, Yao T, Watanabe M, Yoshida M, Kudo SE, Tsuruta O, Sugihara KI, Watanabe T, Saitoh Y, Igarashi M, Toyonaga T, Ajioka Y, Ichinose M, Matsui T, Sugita A, Sugano K, Fujimoto K, Tajiri H. JGES guidelines for colorectal endoscopic submucosal dissection/endoscopic mucosal resection. *Dig Endosc* 2015; **27**: 417-434 [PMID: 25652022 DOI: 10.1111/den.12456]

6 **Ishihara R**, Arima M, Iizuka T, Oyama T, Katada C, Kato M, Goda K, Goto O, Tanaka K, Yano T, Yoshinaga S, Muto M, Kawakubo H, Fujishiro M, Yoshida M, Fujimoto K, Tajiri H, Inoue H; Japan Gastroenterological Endoscopy Society Guidelines Committee of ESD/EMR for Esophageal Cancer. Endoscopic submucosal dissection/endoscopic mucosal resection guidelines for esophageal cancer. *Dig Endosc* 2020; **32**: 452-493 [PMID: 32072683 DOI: 10.1111/den.13654]

7 **Draganov PV**, Wang AY, Othman MO, Fukami N. AGA Institute Clinical Practice Update: Endoscopic Submucosal Dissection in the United States. *Clin Gastroenterol Hepatol* 2019; **17**: 16-25.e1 [PMID: 30077787 DOI: 10.1016/j.cgh.2018.07.041]

8 **Fujishiro M**, Yahagi N, Kakushima N, Kodashima S, Muraki Y, Ono S, Kobayashi K, Hashimoto T, Yamamichi N, Tateishi A, Shimizu Y, Oka M, Ogura K, Kawabe T, Ichinose M, Omata M. Successful nonsurgical management of perforation complicating endoscopic submucosal dissection of gastrointestinal epithelial neoplasms. *Endoscopy* 2006; **38**: 1001-1006 [PMID: 17058165 DOI: 10.1055/s-2006-944775]

9 **Tanaka M**, Ono H, Hasuike N, Takizawa K. Endoscopic submucosal dissection of early gastric cancer. *Digestion* 2008; **77** Suppl 1: 23-28 [PMID: 18204258 DOI: 10.1159/000111484]

10 **Cao Y**, Liao C, Tan A, Gao Y, Mo Z, Gao F. Meta-analysis of endoscopic submucosal dissection versus endoscopic mucosal resection for tumors of the gastrointestinal tract. *Endoscopy* 2009; **41**: 751-757 [PMID: 19693750 DOI: 10.1055/s-0029-1215053]

11 **Yoshizawa Y**, Sugimoto M, Sato Y, Sahara S, Ichikawa H, Kagami T, Hosoda Y, Kimata M, Tamura S, Kobayashi Y, Osawa S, Sugimoto K, Miyajima H, Furuta T. Factors associated with healing of artificial ulcer after endoscopic submucosal dissection with reference to Helicobacter pylori infection, CYP2C19 genotype, and tumor location: Multicenter randomized trial. *Dig Endosc* 2016; **28**: 162-172 [PMID: 26331711 DOI: 10.1111/den.12544]

12 **Otsuka T**, Sugimoto M, Ban H, Nakata T, Murata M, Nishida A, Inatomi O, Bamba S, Andoh A. Severity of gastric mucosal atrophy affects the healing speed of post-endoscopic submucosal dissection ulcers. *World J Gastrointest Endosc* 2018; **10**: 83-92 [PMID: 29774087 DOI: 10.4253/wjge.v10.i5.83]

13 **Yano T**, Tanabe S, Ishido K, Suzuki M, Kawanishi N, Yamane S, Watanabe A, Wada T, Azuma M, Katada C, Koizumi W. Different clinical characteristics associated with acute bleeding and delayed bleeding after endoscopic submucosal dissection in patients with early gastric cancer. *Surg Endosc* 2017; **31**: 4542-4550 [PMID: 28378078 DOI: 10.1007/s00464-017-5513-1]

14 **Sato C**, Hirasawa K, Koh R, Ikeda R, Fukuchi T, Kobayashi R, Kaneko H, Makazu M, Maeda S. Postoperative bleeding in patients on antithrombotic therapy after gastric endoscopic submucosal dissection. *World J Gastroenterol* 2017; **23**: 5557-5566 [PMID: 28852315 DOI: 10.3748/wjg.v23.i30.5557]

15 **Muto M**, Minashi K, Yano T, Saito Y, Oda I, Nonaka S, Omori T, Sugiura H, Goda K, Kaise M, Inoue H, Ishikawa H, Ochiai A, Shimoda T, Watanabe H, Tajiri H, Saito D. Early detection of superficial squamous cell carcinoma in the head and neck region and esophagus by narrow band imaging: a multicenter randomized controlled trial. *J Clin Oncol* 2010; **28**: 1566-1572 [PMID: 20177025 DOI: 10.1200/JCO.2009.25.4680]

16 **Dohi O**, Yagi N, Naito Y, Fukui A, Gen Y, Iwai N, Ueda T, Yoshida N, Kamada K, Uchiyama K, Takagi T, Konishi H, Yanagisawa A, Itoh Y. Blue laser imaging-bright improves the real-time detection rate of early gastric cancer: a randomized controlled study. *Gastrointest Endosc* 2019; **89**: 47-57 [PMID: 30189197 DOI: 10.1016/j.gie.2018.08.049]

17 **Ono S**, Kawada K, Dohi O, Kitamura S, Koike T, Hori S, Kanzaki H, Murao T, Yagi N, Sasaki F, Hashiguchi K, Oka S, Katada K, Shimoda R, Mizukami K, Suehiro M, Takeuchi T, Katsuki S, Tsuda M, Naito Y, Kawano T, Haruma K, Ishikawa H, Mori K, Kato M; LCI-FIND Trial Group. Linked Color Imaging Focused on Neoplasm Detection in the Upper Gastrointestinal Tract : A Randomized Trial. *Ann Intern Med* 2021; **174**: 18-24 [PMID: 33076693 DOI: 10.7326/M19-2561]

18 **Sugimoto M**, Koyama Y, Itoi T, Kawai T. Using texture and colour enhancement imaging to evaluate gastrointestinal diseases in clinical practice: a review. *Ann Med* 2022; **54**: 3315-3332 [PMID: 36420822 DOI: 10.1080/07853890.2022.2147992]

19 **Takizawa K**, Oda I, Gotoda T, Yokoi C, Matsuda T, Saito Y, Saito D, Ono H. Routine coagulation of visible vessels may prevent delayed bleeding after endoscopic submucosal dissection--an analysis of risk factors. *Endoscopy* 2008; **40**: 179-183 [PMID: 18322872 DOI: 10.1055/s-2007-995530]

20 **Muto M**, Katada C, Sano Y, Yoshida S. Narrow band imaging: a new diagnostic approach to visualize angiogenesis in superficial neoplasia. *Clin Gastroenterol Hepatol* 2005; **3**: S16-S20 [PMID: 16012987 DOI: 10.1016/s1542-3565(05)00262-4]

21 **Kim JS**, Kim BW, Shin IS. Efficacy and safety of endoscopic submucosal dissection for superficial squamous esophageal neoplasia: a meta-analysis. *Dig Dis Sci* 2014; **59**: 1862-1869 [PMID: 24619279 DOI: 10.1007/s10620-014-3098-2]

22 **Dubecz A**, Solymosi N, Stadlhuber RJ, Schweigert M, Stein HJ, Peters JH. Does the Incidence of Adenocarcinoma of the Esophagus and Gastric Cardia Continue to Rise in the Twenty-First Century? *J Gastrointest Surg* 2013 [PMID: 24234242 DOI: 10.1007/s11605-013-2345-8]

23 **Yang D**, Zou F, Xiong S, Forde JJ, Wang Y, Draganov PV. Endoscopic submucosal dissection for early Barrett's neoplasia: a meta-analysis. *Gastrointest Endosc* 2018; **87**: 1383-1393 [PMID: 28993137 DOI: 10.1016/j.gie.2017.09.038]

24 **Suzuki H**, Takizawa K, Hirasawa T, Takeuchi Y, Ishido K, Hoteya S, Yano T, Tanaka S, Endo M, Nakagawa M, Toyonaga T, Doyama H, Hirasawa K, Matsuda M, Yamamoto H, Fujishiro M, Hashimoto S, Maeda Y, Oyama T, Takenaka R, Yamamoto Y, Naito Y, Michida T, Kobayashi N, Kawahara Y, Hirano M, Jin M, Hori S, Niwa Y, Hikichi T, Shimazu T, Ono H, Tanabe S, Kondo H, Iishi H, Ninomiya M; Ichiro Oda for J-WEB/EGC group. Short-term outcomes of multicenter prospective cohort study of gastric endoscopic resection: 'Real-world evidence' in Japan. *Dig Endosc* 2019; **31**:

30-39 [PMID: 30058258 DOI: 10.1111/den.13246]

25 **Tanabe S**, Ishido K, Matsumoto T, Kosaka T, Oda I, Suzuki H, Fujisaki J, Ono H, Kawata N, Oyama T, Takahashi A, Doyama H, Kobayashi M, Uedo N, Hamada K, Toyonaga T, Kawara F, Tanaka S, Yoshifuku Y. Long-term outcomes of endoscopic submucosal dissection for early gastric cancer: a multicenter collaborative study. *Gastric Cancer* 2017; **20**: 45-52 [PMID: 27807641 DOI: 10.1007/s10120-016-0664-7]

26 **Zullo A**, Manta R, De Francesco V, Manfredi G, Buscarini E, Fiorini G, Vaira D, Marmo R. Endoscopic submucosal dissection of gastric neoplastic lesions in Western countries: systematic review and meta-analysis. *Eur J Gastroenterol Hepatol* 2021; **33**: e1-e6 [PMID: 32804845 DOI: 10.1097/MEG.0000000000001886]

27 **Tao M**, Zhou X, Hu M, Pan J. Endoscopic submucosal dissection versus endoscopic mucosal resection for patients with early gastric cancer: a meta-analysis. *BMJ Open* 2019; **9**: e025803 [PMID: 31874864 DOI: 10.1136/bmjopen-2018-025803]

28 **Libânio D**, Costa MN, Pimentel-Nunes P, Dinis-Ribeiro M. Risk factors for bleeding after gastric endoscopic submucosal dissection: a systematic review and meta-analysis. *Gastrointest Endosc* 2016; **84**: 572-586 [PMID: 27345132 DOI: 10.1016/j.gie.2016.06.033]

29 **Bureau**. MoIAaCS. Population estimates. [cited 3 April 2023]. Available from: http://wwwstatgojp/data/jinsui/

30 **Sugimoto M**, Hatta W, Tsuji Y, Yoshio T, Yabuuchi Y, Hoteya S, Doyama H, Nagami Y, Hikichi T, Kobayashi M, Morita Y, Sumiyoshi T, Iguchi M, Tomida H, Inoue T, Mikami T, Hasatani K, Nishikawa J, Matsumura T, Nebiki H, Nakamatsu D, Ohnita K, Suzuki H, Ueyama H, Hayashi Y, Murata M, Yamaguchi S, Michida T, Yada T, Asahina Y, Narasaka T, Kuribayashi S, Kiyotoki S, Mabe K, Fujishiro M, Masamune A, Kawai T. Risk Factors for Bleeding After Endoscopic Submucosal Dissection for Gastric Cancer in Elderly Patients Older Than 80 Years in Japan. *Clin Transl Gastroenterol* 2021; **12**: e00404 [PMID: 34644281 DOI: 10.14309/ctg.0000000000000404]

31 **Zou J**, Chai N, Linghu E, Zhai Y, Li Z, Du C, Li L. Clinical outcomes of endoscopic resection for non-ampullary duodenal laterally spreading tumors. *Surg Endosc* 2019; **33**: 4048-4056 [PMID: 30756173 DOI: 10.1007/s00464-019-06698-x]

32 **Inoue T**, Uedo N, Yamashina T, Yamamoto S, Hanaoka N, Takeuchi Y, Higashino K, Ishihara R, Iishi H, Tatsuta M, Takahashi H, Eguchi H, Ohigashi H. Delayed perforation: a hazardous complication of endoscopic resection for non-ampullary duodenal neoplasm. *Dig Endosc* 2014; **26**: 220-227 [PMID: 23621427 DOI: 10.1111/den.12104]

33 **Watanabe D**, Hayashi H, Kataoka Y, Hashimoto T, Ichimasa K, Miyachi H, Tanaka S, Toyonaga T. Efficacy and safety of endoscopic submucosal dissection for non-ampullary duodenal polyps: A systematic review and meta-analysis. *Dig Liver Dis* 2019; **51**: 774-781 [PMID: 31014942 DOI: 10.1016/j.dld.2019.03.021]

34 **Kato M**, Ochiai Y, Fukuhara S, Maehata T, Sasaki M, Kiguchi Y, Akimoto T, Fujimoto A, Nakayama A, Kanai T, Yahagi N. Clinical impact of closure of the mucosal defect after duodenal endoscopic submucosal dissection. *Gastrointest Endosc* 2019; **89**: 87-93 [PMID: 30055156 DOI: 10.1016/j.gie.2018.07.026]

35 **Fuccio L**, Hassan C, Ponchon T, Mandolesi D, Farioli A, Cucchetti A, Frazzoni L, Bhandari P, Bellisario C, Bazzoli F, Repici A. Clinical outcomes after endoscopic submucosal dissection for colorectal neoplasia: a systematic review and meta-analysis. *Gastrointest Endosc* 2017; **86**: 74-86.e17 [PMID: 28254526 DOI: 10.1016/j.gie.2017.02.024]

36 **Hatta W**, Tsuji Y, Yoshio T, Kakushima N, Hoteya S, Doyama H, Nagami Y, Hikichi T, Kobayashi M, Morita Y, Sumiyoshi T, Iguchi M, Tomida H, Inoue T, Koike T, Mikami T, Hasatani K, Nishikawa J, Matsumura T, Nebiki H, Nakamatsu D, Ohnita K, Suzuki H, Ueyama H, Hayashi Y, Sugimoto M, Yamaguchi S, Michida T, Yada T, Asahina Y, Narasaka T, Kuribasyashi S, Kiyotoki S, Mabe K, Nakamura T, Nakaya N, Fujishiro M, Masamune A. Prediction model of bleeding after endoscopic submucosal dissection for early gastric cancer: BEST-J score. *Gut* 2021; **70**: 476-484 [PMID: 32499390 DOI: 10.1136/gutjnl-2019-319926]

37 **Kagawa Y**, Fukuzawa M, Sugimoto M, Nemoto D, Muramatsu T, Shinohara H, Matsumoto T, Madarame A, Yamaguchi H, Uchida K, Morise T, Koyama Y, Sugimoto A, Yamauchi Y, Kono S, Naito S, Yamamoto K, Kishimoto Y, Inuyama M, Kawai T, Itoi T. Validation of the BEST-J score, a prediction model for bleeding after endoscopic submucosal dissection for early gastric cancer: a multicenter retrospective observational study. *Surg Endosc* 2022; **36**: 7240-7249 [PMID: 35194665 DOI: 10.1007/s00464-022-09096-y]

38 **Ban H**, Sugimoto M, Otsuka T, Murata M, Nakata T, Hasegawa H, Fukuda M, Inatomi O, Bamba S, Kushima R, Andoh A. Letter: a potassium-competitive acid blocker vs a proton pump inhibitor for healing endoscopic submucosal dissection-induced artificial ulcers after treatment of gastric neoplasms. *Aliment Pharmacol Ther* 2017; **46**: 564-565 [PMID: 28776744 DOI: 10.1111/apt.14202]

39 **Li R**, Cai S, Sun D, Shi Q, Ren Z, Qi Z, Li B, Yao L, Xu M, Zhou P, Zhong Y. Risk factors for delayed bleeding after endoscopic submucosal dissection of colorectal tumors. *Surg Endosc* 2021; **35**: 6583-6590 [PMID: 33237467 DOI: 10.1007/s00464-020-08156-5]

40 **Seo M**, Song EM, Cho JW, Lee YJ, Lee BI, Kim JS, Jeon SW, Jang HJ, Yang DH, Ye BD, Byeon JS. A risk-scoring model for the prediction of delayed bleeding after colorectal endoscopic submucosal dissection. *Gastrointest Endosc* 2019; **89**: 990-998.e2 [PMID: 30521794 DOI: 10.1016/j.gie.2018.11.029]

41 **Granger CB**, Alexander JH, McMurray JJ, Lopes RD, Hylek EM, Hanna M, Al-Khalidi HR, Ansell J, Atar D, Avezum A, Bahit MC, Diaz R, Easton JD, Ezekowitz JA, Flaker G, Garcia D, Geraldes M, Gersh BJ, Golitsyn S, Goto S, Hermosillo AG, Hohnloser SH, Horowitz J, Mohan P, Jansky P, Lewis BS, Lopez-Sendon JL, Pais P, Parkhomenko A, Verheugt FW, Zhu J, Wallentin L; ARISTOTLE Committees and Investigators. Apixaban versus warfarin in patients with atrial fibrillation. *N Engl J Med* 2011; **365**: 981-992 [PMID: 21870978 DOI: 10.1056/NEJMoa1107039]

42 **Hu PT**, Lopes RD, Stevens SR, Wallentin L, Thomas L, Alexander JH, Hanna M, Lewis BS, Verheugt FW, Granger CB, Jones WS. Efficacy and Safety of Apixaban Compared With Warfarin in Patients With Atrial Fibrillation and Peripheral Artery Disease: Insights From the ARISTOTLE Trial. *J Am Heart Assoc* 2017; **6** [PMID: 28096100 DOI: 10.1161/JAHA.116.004699]

43 **Easton JD**, Lopes RD, Bahit MC, Wojdyla DM, Granger CB, Wallentin L, Alings M, Goto S, Lewis BS, Rosenqvist M, Hanna M, Mohan P, Alexander JH, Diener HC; ARISTOTLE Committees and Investigators. Apixaban compared with warfarin in patients with atrial fibrillation and previous stroke or transient ischaemic attack: a subgroup analysis of the

ARISTOTLE trial. *Lancet Neurol* 2012; **11**: 503-511 [PMID: 22572202 DOI: 10.1016/S1474-4422(12)70092-3]
44 **Rose DK**, Bar B. Direct Oral Anticoagulant Agents: Pharmacologic Profile, Indications, Coagulation Monitoring, and Reversal Agents. *J Stroke Cerebrovasc Dis* 2018; **27**: 2049-2058 [PMID: 29753603 DOI: 10.1016/j.jstrokecerebrovasdis.2018.04.004]
45 **Conway SE**, Hwang AY, Ponte CD, Gums JG. Laboratory and Clinical Monitoring of Direct Acting Oral Anticoagulants: What Clinicians Need to Know. *Pharmacotherapy* 2017; **37**: 236-248 [PMID: 27983747 DOI: 10.1002/phar.1884]
46 **Cuker A**, Siegal DM, Crowther MA, Garcia DA. Laboratory measurement of the anticoagulant activity of the non-vitamin K oral anticoagulants. *J Am Coll Cardiol* 2014; **64**: 1128-1139 [PMID: 25212648 DOI: 10.1016/j.jacc.2014.05.065]
47 **Frost C**, Song Y, Barrett YC, Wang J, Pursley J, Boyd RA, LaCreta F. A randomized direct comparison of the pharmacokinetics and pharmacodynamics of apixaban and rivaroxaban. *Clin Pharmacol* 2014; **6**: 179-187 [PMID: 25419161 DOI: 10.2147/CPAA.S61131]
48 **Reilly PA**, Lehr T, Haertter S, Connolly SJ, Yusuf S, Eikelboom JW, Ezekowitz MD, Nehmiz G, Wang S, Wallentin L; RE-LY Investigators. The effect of dabigatran plasma concentrations and patient characteristics on the frequency of ischemic stroke and major bleeding in atrial fibrillation patients: the RE-LY Trial (Randomized Evaluation of Long-Term Anticoagulation Therapy). *J Am Coll Cardiol* 2014; **63**: 321-328 [PMID: 24076487 DOI: 10.1016/j.jacc.2013.07.104]
49 **Chen A**, Stecker E, A Warden B. Direct Oral Anticoagulant Use: A Practical Guide to Common Clinical Challenges. *J Am Heart Assoc* 2020; **9**: e017559 [PMID: 32538234 DOI: 10.1161/JAHA.120.017559]
50 **Derebail VK**, Rheault MN, Kerlin BA. Role of direct oral anticoagulants in patients with kidney disease. *Kidney Int* 2020; **97**: 664-675 [PMID: 32107019 DOI: 10.1016/j.kint.2019.11.027]
51 **Martin K**, Beyer-Westendorf J, Davidson BL, Huisman MV, Sandset PM, Moll S. Use of the direct oral anticoagulants in obese patients: guidance from the SSC of the ISTH. *J Thromb Haemost* 2016; **14**: 1308-1313 [PMID: 27299806 DOI: 10.1111/jth.13323]
52 **Lee SR**, Choi EK, Park CS, Han KD, Jung JH, Oh S, Lip GYH. Direct Oral Anticoagulants in Patients With Nonvalvular Atrial Fibrillation and Low Body Weight. *J Am Coll Cardiol* 2019; **73**: 919-931 [PMID: 30819360 DOI: 10.1016/j.jacc.2018.11.051]
53 **Fralick M**, Juurlink DN, Marras T. Bleeding associated with coadministration of rivaroxaban and clarithromycin. *CMAJ* 2016; **188**: 669-672 [PMID: 26811362 DOI: 10.1503/cmaj.150580]
54 **Mueck W**, Kubitza D, Becka M. Co-administration of rivaroxaban with drugs that share its elimination pathways: pharmacokinetic effects in healthy subjects. *Br J Clin Pharmacol* 2013; **76**: 455-466 [PMID: 23305158 DOI: 10.1111/bcp.12075]
55 **Ueshima S**, Hira D, Fujii R, Kimura Y, Tomitsuka C, Yamane T, Tabuchi Y, Ozawa T, Itoh H, Horie M, Terada T, Katsura T. Impact of ABCB1, ABCG2, and CYP3A5 polymorphisms on plasma trough concentrations of apixaban in Japanese patients with atrial fibrillation. *Pharmacogenet Genomics* 2017; **27**: 329-336 [PMID: 28678049 DOI: 10.1097/FPC.0000000000000294]
56 **Staatz CE**, Goodman LK, Tett SE. Effect of CYP3A and ABCB1 single nucleotide polymorphisms on the pharmacokinetics and pharmacodynamics of calcineurin inhibitors: Part I. *Clin Pharmacokinet* 2010; **49**: 141-175 [PMID: 20170205 DOI: 10.2165/11317350-000000000-00000]
57 **Ieiri I**. Functional significance of genetic polymorphisms in P-glycoprotein (MDR1, ABCB1) and breast cancer resistance protein (BCRP, ABCG2). *Drug Metab Pharmacokinet* 2012; **27**: 85-105 [PMID: 22123128 DOI: 10.2133/dmpk.dmpk-11-rv-098]
58 **Connolly SJ**, Ezekowitz MD, Yusuf S, Eikelboom J, Oldgren J, Parekh A, Pogue J, Reilly PA, Themeles E, Varrone J, Wang S, Alings M, Xavier D, Zhu J, Diaz R, Lewis BS, Darius H, Diener HC, Joyner CD, Wallentin L; RE-LY Steering Committee and Investigators. Dabigatran versus warfarin in patients with atrial fibrillation. *N Engl J Med* 2009; **361**: 1139-1151 [PMID: 19717844 DOI: 10.1056/NEJMoa0905561]
59 **Giugliano RP**, Ruff CT, Braunwald E, Murphy SA, Wiviott SD, Halperin JL, Waldo AL, Ezekowitz MD, Weitz JI, Špinar J, Ruzyllo W, Ruda M, Koretsune Y, Betcher J, Shi M, Grip LT, Patel SP, Patel I, Hanyok JJ, Mercuri M, Antman EM; ENGAGE AF-TIMI 48 Investigators. Edoxaban versus warfarin in patients with atrial fibrillation. *N Engl J Med* 2013; **369**: 2093-2104 [PMID: 24251359 DOI: 10.1056/NEJMoa1310907]
60 **Patel MR**, Mahaffey KW, Garg J, Pan G, Singer DE, Hacke W, Breithardt G, Halperin JL, Hankey GJ, Piccini JP, Becker RC, Nessel CC, Paolini JF, Berkowitz SD, Fox KA, Califf RM; ROCKET AF Investigators. Rivaroxaban versus warfarin in nonvalvular atrial fibrillation. *N Engl J Med* 2011; **365**: 883-891 [PMID: 21830957 DOI: 10.1056/NEJMoa1009638]
61 **Weitz JI**, Connolly SJ, Patel I, Salazar D, Rohatagi S, Mendell J, Kastrissios H, Jin J, Kunitada S. Randomised, parallel-group, multicentre, multinational phase 2 study comparing edoxaban, an oral factor Xa inhibitor, with warfarin for stroke prevention in patients with atrial fibrillation. *Thromb Haemost* 2010; **104**: 633-641 [PMID: 20694273 DOI: 10.1160/TH10-01-0066]
62 **Salazar DE**, Mendell J, Kastrissios H, Green M, Carrothers TJ, Song S, Patel I, Bocanegra TS, Antman EM, Giugliano RP, Kunitada S, Dornseif B, Shi M, Tachibana M, Zhou S, Rohatagi S. Modelling and simulation of edoxaban exposure and response relationships in patients with atrial fibrillation. *Thromb Haemost* 2012; **107**: 925-936 [PMID: 22398655 DOI: 10.1160/TH11-08-0566]
63 **Sakaguchi T**, Osanai H, Murase Y, Ishii H, Nakashima Y, Asano H, Suzuki S, Takefuji M, Inden Y, Sakai K, Murohara T, Ajioka M. Monitoring of anti-Xa activity and factors related to bleeding events: A study in Japanese patients with nonvalvular atrial fibrillation receiving rivaroxaban. *J Cardiol* 2017; **70**: 244-249 [PMID: 28017463 DOI: 10.1016/j.jjcc.2016.11.013]
64 **Sin CF**, Wong KP, Wong HM, Siu CW, Yap DYH. Plasma Rivaroxaban Level in Patients With Early Stages of Chronic Kidney Disease-Relationships With Renal Function and Clinical Events. *Front Pharmacol* 2022; **13**: 888660 [PMID: 35662694 DOI: 10.3389/fphar.2022.888660]
65 **Chan EW**, Lau WC, Leung WK, Mok MT, He Y, Tong TS, Wong IC. Prevention of Dabigatran-Related Gastrointestinal Bleeding With Gastroprotective Agents: A Population-Based Study. *Gastroenterology* 2015; **149**: 586-95.e3 [PMID: 25960019 DOI: 10.1053/j.gastro.2015.05.002]

66 **Ollier E**, Hodin S, Basset T, Accassat S, Bertoletti L, Mismetti P, Delavenne X. In vitro and in vivo evaluation of drug-drug interaction between dabigatran and proton pump inhibitors. *Fundam Clin Pharmacol* 2015; **29**: 604-614 [PMID: 26392328 DOI: 10.1111/fcp.12154]

67 **Bolek T**, Samoš M, Škorňová I, Galajda P, Staško J, Kubisz P, Mokáň M. Proton Pump Inhibitors and Dabigatran Therapy: Impact on Gastric Bleeding and Dabigatran Plasma Levels. *Semin Thromb Hemost* 2019; **45**: 846-850 [PMID: 31537027 DOI: 10.1055/s-0039-1695735]

68 **Desai J**, Granger CB, Weitz JI, Aisenberg J. Novel oral anticoagulants in gastroenterology practice. *Gastrointest Endosc* 2013; **78**: 227-239 [PMID: 23725876 DOI: 10.1016/j.gie.2013.04.179]

69 **Garcia DA**, Regan S, Henault LE, Upadhyay A, Baker J, Othman M, Hylek EM. Risk of thromboembolism with short-term interruption of warfarin therapy. *Arch Intern Med* 2008; **168**: 63-69 [PMID: 18195197 DOI: 10.1001/archinternmed.2007.23]

70 **Fujimoto K**, Fujishiro M, Kato M, Higuchi K, Iwakiri R, Sakamoto C, Uchiyama S, Kashiwagi A, Ogawa H, Murakami K, Mine T, Yoshino J, Kinoshita Y, Ichinose M, Matsui T; Japan Gastroenterological Endoscopy Society. Guidelines for gastroenterological endoscopy in patients undergoing antithrombotic treatment. *Dig Endosc* 2014; **26**: 1-14 [PMID: 24215155 DOI: 10.1111/den.12183]

71 **Kato M**, Uedo N, Hokimoto S, Ieko M, Higuchi K, Murakami K, Fujimoto K. Guidelines for Gastroenterological Endoscopy in Patients Undergoing Antithrombotic Treatment: 2017 Appendix on Anticoagulants Including Direct Oral Anticoagulants. *Dig Endosc* 2018; **30**: 433-440 [PMID: 29733468 DOI: 10.1111/den.13184]

72 **Veitch AM**, Radaelli F, Alikhan R, Dumonceau JM, Eaton D, Jerrome J, Lester W, Nylander D, Thoufeeq M, Vanbiervliet G, Wilkinson JR, Van Hooft JE. Endoscopy in patients on antiplatelet or anticoagulant therapy: British Society of Gastroenterology (BSG) and European Society of Gastrointestinal Endoscopy (ESGE) guideline update. *Gut* 2021; **70**: 1611-1628 [PMID: 34362780 DOI: 10.1136/gutjnl-2021-325184]

73 **ASGE Standards of Practice Committee**, Acosta RD, Abraham NS, Chandrasekhara V, Chathadi KV, Early DS, Eloubeidi MA, Evans JA, Faulx AL, Fisher DA, Fonkalsrud L, Hwang JH, Khashab MA, Lightdale JR, Muthusamy VR, Pasha SF, Saltzman JR, Shaukat A, Shergill AK, Wang A, Cash BD, DeWitt JM. The management of antithrombotic agents for patients undergoing GI endoscopy. *Gastrointest Endosc* 2016; **83**: 3-16 [PMID: 26621548 DOI: 10.1016/j.gie.2015.09.035]

74 **Lim H**, Gong EJ, Min BH, Kang SJ, Shin CM, Byeon JS, Choi M, Park CG, Cho JY, Lee ST, Kim HG, Chun HJ. Clinical Practice Guideline for the Management of Antithrombotic Agents in Patients Undergoing Gastrointestinal Endoscopy. *Clin Endosc* 2020; **53**: 663-677 [PMID: 33242928 DOI: 10.5946/ce.2020.192]

75 **Chan FKL**, Goh KL, Reddy N, Fujimoto K, Ho KY, Hokimoto S, Jeong YH, Kitazono T, Lee HS, Mahachai V, Tsoi KKF, Wu MS, Yan BP, Sugano K. Management of patients on antithrombotic agents undergoing emergency and elective endoscopy: joint Asian Pacific Association of Gastroenterology (APAGE) and Asian Pacific Society for Digestive Endoscopy (APSDE) practice guidelines. *Gut* 2018; **67**: 405-417 [PMID: 29331946 DOI: 10.1136/gutjnl-2017-315131]

76 **Dunn A**. Perioperative management of oral anticoagulation: when and how to bridge. *J Thromb Thrombolysis* 2006; **21**: 85-89 [PMID: 16475048 DOI: 10.1007/s11239-006-5582-9]

77 **Siegal D**, Yudin J, Kaatz S, Douketis JD, Lim W, Spyropoulos AC. Periprocedural heparin bridging in patients receiving vitamin K antagonists: systematic review and meta-analysis of bleeding and thromboembolic rates. *Circulation* 2012; **126**: 1630-1639 [PMID: 22912386 DOI: 10.1161/CIRCULATIONAHA.112.105221]

78 **Beyer-Westendorf J**, Gelbricht V, Förster K, Ebertz F, Köhler C, Werth S, Kuhlisch E, Stange T, Thieme C, Daschkow K, Weiss N. Peri-interventional management of novel oral anticoagulants in daily care: results from the prospective Dresden NOAC registry. *Eur Heart J* 2014; **35**: 1888-1896 [PMID: 24394381 DOI: 10.1093/eurheartj/eht557]

79 **Shindo Y**, Matsumoto S, Miyatani H, Yoshida Y, Mashima H. Risk factors for postoperative bleeding after gastric endoscopic submucosal dissection in patients under antithrombotics. *World J Gastrointest Endosc* 2016; **8**: 349-356 [PMID: 27076874 DOI: 10.4253/wjge.v8.i7.349]

80 **Yamamoto Y**, Kikuchi D, Nagami Y, Nonaka K, Tsuji Y, Fujimoto A, Sanomura Y, Tanaka K, Abe S, Zhang S, De Lusong MA, Uedo N. Management of adverse events related to endoscopic resection of upper gastrointestinal neoplasms: Review of the literature and recommendations from experts. *Dig Endosc* 2019; **31** Suppl 1: 4-20 [PMID: 30994225 DOI: 10.1111/den.13388]

81 **Jaruvongvanich V**, Sempokuya T, Wijarnpreecha K, Ungprasert P. Continued versus interrupted aspirin use and bleeding risk after endoscopic submucosal dissection of gastric neoplasms: a meta-analysis. *Ann Gastroenterol* 2018; **31**: 344-349 [PMID: 29720860 DOI: 10.20524/aog.2018.0251]

82 **Dong J**, Wei K, Deng J, Zhou X, Huang X, Deng M, Lü M. Effects of antithrombotic therapy on bleeding after endoscopic submucosal dissection. *Gastrointest Endosc* 2017; **86**: 807-816 [PMID: 28732709 DOI: 10.1016/j.gie.2017.07.017]

83 **Nagata N**, Yasunaga H, Matsui H, Fushimi K, Watanabe K, Akiyama J, Uemura N, Niikura R. Therapeutic endoscopy-related GI bleeding and thromboembolic events in patients using warfarin or direct oral anticoagulants: results from a large nationwide database analysis. *Gut* 2018; **67**: 1805-1812 [PMID: 28874418 DOI: 10.1136/gutjnl-2017-313999]

84 **Tomida H**, Yoshio T, Igarashi K, Morita Y, Oda I, Inoue T, Hikichi T, Sumiyoshi T, Doyama H, Tsuji Y, Nishikawa J, Hatta W, Mikami T, Iguchi M, Sumiyama K, Yamamoto K, Kitamura K, Kuribayashi S, Yanagitani A, Uraoka T, Yada T, Hasatani K, Kawaguchi K, Fujita T, Nishida T, Hiasa Y, Fujishiro M; FIGHT-Japan Study Group. Influence of anticoagulants on the risk of delayed bleeding after gastric endoscopic submucosal dissection: a multicenter retrospective study. *Gastric Cancer* 2021; **24**: 179-189 [PMID: 32683602 DOI: 10.1007/s10120-020-01105-0]

85 **Horie Y**, Horiuchi Y, Ishiyama A, Tsuchida T, Yoshimizu S, Hirasawa T, Fujisaki J, Maetani I, Yoshio T. The effect of antithrombotic drug use on delayed bleeding with esophageal endoscopic resection. *J Gastroenterol Hepatol* 2022; **37**: 1792-1800 [PMID: 35844140 DOI: 10.1111/jgh.15944]

86 **Lyman GH**, Carrier M, Ay C, Di Nisio M, Hicks LK, Khorana AA, Leavitt AD, Lee AYY, Macbeth F, Morgan RL, Noble S, Sexton EA, Stenehjem D, Wiercioch W, Kahale LA, Alonso-Coello P. American Society of Hematology 2021 guidelines for management of venous thromboembolism: prevention and treatment in patients with cancer. *Blood Adv* 2021; **5**: 927-974 [PMID: 33570602 DOI: 10.1182/bloodadvances.2020003442]

87 **Samoš M**, Bolek T, Stančiaková L, Péč MJ, Brisudová K, Škorňová I, Staško J, Mokáň M, Kubisz P. Tailored Direct Oral Anticoagulation in Patients with Atrial Fibrillation: The Future of Oral Anticoagulation? *J Clin Med* 2022; **11** [PMID: 36362597 DOI: 10.3390/jcm11216369]

88 **Yoshio T**, Tomida H, Iwasaki R, Horiuchi Y, Omae M, Ishiyama A, Hirasawa T, Yamamoto Y, Tsuchida T, Fujisaki J, Yamada T, Mita E, Ninomiya T, Michitaka K, Igarashi M. Effect of direct oral anticoagulants on the risk of delayed bleeding after gastric endoscopic submucosal dissection. *Dig Endosc* 2017; **29**: 686-694 [PMID: 28295638 DOI: 10.1111/den.12859]

89 **Sanomura Y**, Oka S, Tanaka S, Yorita N, Kuroki K, Kurihara M, Mizumoto T, Yoshifuku Y, Chayama K. Taking Warfarin with Heparin Replacement and Direct Oral Anticoagulant Is a Risk Factor for Bleeding after Endoscopic Submucosal Dissection for Early Gastric Cancer. *Digestion* 2018; **97**: 240-249 [PMID: 29421806 DOI: 10.1159/000485026]

90 **Saito H**, Igarashi K, Hirasawa D, Okuzono T, Suzuki K, Abe Y, Nawata Y, Tanaka Y, Tanaka I, Unno S, Nishikawa Y, Tsubokura M, Nakahori M, Chonan A, Matsuda T. The risks and characteristics of the delayed bleeding after endoscopic submucosal dissection for early gastric carcinoma in cases with anticoagulants. *Scand J Gastroenterol* 2020; **55**: 1253-1260 [PMID: 32924673 DOI: 10.1080/00365521.2020.1817542]

91 **Choi J**, Cho SJ, Na SH, Lee A, Kim JL, Chung H, Kim SG. Use of direct oral anticoagulants does not significantly increase delayed bleeding after endoscopic submucosal dissection for early gastric neoplasms. *Sci Rep* 2021; **11**: 9399 [PMID: 33931685 DOI: 10.1038/s41598-021-88656-z]

92 **Yamashita K**, Oka S, Tanaka S, Boda K, Hirano D, Sumimoto K, Mizumoto T, Ninomiya Y, Tamaru Y, Shigita K, Hayashi N, Sanomura Y, Chayama K. Use of anticoagulants increases risk of bleeding after colorectal endoscopic submucosal dissection. *Endosc Int Open* 2018; **6**: E857-E864 [PMID: 29978006 DOI: 10.1055/a-0593-5788]

93 **Ogiyama H**, Inoue T, Maekawa A, Yoshii S, Yamaguchi S, Nagai K, Yamamoto M, Egawa S, Horimoto M, Ogawa H, Nishihara A, Komori M, Kizu T, Tsutsui S, Tsujii Y, Hayashi Y, Iijima H, Takehara T. Effect of anticoagulants on the risk of delayed bleeding after colorectal endoscopic submucosal dissection. *Endosc Int Open* 2020; **8**: E1654-E1663 [PMID: 33140021 DOI: 10.1055/a-1244-2097]

94 **Harada H**, Nakahara R, Murakami D, Suehiro S, Nagasaka T, Ujihara T, Sagami R, Katsuyama Y, Hayasaka K, Tounou S, Amano Y. The effect of anticoagulants on delayed bleeding after colorectal endoscopic submucosal dissection. *Surg Endosc* 2020; **34**: 3330-3337 [PMID: 31482349 DOI: 10.1007/s00464-019-07101-5]

World Journal of Gastroenterology

Submit a Manuscript: https://www.f6publishing.com

World J Gastroenterol 2023 May 21; 29(19): 2932-2949

DOI: 10.3748/wjg.v29.i19.2932

ISSN 1007-9327 (print) ISSN 2219-2840 (online)

ORIGINAL ARTICLE

Basic Study

TATA-box-binding protein-associated factor 15 is a novel biomarker that promotes cell proliferation and migration in gastrointestinal stromal tumor

Cheng-Ming Guo, Li Tang, Xu Li, Liu-Ye Huang

Specialty type: Gastroenterology and hepatology

Provenance and peer review: Unsolicited article; Externally peer reviewed.

Peer-review model: Single blind

Peer-review report's scientific quality classification

Grade A (Excellent): 0
Grade B (Very good): B
Grade C (Good): C
Grade D (Fair): 0
Grade E (Poor): 0

P-Reviewer: Li S, China; Mankotia DS, India

Received: November 28, 2022
Peer-review started: November 28, 2022
First decision: February 15, 2023
Revised: March 6, 2023
Accepted: April 11, 2023
Article in press: April 11, 2023
Published online: May 21, 2023

Cheng-Ming Guo, Li Tang, Xu Li, Liu-Ye Huang, Department of Gastroenterology, The Affiliated Yantai Yuhuangding Hospital of Qingdao University, Yantai 264000, Shandong Province, China

Corresponding author: Liu-Ye Huang, Professor, Academic Research, Chief Doctor, Chief Physician, Research Scientist, Department of Gastroenterology, The Affiliated Yantai Yuhuangding Hospital of Qingdao University, No. 20 Yuhuangding East Road, Yantai 264000, Shandong Province, China. liuye_huang@163.com

Abstract

BACKGROUND

Gastrointestinal stromal tumor (GIST) is a common neoplasm with high rates of recurrence and metastasis, and its therapeutic efficacy is still not ideal. There is an unmet need to find new molecular therapeutic targets for GIST. TATA-box-binding protein-associated factor 15 (TAF15) contributes to the progress of various tumors, while the role and molecular mechanism of TAF15 in GIST progression are still unknown.

AIM

To explore new molecular therapeutic targets for GIST and understand the biological role and underlying mechanisms of TAF15 in GIST progression.

METHODS

Proteomic analysis was performed to explore the differentially expressed proteins in GIST. Western blotting and immunohistochemical analysis were used to verify the expression level of TAF15 in GIST tissues and cell lines. Cell counting kit-8, colony formation, wound-healing and transwell assay were executed to detect the ability of TAF15 on cell proliferation, migration and invasion. A xenograft mouse model was applied to explore the role of TAF15 in the progression of GIST. Western blotting was used to detect the phosphorylation level and total level of RAF1, MEK and ERK1/2.

RESULTS

A total of 1669 proteins were identified as differentially expressed proteins with 762 upregulated and 907 downregulated in GIST. TAF15 was selected for the further study because of its important role in cell proliferation and migration.

TAF15 was significantly over expressed in GIST tissues and cell lines. Overexpression of TAF15 was associated with larger tumor size and higher risk stage of GIST. TAF15 knockdown significantly inhibited the cell proliferation and migration of GIST *in vitro* and suppressed tumor growth *in vivo*. Moreover, the inhibition of TAF15 expression significantly decreased the phosphorylation level of RAF1, MEK and ERK1/2 in GIST cells and xenograft tissues, while the total RAF1, MEK and ERK1/2 had no significant change.

CONCLUSION

TAF15 is over expressed in GIST tissues and cell lines. Overexpression of TAF15 was associated with a poor prognosis of GIST patients. TAF15 promotes cell proliferation and migration in GIST *via* the activation of the RAF1/MEK/ERK signaling pathway. Thus, TAF15 is expected to be a novel latent molecular biomarker or therapeutic target of GIST.

Key Words: Gastrointestinal stromal tumor; Proteomics; TATA-box-binding protein-associated factor 15; Biomarker; Cell proliferation; Cell migration

Core Tip: TATA-box-binding protein-associated factor 15 (TAF15) was upregulated in gastrointestinal stromal tumor (GIST) cells and tissues and was associated with a poor prognosis in GIST patients. TAF15 promotes cell proliferation and migration of GIST *in vitro* and tumor growth *in vivo via* the activation of the RAF1/MEK/ERK signaling pathway. Therefore, TAF15 is expected to be a novel potential molecular biomarker or therapeutic target of GIST.

Citation: Guo CM, Tang L, Li X, Huang LY. TATA-box-binding protein-associated factor 15 is a novel biomarker that promotes cell proliferation and migration in gastrointestinal stromal tumor. *World J Gastroenterol* 2023; 29(19): 2932-2949

URL: https://www.wjgnet.com/1007-9327/full/v29/i19/2932.htm

DOI: https://dx.doi.org/10.3748/wjg.v29.i19.2932

INTRODUCTION

Gastrointestinal stromal tumor (GIST) is a common neoplasm that arises from the mesenchymal tissue of the gastrointestinal tract and likely originates from the interstitial cells of Cajal[1,2]. Mutations in mast/stem cell growth factor receptor (KIT) and platelet-derived growth factor receptor A (PDGFRA) are considered the primary causes in the pathogenesis of GIST[3]. GIST most commonly occurs in the stomach (50%-60%) and small intestine (30%-35%) but rarely occurs in the colorectum (5%) and esophagus (< 1%)[4]. Previous studies have indicated that GIST accounts for roughly 0.1%-3.0% of gastrointestinal malignances, and 15%-50% of patients present with metastasis at the time of diagnosis [5].

In clinical practice, GIST is liable to recur and distantly metastasize even after the initial tumor excision[6]. In fact, about 40% of patients develop tumor metastasis within 15 years after surgery[7], with a strong tendency to metastasize to the liver and peritoneal surfaces primarily and the lymph nodes and lung less frequently[4,8]. Based on tumor size, mitotic count, tumor site, and tumor rupture, the modified National Institutes of Health (NIH) consensus criteria stratifies GIST into four subgroups: Very low (NIH-VL), low (NIH-L), intermediate (NIH-I), and high risk (NIH-H)[9]. GIST patients with large sized tumors and high mitotic counts are more likely to metastasize to the liver and abdominal cavity and frequently have poor disease-free survival ratios[10].

Before the clinical application of imatinib, a tyrosine kinase inhibitor, surgical resection was the only accepted therapy that could prolong the life of GIST patients who had developed metastasis. Even then, the 5-year overall survival rate of patients was only 27%–34%[11]. Improved treatment with imatinib has been highly effective in advanced or metastatic GIST patients, and approximately 80% of them can reach complete or partial recovery[12,13]. Unfortunately, high rates of drug resistance due to secondary mutations of KIT have rendered imatinib therapy ineffective in recent years[14]. Taken together, the current research shows that the therapeutic efficacy of GIST treatments are still not ideal. Therefore, finding new molecular therapeutic targets for GIST is critical.

In this study, we implemented a proteomic analysis in GIST patients using tandem mass tag (TMT) labeling 10-plex kits to explore potential molecular therapeutic targets for GIST. A total of 4111 proteins were quantified in the GIST samples. Of these, 1669 were identified as significant differentially expressed proteins (DEPs), with 762 upregulated and 907 downregulated proteins. After a systematic

analysis of the top 10 upregulated or downregulated proteins, we selected TATA-box-binding protein-associated factor 15 (TAF15) for further study because of its important role in cell proliferation and migration[15]. TAF15 is a member of the FUS/Ewing sarcoma protein (EWS)/TAF15 (FET) family of RNA- and DNA-binding proteins, which plays an essential role in mRNA transcription, RNA splicing and polyadenylation[16-18].

Previous studies have demonstrated that TAF15 can influence a large number of genes that are closely related to the cell cycle and cell death and that overexpression of TAF15 can promote proliferation in sarcomas, human neuroblastoma and leukemia cells[17,19]. TAF15 mediates resistance to radiation therapy through inhibiting tumor suppressors p53 and p21, and upregulation of TAF15 is closely related to worsened survival in non-small cell lung cancer patients[20]. Additionally, a prior study has described a human anti-TAF15 antibody, PAT-BA4, that targeted a tumor-specific TAF15 antigen and then inhibited cell adhesion and spreading in gastric cancer[21]. Moreover, in a recent study, TAF15 activated the mitogen-activated protein kinase (MAPK) signaling pathway by upregulating the expression of MAPK6 in lung squamous cell carcinoma[22]. Taken together, TAF15 may play an important role in the progression of human cancers. However, the latent functions and molecular mechanism of TAF15 in GIST progression are still unclear and must be further studied.

MATERIALS AND METHODS

Clinical sample collection

One hundred and sixty one patients with GIST were recruited from the Department of Gastrointestinal Surgery, Yantai Yu Huang Ding Hospital of Qing Dao University from March 2020 to June 2022, with ethical permission from the Biomedical Ethics Committee (No.2019–410). All patients were diagnosed with GIST by two independent pathologists based on Chinese clinical guidelines[23]. No patients had received chemotherapy before surgery. Out of the 161 cases, 18 cases had matched tumor (T) and normal (N) tissue samples, and the clinicopathologic features of the paired GIST samples were documented in Table 1. In the remaining 143 cases, only tissue from the tumor site was available. In the beginning we only collected 12 matched samples, which were sent for proteomic analysis, followed by another 6 matched samples. All specimens were immediately frozen in liquid nitrogen within 30 min after excision. All patients provided written informed consent.

Protein extraction and digestion

Tissues from GIST patients were homogenized in RIPA lysis buffer containing protease inhibitors using a mortar and pestle. After homogenizing lightly for 1 min on ice, the lysate was centrifuged twice at 13000 RPM for 10 min at 4 °C, and then the supernatants were transferred to a fresh tube. A BCA assay kit (catalog no.P0010, Beyotime Biotechnology, Shanghai, China) was used to measure the protein concentration of each sample. The protein content of each sample was reduced using 5 mmol/L DL-dithiothreitol at 55 °C for 30 min. Samples were then incubated with 10 mmol/L of iodoacetamide at room temperature for 15 min in the dark to alkylate the protein. Each protein sample was dissolved using triethylammonium bicarbonate buffer and then digested overnight at 37 °C using trypsin.

TMT labeling and fractionation

Tryptic peptides from each sample were labeled with TMT (Thermo Fisher Scientific, Waltham, MA, United States) kits following the manufacturer's protocol. After quenching the reaction using 5% hydroxylamine (Sigma-Aldrich, Saint Louis, MO, United States), the TMT-labeled peptide solution was fractionated using basic pH reversed phase high performance liquid chromatography through an Agilent Zorbax Extend C18 column (5 μm, 150 mm × 2.1 mm). The mobile phase consisted of Buffer A (98% water with 2% acetonitrile) and Buffer B (90% acetonitrile with 10% water). The procedure gradient was run as follows: 0%-8% Buffer B for 0-10 min; 8%-35% Buffer B for 10-80 min; 35%-60% Buffer B for 80-95 min; 60%-70% Buffer B for 95-105 min; 70%-100% Buffer B for 105-120 min. The flow rate was set at 1 mL/min. TMT labeled peptides were separated into 10 fractions by reversed phase high performance liquid chromatography.

Liquid chromatography-tandem mass spectrometry analysis

Liquid chromatography-tandem mass spectrometry (MS) analysis was conducted on a Q Exactive Mass Spectrometer (Thermo Scientific) coupled to an EASY-nanoLC System (Thermo Fisher Scientific). Peptides were loaded onto a reverse-phase C18 column (Thermo Scientific Easy Column, 10 cm long, 75 μm inner diameter, 3μm resin) in Buffer A (0.1% formic acid) and separated with a linear gradient of Buffer B (84% acetonitrile and 0.1% formic acid) at a flow rate of 300 nL/min. The MS was utilized in positive ion mode. MS data were acquired following a data-dependent top10 method, dynamically selecting the most abundant precursor ions from the survey scan (300–1800 m/z). The automatic gain control target was set to $3e^6$ with maximum inject time to 10 ms. Survey scans were acquired from a resolution of 70000 at m/z 200 with an isolation width of 2 m/z.

Table 1 Clinicopathologic features of the collected paired gastrointestinal stromal tumors samples

Case No.	Sex	Age in yr	Location	Tumor size length × width × height in cm	Mitosis count, per 50 HFPs	Risk classification based on NIH
1	Male	74	Stomach	2.8 × 2.8 × 2.0	> 5	High
2	Female	24	Stomach	6.0 × 4.0 × 5.0	> 5	High
3	Male	69	Stomach	7.5 × 5.5 × 4.0	> 10	High
4	Male	46	Small intestine	6.5 × 5.0 × 4.0	> 5	High
5	Female	65	Small intestine	6.5 × 5.5 × 5.0	> 5	High
6	Female	61	Stomach	5.5 × 3.5 × 4.0	> 5	High
7	Female	49	Stomach	8.5 × 8.0 × 7.0	< 5	Intermediate
8	Male	77	Stomach	6.0 × 6.0 × 5.0	< 5	Intermediate
9	Female	54	Stomach	6.0 × 4.5 × 3.5	< 5	Intermediate
10	Female	43	Stomach	5.5 × 4.5 × 3.0	< 5	Intermediate
11	Male	70	Stomach	7.0 × 7.0 × 5.5	< 5	Intermediate
12	Female	55	Stomach	8.0 × 8.0 × 7.0	< 5	Intermediate
13	Male	63	Small intestine	5.0 × 3.5 × 3.0	< 5	Low
14	Male	67	Stomach	2.3 × 1.5 × 1.5	< 5	Low
15	Male	44	Stomach	3.0 × 2.7 × 1.3	< 5	Low
16	Female	49	Stomach	1.0 × 0.8 × 0.8	< 5	Very low
17	Female	66	Stomach	2.0 × 1.8 × 1.0	< 5	Very low
18	Female	57	Stomach	2.0 × 1.8 × 1.5	< 5	Very low

HPF: High-powered field; NIH: National Institutes of Health.

Data processing and analysis

Data for each sample were processed using the Swiss-Prot *Homo sapiens* database (20413 entries, January 14, 2017). The parameters of the procedures were as follows: Cysteine carbamidomethylation was set to fixed modification; oxidation was set to variable modification; peptide mass tolerance was 20 ppm, trypsin digestion, max 2 missed cleavages; and the false discovery rate was less than 1%. Proteins with a fold change of > 1.2 or < 0.83 and a P value < 0.05 were identified as significantly upregulated or downregulated.

Western blotting analysis

Western blot analysis was performed using 10% sodium dodecyl sulfonate-polyacrylamide gel electrophoresis to separate equal amounts (25 μg/load) of protein samples. Protein samples were transferred onto polyvinylidenedifluoride membranes. The membranes were blocked at room temperature for 1 h with 5% nonfat milk in TBS-T buffer and subsequently incubated with primary antibodies at 4 °C overnight. Secondary antibodies were incubated for 1 hat room temperature. Protein samples were visualized using ECL reagents (MA0186, Meilunbio, Dalian, China) using the ChemiScope 6200 Touch Imaging System (CLINX, Shanghai, China). Some membranes were recycled using stripping buffer (SL1340, Coolaber, Beijing, China) and incubated with other primary antibodies. The primary antibodies were used and obtained as follows: TAF15 (1:3000, ab134916, Abcam, United States); GAPDH (1:5000, D110016, Sangon Biotech, Shanghai, China); RAF1 (1:500, D155090, Sangon Biotech, Shanghai, China); p-RAF1 (1:1000, 66592-1-lg, Proteintech, Wuhan, China); MEK1/2 (1:1000, 11049-1-AP, Proteintech, Wuhan, China); p-MEK1 (1:1000, 28930-1-AP, Proteintech, Wuhan, China); ERK1/2 (1:1000, 16443-1-AP, Proteintech, Wuhan, China); and p-ERK1/2 (1:1000, 28733-1-AP, Proteintech, Wuhan, China). The secondary antibodies were used and obtained as follows: HRP goat anti-rabbit immunoglobulin G (IgG) (1:3000, D110058, Sangon Biotech, shanghai, China); and HRP goat anti-mouse IgG (1:3000, D110058, Sangon Biotech, Shanghai, China). Three independent tests were performed.

Immunohistochemistry

Tissue specimens were cut into 4 μm sections and processed by deparaffinization and rehydration. Slides were incubated with 3% hydrogen peroxide for 20 min at room temperature to block endogenous peroxidase activity. Tissue sections were incubated with primary antibody TAF15 (1:100, ab134916, Abcam, United States) at 4 °C in a wet chamber overnight and then incubated with secondary antibody HRP goat anti-rabbit IgG (1:100, D110058, Sangon Biotech, Shanghai, China) for 1 h in a wet chamber at room temperature. Color was developed using diaminobenzidine and hematoxylin. Two independent pathologists evaluated the samples by randomly selecting and evaluating five × 400 microscopic fields per slide. The percentage of stained tumor cells was scored as follows: 0, < 5% positive cells; 1, 5%-24% positive cells; 2, 25%-49% positive cells; 3, 50%-74% positive cells; and 4, ≥ 75% positive cells. The staining intensity was scored as follows: 0 for absence; 1 for weak; 2 for moderate; and 3 for strong. The total stained index was equivalent to intensity score × positive score. A total score ≥ 4 was considered positive expression, and < 4 was treated as negative expression.

Cell lines and culture

GIST-882 and GIST-T1 cell lines were obtained from the Shanghai Cancer Institute, and GIST-48 cell lines were kindly provided by Professor Jonathan Fletcher (Harvard Medical School, United States). GIST-882 and GIST-T1 cells were cultured with RPMI 1640 medium (Gibco, United States), and GIST-48 cells were cultured with DMEM (BioInd, Israel). Both medium preparations contained 10% fetal bovine serum (FBS) (Gibco, United States) and 1% penicillin-streptomycin in a humidified incubator at 37 °C with 5% CO2.

Cell transfection

The lentivirus for knocking down TAF15 (shRNA1, shRNA2, shRNA3) and control scrambled lentivirus (sh-scrambled) were purchased from Genomeditech (Shanghai, China). GIST-882 and GIST-T1 cells were seeded in a 12-well plate(Corning Life Sciences) at 1×10^5 cells per well, and the transfection was performed when the cell density reached about 50%. Cells were cultured in fresh medium after being infected with lentivirus for 72 h. The multiplicity of infection of lentivirus to GIST-882 and GIST-T1 was 30. Stable cell lines were generated through selection with puromycin (2 μg/mL). Transfection efficiency was detected using western blot analysis.

Cell immunofluorescence

Transfected cells were cultured in 12-well plates. When the cell density reached 50%-65%, cells were fixed using 4% paraformaldehyde for 30 min to make slides. 0.5% Triton X-100 was added to slides to allow for cell penetration, and 10% goat serum was used to block cells for 2 h at room temperature. Slides were then incubated with the TAF15 primary antibody (1:500, ab134916, Abcam, United States) at 4 °C overnight and then incubated with secondary antibodies for 1 h at room temperature. DAPI was used to stain the cell nuclei, and images were photographed using a fluorescent microscope. The fluorescent intensity of cells were measured using Image J software (version 3.2.0.8).

Cell counting kit-8 assay and colony formation assay

The cell counting kit (CCK)-8 (Dojindo, Tokyo, Japan) assay was performed according to the manufacturer's instructions. Briefly, different groups of cells were seeded onto 96-well plates at 1×10^3 cells per well. The CCK-8 reagent was added (10 μL/well) into the individual wells during the last hour. A microplate reader (Bio-Rad) was used to measure the optical density of the samples at 450 nm, as a measure of cell proliferation. With respect to the colony formation assay, different groups of cells were cultured in 6-well plates (500 cells/well) for 2 wk. Cell colonies were fixed with 4% paraformaldehyde for 30 min and stained with 1% crystal violet for 15 min at the room temperature. Colonies consisting of 50 or more cells were counted.

Transwell experiment

GIST-882 and GIST-T1 cells (3×10^4 cells/well) were inoculated into the upper polycarbonate membrane chambers of a 12-well plate without FBS, while the lower chamber contained RPMI 1640 medium with 10% FBS. To detect the cell invasion ability, matrix gel was in advance added to the polycarbonate membrane chambers. After being cultured for 48 h, the cells attached to the lower side were fixed with 4% paraformaldehyde for 30 min and stained with 1% crystal violet for 15 min at the room temperature. Five fields were selected randomly to count using an inverted microscope.

Wound healing assay

GIST-882 and GIST-T1 cells were cultured up to 90% confluency and then serum-starved for 12 h. The cell monolayer was scratched using a 1 mL plastic pipette tip. Culture medium was used to wash away the cell debris twice, and then cells were incubated in respective culture medium containing 10% FBS. Samples were photographed at 0 h, 12 h and 24 h post scratch using an Olympus microscope. The percentage of wound healing was evaluated using Image J software.

Modeling of GIST xenografts in nude mice

Nude mice aged 4 wk were purchased from the Beijing Vital River Laboratory Animal Technology Co., Ltd (Beijing, China). All animal care and processing were performed according to the Institutional Animal Care and Use Committee of Qingdao University guidelines. Twenty mice were divided randomly into two groups (10 mice per group) and then subcutaneously injected in the axillary region with stable cells (2×10^6 cells) transfected with sh-TAF15 or sh-scrambled. The volume (volume = length × width × width/2) of tumors were measured every 2 d. The mice were humanely sacrificed using the cervical dislocation method after anesthesia with 0.7% sodium pentobarbital. Tumor tissues were then excised, photographed and weighed.

Statistical analysis

Statistical analyses were performed using GraphPad Prism 9.3.1. The data analyses were conducted using Student's *t*-test, χ^2 test, one-way analysis of variance or Mann-Whitney *U* test. Data were expressed as mean ± standard deviation. $P < 0.05$ was considered statistically significant, and significance was indicated in each graph.

RESULTS

Quantification of DEPs by TMT

In total, 4111 proteins were quantified with a false discovery rate < 0.01 in all 12 GIST matched samples. Of these, 1669 were identified as significant DEPs on the basis of the filtering criteria of fold change > 1.2 or < 0.83 and *P* value < 0.05, including 762 upregulated proteins and 907 downregulated proteins (Figure 1A and Supplementary Table 1). Notably, the key proteins used for diagnosing GIST, including KIT, DOG1 and hematopoietic progenitor cell antigen CD34 (CD34), were all contained in the upregulated protein category (Supplementary Table 1), suggesting that our proteomic data were reliable. Moreover, 667, 686, 840 and 974 significant DEPs were identified in the NIH-H, NIH-I, NIH-L and NIH-VL subgroups, respectively (Figure 1B and Supplemental Table 2). After our systematic analysis of the top 10 upregulated and downregulated proteins (Table 2), we decided to focus on the protein TAF15 due to its important role in cell proliferation and migration.

Identification of TAF15 by western blotting analysis

Western blotting was used to further identify the expression levels of TAF15 in GIST. We detected the extracted proteins from tumor tissues (T) and matched normal tissues (N) of 18 GIST patients, including 6 NIH-H, 6 NIH-I, 3 NIH-L, and 3 NIH-VL cases. The results showed that the expression levels of TAF15 were significantly increased in tumor tissues compared with matched normal tissues (Figure 1C and D), which were in agreement with the results of our quantitative proteomics analysis (Table 2 and Supplemental Table 2).

Validation of TAF15 expression by immunohistochemical analysis

We evaluated the expression level of TAF15 in GIST patients using immunohistochemical (IHC) analysis of tumor tissues (T) from 161 patients and 18 matched normal tissues (N). We found significantly higher levels of expression of TAF15 in tumor tissues compared to matched normal tissues (red arrows, Figure 1E and F, Supplemental Table 3). Moreover, subgroup analyses showed that the expression level of TAF15 was significantly higher in the NIH-H subgroup than in the NIH-I, NIH-L and NIH-VL subgroups and that the expression level of TAF15 was significantly higher in the NIH-I subgroup than the NIH-VL subgroup (Figure 1G and Supplemental Table 3). We found no significant difference in the expression of TAF15 between the NIH-L and NIH-VL subgroups and between the NIH-I and NIH-L subgroups. Furthermore, based on our IHC data, we found that the overexpression level of TAF15 was positively correlated with tumor size and GIST risk stage but was not significantly correlated with gender, age or tumor metastasis (Table 3). These results provided evidence that the higher expression of TAF15 may contribute to malignant progression of GIST and that TAF15 may be a latent promoter or biomarker of GIST.

Knockdown of TAF15 inhibited the proliferation and migration of GIST cells

In order to understand the real role of TAF15 in GIST progression, short-hairpin RNAs (shRNAs) were used to knock down TAF15 in GIST-882 and GIST-T1 cells. GIST-882 and GIST-T1 cells were used instead of GIST-48 cells, as the expression level of TAF15 was higher in the former cell lines (Figure 2A). Three shRNAs targeting TAF15 (sh1, sh2 and sh3) were applied to knock down TAF15 protein. The results showed that sh2 and sh3 could significantly reduce the expression of TAF15 when compared to scrambled shRNA (scr), as tested by western blotting analysis (Figure 2B and C) and cell immunofluorescence assays (Figure 2D and E). Therefore, sh2 and sh3 were used to perform further experiments.

Table 2 The top 10 upregulated and downregulated proteins

Category	Accession	Protein name	FC,T *vs* N	*P* value
Up	P29400	COL4A5	3.129881192	0.001086699
	O94772	LY6H	2.995133385	0.012292301
	P05204	HMGN2	2.92528705	2.10765E-07
	O00479	HMGN4	2.900071252	3.22924E-09
	P20930	FLG	2.87152332	0.002555182
	P52926	HMGA2	2.687785701	0.008942412
	Q6UX72	B3GNT9	2.576105848	4.91404E-09
	Q92804	TAF15	2.456058544	1.54458E-05
	O95081	AGFG2	2.441304592	2.93054E-06
	P09936	UCHL1	2.157884674	7.498E-07
Down	Q96BQ1	FAM3D	0.225135868	0.022611851
	Q5DID0	UMODL1	0.242287446	0.00020958
	P25815	S100P	0.267045455	3.77116E-06
	P13640	MT1G	0.274242	0.0028833
	P42330	AKR1C3	0.290893518	6.40059E-07
	Q9UBU3	GHRL	0.293081189	0.000379102
	Q9NS71	GKN1	0.311488849	6.5931E-06
	O95994	AGR2	0.330784665	9.59846E-06
	P19075	TSPAN8	0.350779233	7.40703E-09
	P55087	AQP4	0.352590936	0.035544439

T: Tumor tissues; N: Matched tumor normal tissues; FC: Fold change.

The results of the CCK-8 assay and the colony formation assay indicated that TAF15 knockdown (sh2 and sh3) exhibited a significant decrease in proliferative and colony forming ability in GIST-882 and GIST-T1 cells when compared with the scr (Figure 3A-D). Transwell assay showed that the sh-TAF15 group (sh2 and sh3) exhibited significantly weaker migratory abilities compared to the scr in GIST-882 and GIST-T1 cells (Figure 3E and F). However, there was no significant difference in the invasion ability of GIST-882 and GIST-T1 cells between the sh-TAF15 group (sh2 and sh3) and sh-scrambled group (Figure 3G and H). The results of the wound healing assay also showed that migratory abilities significantly decreased in the sh-TAF15 group (sh2 and sh3) compared to the scr in GIST-882 and GIST-T1 cells (Figure 3I-K). These findings indicated that TAF15 knockdown can significantly inhibit GIST cell proliferation and migration.

TAF15 promoted GIST progression by activating the RAF1/MEK/ERK signaling pathway

Previous studies have shown that EWS, one of the members of the FET family proteins, forms a fusion oncoprotein EWS-FLI1 whose expression leads to the activation of ERK1/2 signaling in zebrafish embryos and adult tumors[24]. In consideration of the important role of the ERK signaling pathway in many human tumors[25], we speculated that TAF15 could promote cell proliferation and migration directly through the activation of the ERK signaling pathway in GIST. Therefore, we assessed the phosphorylation level of RAF1, MEK and ERK1/2 in GIST-882 and GIST-T1 by western blotting. The results showed that the phosphorylation levels of RAF1, MEK and ERK1/2 were significantly decreased following TAF15 knockdown (sh2 and sh3). However, there was no significant change in levels of total RAF1, MEK and ERK1/2 (Figure 4). Collectively, these findings suggest that TAF15 may promote cell proliferation and migration through the activation of the RAF1/MEK/ERK signaling pathway in GIST.

TAF15 promoted the growth of GIST in vivo

To further confirm the role of TAF15 in the progression of GIST, we established a xenograft mouse model utilizing GIST-882 cells due to their enhanced proliferative and migratory ability. sh2 was used in this experiment because of its higher knockdown efficiency, with scr as a control. Twenty nude female mice were randomly divided into two groups, and each mouse was then subcutaneously injected with

Table 3 Correlation between the expression of TATA-box-binding protein-associated factor 15 and clinicopathological characteristics in gastrointestinal stromal tumors

Characteristics	TAF15 expression		*P* value
	Negative	Positive	
Total number	31	130	
Sex			0.2730[a]
Male	16 (9.9)	53 (32.9)	
Female	15 (9.3)	77 (58.7)	
Age in yr			0.8228[a]
≤ 60	15 (9.3)	60 (37.2)	
> 60	16 (9.9)	70 (43.5)	
Tumor size			
Maximum diameter in cm			
≤ 5	29 (18.0)	74 (46.0)	0.0001[a]
> 5	2 (1.2)	56 (34.8)	
GIST risk stage			0.0021[b]
Very low risk	15 (9.3)	30 (18.6)	
Low risk	11 (6.8)	31 (19.3)	
Intermediate risk	3 (1.9)	29 (18.0)	
High risk	2 (1.2)	40 (24.8)	
Metastasis			0.1316[a]
-	31 (19.3)	121 (75.2)	
+	0 (0.0)	9 (5.6)	

[a]*P* values were calculated by χ^2 test.
[b]*P* values were calculated by Mann-Whitney *U* test.
Total patients of 161. Data are presented as *n*(%). TAF15: TATA-box-binding protein-associated factor 15; GIST: Gastrointestinal stromal tumor.

either sh2 or scr cells. Unfortunately, one mouse in the scr group died on day 7 post-injection for an unknown reason. Ten days after injection, xenograft tumors in the remaining mice were detectable. The results showed that TAF15 knockdown significantly suppressed tumor growth and tumor weight (Figure 5A-C). Furthermore, western blotting analysis was used to confirm the level of TAF15 in the xenograft tumors. The results showed that the levels of TAF15 were significantly decreased in the sh2 group compared to the scr group (Figure 5D and E). Additionally, three xenograft tumors of the sh2 group and three xenograft tumors of the scr group were randomly selected to test the levels of RAF1, MEK and ERK1/2 by western blotting. The results indicated that the phosphorylation levels of RAF1, MEK and ERK also decreased significantly in the sh2 group, while the levels of total RAF1, MEK and ERK showed no significant change (Figure 5F-I). These data indicated that TAF15 may promote the growth of GIST *in vivo via* the activation of the RAF1/MEK/ERK signaling pathway.

DISCUSSION

KIT and PDGFRA mutations are considered to be two major factors in GIST pathogenesis[3,26], and drugs targeting KIT and PDGFRA pathways have achieved great success in the treatment of this disease [27,28]. However, GIST patients gradually become resistant to current targeted drug treatment in recent years[14,28]. Therefore, there is an unmet need to explore other latent targets.

An increasing number of biomarkers or targets have been reported to be important to GIST progression. For example, p53 is a biomarker and potential target in GIST; targeting the p53 pathway is a novel additional treatment strategy for GIST[29]. High expression of carbohydrate antigen 125 is an independent risk factor for GIST progression, and it is a significant biomarker in the overall management of GIST patients[30]. Brain-derived neurotrophic factor is over expressed in high-risk GIST patients, and it may serve as a significant prognostic factor[31].In the present study, proteomic analysis

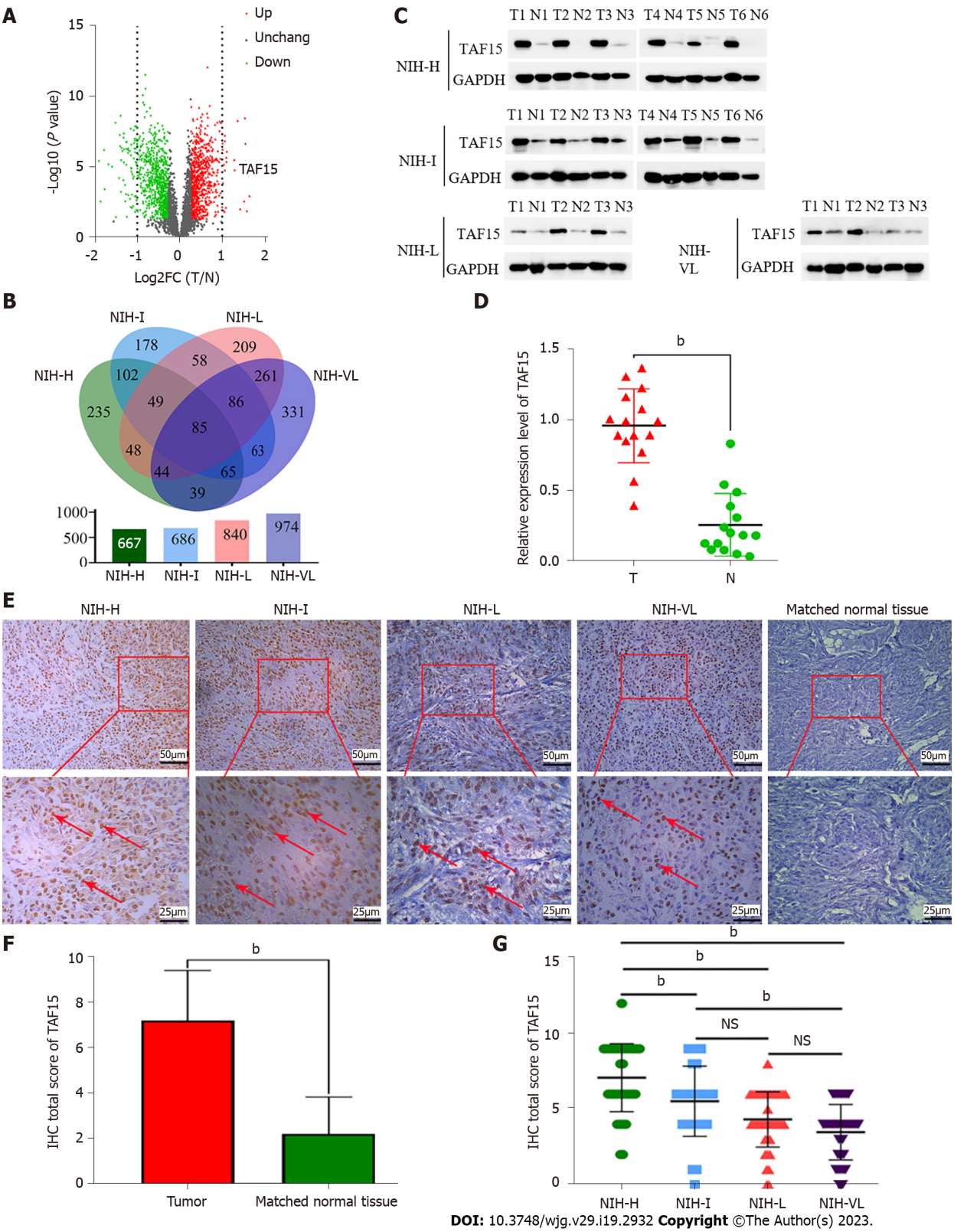

DOI: 10.3748/wjg.v29.i19.2932

Figure 1 Differentially expressed proteins in gastrointestinal stromal tumor samples. A: Proteomic analysis identified the differentially expressed proteins in gastrointestinal stromal tumor (GIST) patients; B: Venn diagram showed the number of identified differentially expressed proteins in the subgroups of GIST; C and D: Western blotting identified that the expression level of TATA-box-binding protein-associated factor 15 (TAF15) was significantly increased in tumor tissues compared with matched normal tissues in all 18 GIST samples. *P* values were calculated using the Student's *t*-test; E: Immunohistochemical analysis verified the expression of TAF15 using 161 GIST tumor tissues and 18 matched normal tissues (representative images are shown and red arrows indicate positive staining); F: Total immunostaining score of TAF15 protein in tumor tissues and matched normal tissues of GIST; G: Total immunostaining score of TAF15 proteins in the GIST subgroup. *P* values were calculated using the Student's *t*-test or one-way analysis of variance. $^{b}P < 0.01$. NS: No significance between groups; NIH-H: National Institutes of Health high risk; NIH-I: National Institutes of Health intermediate risk; NIH-L: National Institutes of Health low risk; NIH-VL: National Institutes of Health very low risk; IHC: Immunohistochemical; T: Tumor tissues; N: Normal tissues; FC: Fold change; TAF15: TATA-box-binding protein-associated factor 15.

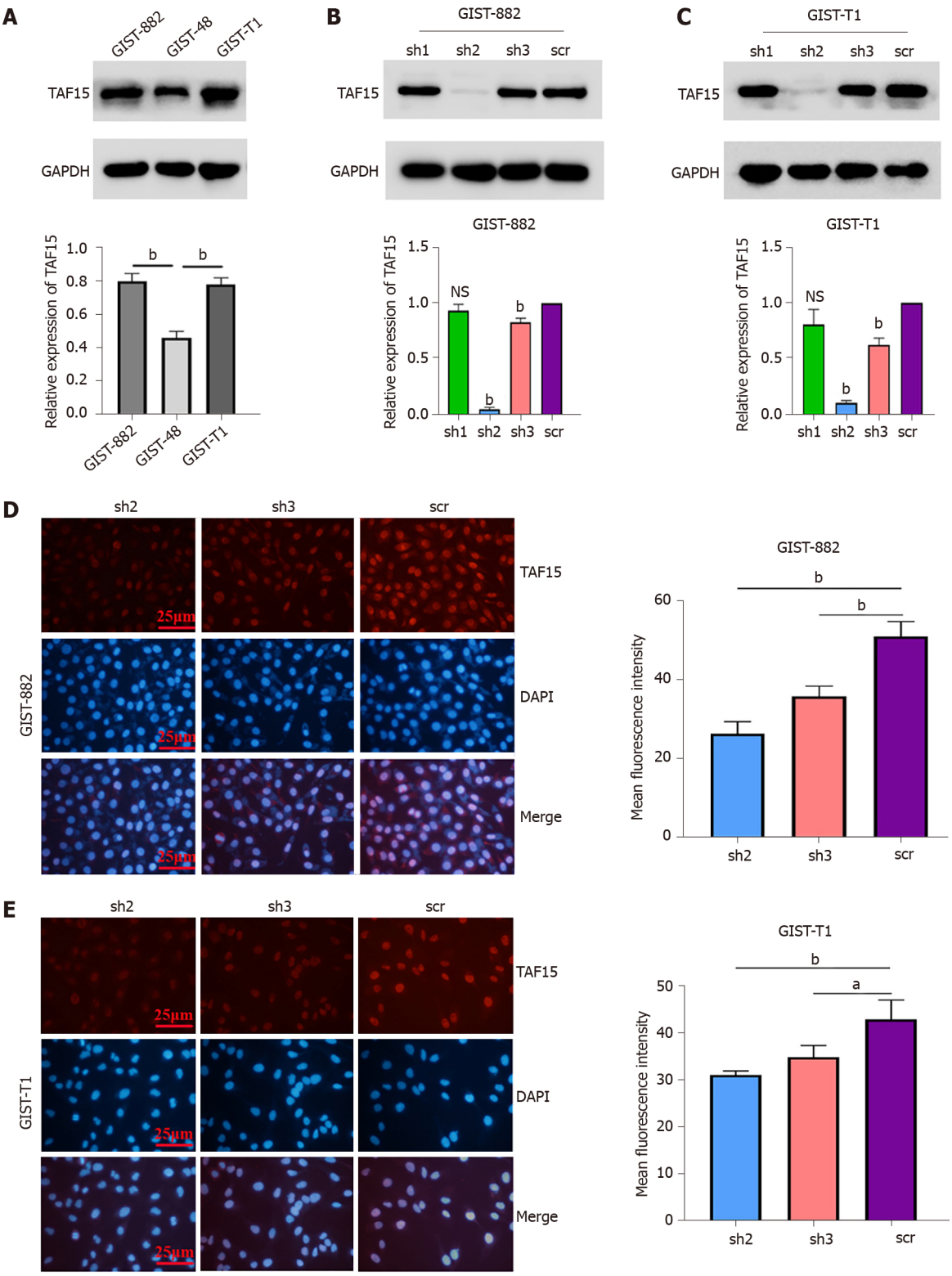

DOI: 10.3748/wjg.v29.i19.2932

Figure 2 The knockdown efficiency of short hairpin-TATA-box-binding protein-associated factor 15 in gastrointestinal stromal tumor cell lines. A: Western blotting to detect the expression level of TATA-box-binding protein-associated factor 15 (TAF15) in gastrointestinal stromal tumor(GIST) cell lines. *P* values were calculated by one-way analysis of variance; B and C: TAF15 was knocked down using three short hairpin (sh) RNAs (sh1, sh2, and sh3) and scrambled shRNA (scr) as control in GIST-882 and GIST-T1 cells. The results showed that sh2 and sh3 could reduce the expression level of TAF15 significantly when compared to scr as tested by western blotting analysis; D and E: The fluorescence intensity of TAF15 in sh2 and sh3 was reduced significantly when compared to scr in GIST-882 and GIST-T1 cells as tested by a cell immunofluorescence assay. *P* values were calculated using the Student's *t*-test. $^{a}P < 0.05$, $^{b}P < 0.01$. NS: No significance between groups; GIST: Gastrointestinal stromal tumor; TAF15: TATA-box-binding protein-associated factor 15; sh1: shRNA1 targeting TATA-box-binding protein-associated factor 15; sh2: shRNA2 targeting TATA-box-binding protein-associated factor 15; sh3: shRNA3 targeting TATA-box-binding protein-associated factor 15; scr: Scrambled shRNA.

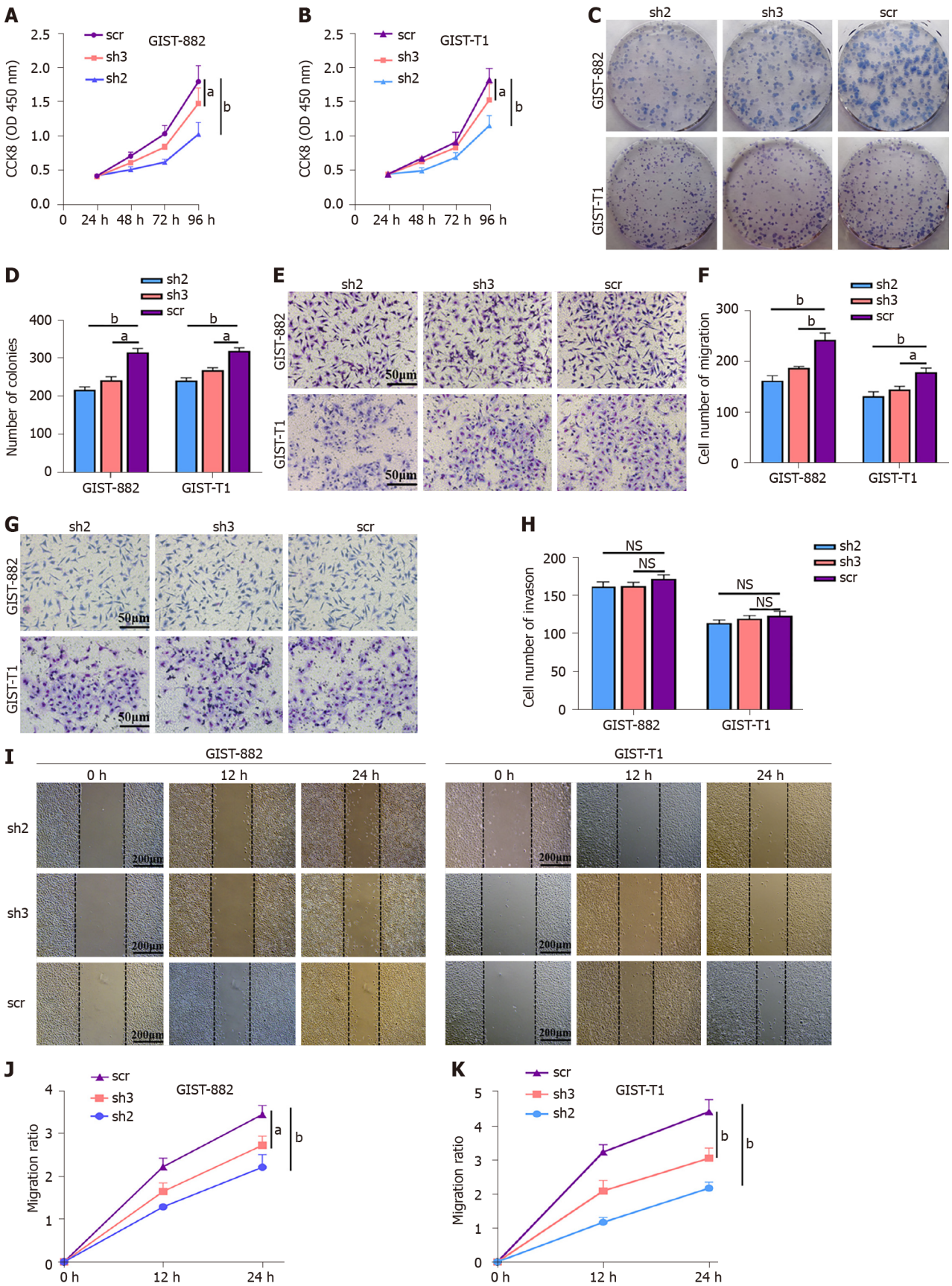

DOI: 10.3748/wjg.v29.i19.2932 **Copyright** ©The Author(s) 2023.

Figure 3 TATA-box-binding protein-associated factor 15 regulated the proliferation and migration of gastrointestinal stromal tumor cells. A and B: Cell counting kit-8 assay was performed to detect the proliferation of gastrointestinal stromal tumor (GIST)-882 and GIST-T1 after cell transfection. *P* values were calculated using the Student's *t*-test; C and D: A colony formation assay identified the proliferative ability of GIST-882 and GIST-T1 after cell transfection. Statistical analyses were performed using the Student's *t*-test; E-H: A transwell assay was performed to analyze the migratory and invasive ability of GIST-882 and

GIST-T1 cells after transfection. *P* values were calculated using the Student's *t*-test; I-K: A wound healing assay was conducted to confirm the migratory ability of GIST-882 and GIST-T1 cells after transfection. *P* values were calculated using the Student's *t*-test. $^{a}P < 0.05$, $^{b}P < 0.01$. GIST: Gastrointestinal stromal tumor; NS: No significance between groups; sh2: shRNA2 targeting TATA-box-binding protein-associated factor 15; sh3: shRNA3 targeting TATA-box-binding protein-associated factor 15; scr: Scrambled shRNA; CCK8: Cell counting kit-8.

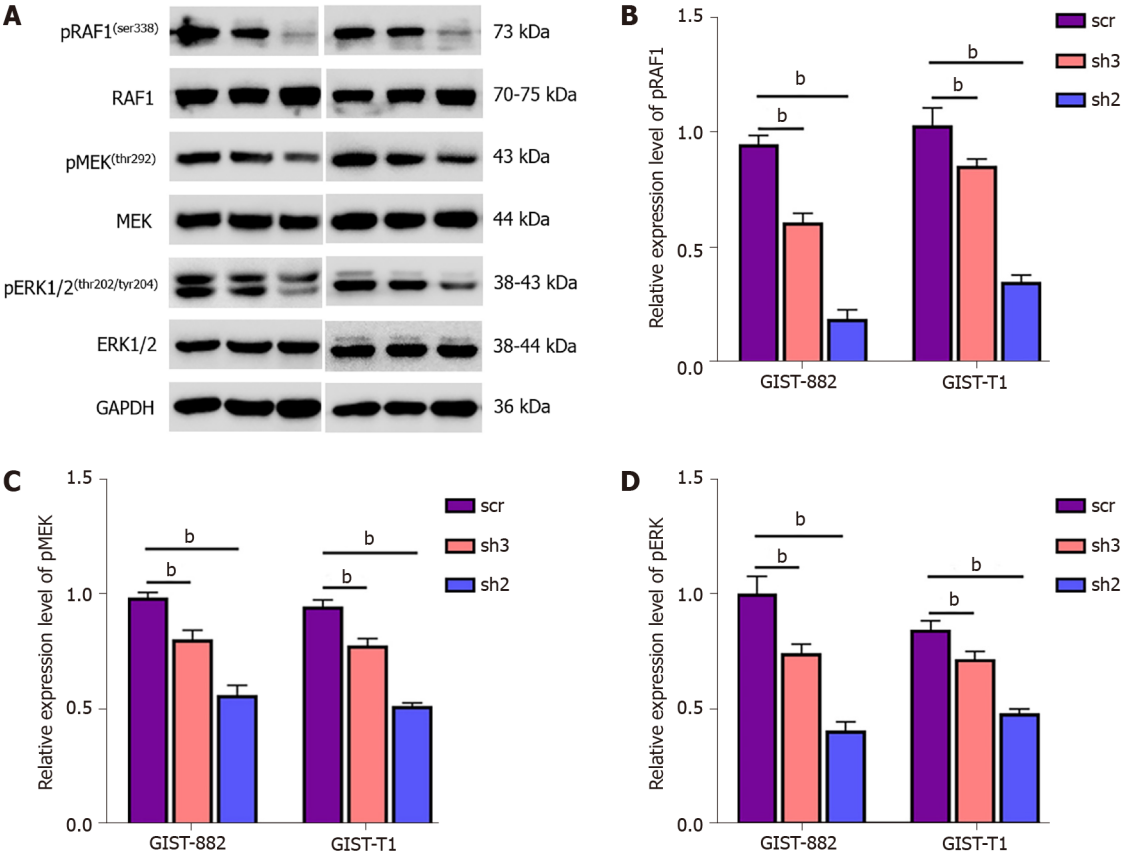

DOI: 10.3748/wjg.v29.i19.2932

Figure 4 TATA-box-binding protein-associated factor 15 promoted the proliferation and migration of gastrointestinal stromal tumor cells by activating the RAF1/MEK/ERK pathway. A: Western blotting analysis detected the protein level of pRAF1/RAF1, pMEK/MEK and pERK/ERK in gastrointestinal stromal tumor (GIST)-882 and GIST-T1 after cell transfection; B-D: The phosphorylation levels of RAF1, MEK and ERK1/2 were significantly decreased inshRNA2 targeting TATA-box-binding protein-associated factor 15 and shRNA3 targeting TATA-box-binding protein-associated factor 15 when compared to the scrambled shRNA in GIST cell lines. Statistical analyses were executed by the Student's *t*-test. $^{b}P < 0.01$. GIST: Gastrointestinal stromal tumor; sh2: shRNA2 targeting TATA-box-binding protein-associated factor 15; sh3: shRNA3 targeting TATA-box-binding protein-associated factor 15; scr: Scrambled shRNA.

was performed in patients with GIST to explore the potential molecular biomarkers for prediction, early diagnosis or treatment.

A total of 4111 quantified proteins with 1669 DEPs (762 upregulated and 907 downregulated proteins) were revealed in our study. Among the top 10 DEPs identified, TAF15 was interesting due to its key role in promoting growth in other human tumors such as extraskeletalmyxoid sarcomas, leukemia, Ewing's sarcomas, human neuroblastoma and lung squamous cell carcinoma[15,17,19,20,32]. TAF15 was first reported as an RNA or DNA binding protein, while more recent studies have shown that TAF15 also plays important roles in cellular stress responses, cell spreading and cell adhesion[33,34]. GAS5 binding to TAF15 could upregulate expression of HIF1A,thus promoting wound healing in diabetic foot ulcers [35].

We believe our study is the first to confirm that TAF15 is over expressed in GIST tissues and cell lines and that high expression levels of TAF15 are positively correlated with tumor size and GIST risk stage. Previous studies have shown that the inhibition of TAF15 expression could significantly reduce cellular proliferation in melanoma and lung cancer[20,21]. Similarly, our study demonstrated that TAF15 knockdown could significantly inhibit proliferation and migration of GIST cells *in vitro* and suppress tumor growth *in vivo*. These data provided evidence that overexpression of TAF15 may contribute to the malignant progression of GIST.

The latent molecular mechanism of TAF15 in GIST was also first investigated in this study. Previous studies have shown that FET family proteins are mainly present in the nucleus[34], but it is now known that they also shuttle between the nucleus and cytoplasm[36-38]. They have an extensive functionality

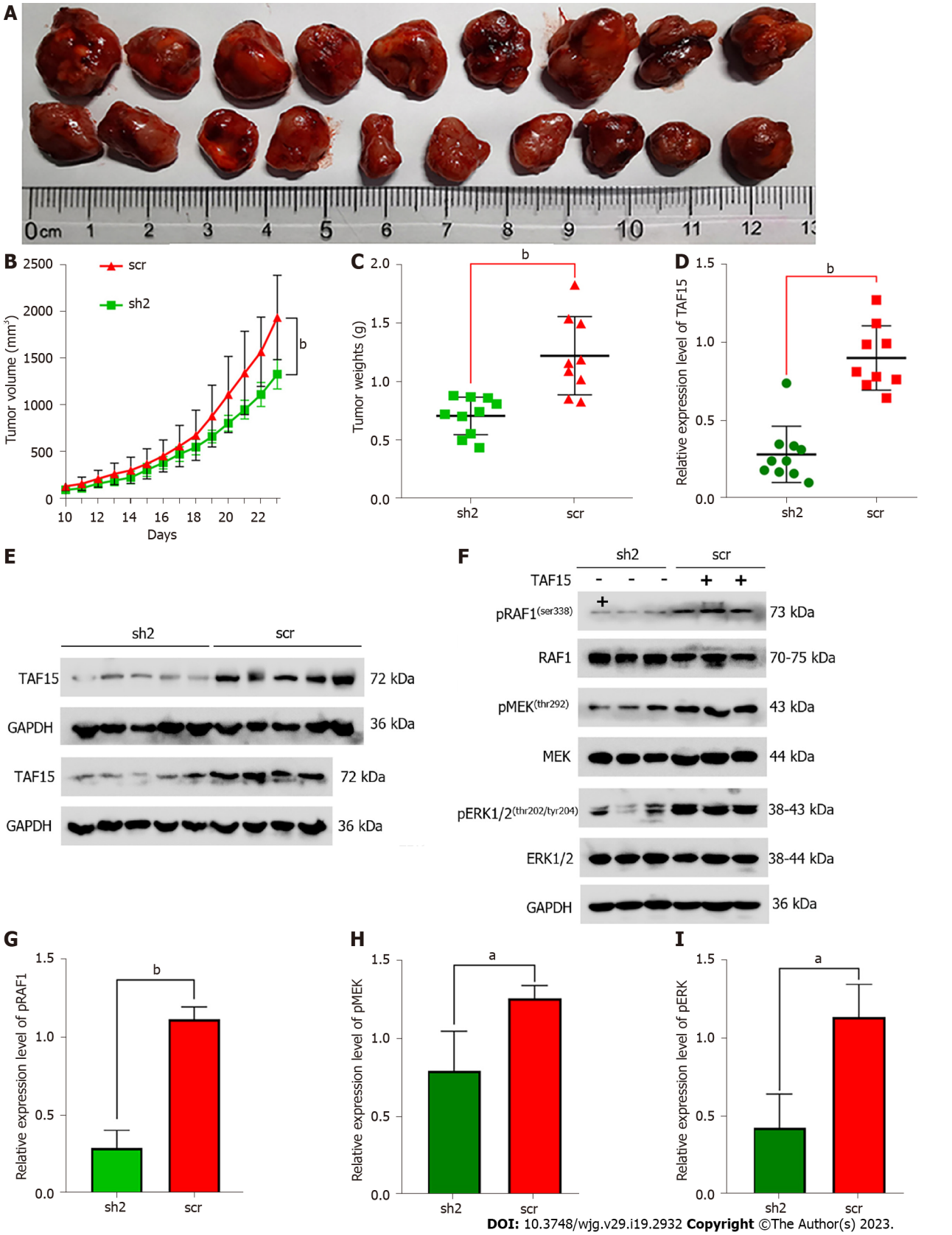

DOI: 10.3748/wjg.v29.i19.2932

Figure 5 TATA-box-binding protein-associated factor 15 suppressed tumor growth of gastrointestinal stromal tumor cells *in vivo*. A-C: The volumes and weights of tumors in the shRNA2 targeting TATA-box-binding protein-associated factor 15 group were significantly smaller than the scrambled shRNA group. Statistical analyses were performed using the Student's *t*-test; D and E: Western blotting analysis was used to confirm the expression levels of TATA-box-binding protein-associated factor 15 in xenograft tumors; F-I: Western blotting analysis confirmed the protein levels of pRAF1/RAF1, pMEK/MEK and pERK/ERK in xenograft tumors. *P* values were calculated using the Student's *t*-test. $^{a}P < 0.05$, $^{b}P < 0.01$. TAF15: TATA-box-binding protein-associated factor 15; sh2: shRNA2 targeting TATA-box-binding protein-associated factor 15; scr: Scrambled shRNA.

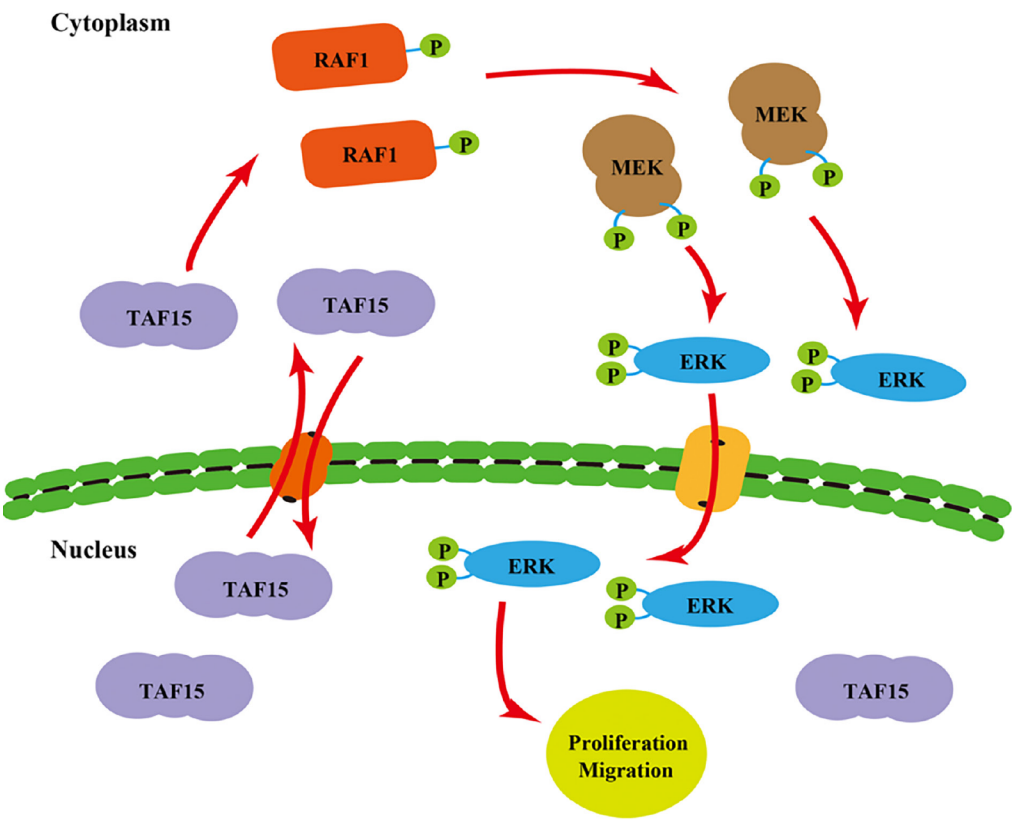

DOI: 10.3748/wjg.v29.i19.2932

Figure 6 A schematic diagram of the mechanism of action of TATA-box-binding protein-associated factor 15 in gastrointestinal stromal tumors. TATA-box-binding protein-associated factor 15 shuttles between the nucleus and cytoplasm and promotes proliferation and migration of gastrointestinal stromal tumor cells by activating the RAF1/MEK/ERK pathway. TAF15: TATA-box-binding protein-associated factor 15.

including regulation and interaction with various proteins[39,40]. Moreover, recent work demonstrated that EWS-FLI1 fusion protein expression leads to activation of ERK1/2 signaling in zebrafish embryos and adult tumors[24]. Additionally, it is well known that the RAF/MEK/ERK signaling pathway plays an essential role in promoting cellular proliferation and survival[41].

In our study, we found TAF15 knockdown could significantly decrease the phosphorylation levels of RAF1, MEK and ERK, without significantly changing the total amounts of RAF1, MEK and ERK in GIST cell lines and xenograft tumors. Similarly, TAF15 is involved in the promotion of cell proliferation, migration and invasion of lung squamous cell carcinoma by activating the MAPK signaling pathway [22]. These results suggested that the activation of the ERK pathway may represent a new function of the TAF15 protein beyond DNA binding, mRNA splicing and mRNA transport. Taken together, these findings suggested that TAF15 shuttles between the nucleus and cytoplasm and may promote cell proliferation and migration directly through the activation of the RAF1/MEK/ERK signaling pathway in GIST (Figure 6). These observations greatly extend the functional repertoire of TAF15.

However, due to difficulty of obtaining matched tumor tissues after surgery[23], the number of paired samples used in this study for proteomic analysis, western blotting and IHC were small. Thus, we acknowledge that the accuracy of the proteomic analysis, western blotting and IHC in this research may be affected by the sample size and that the statistical analyses may be less robust due to the small sample size. Further studies will help validate some of the important and interesting findings of this study in larger GIST cohorts when available. Additional roles of TAF15 in GIST remain to be explored, as hundreds of genes lie downstream of TAF15[42].

CONCLUSION

In summary, this study utilized a proteomic analysis to find new molecular therapeutic targets for GIST and analyzed the expression level and underlying biological functions of TAF15 in GIST. Moreover, our study may be the first to demonstrate that TAF15 expression may contribute to malignant progression of GIST. TAF15promoted cell proliferation and migration in GIST *via* the RAF1/MEK/ERK signaling pathway. Therefore, TAF15 is expected to be a novel latent molecular biomarker or therapeutic target of GIST.

ARTICLE HIGHLIGHTS

Research background

Gastrointestinal stromal tumors (GIST) are a common neoplasm with high rates of recurrence and metastasis, and its therapeutic efficacy is still not ideal. There is an unmet need to find new molecular therapeutic targets for GIST. TATA-box-binding protein-associated factor 15 (TAF15) contributes to the progress of various tumors, while the role and molecular mechanism of TAF15 in GIST progression are still unknown.

Research motivation

To explore the novel early diagnostic markers or therapeutic targets for the diagnosis and treatment of GIST.

Research objectives

To investigate new molecular therapeutic targets for GIST and explore the role and potential molecular mechanism of TAF15 in GIST progression.

Research methods

Proteomic analysis was performed to explore the differentially expressed proteins in GIST. Western blotting and immunohistochemical analysis were used to verify expression levels of TAF15 in GIST tissues and cell lines. Cell counting kit-8, colony formation, transwell, wound healing and western blotting assays were applied to explore the effect and the molecular mechanism of TAF15 in GIST. The role of TAF15 *in vivo* was confirmed using a xenograft mouse model assay.

Research results

A total of 1669 proteins were identified as differentially expressed proteins with 762 upregulated and 907 downregulated in GIST. TAF15 was significantly upregulated in GIST tissues and cell lines. Overexpression of TAF15 was associated with larger tumor size and higher risk stage of GIST. TAF15 knockdown suppressed proliferation and migration of GIST cells *in vitro* and inhibited the growth of GIST *in vivo*. Moreover, the inhibition of TAF15 expression significantly decreased the phosphorylation level of RAF1, MEK and ERK1/2 in GIST cells and xenograft tissues, while the total levels of RAF1, MEK and ERK1/2 had no significant changes.

Research conclusions

TAF15 may contribute to malignant progression of GIST and promote cell proliferation and migration in GIST *via* the activation of the RAF1/MEK/ERK signaling pathway.

Research perspectives

TAF15 is expected to be a novel latent molecular biomarker or therapeutic target of GIST.

FOOTNOTES

Author contributions: Guo CM and Tang L contributed equally to this work; Guo CM and Tang L performed the data acquisition, drafted the manuscript and executed the *in vitro* experiments; Guo CM completed the statistical analyses; Guo CM and Li X executed the animal experiments; Huang LY designed the work and revised the manuscript.

Supported by National Natural Science Foundation of China, No. 81870453.

Institutional review board statement: The study was conducted according to the guidelines of the Declaration of Helsinki, and approved by Ethics Committee of Yantai Yuhuangding Hospital,No.2019-410.

Institutional animal care and use committee statement: All animal experiments were approved by the Affiliated Yantai Yuhuangding Hospital of Qingdao University for Laboratory Animal Welfare and Ethical Review, No. 2022-A56.

Informed consent statement: All study participants or their legal guardian provided informed written consent about personal and medical data collection prior to study enrolment.

Conflict-of-interest statement: All authors report having no relevant conflicts of interest for this article.

Data sharing statement: The data can be obtained from the corresponding author upon reasonable request.

ARRIVE guidelines statement: The authors have read the ARRIVE guidelines, and the manuscript was prepared and

revised according to the ARRIVE guidelines.

Country/Territory of origin: China

ORCID number: Cheng-Ming Guo 0000-0002-6844-6223; Li Tang 0000-0002-1491-2129; Xu Li 0000-0002-4389-0352; Liu-Ye Huang 0000-0002-5016-0331.

S-Editor: Fan JR
L-Editor: Filipodia
P-Editor: Yu HG

REFERENCES

1 **Wu CE**, Tzen CY, Wang SY, Yeh CN. Clinical Diagnosis of Gastrointestinal Stromal Tumor (GIST): From the Molecular Genetic Point of View. *Cancers (Basel)* 2019; **11** [PMID: 31100836 DOI: 10.3390/cancers11050679]

2 **Casali PG**, Abecassis N, Aro HT, Bauer S, Biagini R, Bielack S, Bonvalot S, Boukovinas I, BoveeJVMG, Brodowicz T, Broto JM, Buonadonna A, De Álava E, Dei Tos AP, Del MuroXG, Dileo P, Eriksson M, Fedenko A, Ferraresi V, Ferrari A, Ferrari S, Frezza AM, Gasperoni S, Gelderblom H, Gil T, Grignani G, Gronchi A, Haas RL, Hassan B, Hohenberger P, Issels R, Joensuu H, Jones RL, Judson I, Jutte P, Kaal S, Kasper B, Kopeckova K, Krákorová DA, Le Cesne A, Lugowska I, Merimsky O, Montemurro M, Pantaleo MA, Piana R, Picci P, Piperno-Neumann S, Pousa AL, Reichardt P, Robinson MH, Rutkowski P, Safwat AA, Schöffski P, Sleijfer S, Stacchiotti S, Sundby Hall K, Unk M, Van Coevorden F, van der Graaf WTA, Whelan J, Wardelmann E, Zaikova O, Blay JY; ESMO Guidelines Committee and EURACAN. Gastrointestinal stromal tumours: ESMO-EURACAN Clinical Practice Guidelines for diagnosis, treatment and follow-up. *Ann Oncol* 2018; **29**: iv267 [PMID: 30188977 DOI: 10.1093/annonc/mdy320]

3 **Heinrich MC**, Corless CL, Duensing A, McGreevey L, Chen CJ, Joseph N, Singer S, Griffith DJ, Haley A, Town A, Demetri GD, Fletcher CD, Fletcher JA. PDGFRA activating mutations in gastrointestinal stromal tumors. *Science* 2003; **299**: 708-710 [PMID: 12522257 DOI: 10.1126/science.1079666]

4 **Miettinen M**, Lasota J. Gastrointestinal stromal tumors. *Gastroenterol Clin North Am* 2013; **42**: 399-415 [PMID: 23639648 DOI: 10.1016/j.gtc.2013.01.001]

5 **Xue A**, Gao X, He Y, Shu P, Huang X, Sun J, Lu J, Hou Y, Fang Y, Shen K. Role of Surgery in the Management of Liver Metastases From Gastrointestinal Stromal Tumors. *Front Oncol* 2022; **12**: 903487 [PMID: 35847933 DOI: 10.3389/fonc.2022.903487]

6 **Zhang D**, He C, Guo Y, Li J, Li B, Zhao Y, Yu L, Chang Z, Pei H, Yang M, Li N, Zhang Q, He Y, Pan Y, Zhao ZJ, Zhang C, Chen Y. Efficacy of SCF drug conjugate targeting c-KIT in gastrointestinal stromal tumor. *BMC Med* 2022; **20**: 257 [PMID: 35999600 DOI: 10.1186/s12916-022-02465-3]

7 **Joensuu H**, Vehtari A, Riihimäki J, Nishida T, Steigen SE, Brabec P, Plank L, Nilsson B, Cirilli C, Braconi C, Bordoni A, Magnusson MK, Linke Z, Sufliarsky J, Federico M, Jonasson JG, Dei Tos AP, Rutkowski P. Risk of recurrence of gastrointestinal stromal tumour after surgery: an analysis of pooled population-based cohorts. *Lancet Oncol* 2012; **13**: 265-274 [PMID: 22153892 DOI: 10.1016/S1470-2045(11)70299-6]

8 **Fletcher CD**, Berman JJ, Corless C, Gorstein F, Lasota J, Longley BJ, Miettinen M, O'Leary TJ, Remotti H, Rubin BP, Shmookler B, Sobin LH, Weiss SW. Diagnosis of gastrointestinal stromal tumors: A consensus approach. *Hum Pathol* 2002; **33**: 459-465 [PMID: 12094370 DOI: 10.1053/hupa.2002.123545]

9 **Li S**, Chen D, Li S, Zhao Z, Yang H, Wang D, Zhang Z, Fu W. Novel Prognostic Nomogram for Recurrence-Free Survival of Patients With Primary Gastrointestinal Stromal Tumors After Surgical Resection: Combination of Prognostic Nutritional Index and Basic Variables. *Front Oncol* 2020; **10**: 581855 [PMID: 33585198 DOI: 10.3389/fonc.2020.581855]

10 **Bang YH**, Ryu MH, Kim HD, Lee HE, Kang YK. Clinical outcomes and prognostic factors for patients with high-risk gastrointestinal stromal tumors treated with 3-year adjuvant imatinib. *Int J Cancer* 2022; **151**: 1770-1777 [PMID: 35678337 DOI: 10.1002/ijc.34157]

11 **Nunobe S**, Sano T, Shimada K, Sakamoto Y, Kosuge T. Surgery including liver resection for metastatic gastrointestinal stromal tumors or gastrointestinal leiomyosarcomas. *Jpn J Clin Oncol* 2005; **35**: 338-341 [PMID: 15928191 DOI: 10.1093/jjco/hyi091]

12 **Keung EZ**, Raut CP, Rutkowski P. The Landmark Series: Systemic Therapy for Resectable Gastrointestinal Stromal Tumors. *Ann Surg Oncol* 2020; **27**: 3659-3671 [PMID: 32734368 DOI: 10.1245/s10434-020-08869-w]

13 **Hemming ML**, Heinrich MC, Bauer S, George S. Translational insights into gastrointestinal stromal tumor and current clinical advances. *Ann Oncol* 2018; **29**: 2037-2045 [PMID: 30101284 DOI: 10.1093/annonc/mdy309]

14 **Joensuu H**, Rutkowski P, Nishida T, Steigen SE, Brabec P, Plank L, Nilsson B, Braconi C, Bordoni A, Magnusson MK, Sufliarsky J, Federico M, Jonasson JG, Hostein I, Bringuier PP, Emile JF. KIT and PDGFRA mutations and the risk of GI stromal tumor recurrence. *J Clin Oncol* 2015; **33**: 634-642 [PMID: 25605837 DOI: 10.1200/JCO.2014.57.4970]

15 **Lindén M**, Vannas C, Österlund T, Andersson L, Osman A, Escobar M, Fagman H, Ståhlberg A, Åman P. FET fusion oncoproteins interact with BRD4 and SWI/SNF chromatin remodelling complex subtypes in sarcoma. *Mol Oncol* 2022;

16: 2470-2495 [PMID: 35182012 DOI: 10.1002/1878-0261.13195]

16 **Glisovic T**, Bachorik JL, Yong J, Dreyfuss G. RNA-binding proteins and post-transcriptional gene regulation. *FEBS Lett* 2008; **582**: 1977-1986 [PMID: 18342629 DOI: 10.1016/j.febslet.2008.03.004]

17 **Zuo L**, Zhang G, Massett M, Cheng J, Guo Z, Wang L, Gao Y, Li R, Huang X, Li P, Qi Z. Loci-specific phase separation of FET fusion oncoproteins promotes gene transcription. *Nat Commun* 2021; **12**: 1491 [PMID: 33674598 DOI: 10.1038/s41467-021-21690-7]

18 **Wang J**, Cai Y, Lu H, Zhang F, Zheng J. LncRNA APOA1-AS facilitates proliferation and migration and represses apoptosis of VSMCs through TAF15-mediated SMAD3 mRNA stabilization. *Cell Cycle* 2021; **20**: 1642-1652 [PMID: 34382908 DOI: 10.1080/15384101.2021.1951940]

19 **Ballarino M**, Jobert L, Dembélé D, de la Grange P, Auboeuf D, Tora L. TAF15 is important for cellular proliferation and regulates the expression of a subset of cell cycle genes through miRNAs. *Oncogene* 2013; **32**: 4646-4655 [PMID: 23128393 DOI: 10.1038/onc.2012.490]

20 **Singh AK**, Kapoor V, Thotala D, Hallahan DE. TAF15 contributes to the radiation-inducible stress response in cancer. *Oncotarget* 2020; **11**: 2647-2659 [PMID: 32676166 DOI: 10.18632/oncotarget.27663]

21 **Schatz N**, Brändlein S, Rückl K, Hensel F, Vollmers HP. Diagnostic and therapeutic potential of a human antibody cloned from a cancer patient that binds to a tumor-specific variant of transcription factor TAF15. *Cancer Res* 2010; **70**: 398-408 [PMID: 20048082 DOI: 10.1158/0008-5472.CAN-09-2186]

22 **Zhu H**, Liu Q, Yang X, Ding C, Wang Q, Xiong Y. LncRNA LINC00649 recruits TAF15 and enhances MAPK6 expression to promote the development of lung squamous cell carcinoma *via* activating MAPK signaling pathway. *Cancer Gene Ther* 2022; **29**: 1285-1295 [PMID: 35228660 DOI: 10.1038/s41417-021-00410-9]

23 **Li J**, Ye Y, Wang J, Zhang B, Qin S, Shi Y, He Y, Liang X, Liu X, Zhou Y, Wu X, Zhang X, Wang M, Gao Z, Lin T, Cao H, Shen L; Chinese Society Of Clinical Oncology Csco Expert Committee On Gastrointestinal Stromal Tumor. Chinese consensus guidelines for diagnosis and management of gastrointestinal stromal tumor. *Chin J Cancer Res* 2017; **29**: 281-293 [PMID: 28947860 DOI: 10.21147/j.issn.1000-9604.2017.04.01]

24 **Vasileva E**, Warren M, Triche TJ, Amatruda JF. Dysregulated heparan sulfate proteoglycan metabolism promotes Ewing sarcoma tumor growth. *Elife* 2022; **11** [PMID: 35285802 DOI: 10.7554/eLife.69734]

25 **Ullah R**, Yin Q, Snell AH, Wan L. RAF-MEK-ERK pathway in cancer evolution and treatment. *Semin Cancer Biol* 2022; **85**: 123-154 [PMID: 33992782 DOI: 10.1016/j.semcancer.2021.05.010]

26 **Miettinen M**, Sarlomo-Rikala M, Lasota J. Gastrointestinal stromal tumors: recent advances in understanding of their biology. *Hum Pathol* 1999; **30**: 1213-1220 [PMID: 10534170 DOI: 10.1016/s0046-8177(99)90040-0]

27 **Serrano C**, Mariño-Enríquez A, Tao DL, Ketzer J, Eilers G, Zhu M, Yu C, Mannan AM, Rubin BP, Demetri GD, Raut CP, Presnell A, McKinley A, Heinrich MC, Czaplinski JT, Sicinska E, Bauer S, George S, Fletcher JA. Complementary activity of tyrosine kinase inhibitors against secondary kit mutations in imatinib-resistant gastrointestinal stromal tumours. *Br J Cancer* 2019; **120**: 612-620 [PMID: 30792533 DOI: 10.1038/s41416-019-0389-6]

28 **Demetri GD**, Reichardt P, Kang YK, Blay JY, Rutkowski P, Gelderblom H, Hohenberger P, Leahy M, von Mehren M, Joensuu H, Badalamenti G, Blackstein M, Le Cesne A, Schöffski P, Maki RG, Bauer S, Nguyen BB, Xu J, Nishida T, Chung J, Kappeler C, Kuss I, Laurent D, Casali PG; GRID study investigators. Efficacy and safety of regorafenib for advanced gastrointestinal stromal tumours after failure of imatinib and sunitinib (GRID): an international, multicentre, randomised, placebo-controlled, phase 3 trial. *Lancet* 2013; **381**: 295-302 [PMID: 23177515 DOI: 10.1016/S0140-6736(12)61857-1]

29 **Wu CE**, Chen CP, Huang WK, Pan YR, Aptullahoglu E, Yeh CN, Lunec J. p53 as a biomarker and potential target in gastrointestinal stromal tumors. *Front Oncol* 2022; **12**: 872202 [PMID: 35965531 DOI: 10.3389/fonc.2022.872202]

30 **Sui C**, Lin C, Tao T, Guan W, Zhang H, Tao L, Wang M, Wang F. Prognostic significance of serum CA125 in the overall management for patients with gastrointestinal stromal tumors. *BMC Gastroenterol* 2023; **23**: 25 [PMID: 36703123 DOI: 10.1186/s12876-023-02655-0]

31 **Tian GA**, Xu WT, Sun Y, Wang J, Ke Q, Yuan MJ, Wang JJ, Zhuang C, Gong Q. BDNF expression in GISTs predicts poor prognosis when associated with PD-L1 positive tumor-infiltrating lymphocytes. *Oncoimmunology* 2021; **10**: 2003956 [PMID: 34804639 DOI: 10.1080/2162402X.2021.2003956]

32 **Xiong Y**, Yang C, Yang X, Ding C, Wang Q, Zhu H. LncRNA MIR9-3HG enhances LIMK1 mRNA and protein levels to contribute to the carcinogenesis of lung squamous cell carcinoma *via* sponging miR-138-5p and recruiting TAF15. *Pathol Res Pract* 2022; **237**: 153941 [PMID: 35933883 DOI: 10.1016/j.prp.2022.153941]

33 **de Hoog CL**, Foster LJ, Mann M. RNA and RNA binding proteins participate in early stages of cell spreading through spreading initiation centers. *Cell* 2004; **117**: 649-662 [PMID: 15163412 DOI: 10.1016/s0092-8674(04)00456-8]

34 **Andersson MK**, Ståhlberg A, Arvidsson Y, Olofsson A, Semb H, Stenman G, Nilsson O, Aman P. The multifunctional FUS, EWS and TAF15 proto-oncoproteins show cell type-specific expression patterns and involvement in cell spreading and stress response. *BMC Cell Biol* 2008; **9**: 37 [PMID: 18620564 DOI: 10.1186/1471-2121-9-37]

35 **Peng WX**, He PX, Liu LJ, Zhu T, Zhong YQ, Xiang L, Peng K, Yang JJ, Xiang GD. LncRNA GAS5 activates the HIF1A/VEGF pathway by binding to TAF15 to promote wound healing in diabetic foot ulcers. *Lab Invest* 2021; **101**: 1071-1083 [PMID: 33875793 DOI: 10.1038/s41374-021-00598-2]

36 **Marko M**, Vlassis A, Guialis A, Leichter M. Domains involved in TAF15 subcellular localisation: dependence on cell type and ongoing transcription. *Gene* 2012; **506**: 331-338 [PMID: 22771914 DOI: 10.1016/j.gene.2012.06.088]

37 **Zinszner H**, Sok J, Immanuel D, Yin Y, Ron D. TLS (FUS) binds RNA *in vivo* and engages in nucleo-cytoplasmic shuttling. *J Cell Sci* 1997; **110** (Pt 15): 1741-1750 [PMID: 9264461 DOI: 10.1242/jcs.110.15.1741]

38 **Zakaryan RP**, Gehring H. Identification and characterization of the nuclear localization/retention signal in the EWS proto-oncoprotein. *J Mol Biol* 2006; **363**: 27-38 [PMID: 16965792 DOI: 10.1016/j.jmb.2006.08.018]

39 **Law WJ**, Cann KL, Hicks GG. TLS, EWS and TAF15: a model for transcriptional integration of gene expression. *Brief Funct Genomic Proteomic* 2006; **5**: 8-14 [PMID: 16769671 DOI: 10.1093/bfgp/ell015]

40 **Rual JF**, Venkatesan K, Hao T, Hirozane-Kishikawa T, Dricot A, Li N, Berriz GF, Gibbons FD, Dreze M, Ayivi-

Guedehoussou N, Klitgord N, Simon C, Boxem M, Milstein S, Rosenberg J, Goldberg DS, Zhang LV, Wong SL, Franklin G, Li S, Albala JS, Lim J, Fraughton C, Llamosas E, Cevik S, Bex C, Lamesch P, Sikorski RS, Vandenhaute J, Zoghbi HY, Smolyar A, Bosak S, Sequerra R, Doucette-Stamm L, Cusick ME, Hill DE, Roth FP, Vidal M. Towards a proteome-scale map of the human protein-protein interaction network. *Nature* 2005; **437**: 1173-1178 [PMID: 16189514 DOI: 10.1038/nature04209]

41 **Yaeger R**, Corcoran RB. Targeting Alterations in the RAF-MEK Pathway. *Cancer Discov* 2019; **9**: 329-341 [PMID: 30770389 DOI: 10.1158/2159-8290.CD-18-1321]

42 **Kume K**, Ikeda M, Miura S, Ito K, Sato KA, Ohmori Y, Endo F, Katagiri H, Ishida K, Ito C, Iwaya T, Nishizuka SS. α-Amanitin Restrains Cancer Relapse from Drug-Tolerant Cell Subpopulations *via* TAF15. *Sci Rep* 2016; **6**: 25895 [PMID: 27181033 DOI: 10.1038/srep25895]

World Journal of Gastroenterology

Submit a Manuscript: https://www.f6publishing.com

World J Gastroenterol 2023 May 21; 29(19): 2950-2960

DOI: 10.3748/wjg.v29.i19.2950

ISSN 1007-9327 (print) ISSN 2219-2840 (online)

ORIGINAL ARTICLE

Basic Study

Susceptibility patterns and virulence genotypes of *Helicobacter pylori* affecting eradication therapy outcomes among Egyptian patients with gastroduodenal diseases

Ahmed Morad Asaad, Gasser El-Azab, Eman Abdelsameea, Osama Elbahr, Ahmed Kamal, Mohamed Abdel-Samiee, Ahmed Abdelfattah, Heba Abdallah, Doha Maher, Ahmed El-Refaie, Samar Ebrahim Ghanem, Shamshul Ansari, Samah Mohammed Awad

Specialty type: Gastroenterology and hepatology

Provenance and peer review: Invited article; Externally peer reviewed.

Peer-review model: Single blind

Peer-review report's scientific quality classification

Grade A (Excellent): A
Grade B (Very good): B
Grade C (Good): C, C, C
Grade D (Fair): D
Grade E (Poor): 0

P-Reviewer: Abadi ATB, Iran; Bordin DS, Russia; Kirkik D, Turkey; Koga Y, Japan; Machado NC, Brazil

Received: December 7, 2022
Peer-review started: December 7, 2022
First decision: January 22, 2023
Revised: February 11, 2023
Accepted: April 25, 2023
Article in press: April 25, 2023
Published online: May 21, 2023

Ahmed Morad Asaad, Department of Microbiology, College of Medicine, Zagazig University, Zagazig 44519, Egypt

Gasser El-Azab, Eman Abdelsameea, Osama Elbahr, Ahmed Kamal, Mohamed Abdel-Samiee, Ahmed Abdelfattah, Department of Hepatology and Gastroenterology, National Liver Institute, Menoufia University, Shebin El-Kom 32511, Egypt

Heba Abdallah, Department of Clinical Pathology, National Liver Institute, Menoufia University, Shebin El-Kom 32511, Egypt

Doha Maher, Ahmed El-Refaie, Department of Pathology, National Liver Institute, Menoufia University, Shebin El-Kom 32511, Egypt

Samar Ebrahim Ghanem, Department of Clinical Biochemistry and Molecular Diagnostics, National Liver Institute, Menoufia University, Shebin El-Kom 32511, Egypt

Shamshul Ansari, Department of Health Sciences, Higher Colleges of Technology, Abu Dhabi Women's College, Abu Dhabi 25026, United Arab Emirates

Samah Mohammed Awad, Department of Clinical Microbiology and Immunology, National Liver Institute, Menoufia University, Shebin El-Kom 32511, Egypt

Corresponding author: Shamshul Ansari, MSc, PhD, Assistant Professor, Department of Health Sciences, Higher Colleges of Technology, Abu Dhabi Women's College, Hazza Bin Zayed Street, Al Dhafrah-Abu Dhabi, Abu Dhabi 25026, United Arab Emirates.
shamshulansari483@yahoo.com

Abstract

BACKGROUND

Helicobacter pylori (*H. pylori*) is a significant human pathogen that is responsible for a variety of illnesses, including mucosa-associated lymphoid tissue lymphoma, gastric cancer, peptic ulcers, and gastritis.

AIM

To investigate the frequency of *H. pylori* infection and its resistance patterns among Egyptian patients and to determine the influence of *H. pylori* virulence genetic determinants on the eradication success of 14-d triple therapy regimen.

METHODS

H. pylori infections were investigated in 72 patients with gastroduodenal complications suggestive of *H. pylori* infection. The *cagA* and *vacA* genotypes of cultured strains were studied using polymerase chain reaction. The patients underwent 14 d of triple-therapy treatment. The treatment response was examined using histology and a rapid urease test 6 wk after therapy discontinuation.

RESULTS

The intention-to-treat eradication rate was 59.2% (95%CI: 48.2%–70.3%). Rates of *H. pylori* resistance to clarithromycin, amoxicillin, and metronidazole were 52.8%, 81.9%, and 100%, respectively. Successful eradication of *H. pylori* was more significantly associated with *vacA* s1-positive strains [adjusted odds ratio (aOR) = 0.507, 95%CI: 0.175–0.822]. A significant association was found between failed eradication rate and *H. pylori* strains resistant to clarithromycin (aOR = 0.204, 95%CI: –0.005 to 0.412) and amoxicillin (aOR = 0.223, 95%CI: 0.026–0.537).

CONCLUSION

This study's low *H. pylori* eradication rate following 14-d triple therapy is concerning and worrying. *H. pylori* pan-resistance to metronidazole followed by the high resistance to ciprofloxacin, amoxicillin, and clarithromycin in this research is challenging and of great concern.

Key Words: *Helicobacter pylori*; Eradication therapy; Virulence; Clarithromycin resistance; *cagA* gene; *vacA* gene

Core Tip: In this study, 72 patients with *Helicobacter pylori* infections were investigated. Half of the *Helicobacter pylori* strains had the *cagA* gene, and more than half of the strains were resistant to antibiotics except tetracycline and clarithromycin (CLR). However, CLR and tetracycline were effective at higher doses to achieve effective eradication by the CLR-based therapy. Most importantly, this study demonstrated that an alternative therapeutic regimen should be adopted to achieve effective infection eradication in Egypt.

Citation: Asaad AM, El-Azab G, Abdelsameea E, Elbahr O, Kamal A, Abdel-Samiee M, Abdelfattah A, Abdallah H, Maher D, El-Refaie A, Ghanem SE, Ansari S, Awad SM. Susceptibility patterns and virulence genotypes of *Helicobacter pylori* affecting eradication therapy outcomes among Egyptian patients with gastroduodenal diseases. *World J Gastroenterol* 2023; 29(19): 2950-2960

URL: https://www.wjgnet.com/1007-9327/full/v29/i19/2950.htm

DOI: https://dx.doi.org/10.3748/wjg.v29.i19.2950

INTRODUCTION

Helicobacter pylori (H. pylori) is a prominent human pathogen and is responsible for a variety of diseases, such as mucosa-associated lymphoid tissue lymphoma, duodenal or peptic ulcer, gastritis, and gastric cancer[1,2]. As a result of its causative relationship to gastric adenocarcinoma, the World Health Organization has identified this pathogen as a class I carcinogen[3]. According to the global estimate, *H. pylori* infects roughly 4.4 billion people with prevalence rates ranging from 20%-90% in developed and underdeveloped nations, accordingly[2].

Pathologically, the existence of gastric mucosa inflammatory changes in areas with abundant *H. pylori* organisms together with the pathognomonic existence of either lymphoid aggregates and/or follicles with germinal centers and neutrophilic infiltration constitutes the definition of chronic *H. pylori* gastritis [2,3].

Previous epidemiological research has produced a long list of microbial virulence factors that have a crucial role in *H. pylori* colonization, persistence, serotype/genotype diversity, host immune responses, pathogenicity, and disease severity. These factors involve the outer inflammatory protein (*oipA*) gene, the cytotoxin-associated gene (*cagA*), the vacuolating cytotoxin gene (*vacA*), the *babA2* adhesin gene, the epithelium gene A (*iceA*), and the duodenal ulcer-promoting gene (*dupA*)[4-7].

The variability of *H. pylori* strains is believed to be related to the genetic structural diversity with associated polymorphic arrangements of different virulence determinant genes[4]. For example, the *vacA* gene, which encodes a vacuolating toxin, is found in the vast majority of *H. pylori* strains and is an important virulence factor. Because of sequence variability in the middle region (m), m1 and m2 alleles, signal region (s), s1 or s2 alleles, and the intermediate region I subtypes 1 or 2, notable diversity in the vacuolating activity of different strains is found. *iceA1* and *iceA2* are two major alleles of the *iceA* gene, which is another example of microbial genetic variation[8].

Triple therapy for 14 d with proton pump inhibitors and a mixture of two antibiotics, clarithromycin (CLR) and amoxicillin (AMX) or metronidazole (MNZ) is the standard treatment for *H. pylori* infections [9,10]. CLR is the preferred antibiotic in areas in which resistance to this antibiotic is < 15%[10]. However, the continuous surge in antimicrobial resistance, including CLR-resistance, has been accompanied by a failure to eradicate *H. pylori* infections in a significant proportion of cases worldwide. The prevalence of *H. pylori* resistance to CLR ranges from 11.1% in Europe to 92.3% in Africa, reaching 18.9% in Asia and 29.3% in America as described in clinical reports[11-13].

Only a few studies addressing *H. pylori* infections, pathogenicity, and epidemiology among Egyptian patients are available. Besides, data regarding *H. pylori* resistance to CLR is scarce. Therefore, this research aimed to determine the *H. pylori* infection frequency and its resistance patterns among Egyptian patients and to determine the influence of *H. pylori* virulence genetic determinants on the eradication success of a 14-d triple therapy regimen.

MATERIALS AND METHODS

This cross-sectional observational study was completed from August 2021 to June 2022 at the National Liver Institute (NLI), a 760-bed tertiary care hospital in Shebin El-Kom, Egypt. The research adhered to the Helsinki Declaration principles and received ethical approval from the ethics NLI research committee, No. 00308/2022. Written consent was obtained from all participants. The research followed the international principles of strengthening the reporting of observational studies in epidemiology[14]. During the research period, 86 adult cases with different dyspepsia symptoms (vomiting, epigastric, abdominal pain, and/or heartburn) and/or other symptoms indicative of *H. pylori* infection and likely to require *H. pylori* eradication therapy were enrolled in this research.

All cases provided a medical history and underwent a physical examination, a quick urease test, and inspection of the esophagus, stomach, and duodenum using an upper endoscopy.

Endoscopy

Under topical lignocaine anesthesia, each patient underwent an upper gastrointestinal endoscopy (Olympus X Q40; Olympus Optical, Tokyo, Japan). Each patient's antrum and stomach corpus were biopsied during the endoscopy to obtain two sets of biopsy samples. The first set of biopsies was utilized for a rapid urease test utilizing a rapid urease test kit (CLO test; Kimberly-Clark Ltd., Draper, UT, United States). Three hours later, the second set was transferred on ice to the laboratory for bacteriological culture after being packed in 3 mL of sterile normal saline. For histopathological analysis, the third specimen was immediately fixed in 10% formalin. The fourth section was added to a buffered solution (10 mmol/LTris, pH 8, 10 mmol/L ethylenediaminetetraacetic acid, and 0.5% sodium dodecyl sulfate) and then frozen at –80 °C for DNA extraction and polymerase chain reaction (PCR) assays. *H. pylori* was diagnosed using three techniques: (1) *H. pylori* culture; (2) Histopathology using hematoxylin and eosin and Giemsa staining; and (3) Rapid urease test. At baseline, a patient was considered *H. pylori* -positive if he had a positive culture or rapid urease test that was validated by histological features (foveolar-neutrophilic infiltration, lymphoid follicles and/or aggregates, and verified positive Giemsa stained I rods). Six weeks after the triple therapy cessation, a second gastrointestinal endoscopy was completed to determine and confirm the presence of *H. pylori* and whether or not the duodenal ulcer had been successfully cured. Eradication was defined as the absence of histological evidence and a negative result on the rapid urease test.

H. pylori culture and antimicrobial susceptibility testing

Using a tissue grinder, the biopsy specimen was homogenized and plated onto brain-heart infusion agar plates (Difco, Detroit, MI, United States) that were supplemented with vancomycin (6 mg/mL), amphotericin B (8 mg/mL), trimethoprim (5 mg/mL), and 10% glycerol. Under microaerophilic conditions (85% N_2, 5% O_2, and 10% CO_2) in a humid atmosphere, the plates were incubated at 37 °C for 3-5 d. *H. pylori* was recognized based on Gram staining, helical shape, and biochemical assays that were positive for oxidase, catalase, and urease[15].

As suggested by the European committee on antimicrobial susceptibility testing, the E-test minimum inhibitory concentration technique was used to test for antimicrobial susceptibility. Tests were done on Mueller–Hinton agar plates enriched with 7% horse blood (bioMérieux Inc., Marcy-l'Étoile, France) using E-test strips (AB Biodisk, Slona, Sweden)[16]. Tetracycline (TET), CLR, AMX, rifampicin (RIF), and ciprofloxacin (CIP) were among the antibiotics that were evaluated. The isolate was considered

resistant to AMX, CLR, and MNZ if minimal inhibitory concentrations (MICs) were > 0.125 mg/L, > 0.5 mg/L, and > 8 mg/L, respectively. Besides, the isolate was considered resistant to CIP, RIF, and TET if MICs were > 1 mg/L[16].

DNA extraction

Each *H. pylori* isolate was sub-cultured and incubated for 72 h after which 7-10 colonies were pooled together. DNA was extracted according to the manufacturer's instructions using the QIAamp DNA micro kit (Qiagen, Hilden, Germany) and then was eluted in 200 μL of 1x TE buffer (10 mM Tris-HCl, 1 mM ethylenediaminetetraacetic acid; pH 8.0) and stored at –20 °C until PCR amplification.

Molecular identification of cagA and vacA genotypes of H. pylori

As previously disclosed, all isolates were subject to multiplex PCR to determine *cagA* and *vacA* genotypes[17-19]. Table 1 contains a list of all primers utilized for this research. Multiplex PCR was carried out in a thermocycler (Cyclogene; Bio-Techne, Minneapolis, MN, United Kingdom) in a reaction mixture volume of 50 μL. Each reaction contained 25 μL of 2 × multiplex PCR Master mix (Hot start DNA polymerase, multiplex buffer, dNTP mix $MgCl_2$; ThermoScientific, Vilinus, Lithuania), 2 μL of each primer (40 pmol), and 200 ng of template DNA (6 μL) according to DNA concentration in yield. The reaction volume was brought to 50 μL with the addition of nuclease free water. PCR grade water and DNA from *H. pylori* strain American Type Culture Collection 43504 were used as negative and positive controls, respectively. Multiplex PCR was carried out by the simultaneous addition of primers in the same reaction mixture after test of each primer pair separately: (1) 35 cycles of 95 °C for 1 min; (2) Annealing at 54 °C for 1.5 min; (3) Extension at 72 °C for 1 min; and (4) A final extension at 72 °C for 10 min. The amplified PCR products were electrophoresed on 1.5% agarose gels using 1 × TBE after which the gel was stained with ethidium bromide using a 100 bp ladder as the molecular weight standard, visualized under an ultraviolet light source, and photographed using a BioRad Gel Doc device.

H. pylori eradication therapy and follow-up

Patients were given omeprazole (20 mg) and two antibiotics, AMX (1 g) and CLR (500 mg), twice daily for 14 d[9]. Clinical follow-up, including side-effect monitoring, was performed until the medication was completed. Using a rapid urease test, the therapeutic response was examined 6 wk following the termination of therapy. Successful eradication of *H. pylori* was indicated by a negative result from the rapid urease test and microbiological cultures and by the absence of neutrophilic infiltration with a decrease in lymphoid inflammatory changes in the biopsy tissue following treatment[9,20].

Statistical analysis

Coding, validating, and analyzing the data required the use of SPSS version 22 (IBM Corp., Armonk, NY, United States). Data were shown using average, median, and frequencies (%). A χ^2 test or Fisher's exact test was used to compare categorical data, and the Student's *t*-test was used for numerical data. *P* values ≤ 0.05 based on a two-tail test were considered to be significant. Potential risk factors were identified using a binary logistic regression analysis that included an antecedent 95%CI and adjusted odds ratio (aOR).

RESULTS

Patients characteristics and H. pylori infection

Table 2 shows the demographic and clinical characteristics of the patients. The age of the patients ranged from 19 years to 59 years (median: 39.5 years), and 57 (79.2%) were males. Based on endoscopic examination, more than half of the patients (54.2%) had gastritis, while 33.3% and 12.5% of patients had gastric ulcer and duodenitis, respectively. Based on histopathological examination of the tissue biopsy, features of chronic gastritis and rods of *H. pylori* were seen based on Giemsa stain (Figure 1).

Thirty-six (50%) strains were *cagA*-positive among 72 *H. pylori* isolates in this study, and in 50 (69.4%) of the *H. pylori* strains, the *vacA* gene was detected. For the *vacA* gene s and m region sub-typing, 42 and 18 strains were positive for s1 and s2, respectively, while 27 and 33 isolates were positive for m1 and m2, respectively (Figure 2).

Antimicrobial susceptibility test outcomes

During the research period, a total of 86 patients were recruited. Among them, 10 patients were negative for *H. pylori* infection, and 4 patients failed to complete treatment, leaving 72 patients eligible for the study protocol. Among the 72 *H. pylori* isolates, the resistance rates to MNZ, AMX, RIF, CLR, CIP, and TET were 100%, 81.9%, 62.5%, 52.8%, 41.7%, and 37.5%, respectively.

Triple therapy outcomes

The eligible patients underwent 14-d triple therapy with two antibiotics: (1) AMX (1 g); (2) CLR (500

Table 1 Primers used in this study for multiplex polymerase chain reaction for detection of *vacA* and *cagA* genotypes in *Helicobacter pylori* isolates

Primer	Nucleotide sequence, 5'—3'	Gene	Size, bp
vacA			
VA1-F	ATGGAAATACAACAAACACAC	*vacA* s1/s2	259/286
VA1-R	CTGCTTGAATGCGCCAAAC		
VA2-F	CAATCTGTCCAATCAAGCGAG	*vacA* m1/m2	570/645
VA2-R	GCGTCAAAATAATTCCAAGG		
Cag-F	GTTGATAACGCTGTCGCTTC	*cagA*	349
Cag-R	GGGTTGTATGATATTTTCCATAA		

m1/m2: Middle regions; s1/s2: Signal regions.

Table 2 Patient demographic and clinical characteristics

Variable	*n* (%)
Mean age in yr	39.5 ± 12.9
Male sex	57 (79.2)
History of smoking	22 (30.6)
History of upper abdominal pain	48 (66.7)
Endoscopic finding	
Gastritis	39 (54.2)
Gastric ulcer	24 (33.3)
Duodenitis	9 (12.5)
Co-morbid conditions	
Liver cirrhosis	15 (20.8)
Diabetes mellitus	9 (12.5)
Hypertension	3 (4.2)
cagA	36 (50.0)
vacA	60 (83.3)
s1	42 (58.3)
s2	18 (25.0)
m1	27 (37.5)
m2	33 (45.8)

m1/m2: Middle regions; s1/s2: Signal regions.

mg); and (3) Omeprazole (20 mg). In 45 individuals, the 14-d triple therapy was successful in completely eliminating *H. pylori*; however, in the other 27 patients, the infection persisted despite treatment. *H. pylori* eradication rates were 59.2% (95%CI: 48.2–70.3%) for intention-to-treat (ITT) and 62.5% (95%CI: 51.3%–73.7%) for per protocol treatment.

In patients with *vacA* s1-positive (P = 0.02), s2-positive (P = 0.03), or m1-positive (P = 0.01) strains, *H. pylori* eradication occurred more frequently. It was not surprising that the rates of resistance to AMX (P = 0.012) and CLR were higher in *H. pylori* isolates from patients who experienced unsuccessful eradication (P = 0.005). However, no significant association with eradication therapy and resistance rates to CIP, TET, and RIF was found (Table 3).

With 95%CI and aOR the multiple logistic regression analysis revealed possible risk factors associated with *H. pylori* eradication therapy (Table 4). Successful eradication of *H. pylori* was more significantly associated with strains harboring the *vacA* s1 genotype (aOR = 0.507, 95%CI: 0.175–0.822). In contrast,

Table 3 Relationship between risk factors and outcomes of *Helicobacter pylori* eradication therapy, *n* (%)

Variable	Successful, *n* = 45	Unsuccessful, *n* = 27	*P* value
Mean age in yr	43.13 ± 12.19	39.22 ± 11.91	0.188
Male sex	36	21	0.524
Smoking	15	12	0.349
cagA	21 (46.7)	15 (55.6)	0.313
s1	31 (68.9)	11 (40.7)	0.022
s2	15 (33.3)	3 (11.1)	0.031
m1	22 (48.9)	5 (18.5)	0.014
m2	21 (46.7)	12 (44.4)	0.525
AMX	33 (73.3)	26 (96.3)	0.012
CIP	18 (40.0)	12 (44.4)	0.45
TET	15 (33.3)	12 (44.4)	0.244
CLR	18 (40.0)	20 (74.1)	0.005
RIF	27 (60.0)	18 (40.0)	0.379

AMX: Amoxicillin; CIP: Ciprofloxacin; CLR: Clarithromycin; m1/m2: Middle region; RIF: Rifampicin; s1/s2: Signal region; TET: Tetracycline.

Table 4 Multivariate analysis of risk factors accompanied with eradication therapy of *Helicobacter pylori*

Variable	aOR (95%CI)	*P* value
s1	0.507 (0.175–0.822)	0.003
s2	0.074 (-0.227 to 0.393)	0.595
m1	-0.028 (-0.291 to 0.234)	0.83
AMX	0.223 (0.026–0.537)	0.032
CLR	0.204 (-0.005 to 0.412)	0.036

aOR: Adjusted odds ratio; AMX: Amoxicillin; CI: Confidence interval; CLR: Clarithromycin; m1: Middle region; s1/s2: Signal region.

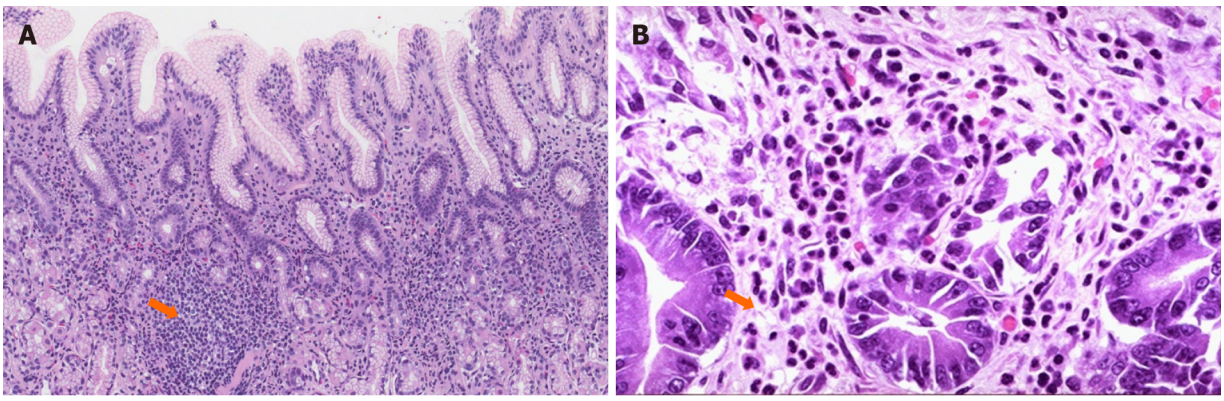

DOI: 10.3748/wjg.v29.i19.2950

Figure 1 *Helicobacter pylori* associated chronic gastritis with lymphoid aggregates and curved rods of *Helicobacter pylori* carpeting the mucosal surface. A: Hematoxylin and eosin staining, × 200; B: Hematoxylin and eosin staining, × 400.

failed eradication rates were significantly associated with *H. pylori* strains resistant to AMX (aOR = 0.223, 95%CI: 0.026–0.537) and CLR (aOR = 0.204, 95%CI: –0.005 to –0.036).

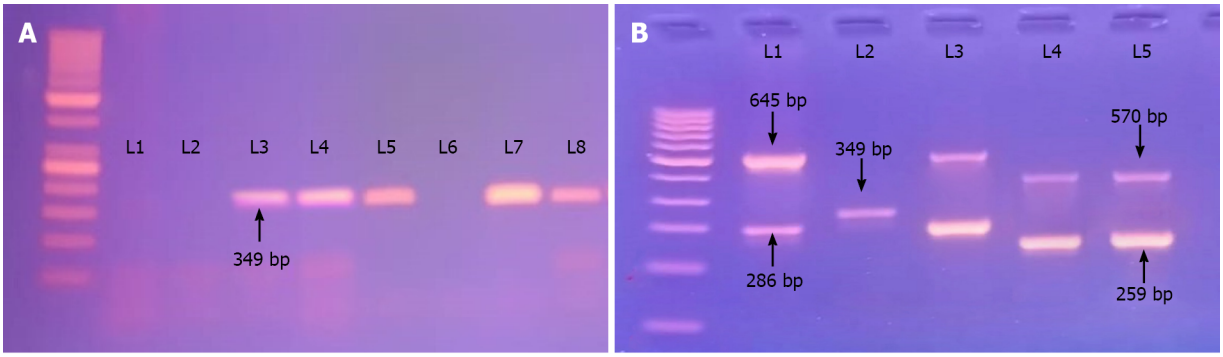

DOI: 10.3748/wjg.v29.i19.2950

Figure 2 Polymerase chain reaction amplification of *cagA* and *vacA* genotypes using 100 bp ladder. A: Lanes 1, 2, 6 *cagA*-negative and lanes 3, 4, 5, 7, and 8 *cagA*-positive; B: Lanes 1 and 3 *vacA* genotype s2m2 and lanes 4 and 5 *vacA* genotype s1m1.

DISCUSSION

Eradication therapy of *H. pylori* infections has been deemed beneficial for cases with gastroduodenal disorders, such as gastric MALT lymphoma, peptic ulcer disease history, gastric cancer, dyspepsia, atrophic gastritis, and hyperplastic polyps, and for cases with certain extragastrointestinal disorders, such as unexplained iron-deficiency anemia, chronic idiopathic urticaria, and idiopathic thrombocytopenic purpura[1,21].

Despite establishment of multiple *H. pylori* eradication treatment regimens in different worldwide regions, the usual 14-d triple therapy [piperacillin/AMX/CLR (PAC)] produces adequate eradication rates for both adults and children in Egypt[21-23]. However, cure rates in this study were found to be unsatisfactory and disappointing. Our findings showed that the 14-d triple therapy efficacy of *H. pylori* eradication (59%) was lower than that reported from previous Egyptian studies (ITT range: 72%–83%) [22,23]. A previous meta-analysis investigated the global trend in eradication rates of two different first-line therapeutic regimens (PAC and piperacillin/AMX/MNZ) for 8061 patients infected with *H. pylori* from 30 countries[24]. In this report, the cure rate of PAC (77.1%, 95%CI = 75%–79%) was significantly higher than piperacillin /AMX/MNZ (70%, 95%CI = 67.7%–72.3%) (OR = 0.70, 95%CI = 0.56–0.88; P < 0.002). Previous clinical studies worldwide showed an unacceptable and continuous decrease in *H. pylori* triple eradication therapy-associated cure rates[13,25]. It is noteworthy that the overall global cure rates of these protocols are < 80%, which have recently been considered regimens with disappointing efficacy.

Inadequate treatment duration, antimicrobial resistance, inadequate stomach acid suppression, poor adherence to eradication regimens, and quick metabolism of proton pump inhibitors have all been implicated in the failure of the traditional triple therapy to eradicate a pathogen according to previous ecological research[26,27]. CLR resistance has been recognized as the primary cause of routine triple treatment failure. In a recent meta-analysis investigating 66142 patients from 65 countries, failure to achieve eradication was 7-fold higher in patients with CLR-resistant *H. pylori* infections (OR: 6.97; 95%CI: 5.23–9.01; P = 0.001) when treated with a CLR-containing regimen than patients with susceptible strains[13]. Therefore, in nations with a high prevalence of CLR resistance (> 15%–20%), bismuth quadruple treatment is recommended.

Pooled data from 25 randomized trials including 3990 patients showed that the ITT eradication rate of standard triple therapy (65.7%) was significantly lower than bismuth-containing regimens (74.9%; OR: 1.60; 95%CI: 1.07–2.39). In addition, in the per protocol analysis, the pooled eradication rate for bismuth-containing regimens was 86.7% *vs* 33.3% for the usual triple regimen (OR: 10.64; 95%CI: 2.96–39.53)[28]. It is noteworthy that all isolates in this study were MNZ-resistant, and more than half of the isolates were resistant to AMX and CLR. These findings are not surprising as MNZ has been abused by the public without prescription for various gastrointestinal infections and diarrhea, while both AMX and CLR have been included in empiric therapies for respiratory infections or non-tuberculous mycobacterial infections in our region. Therefore, continuous monitoring of susceptibility patterns of *H. pylori* to various antimicrobials seems crucial as multidrug resistant *H. pylori* strains undoubtedly induce failure of *H. pylori* eradication therapy.

H. pylori cagA and *vacA* genotypes are among the most important factors implicated in the pathogenesis of gastroduodenal diseases and in influencing the sequelae of treatment protocols. The association of *cagA*-positive strains with the *H. pylori* eradication therapy outcomes were demonstrated by former clinical and ecological investigations[4-9]. However, the results from these studies were inconsistent and controversial. In this study, strains with or without *cagA* had no effect on eradication rates, a finding that is similar to previous reports. In a previous meta-analysis including 25 studies, the influence of the virulence factors, *vacA* and *cagA*, on *H. pylori* eradication therapy in 2693 cases was investigated by Wang *et al*[29]. In their report, the pooled *H. pylori* eradication rate was 77% (95%CI:

70%–83%) for *cagA*-negative patients and 85% (95%CI: 81%–89%) for *cagA*-positive with an 8% higher eradication rate among *cagA*-positive strains. In addition, using subgroup analyses based on clinical presentations, eradication detection method, location, and therapeutic regimen types, the authors concluded that *cagA*-negative strains responded to successful *H. pylori* therapy eradication rates than *cagA*-positive strains with pooled risk ratios (RR) of 1.118 (95%CI: 1.051–1.189; $P < 0.001$) for Asia and 1.138 (95%CI: 1.000–1.295; $P = 0.049$) for Europe. In South America, *cagA*-positive strains and *cagA*-negative strains exhibited comparable *H. pylori* treatment rates (RR: 1.104, 95%CI: 0.953–1.279; $P = 0.186$).

The *vacA* s1-positive *H. pylori* strains are typically more virulent and more closely linked to progressive gastroduodenal disorders as reported in many previous studies[29]. An increase in blood flow to the site of infection and stronger inflammatory responses were stimulated by more virulent strains as reported by clinical and epidemiological-based evidence. In addition, the more virulent strains are usually more susceptible to antimicrobials because of faster replication. *H. pylori* strains containing *vacA* s1 were substantially related to a greater *H. pylori* eradication rate in the current investigation.

This result is consistent with earlier findings in which *vacA* s1-positive strains posed a significant risk for the development of gastric illnesses with easier eradication in diseased people. Wang *et al*[29] discovered that the pooled *H. pylori* eradication rate was 73% (95%CI: 61%–85%) for *vacA* s2 and 83% (95%CI: 75%–91%) for *vacA* s1 with a 10% improvement in eradication rates in the *vacA* s1 group compared to the *vacA* s2 group (95%CI: 1.040–1.303; $P = 0.008$). In their meta-analysis, *vacA* s1 status was associated with better eradication rates in the triple therapy subgroup according to an examination of subgroups based on different worldwide locations (RR: 1.175, 95%CI: 1.012–1.360)[29]. Brennan *et al*[7] reported that the incidence of the more virulent s1 genotype was substantially lower among previously treated individuals than among those who had never received therapy (58.3% *vs* 74.3%). A significant increase in the frequency of the least pathogenic s2/m2 genotype was seen in previously treated individuals (36.7% *vs* 21.0%)[7]. Our findings and results of other studies clearly demonstrated that the *vacA* s1 genotype would be useful for predicting successful outcomes of *H. pylori* eradication therapy.

This study had some limitations. First, this research may have been limited in its capability to investigate other virulence marker-associated pathogenic roles due to the lack of molecular analysis beyond PCR and genome sequencing. Second, this study was conducted within a single center. Therefore, our findings cannot be applied to other situations. To further understand the phenotypic and genotypic links between *H. pylori* virulence, antibiotic resistance, and the efficacy of eradication therapy, further molecular-based epidemiological multicenter investigations with longer monitoring durations are required.

CONCLUSION

This low *H. pylori* eradication rate following 14-d triple therapy is concerning and worrying. The pan-resistance of *H. pylori* to MNZ followed by the high resistance to AMX, CLR, and CIP in this research is challenging and of great concern. These findings draw attention to the urgent need for performing *H. pylori* antimicrobial susceptibility testing before starting eradication therapy in addition to continuous surveillance of *H. pylori* resistance patterns in our region to provide data that can guide empirical treatment. In addition, the *vacA* s1-positive *H. pylori* isolates are easier to eradicate and could be used as an indicator to predict the successful outcome of eradication therapy.

ARTICLE HIGHLIGHTS

Research background

Helicobacter pylori (*H. pylori*) has been implicated in the development of gastric cancer and gastric mucosa-associated lymphoid tissue lymphoma. However, the bacterial eradication reduces the risk of theses gastric complications. The therapeutic regimens currently in use and the duration of therapy differ in different countries, which affects the therapy outcomes. The therapeutic outcomes have been found to be affected by the virulence characteristics of the infecting strains. The strains with more virulent characteristics possessing *vacA* s1 and m1 are eradicated more efficiently than the strains harboring less virulent characteristics.

Research motivation

To demonstrate that the infecting strains possessing more virulent characteristics are eradicated efficiently with a 14-d triple therapy. The *vacA* s1-positive *H. pylori* isolates are easier to eradicate and could be used as an indicator to predict the successful outcome of eradication therapy.

Research objectives

To evaluate the *H. pylori* infection frequency and its resistance patterns among Egyptian patients and to determine the *H. pylori* virulence characteristics influencing the eradication success of the 14-d triple therapy regimen.

Research methods

The patients suggestive of *H. pylori* infections were subjected to endoscopy-based biopsy specimen collection. The collected biopsy specimens were used to evaluate the *H. pylori* infection by a combination of diagnostic tests that included urease test, bacterial culture, and histopathological investigation. The extracted DNA was subjected to PCR-based *cagA* and *vacA* genotype investigation. The *H. pylori*-infected patients received triple therapy for 14 d. Six weeks after completion of the therapy, the treatment response was examined utilizing histology and the rapid urease test.

Research results

Among the 86 recruited patients, infection was found in 76 individuals. All of the strains were resistant to metronidazole (MNZ), while 52.8% and 81.9% of the isolates were resistant to clarithromycin (CLR) and amoxicillin (AMX), respectively. Successful eradication of *H. pylori* was significantly associated with *vacA* s1-positive strains [adjusted odds ratio (aOR) = 0.507, 95%CI: 0.175–0.822]. *H. pylori* strains resistant to CLR (aOR = 0.204, 95%CI: -0.005 to 0.412) and AMX (aOR = 0.223, 95%CI: 0.026–0.537) were significantly associated with failed eradication rate.

Research conclusions

The low eradication rate of 14-d triple therapy in this study is worrisome and indicates that an alternative therapy to achieve effective eradication must be identified. The findings of complete failure of MNZ and reduced efficacy of AMX, CLR, and ciprofloxacin draw attention to the urgent need of antimicrobial susceptibility testing-guided eradication therapy. In addition, the strains with virulent properties of *vacA* s1 are easier to eradicate and could be used as an indicator to predict the successful outcome of eradication therapy.

Research perspectives

CLR, AMX, and MNZ-based 14-d eradication therapy is ineffective and discouraged in these populations. Extensive nationwide studies should be considered to document the efficacy and to find alternative therapeutic regimens in respect to the duration. Furthermore, antimicrobial susceptibility testing based therapy should be encouraged to help reduce the development of antimicrobial resistance.

ACKNOWLEDGEMENTS

The authors would like to thank the colleagues in the Department of Laboratory and Microbiology and Endoscopy and the patients in the National Liver Institute who aided this research.

FOOTNOTES

Author contributions: Asaad AM and Awad SM conceived and designed the study; El-Azab G, Abdelsameea E, El-Bahr O, Kamal A, Abdel-Samiee M, and Abdelfattah A collected the data and performed the clinical part of the study; Abdallah H, Maher D, El-Refaie A, Ghanem SE, and Awad SM contributed to the laboratory investigations of the study; Ghanem SE and Awad SM performed the data analysis; Asaad AM, Ansari S, and Awad SM wrote the paper; All authors extensively revised the manuscript.

Institutional review board statement: The study protocol was approved by the local ethics committee of National Liver Institute Menoufia University, No. 00308/2022.

Informed consent statement: Patient consent was taken from all studied patients before the start of the study. The authors affirm that human research participants provided informed consent for publication.

Conflict-of-interest statement: All the authors report having no relevant conflicts of interest for this article.

Data sharing statement: The datasets generated and/or analyzed during the current study are not publicly available due to confidential and institutional ethical issues.

Country/Territory of origin: Egypt

ORCID number: Ahmed Morad Asaad 0000-0002-1422-1117; Eman Abdelsameea 0000-0002-3225-7164; Mohamed Abdel-Samiee 0000-0002-8970-0286; Heba Abdallah 0000-0001-6336-9786; Samar Ebrahim Ghanem 0000-0003-2798-9720; Shamshul Ansari 0000-0003-1846-1377.

S-Editor: Li L
L-Editor: Filipodia
P-Editor: Fan JR

REFERENCES

1 **Leja M**, Axon A, Brenner H. Epidemiology of Helicobacter pylori infection. *Helicobacter* 2016; **21** Suppl 1: 3-7 [PMID: 27531531 DOI: 10.1111/hel.12332]
2 **Atherton JC**. The pathogenesis of Helicobacter pylori-induced gastro-duodenal diseases. *Annu Rev Pathol* 2006; **1**: 63-96 [PMID: 18039108 DOI: 10.1146/annurev.pathol.1.110304.100125]
3 **Herrero R**, Parsonnet J, Greenberg ER. Prevention of gastric cancer. *JAMA* 2014; **312**: 1197-1198 [PMID: 25247512 DOI: 10.1001/jama.2014.10498]
4 **Sukri A**, Hanafiah A, Mohamad Zin N, Kosai NR. Epidemiology and role of Helicobacter pylori virulence factors in gastric cancer carcinogenesis. *APMIS* 2020; **128**: 150-161 [PMID: 32352605 DOI: 10.1111/apm.13034]
5 **Sugimoto M**, Yamaoka Y. Virulence factor genotypes of Helicobacter pylori affect cure rates of eradication therapy. *Arch Immunol Ther Exp (Warsz)* 2009; **57**: 45-56 [PMID: 19219527 DOI: 10.1007/s00005-009-0007-z]
6 **Oktem-Okullu S**, Cekic-Kipritci Z, Kilic E, Seymen N, Mansur-Ozen N, Sezerman U, Gurol Y. Analysis of Correlation between the Seven Important Helicobacter pylori (H. pylori) Virulence Factors and Drug Resistance in Patients with Gastritis. *Gastroenterol Res Pract* 2020; **2020**: 3956838 [PMID: 32908495 DOI: 10.1155/2020/3956838]
7 **Brennan DE**, Dowd C, O'Morain C, McNamara D, Smith SM. Can bacterial virulence factors predict antibiotic resistant Helicobacter pylori infection? *World J Gastroenterol* 2018; **24**: 971-981 [PMID: 29531461 DOI: 10.3748/wjg.v24.i9.971]
8 **Gangwer KA**, Shaffer CL, Suerbaum S, Lacy DB, Cover TL, Bordenstein SR. Molecular evolution of the Helicobacter pylori vacuolating toxin gene *vac*A. *J Bacteriol* 2010; **192**: 6126-6135 [PMID: 20870762 DOI: 10.1128/JB.01081-10]
9 **Malfertheiner P**, Megraud F, Rokkas T, Gisbert JP, Liou JM, Schulz C, Gasbarrini A, Hunt RH, Leja M, O'Morain C, Rugge M, Suerbaum S, Tilg H, Sugano K, El-Omar EM; European Helicobacter and Microbiota Study group. Management of Helicobacter pylori infection: the Maastricht VI/Florence consensus report. *Gut* 2022 [PMID: 35944925 DOI: 10.1136/gutjnl-2022-327745]
10 **De Francesco V**, Bellesia A, Ridola L, Manta R, Zullo A. First-line therapies for Helicobacter pylori eradication: a critical reappraisal of updated guidelines. *Ann Gastroenterol* 2017; **30**: 373-379 [PMID: 28655973 DOI: 10.20524/aog.2017.0166]
11 **Wu W**, Yang Y, Sun G. Recent Insights into Antibiotic Resistance in Helicobacter pylori Eradication. *Gastroenterol Res Pract* 2012; **2012**: 723183 [PMID: 22829809 DOI: 10.1155/2012/723183]
12 **Papastergiou V**, Georgopoulos SD, Karatapanis S. Treatment of Helicobacter pylori infection: meeting the challenge of antimicrobial resistance. *World J Gastroenterol* 2014; **20**: 9898-9911 [PMID: 25110420 DOI: 10.3748/wjg.v20.i29.9898]
13 **Savoldi A**, Carrara E, Graham DY, Conti M, Tacconelli E. Prevalence of Antibiotic Resistance in Helicobacter pylori: A Systematic Review and Meta-analysis in World Health Organization Regions. *Gastroenterology* 2018; **155**: 1372-1382.e17 [PMID: 29990487 DOI: 10.1053/j.gastro.2018.07.007]
14 **Strengthening the reporting of observational studies in epidemiology**. STROBE checklist, version 4. 2007. [cited 22 October 2018]. Available from: http://www.strobe-statement.org/index.php?id=available-checklists
15 **Mégraud F**, Lehours P. Helicobacter pylori detection and antimicrobial susceptibility testing. *Clin Microbiol Rev* 2007; **20**: 280-322 [PMID: 17428887 DOI: 10.1128/CMR.00033-06]
16 **European committee on antimicrobial susceptibility testing**. Breakpoint Tables for Interpretation of MICs and Zone Diameters, Version 9.0. 2019. [cited 1 January 2019]. Available from: http://www.eucast.org
17 **Tummuru MK**, Cover TL, Blaser MJ. Cloning and expression of a high-molecular-mass major antigen of Helicobacter pylori: evidence of linkage to cytotoxin production. *Infect Immun* 1993; **61**: 1799-1809 [PMID: 8478069 DOI: 10.1128/iai.61.5.1799-1809.1993]
18 **Atherton JC**, Cao P, Peek RM Jr, Tummuru MK, Blaser MJ, Cover TL. Mosaicism in vacuolating cytotoxin alleles of Helicobacter pylori. Association of specific *vac*A types with cytotoxin production and peptic ulceration. *J Biol Chem* 1995; **270**: 17771-17777 [PMID: 7629077 DOI: 10.1074/jbc.270.30.17771]
19 **Yamaoka Y**, Kodama T, Gutierrez O, Kim JG, Kashima K, Graham DY. Relationship between Helicobacter pylori *ice*A, cagA, and *vac*A status and clinical outcome: studies in four different countries. *J Clin Microbiol* 1999; **37**: 2274-2279 [PMID: 10364597 DOI: 10.1128/JCM.37.7.2274-2279.1999]
20 **Alboraie M**, Elhossary W, Aly OA, Abbas B, Abdelsalam L, Ghaith D, Shady Z, Gaber Y, Adel E, Peura D, Armstrong D, Esmat G; special interest group; Egyptian Association for Study of Gastrointestinal Diseases and Liver (E A S G L D). Egyptian recommendations for management of Helicobacter pylori infection: 2018 report. *Arab J Gastroenterol* 2019; **20**: 175-179 [PMID: 31564518 DOI: 10.1016/j.ajg.2019.09.001]
21 **Kamboj AK**, Cotter TG, Oxentenko AS. Helicobacter pylori: The Past, Present, and Future in Management. *Mayo Clin Proc* 2017; **92**: 599-604 [PMID: 28209367 DOI: 10.1016/j.mayocp.2016.11.017]
22 **Ismail WA**, Mostafa EF. A comparison between conventional triple therapy and sequential therapy on tolerance of

treatment and eradication of Helicobacter pylori infection in Egyptian patients. *Egy J Int Med* 2018; **30**: 90-95 [DOI: 10.4103/ejim.ejim_6_18]

23 **Abd-Elsalam S**, Kobtan A, El-Kalla F, Elkhalawany W, Nawasany SE, Saif SA, Yousef M, Ali LA, Soliman S, Mansour L, Habba E, Soliman H, Rizk F, Shehata MA. A 2-week Nitazoxanide-based quadruple treatment as a rescue therapy for Helicobacter pylori eradication: A single center experience. *Medicine (Baltimore)* 2016; **95**: e3879 [PMID: 27310977 DOI: 10.1097/MD.0000000000003879]

24 **Puig I**, Baylina M, Sánchez-Delgado J, López-Gongora S, Suarez D, García-Iglesias P, Muñoz N, Gisbert JP, Dacoll C, Cohen H, Calvet X. Systematic review and meta-analysis: triple therapy combining a proton-pump inhibitor, amoxicillin and metronidazole for Helicobacter pylori first-line treatment. *J Antimicrob Chemother* 2016; **71**: 2740-2753 [PMID: 27342548 DOI: 10.1093/jac/dkw220]

25 **Li B**, Lan X, Wang L, Zhao J, Ding J, Ding H, Lei J, Wei Y, Zhang W. Proton-pump inhibitor and amoxicillin-based triple therapy containing clarithromycin *vs* metronidazole for Helicobacter pylori: A meta-analysis. *Microb Pathog* 2020; **142**: 104075 [PMID: 32074497 DOI: 10.1016/j.micpath.2020.104075]

26 **Zullo A**, De Francesco V, Hassan C. Predicting Helicobacter pylori eradication: how to teach an old dog new tricks! *J Clin Gastroenterol* 2012; **46**: 259-261 [PMID: 22395061 DOI: 10.1097/MCG.0b013e318247177e]

27 **Kotilea K**, Mekhael J, Salame A, Mahler T, Miendje-Deyi VY, Cadranel S, Bontems P. Eradication rate of Helicobacter Pylori infection is directly influenced by adherence to therapy in children. *Helicobacter* 2017; **22** [PMID: 28303625 DOI: 10.1111/hel.12383]

28 **Ko SW**, Kim YJ, Chung WC, Lee SJ. Bismuth supplements as the first-line regimen for Helicobacter pylori eradication therapy: Systemic review and meta-analysis. *Helicobacter* 2019; **24**: e12565 [PMID: 30698318 DOI: 10.1111/hel.12565]

29 **Wang D**, Li Q, Gong Y, Yuan Y. The association between *vac*A or cagA status and eradication outcome of Helicobacter pylori infection: A meta-analysis. *PloS One* 2017; **12**: e0177455 [PMID: 28493953 DOI: 10.1371/journal.pone.0177455]

World Journal of Gastroenterology

Submit a Manuscript: https://www.f6publishing.com

World J Gastroenterol 2023 May 21; 29(19): 2961-2978

DOI: 10.3748/wjg.v29.i19.2961

ISSN 1007-9327 (print) ISSN 2219-2840 (online)

ORIGINAL ARTICLE

Basic Study

MMP14 is a diagnostic gene of intrahepatic cholangiocarcinoma associated with immune cell infiltration

Jun Wu, Yang Guo, Zhi-Fan Zuo, Zi-Wei Zhu, Lei Han

Specialty type: Oncology

Provenance and peer review: Unsolicited article; Externally peer reviewed.

Peer-review model: Single blind

Peer-review report's scientific quality classification

Grade A (Excellent): A
Grade B (Very good): B, B
Grade C (Good): 0
Grade D (Fair): 0
Grade E (Poor): 0

P-Reviewer: Bleszynski MS, Canada; Ishii T, Japan; Quaresima S, Italy

Received: February 28, 2023
Peer-review started: February 28, 2023
First decision: March 14, 2023
Revised: March 24, 2023
Accepted: April 23, 2023
Article in press: April 23, 2023
Published online: May 21, 2023

Jun Wu, Zi-Wei Zhu, China Medical University, The General Hospital of Northern Theater Command Training Base for Graduate, Shenyang 110016, Liaoning Province, China

Yang Guo, Lei Han, Department of Hepatobiliary Surgery, The General Hospital of Northern Theater Command, Shenyang 110016, Liaoning Province, China

Zhi-Fan Zuo, Gynecological Radiotherapy Ward, Liaoning Provincial Cancer Hospital, Shenyang 110801, Liaoning province, China

Corresponding author: Lei Han, MD, Associate Chief Physician, Deputy Director, Department of Hepatobiliary Surgery, The General Hospital of Northern Theater Command, No. 83 Wenhua Road, Shenyang 110016, Liaoning Province, China. hanlei1974@sina.com

Abstract

BACKGROUND

Intrahepatic cholangiocarcinoma (ICC) is a malignant tumor of the hepatobiliary system with concealed onset, strong invasiveness and poor prognosis.

AIM

To explore the disease characteristic genes that may be helpful in the diagnosis of ICC and affect immune cell infiltration.

METHODS

We downloaded two ICC-related human gene expression profiles from GEO database as the training group (GSE26566 and GSE32958 datasets) for difference analysis, and performed enrichment analysis on differential genes. The least absolute shrinkage and selection operator (LASSO), support vector machine-recursive feature elimination (SVM-RFE) and random forest (RF), three machine learning algorithms, were used to screen the characteristic genes. Double verification was carried out on GSE107943 and The Cancer Genome Atlas, two verification groups. Receiver operating characteristic curve and area under the curve (AUC) were used to evaluate the diagnostic efficacy of genes for ICC. CIBERSORT and ssGSEA algorithms were used to evaluate the effect of characteristic genes on immune infiltration pattern. Human Protein Atlas (HPA) was used to analyze the protein expression level of the target gene.

RESULTS

A total of 1091 differential genes were obtained in the training group. Enrichment

analysis showed that the above genes were mainly enriched in small molecular catabolism, complement and coagulation cascade, bile secretion and other functions and pathways. Twenty-five characteristic genes were screened by LASSO regression, 19 by SVM-RFE algorithm, and 30 by RF algorithm. Three algorithms were used in combination to determine the characteristic gene of ICC: *MMP14*. The verification group confirmed that the genes had a high diagnostic accuracy (AUC values of the training group and the verification group were 0.960, 0.999, and 0.977, respectively). Comprehensive analysis of immune infiltration showed that *MMP14* could affect the infiltration of monocytes, activated memory CD4 T cells, resting memory CD4 T cells, and other immune cells, and was closely related to the expression of CD200, cytotoxic T-lymphocyte-associated antigen 4, CD14, CD44, and other immune checkpoints. The results of immunohistochemistry in HPA database showed was indeed overexpressed in ICC.

CONCLUSION

MMP14 can be used as a disease characteristic gene of ICC, and may regulate the distribution of immune-infiltrating cells in the ICC tumor microenvironment, which provides a new method for the determination of ICC diagnostic markers and screening of therapeutic targets.

Key Words: Intrahepatic cholangiocarcinoma; MMP14; Machine learning; Immune infiltration; Characteristic gene; Diagnostic markers

Core Tip: This study demonstrates that a new candidate molecular marker: MMP14 that is important for the diagnosis of intrahepatic cholangiocarcinoma, and MMP14 was related to a variety of immune cell components and participated in the occurrence and development in intrahepatic cholangiocarcinoma.

Citation: Wu J, Guo Y, Zuo ZF, Zhu ZW, Han L. *MMP14* is a diagnostic gene of intrahepatic cholangiocarcinoma associated with immune cell infiltration. *World J Gastroenterol* 2023; 29(19): 2961-2978
URL: https://www.wjgnet.com/1007-9327/full/v29/i19/2961.htm
DOI: https://dx.doi.org/10.3748/wjg.v29.i19.2961

INTRODUCTION

Intrahepatic cholangiocarcinoma (ICC) is the second most common primary tumor of the liver, which originates from intrahepatic bile duct epithelial cells and accounts for about 20% of primary liver malignant tumors[1]. Its incidence is on the rise worldwide, with the highest incidence in Southeast Asia, and the second highest incidence in China after Thailand[2,3]. Pathological changes such as chronic cholangitis, cholestasis, intrahepatic bile duct stones, and liver cirrhosis all increase the incidence of ICC[4]. At present, due to the poor efficacy of radiotherapy and chemotherapy for ICC, surgical treatment is currently the main treatment method for ICC. However, patients with ICC may be asymptomatic in the early stage, and most patients have intrahepatic metastasis, lymph node metastasis, or even distant metastasis at the first time of diagnosis. Only 9% of patients with advanced ICC can survive for 5 years[5-8]. Despite the continuous improvement in imaging and laboratory tests, the early diagnosis of ICC is still not ideal. Currently, the biomarkers of ICC mainly include carcinoembryonic antigen, carbohydrate antigen 19-9 and a-fetoprotein, but the sensitivity and specificity are not satisfactory[9]. Hence, it is crucial to find new biomarkers for early screening and diagnosis of ICC.

Many studies on the tumor microenvironment have confirmed that a variety of immune regulatory mechanisms play an important role in the malignant biological behavior of tumors. Therefore, immunotherapy has gradually been paid attention in various treatments for solid tumors, and as an emerging and effective anticancer treatment, it has also been widely used for ICC. However, the improvement of the efficacy of immunotherapy and the development of effective drugs targeting specific immune targets are still problems to be solved[10].

Machine learning is a part of the field of artificial intelligence, which can find rules through the analysis of data, and can be conducive to the prediction of similar unknown data. And the existing knowledge structure can be constantly updated to improve its own performance[11]. With the continuous progress of machine learning, the development of more accurate machine learning algorithms makes it possible for us to find new disease-related genes[12]. At the same time, second-generation sequencing technology has made convenient screening of ICC diagnostic targets, and provided a solid foundation for precise treatment of patients and selection of personalized drugs[13].

In this study, using the ICC-related data in the GEO and The Cancer Genome Atlas (TCGA) databases, bioinformatics and machine learning algorithms were used to comprehensively analyze and obtain reliable disease-characteristic genes, and in-depth exploration found that this gene may regulate the progression of ICC by mediating the composition of immune-infiltrating cells. The above preliminary research results can provide important references for the identification of early diagnostic markers for ICC and the mining of potential intervention targets for immunotherapy.

MATERIALS AND METHODS

Download of the sample datasets

The gene expression data of ICC cancer tissues and paracancerous tissues were obtained by using the three datasets GSE26566, GSE32958, and GSE107943 in GEO database. The transcriptome gene expression data of cancer and paracancerous samples of ICC patients were obtained from TCGA database. The relevant datasets were sorted, and samples other than cancer and paracancerous tissues of ICC patients were deleted. The two datasets of GSE26566 and GSE32958 were combined as the training group. The GSE107943 dataset was used as the verification group, while the TCCG dataset was used as the external database verification group.

Screening of differential genes

The Limma package was used to analyze the differences between the GSE26566 and GSE32958 datasets after merging the training groups. Genes that met the conditions $|\log2FC| > 2$ and adj. $P < 0.05$ were considered to be differential genes. The first 50 genes with the most significant difference between upregulated and downregulated genes were selected for heat mapping using the pheatmap package. The volcanic map was plotted using ggplot2 and ggrepel packages to visualize significantly different genes.

Functional enrichment analysis

According to the results of differential expression analysis, the org.Hs.eg.db, enrichplot, clusterProfiler, DOSE and GSEABase package were used for GO functional enrichment analysis, KEGG pathway enrichment analysis, DO disease enrichment analysis and GSEA enrichment analysis, respectively. The top 10 most significantly enriched functions in biological processes (BP), CC and molecular functions (MF) were visualized by drawing bubble plots. The top 30 pathways or diseases with the most significant enrichment were selected for KEGG enrichment analysis and DO enrichment analysis bubble diagram drawing. GSEA enrichment analysis was carried out on the experimental group (cancer tissue samples) and the control group (paracancerous tissue samples), and the first five functions and pathways that were most significantly enriched in the experimental group and the control group were visualized respectively.

Screening disease characteristic genes by machine learning

Based on the differential gene expression, least absolute shrinkage and selection operator (LASSO) regression, support vector machine-recursive feature elimination (SVM-RFE) algorithm and random forest (RF) algorithm were used to screen disease characteristic genes. The genes screened by the three algorithms were intersected to obtain the final disease characteristic gene, which was the new characteristic gene for ICC diagnosis. The diagnostic genes obtained by the comprehensive analysis of the above three machine learning algorithms had stronger persuasion and higher accuracy. The LASSO regression algorithm was based on the glmnet package. When the parameters were set to a = 1, type.measure = deviance and nfolds = 10, the number of genes corresponding to the point with the smallest cross-validation error was the target gene. The SVM-RFE algorithm was based on the e1071, kernlab and caret packages. The method adopted was svmRadial, and the number of genes corresponding to the point with the smallest cross-validation error was selected as the disease characteristic gene. The RF algorithm was based on the randomForest package. The differentially expressed genes were used to train the RF model. The number of forest trees was set to 500, and the number of corresponding trees with the smallest cross-verification error was found to reconstruct the RF model for training. The importance score of the gene was obtained. We sorted from high to low according to the scores, and selected the 30 genes with the highest importance scores as the feature gene set.

Assessing the diagnostic value of ICC signature genes

The limma package was used to analyze the differences between the two verification groups of GSE107943 and TCGA to determine whether the differential expression of disease characteristic genes in the verification group was consistent with that of the training group. We used the ggpubr package to visualize and draw a boxplot. The receiver operating characteristic (ROC) curve was drawn based on the pROC package to evaluate the efficiency of characteristic genes in the diagnosis of ICC. Area under the curve (AUC) value was used as an index to evaluate the diagnostic value of characteristic genes in

Table 1 Number of data set samples

Dataset	Number of cancer samples	Number of paracancerous samples	Total
GSE26566	104	59	163
GSE32958	16	7	23
GSE107943	30	27	57
TCGA	33	8	41
Total	183	101	284

TCGA: The Cancer Genome Atlas.

the training and test groups. The 95% confidence interval (CI) of AUC value was extracted and calculated by bootstrap method.

Comprehensive analysis of immune infiltration pattern in ICC

According to the gene expression level of each sample, CIBERSORT algorithm was used to quantify the relative content of immune cells in each sample with the help of e1071 and preprocessCore package, so as to obtain the proportion of different immune cells in each sample, and a bar chart was drawn. The corrplot package was used to analyze the correlation of immune cells and draw the correlation heat map. The vioplot package was used to analyze the difference in immune cell infiltration between cancer tissue and paracancerous tissue of ICC patients, and the violin picture was drawn. The CIBERSORT and ssGSEA algorithms were used to evaluate the relationship between ICC characteristic genes and tumor immune-infiltrating cells, in order to explore the effect of ICC characteristic genes on tumor immune microenvironment. Finally, 46 immune checkpoint related genes (including *CD274*, *PDCD1*, *CTLA4*, *CD14*, *LAG3*, and *TNFRSF9*) were found through the literature. We used the limma and corrplot packages, *etc.* to analyze whether the disease signature genes had a regulatory effect on the expression of immune checkpoints.

Analysis of protein expression level of disease characteristic genes by Human Protein Atlas database

The Human Protein Atlas (HPA) database provides the expression and distribution of all available proteins in human tissues and organs. Therefore, protein expression data of disease-characteristic genes in ICC and paracancerous tissues were obtained from this database for comparative analysis.

Statistical analysis

All statistical analyses in this study were conducted in R version 4.2.0. ICC characteristic genes were screened by LASSO regression, SVM-RFE and RF machine learning algorithms. The diagnostic efficacy of diagnostic biomarkers was evaluated by ROC curve. The relationship between the expression of characteristic genes and immune cell infiltration and immune checkpoint was analyzed by Spearman and Pearson correlation. Statistical significance was identified based on $P < 0.05$.

RESULTS

Downloading and sorting of sample data

Table 1 shows the three datasets (GSE26566, GSE32958, and GSE107943) in the GEO database and the ICC-related information obtained from the TCGA database. Two hundred and eighty-four samples were collected, including 120 cancer tissues and 66 paracancerous tissues in the training group. In the two verification groups, cancer tissue samples were from 30 and 33 cases, respectively, and paracancerous tissue samples from 27 and eight cases, respectively.

Screening of differential genes

By the difference analysis of the training group, 1091 differential mRNAs were obtained, including 463 upregulated and 628 downregulated mRNAs (Figure 1A and B). There were many genes with multiple differences in ICC cancer and paracancerous tissues; therefore, it was important to screen characteristic genes that mediated the occurrence and development of ICC, which laid a foundation for the following mechanistic exploration and target gene identification.

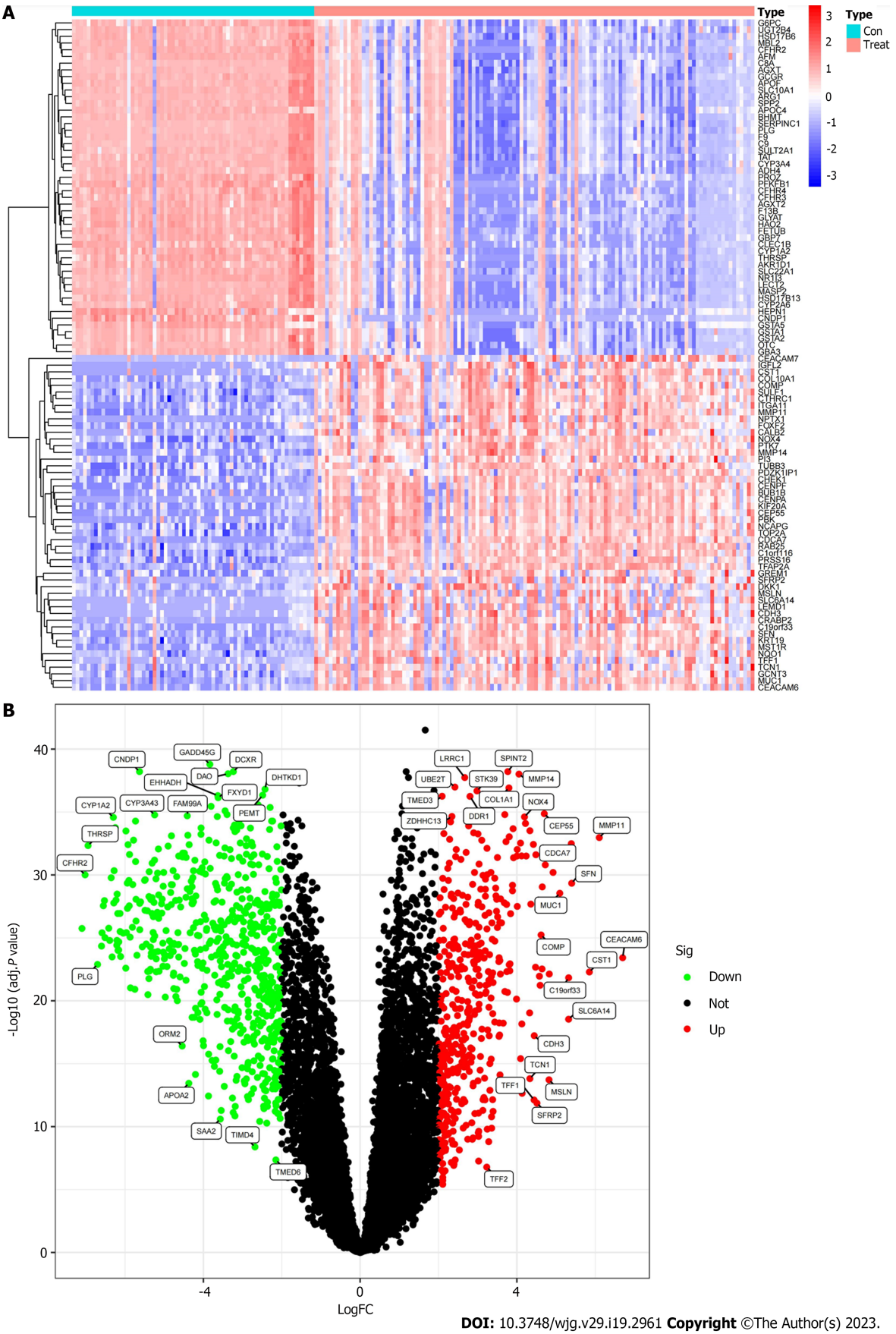

DOI: 10.3748/wjg.v29.i19.2961

Figure 1 The differentially expressed mRNA of intrahepatic cholangiocarcinoma patients was screened based on GEO database training group. A: The heat map of differential gene expression in cancer tissues (Treat) and paracancerous tissues (Con); B: The Volcano map of differential gene expression between cancer and paracancerous tissues.

Biological functions of differential genes

Through GO functional enrichment analysis, we found that in terms of BP, processes such as small molecule catabolic process, response to xenobiotic stimulus, and carboxylic acid catabolic process had the largest number of enrichment genes. In terms of CC, collagen-containing extracellular matrix (ECM), apical part of cell and other CC had the largest number of enriched genes. In terms of MF, sulfur compound binding, glycosaminoglycan binding, serine hydrolase activity and iron ion binding had the largest number of enriched genes (Figure 2A). KEGG pathway enrichment analysis showed that the differential genes were mainly enriched in 56 related regulatory mechanisms, which were mainly involved in complement and coagulation cascades, bile secretion, biosynthesis of cofactors, drug metabolism cytochrome P450, chemical carcinogenesis DNA adducts, retinol metabolism and other pathways (Figure 2B). DO disease enrichment analysis showed that differential genes were closely related to cardiovascular disease, urinary system disease, fatty liver and cholangiocarcinoma (Figure 2C). GSEA enrichment analysis was carried out on the experimental and control groups. GO enrichment analysis showed that acylglycerol homeostasis and alcohol metabolic process were mainly enriched in paracancerous tissues (Figure 3A). In ICC cancer tissues, differential genes were mainly enriched in cell division, chromosome segregation, embryonic organ development and other functions (Figure 3B). KEGG enrichment analysis showed that complement, coagulation cascades and drug metabolism cytochrome P450 were actively expressed in para-cancerous tissues (Figure 3C), while cell cycle, ECM receptor interaction and pathways in cancer were actively expressed in cancer tissues (Figure 3D).

Determination of diagnostic markers for ICC

To identify the specific genes of value in the diagnosis of ICC, we used machine learning to filter the above 1091 differential genes. A total of 25 genes were screened by LASSO regression algorithm, namely: *MMP14*, *CDCA8*, *ZDHHC13*, *NOX4*, *HEPN1*, *LRRC49*, *PDZK1IP1*, *OR1L4*, *FAP*, *NDST3*, *FXN*, *PYCR1*, *PRR11*, *SPAM1*, *MAD2L1*, *APOBEC3G*, *PI3*, *CYP7A1*, *RNF165*, *MT1M*, *GREM1*, *EME1*, *ENAH*, *CDKN2B* and *FOSB* (Figure 4A). After screening by SVM-RFE algorithm, 19 genes were retained, namely: *CFHR2*, *PROC*, *UBE2T*, *HGD*, *AGMAT*, *ACSL1*, *GADD45G*, *DCXR*, *HGFAC*, *DTL*, *MMP14*, *ADHFE1*, *SLC22A1*, *CBS*, *PIPOX*, *SHMT1*, *RDH5*, *F12*, and *F9* (Figure 4B). After screening by RF algorithm, the first 30 genes obtained good diagnostic effect, namely: *SLC10A1*, *CYP3A43*, *COL8A1*, *CDH13*, *ALDH1A1*, *ITPR3*, *MT1H*, *NRCAM*, *TMOD1*, *TNFAIP6*, *SH2D3A*, *OLFML2A*, *WNT10A*, *ACAA2*, *RGN*, *GADD45G*, *CNDP1*, *SPINT2*, *DCXR*, *DAO*, *MMP14*, *LRRC1*, *UBE2T*, *COL1A1*, *DHTKD1*, *STK39*, *PEMT*, *EHHADH*, *TMED3*, and *DDR1* (Figure 4C and D). After the intersection of the genes determined by the above three results, the best disease characteristic gene was obtained: *MMP14* (Figure 4E).

Feasibility analysis of disease characteristic genes as ICC diagnostic markers

Previous studies had shown that *MMP14* was highly expressed in cancer tissues of ICC patients in the training group, so it was important to clarify its expression in two independent verification groups before evaluating the accuracy of this gene as a disease signature gene. In the GSE107943 dataset, the expression of MMP14 in ICC cancer tissues was apparently higher than that in paracancer tissue (Figure 5A). The same result was obtained by external database verification of *MMP14* in the TCGA database (Figure 5B). ROC curves were drawn for the training and validation groups, which showed that in the training group, AUC was 0.960 (95%CI: 0.932-0.983) (Figure 5C). In the GSE107943 verification group, AUC was 0.999 (95%CI: 0.993-1.000) (Figure 5D), and in the TCGA verification group, AUC was 0.977 (95%CI: 0.924-1.000) (Figure 5E). AUC in the verification group was higher than in the training group, and AUC values were all > 0.9. This showed that *MMP14* had good diagnostic efficiency and could be used as a characteristic gene of ICC, which provided a new reference marker for the selection of gene targets for diagnosis of ICC.

Immune cell infiltration in ICC

To explore the infiltration of immune cells in the immune microenvironment of ICC, the proportion of 22 types of immune cells in each sample of ICC cancer and paracancerousl tissues was clarified (Figure 6A). The positive correlation between resting dendritic cells resting and resting memory CD4 T cells resting was the strongest (r = 0.45), and the negative correlation between mast cells resting and mast cells activated was the strongest (r = 0.40) (Figure 6B). We then analyzed the infiltration of immune cells in cancer and paracancerous tissues, and was significant for monocytes, M0 macrophages, activated mast cells, and eosinophils. Compared with paracancerous tissues, expression of M0 macrophages in tumor tissues was greatly higher (P = 0.040), while expression of monocytes (P = 0.002) and activated mast cells (P = 0.037) was significantly lower in tumor tissues (Figure 6C).

Correlation analysis of ICC disease signature genes and immune infiltration patterns

There were differences in the distribution of immune infiltrating cells between ICC cancer tissues and paracancerous tissues. To analyze its potential regulatory factors, we explored the correlation between ICC disease signature genes and immune microenvironment. CIBERSORT algorithm analysis showed that among the immune cells, *MMP14* was significantly correlated with the number of seven types of

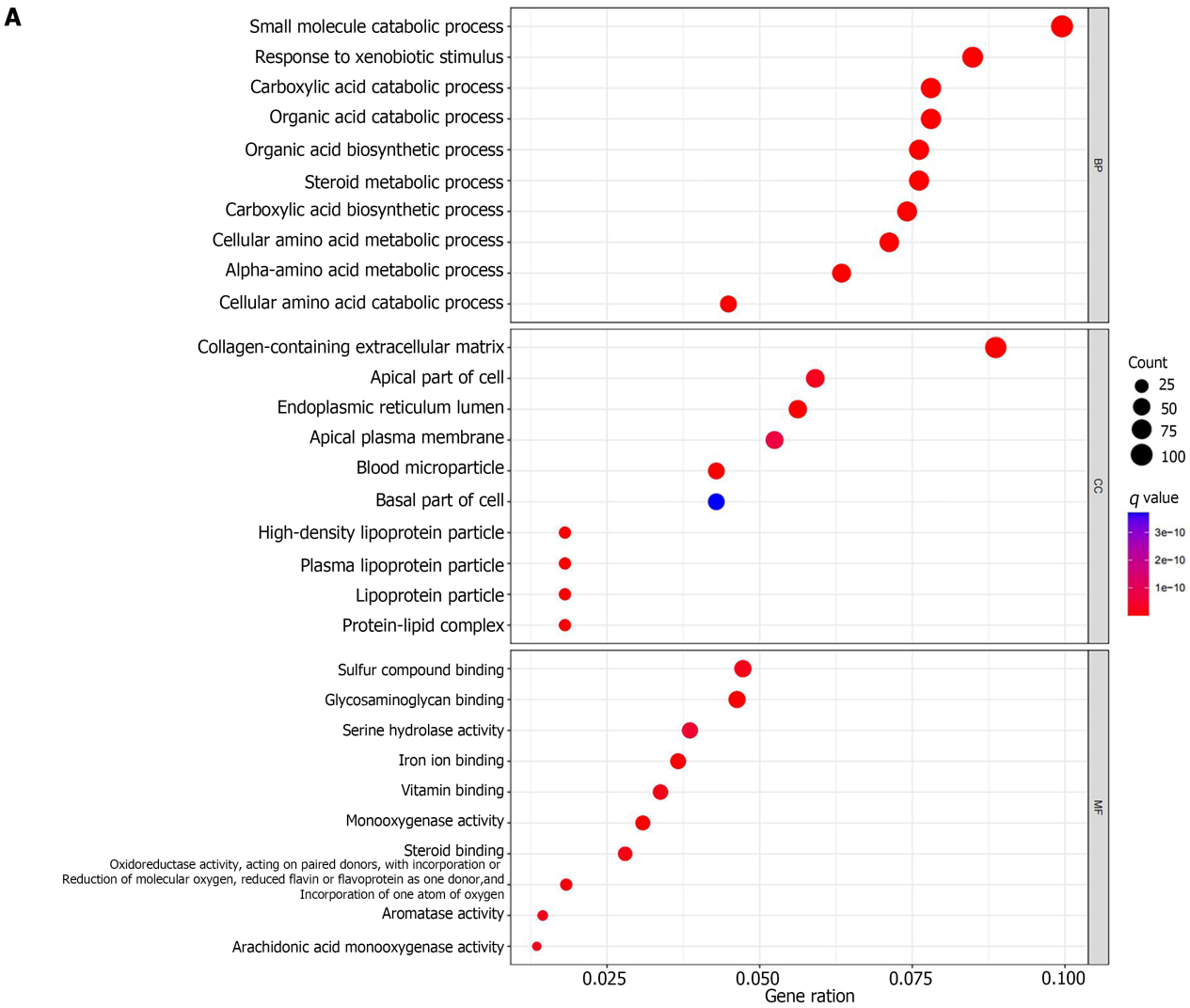
A
Small molecule catabolic process
Response to xenobiotic stimulus
Carboxylic acid catabolic process
Organic acid catabolic process
Organic acid biosynthetic process
Steroid metabolic process
Carboxylic acid biosynthetic process
Cellular amino acid metabolic process
Alpha-amino acid metabolic process
Cellular amino acid catabolic process
BP
Collagen-containing extracellular matrix
Apical part of cell
Endoplasmic reticulum lumen
Apical plasma membrane
Blood microparticle
Basal part of cell
High-density lipoprotein particle
Plasma lipoprotein particle
Lipoprotein particle
Protein-lipid complex
CC
Sulfur compound binding
Glycosaminoglycan binding
Serine hydrolase activity
Iron ion binding
Vitamin binding
Monooxygenase activity
Steroid binding
Oxidoreductase activity, acting on paired donors, with incorporation or Reduction of molecular oxygen, reduced flavin or flavoprotein as one donor,and Incorporation of one atom of oxygen
Aromatase activity
Arachidonic acid monooxygenase activity
MF
0.025
0.050
0.075
0.100
Gene ration
Count
25
50
75
100
q value
3e−10
2e−10
1e−10

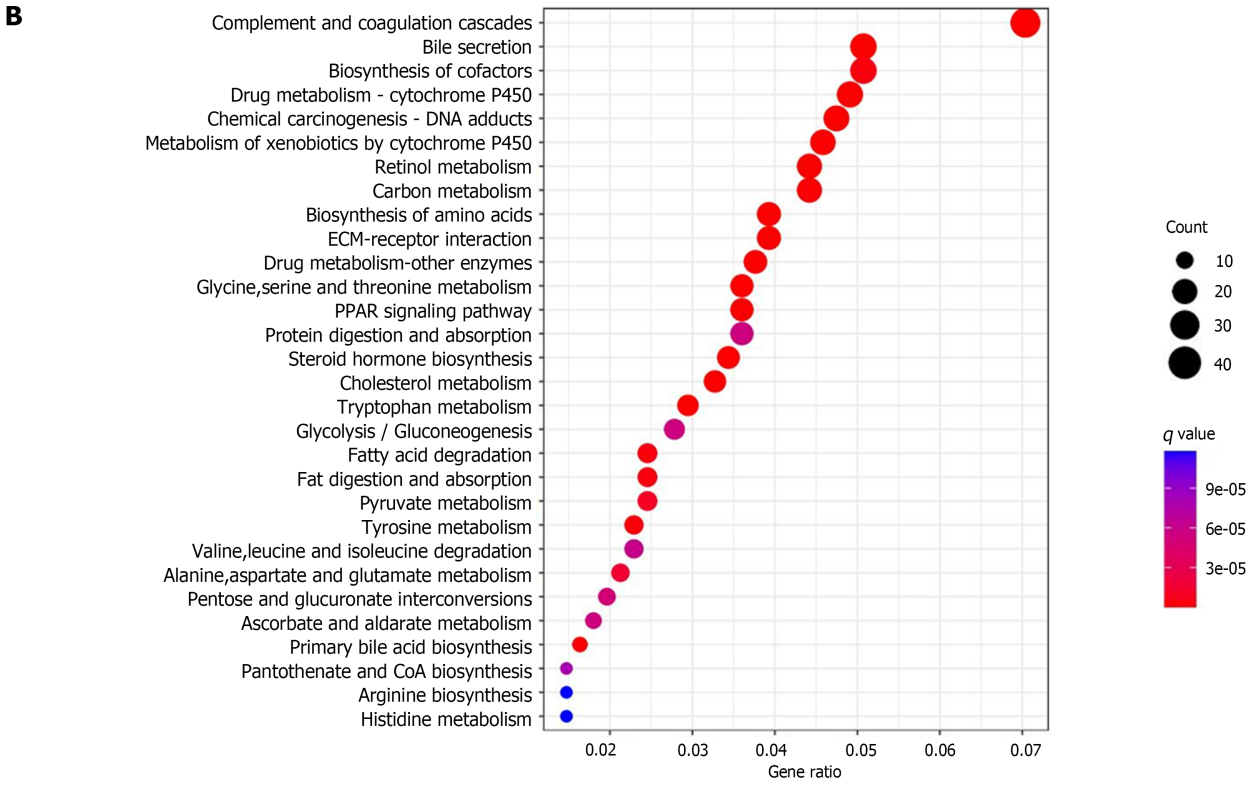
B
Complement and coagulation cascades
Bile secretion
Biosynthesis of cofactors
Drug metabolism - cytochrome P450
Chemical carcinogenesis - DNA adducts
Metabolism of xenobiotics by cytochrome P450
Retinol metabolism
Carbon metabolism
Biosynthesis of amino acids
ECM-receptor interaction
Drug metabolism-other enzymes
Glycine,serine and threonine metabolism
PPAR signaling pathway
Protein digestion and absorption
Steroid hormone biosynthesis
Cholesterol metabolism
Tryptophan metabolism
Glycolysis / Gluconeogenesis
Fatty acid degradation
Fat digestion and absorption
Pyruvate metabolism
Tyrosine metabolism
Valine,leucine and isoleucine degradation
Alanine,aspartate and glutamate metabolism
Pentose and glucuronate interconversions
Ascorbate and aldarate metabolism
Primary bile acid biosynthesis
Pantothenate and CoA biosynthesis
Arginine biosynthesis
Histidine metabolism
0.02
0.03
0.04
0.05
0.06
0.07
Gene ratio
Count
10
20
30
40
q value
9e-05
6e-05
3e-05

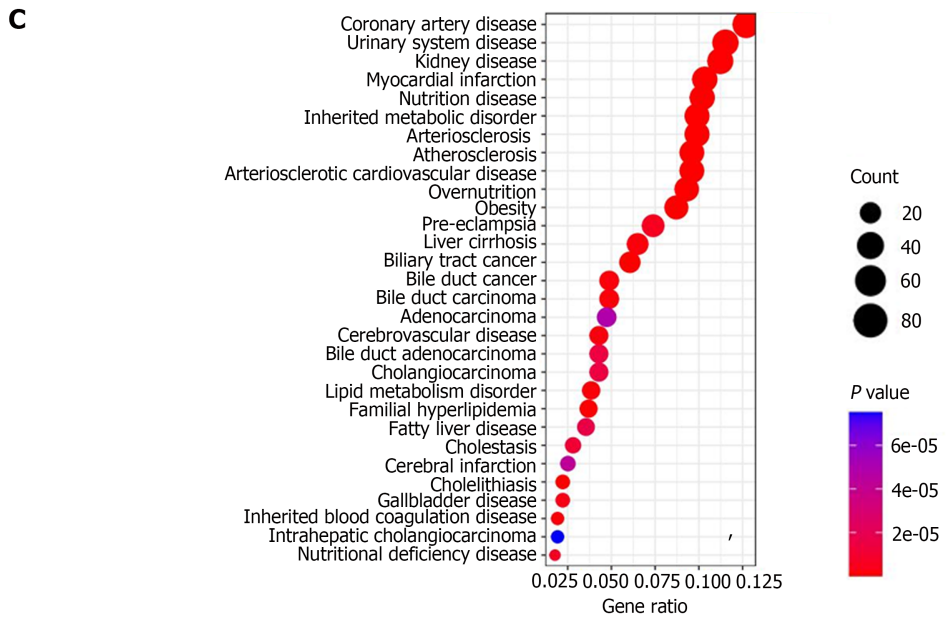

DOI: 10.3748/wjg.v29.i19.2961

Figure 2 Enrichment analysis of differential genes. A: GO functional enrichment analysis; B: KEGG pathway enrichment analysis; C: DO disease enrichment analysis.

immune cells. Expression of MMP14 was positively related with M0 macrophages M0 (r = 0.40, P = 0.0023), activated dendritic cells (r = 0.32, P = 0.0180) and follicular helper T cells (r = 0.29, P = 0.0300) (Figure 7A-C), and negatively related with activated memory CD4 T cells (r = -0.33, P = 0.0130), monocytes (r = -0.32, P = 0.0190), M1 macrophages (r = -0.28, P = 0.0420) and resting memory CD4 T cells (r = -0.27, P = 0.0440) (Figure 7D-G). The final results of *MMP14* and immune cell infiltration based on the above CIBERSORT algorithm are summarized (Figure 8A). ssGSEA algorithm analysis showed that there was a significant correlation between *MMP14* and the number of four types of immune cells and 28 types of immune cells. It was significantly negatively correlated with the number of neutrophils, monocytes, central memory CD8 T cells and central memory CD4 T cells (Figure 8B). *MMP14* was positively correlated with the expression of *CD200*, *CD40*, *CD44*, *CD70*, *CTLA4*, *HHLA2*, *LGALS9*, *TNFRSF14*, *TNFRSF18*, *TNFRSF25*, *TNFSF4* and *TNFSF9*. However, it was negatively correlated with the expression of *CD14*, *CD160*, *TMIGD2*, and *TNFSF14* (Figure 8C). In summary, *MMP14* regulates the composition of immune infiltrating cells in the tumor microenvironment of ICC and may affect the efficacy of immunotherapy by mediating the expression of immune cell surface markers.

Expression of disease characteristic genes in ICC

HPA database analysis showed that expression of MMP14 protein in ICC cancer tissue was higher than that in paracancerous tissue (Figure 9). It was consistent with the trend in mRNA expression levels in the training and verification groups, which confirmed that *MMP14* could be used as a disease characteristic diagnostic gene of ICC.

DISCUSSION

Although there has been some improvement in the treatment of ICC in recent years, the disease control rate is still low[14]. There is no definite marker for early diagnosis of ICC[15]. Individualized treatment has not yet achieved satisfactory results in ICC patients[16]. At present, immunotherapy is a research hot spot in the field of cancer treatment worldwide, and it has widespread prospects for treatment of cholangiocarcinoma[17]. Therefore, the present study focused on discovering new diagnostic markers and improving immunotherapy and determining synergistic therapeutic targets for ICC. Recently, similar ideas have been developed in the research of a variety of tumors and other diseases. More researchers have begun to identify new disease signature genes and explore their potential links with immune cell infiltration. For example, in chronic obstructive pulmonary disease (COPD), STAU1 and SLC27A3 are considered to be important diagnostic biomarkers. The pathogenesis of COPD is largely affected by the pattern of immune cell infiltration. It has been confirmed that STAU1 and SLC27A3 are important factors in regulating the content of plasma cells, resting NK cells, CD8 T cells, and other immune cells[18]. Studies have pointed out that LTBP2 is a highly effective biomarker for prostate cancer, which may inhibit the proliferation and metastasis of prostate cancer through the PI3K/AKT

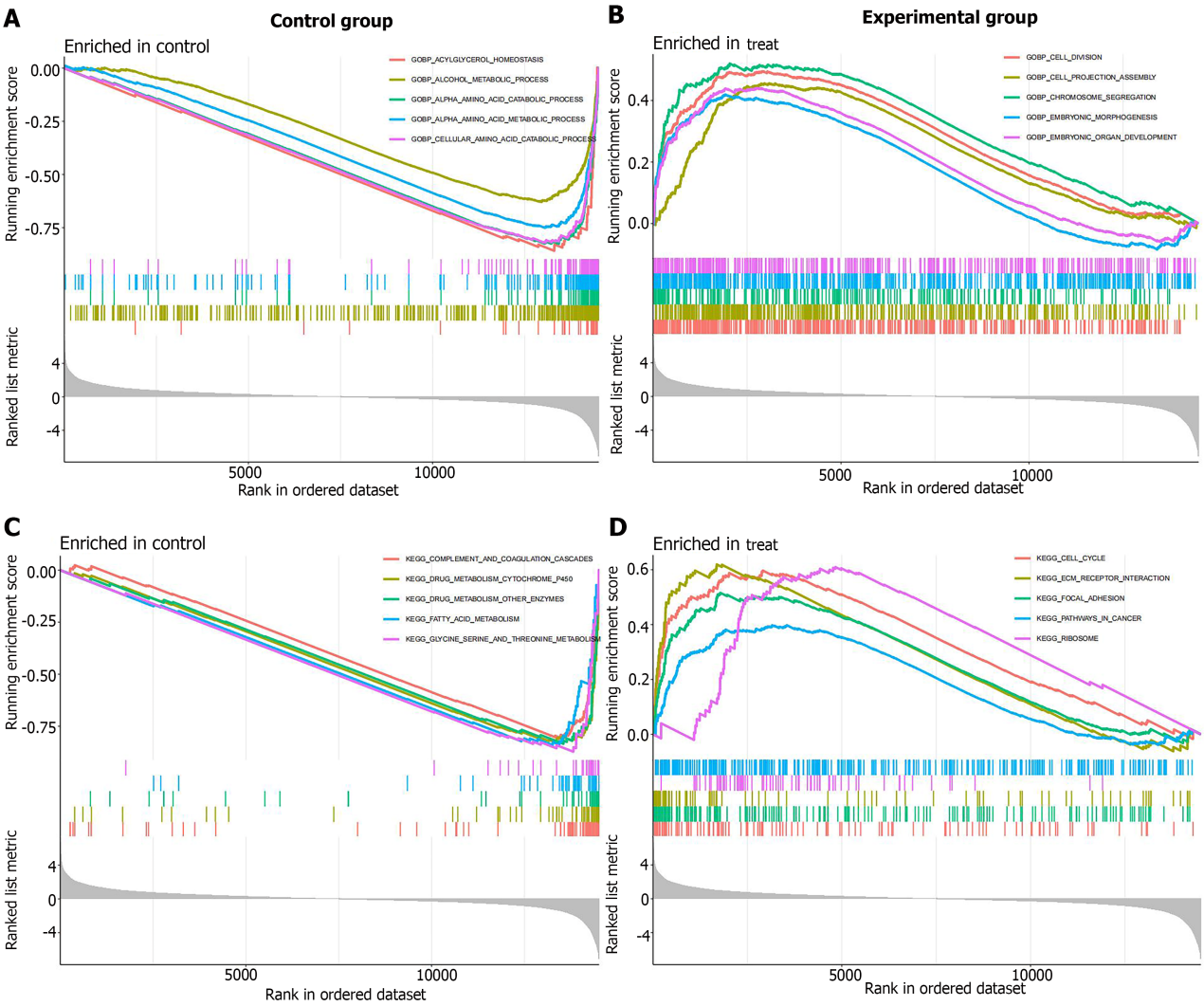

DOI: 10.3748/wjg.v29.i19.2961

Figure 3 GSEA enrichment analysis of differential genes. A: GO enrichment analysis in the control group; B: GO enrichment analysis in the experimental group; C: KEGG enrichment analysis in the control group; D: KEGG enrichment analysis in the experimental group.

signaling pathway, and is related to CD4 T-cell infiltration and the response to anti-PD-1/PD-L1 immunotherapy[19]. However, for ICC with poor prognosis, there have been few studies on potential diagnostic markers and their correlation with immune cell infiltration. Therefore, we hope to find diagnostic biomarkers for ICC and investigate their relationship with immune cell infiltration.

The present study was a series of retrospective studies based on the gene expression matrix of ICC patients in the GEO and TCGA databases, looking for new diagnostic genes for ICC and analyzing the significance of immune cell infiltration. The results obtained are consistent with previous studies that complex metabolic changes occurred in the entire process of cholangiocarcinoma development, and metabolic reprogramming mechanisms such as glucose metabolism, amino acid metabolism, and lipid metabolism all mediate tumor proliferation and invasion are involved[20]. Mechanisms such as ECM-receptor interaction, cell cycle disorder, and stem cell self-renewal have also been confirmed to affect the development of ICC, which is consistent with our enrichment analysis[21-23]. To accurately screen for disease characteristic genes, we used LASSO regression, SVM-RFE, and RF learning algorithms for joint analysis. After the joint verification of another data set in the GEO and TCGA databases, we identified *MMP14* as having high diagnostic accuracy for ICC.

The MMP family are proteolytic enzymes closely related to angiogenesis and tumor progression. MMP14 was the first transmembrane protein found in the family[24]. Previous studies have indicated that MMP14 plays a key role in the malignant transformation of liver cancer, pancreatic cancer, colorectal cancer and other tumors[25-28]. In primary liver cancer, the expression of MMP14 in cancer tissues is significantly higher than that in paracancerous tissues. The expression level of MMP14 is positively correlated with tumor size, Edmondson-Steiner grade and α-fetoprotein level, and mediates the poor prognosis of patients with primary liver cancer[29]. In renal cell carcinoma, MMP14, as a member of the circPTCH1/miR-485-5p/MMP14 endogenous competitive network, participates in promoting metastasis and activating epithelial-mesenchymal transformation of renal cell carcinoma

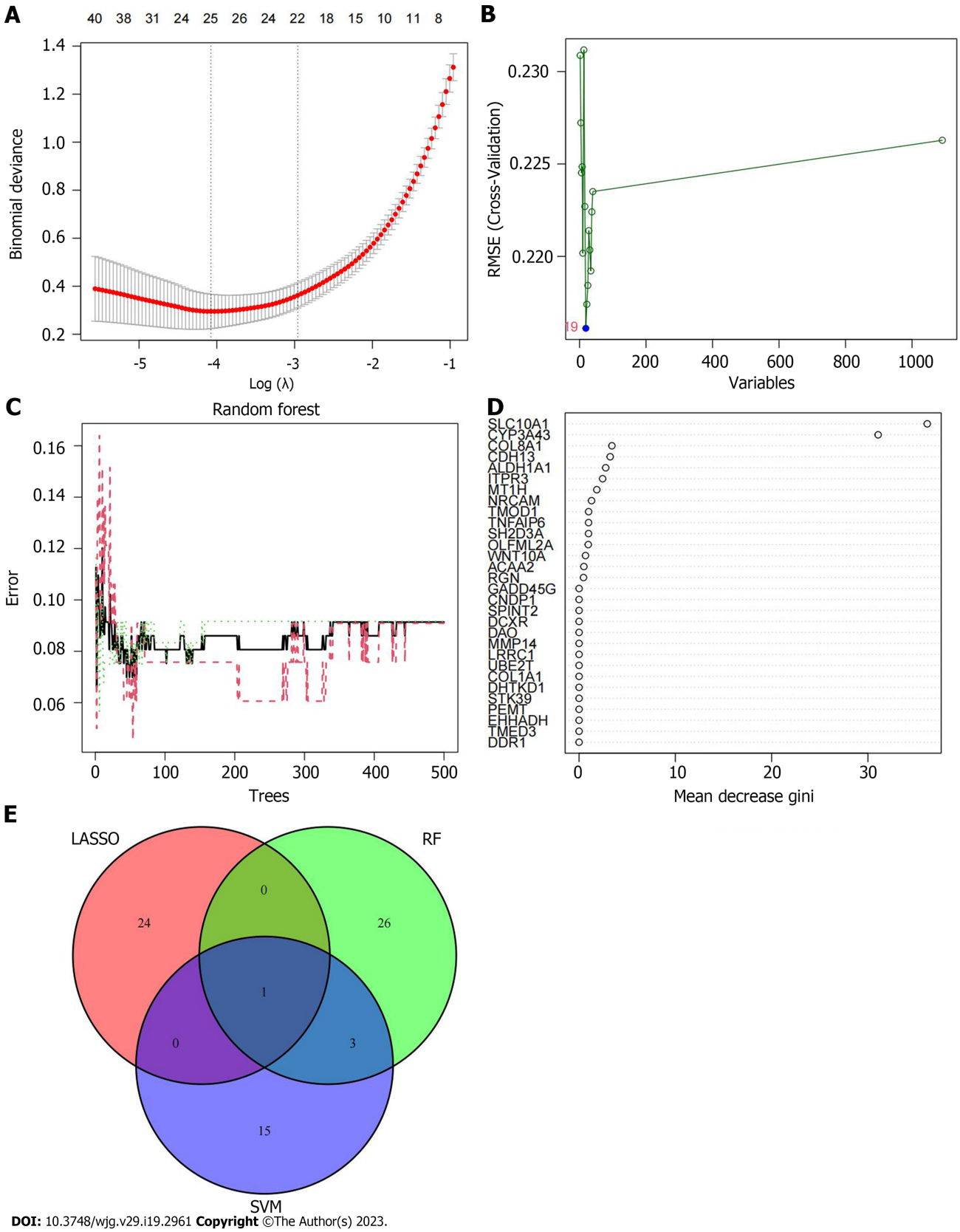

DOI: 10.3748/wjg.v29.i19.2961

Figure 4 Screening of disease signature genes. A: The process of least absolute shrinkage and selection operator regression screening of characteristic genes; B: The relationship between the error and the number of variables in support vector machine-recursive feature elimination; C: The impact of the amount of decision trees on the error rate; D: The name of the characteristic gene and the score of gene importance obtained by RF screening; E: The Venn diagrams of the intersection eigengenes obtained by the three algorithms. SVM: Support vector machine; LASSO: The least absolute shrinkage and selection operator; RF: Random forest.

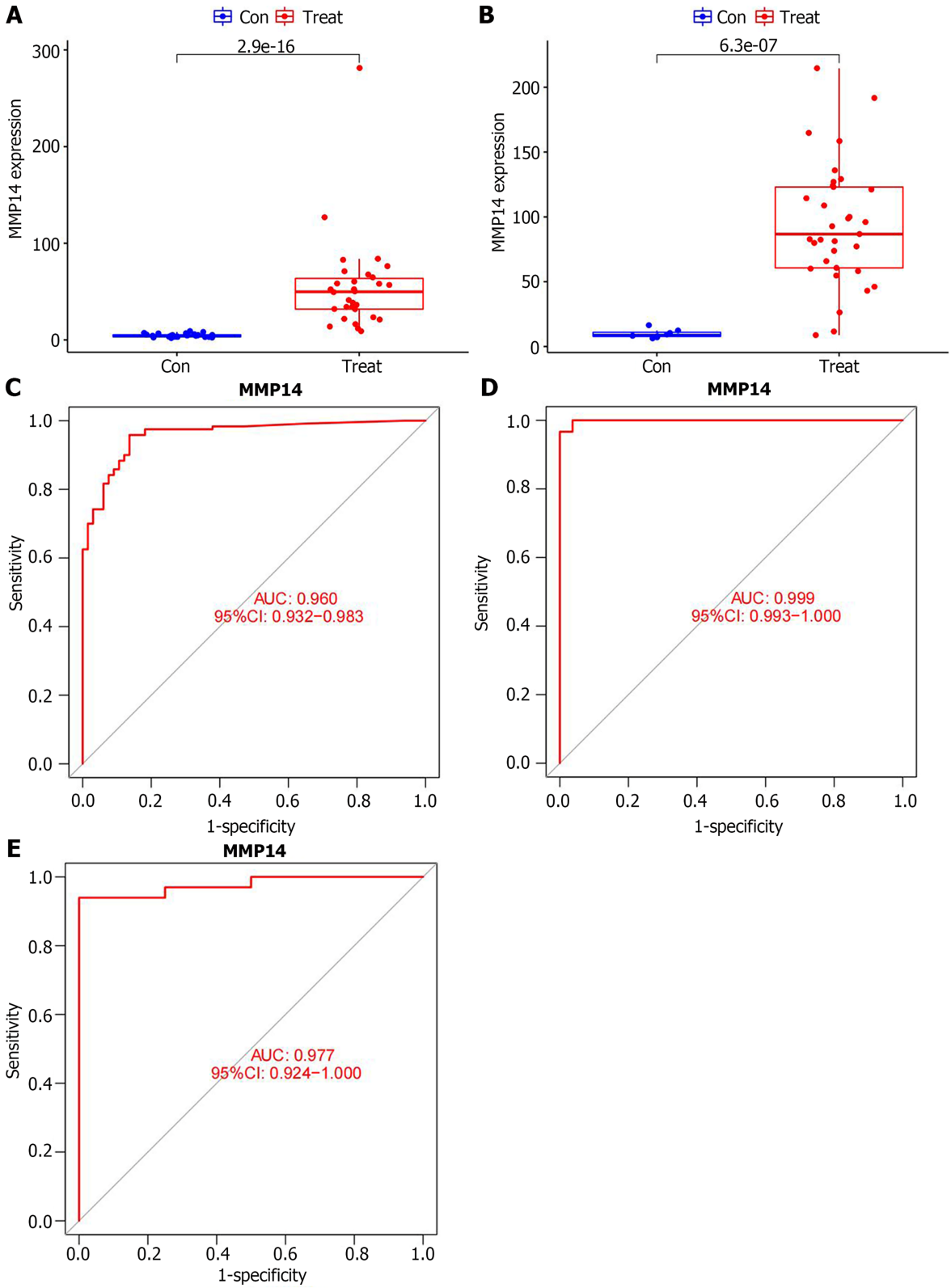

DOI: 10.3748/wjg.v29.i19.2961

Figure 5 Analysis of the diagnostic value of intrahepatic cholangiocarcinoma characteristic genes. A: The boxplot of the differential expression of MMP14 in the GSE107943 dataset; B: The boxplot of the differential expression of MMP14 in the The Cancer Genome Atlas (TCGA) database; C: In the training group, the receiver operating characteristic (ROC) curve of MMP14 to evaluate the diagnostic efficacy of intrahepatic cholangiocarcinoma (ICC); D: In the GSE107943 dataset of the verification group, the ROC curve of MMP14 to evaluate the diagnostic efficacy of ICC; E: In the TCGA dataset of the verification group, the ROC curve of MMP14 to evaluate the diagnostic efficacy of ICC. AUC: Area under the curve; 95%CI: 95% confidence interval.

[30]. Direct degradation of ECM or indirect activation of MMP2 is also the main way for MMP14 to promote the invasion and metastasis of many types of tumors[31,32]. Ragusa and colleagues found that, in a chemotherapy-resistant, aggressive, matrix-rich colorectal cancer subtype, fluctuations in tumor

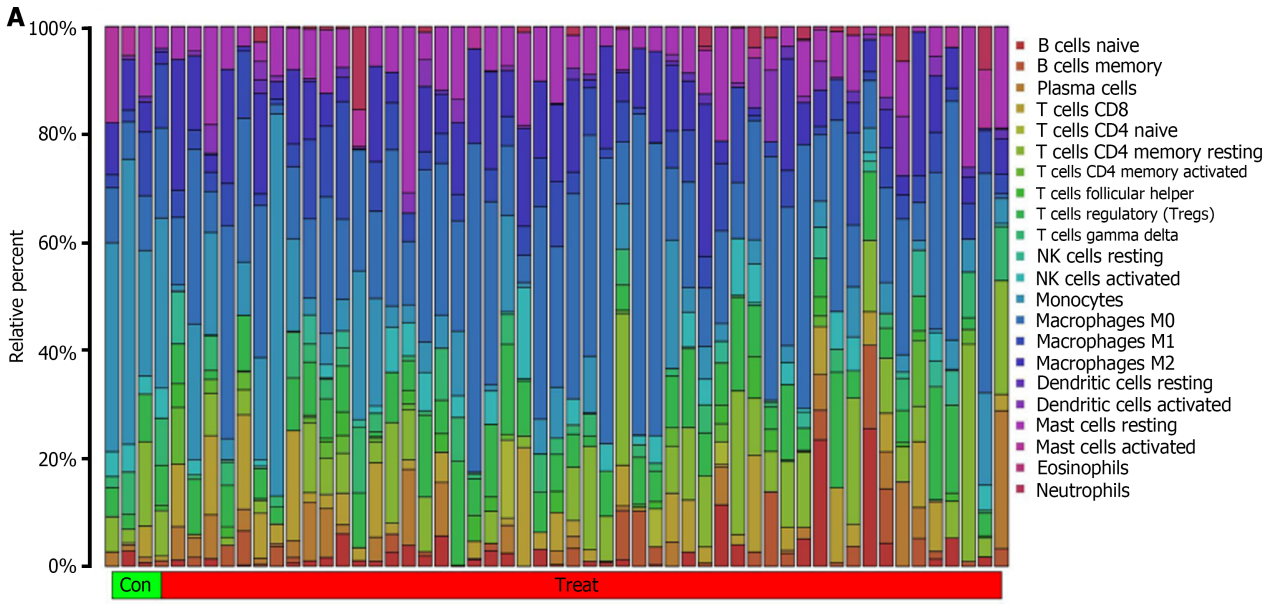
A
100%
80%
60%
40%
20%
0%
Relative percent
Con
Treat
B cells naive
B cells memory
Plasma cells
T cells CD8
T cells CD4 naive
T cells CD4 memory resting
T cells CD4 memory activated
T cells follicular helper
T cells regulatory (Tregs)
T cells gamma delta
NK cells resting
NK cells activated
Monocytes
Macrophages M0
Macrophages M1
Macrophages M2
Dendritic cells resting
Dendritic cells activated
Mast cells resting
Mast cells activated
Eosinophils
Neutrophils

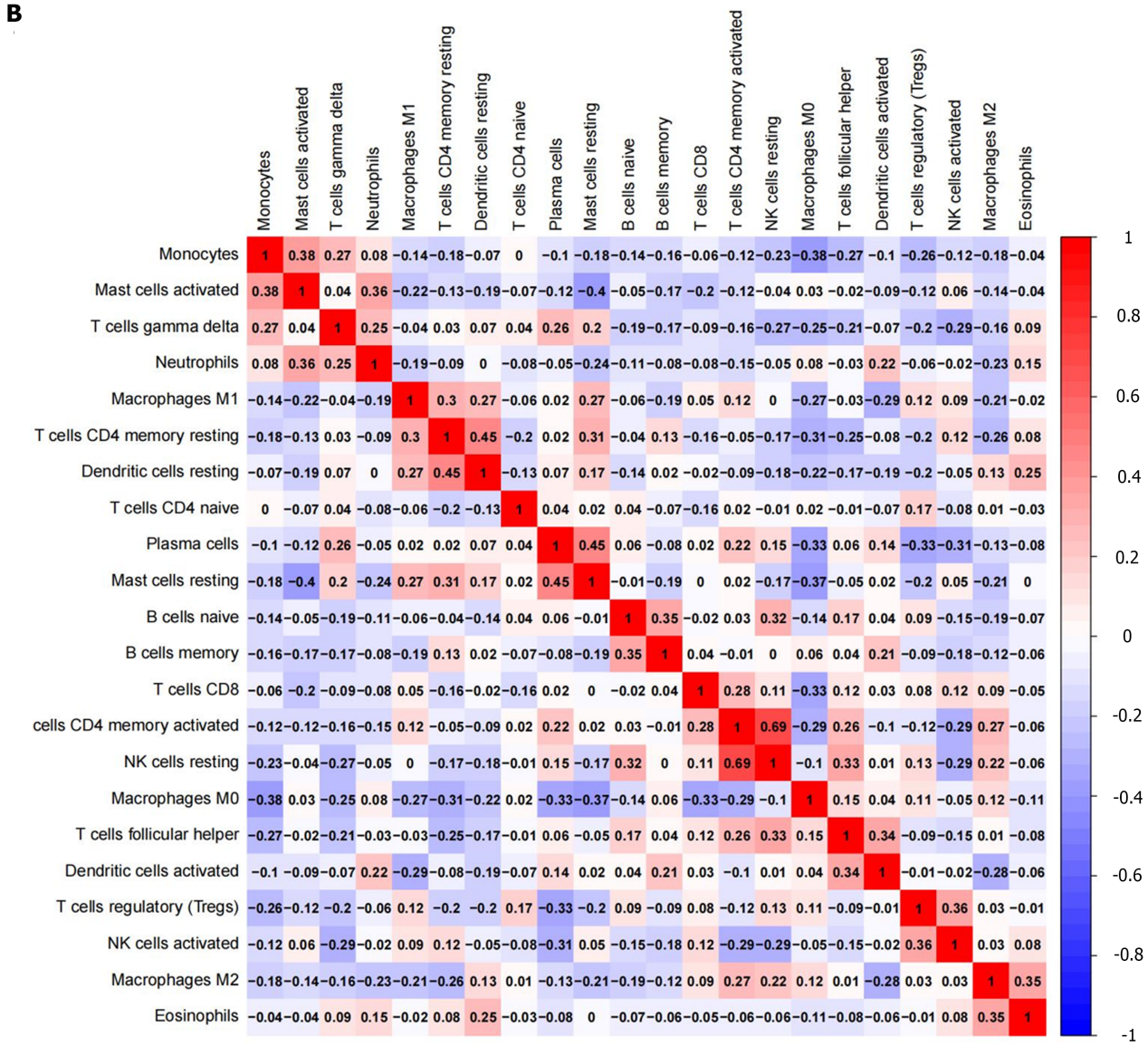
B
Monocytes
Mast cells activated
T cells gamma delta
Neutrophils
Macrophages M1
T cells CD4 memory resting
Dendritic cells resting
T cells CD4 naive
Plasma cells
Mast cells resting
B cells naive
B cells memory
T cells CD8
T cells CD4 memory activated
NK cells resting
Macrophages M0
T cells follicular helper
Dendritic cells activated
T cells regulatory (Tregs)
NK cells activated
Macrophages M2
Eosinophils
1
0.8
0.6
0.4
0.2
0
-0.2
-0.4
-0.6
-0.8
-1

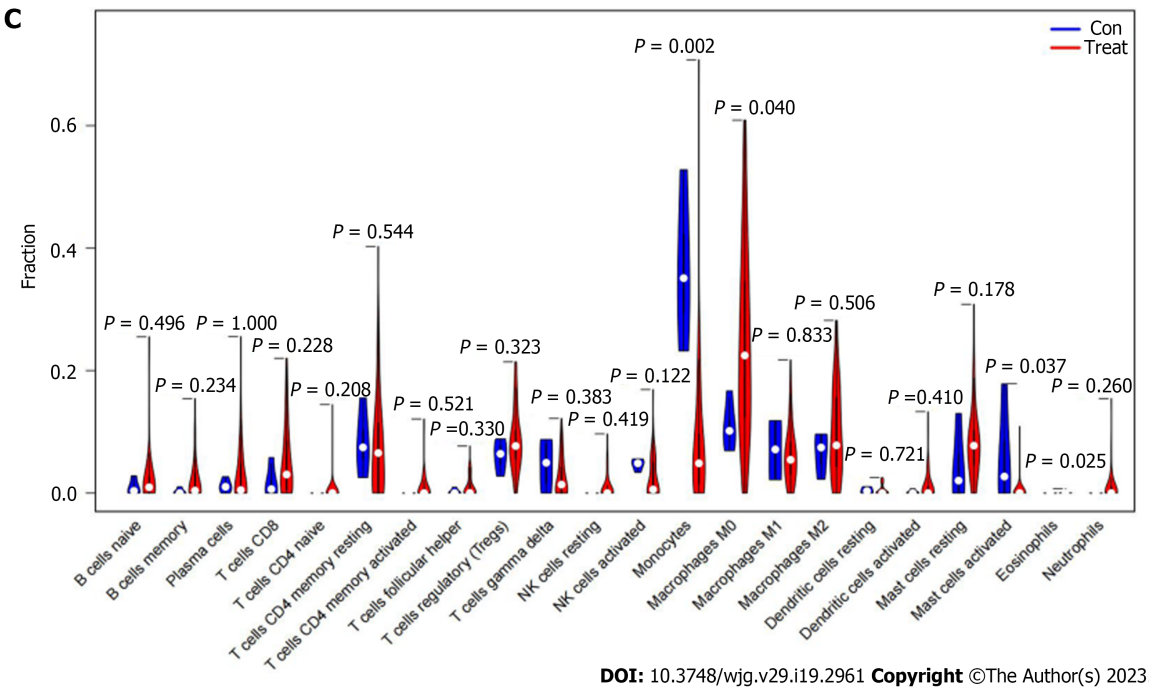

DOI: 10.3748/wjg.v29.i19.2961

Figure 6 The distribution of immune infiltrating cells in intrahepatic cholangiocarcinoma. A: The relative content of immune infiltrating cells in each sample; B: The correlation heatmap composed of cells in all samples; C: The violin plot of the difference in immune cell infiltration between intrahepatic cholangiocarcinoma cancer and paracancerous tissues.

signals triggered a decrease in PROX1 Levels and upregulation of MMP14 through the WNT and Notch pathways, which promoted a series of adverse tumor microenvironmental changes, including activation of fibroblasts, vascular dysfunction, and inability of cytotoxic T cells to enter the tumor[33]. It can be seen that, as a clear tumor-promoting factor, MMP14 is a key regulator in the tumor microenvironment, tumor immune infiltration and tumorigenesis, but its effect on disease diagnosis and tumor immune microenvironment in ICC has not been reported, so our research is important.

Tumor microenvironment plays an important role in the occurrence, development and prognosis of tumor. As an important part of tumor microenvironment, immune cells are involved in the prognosis of the disease and guidance of clinical treatment[34-36]. We calculated the profiles of immune cell infiltration in ICC cancer and paracancerous tissues, and elucidated ICC-associated immune cell subtypes and their potential relationships. Compared with paracancerous tissues, the infiltration of M0 macrophages in ICC tissues was significantly increased, while the proportion of monocytes and mast cells activated was significantly decreased. The correlation analysis between MMP14 and immune cells showed that it was positively correlated with M0 macrophages, activated dendritic cells and follicular helper T cells, and negatively correlated with activated memory CD4 T cells, monocytes, M1 macrophages and resting memory CD4 T cells. The ssGSEA algorithm showed that MMP14 was closely related to the degree of immune cell infiltration, and the number of central memory CD8 T cells, neutrophils, monocytes and central memory CD4 T cells decreased significantly in ICC patients with high expression of MMP14. We found that MMP14 was positively correlated with expression of 12 molecules, including CTLA4 and CD40, and negatively correlated with expressions of four molecules, including CD14 and CD160. Differential regulatory mechanisms of the tumor microenvironment in ICC patients may help explain individual differences in immunotherapy. The expression of MMP14 was negatively regulated by the distribution of monocytes and CD4 T cells in the analysis of CIBERSORT and ssGSEA algorithms. Coincidentally, in the correlation analysis with immune checkpoints, we found that MMP14 was related to the expression of many important molecules, such as monocyte surface marker CD14 and transmembrane receptor CTLA4 on T cells. As an important part of effective antitumor immunity, CD4 T cells can directly eliminate tumor cells through cytolytic mechanisms, or indirectly target tumor cells by regulating the tumor microenvironment to kill tumor cells[37]. Different subpopulations of monocytes perform exclusive functions for tumor promotion or antitumor immunity [38]. It has been reported that CD14 and CD16 monocyte subsets can induce cancer cell death through antibody-dependent cytotoxicity[24,39]. Therefore, we have the reason to speculate that MMP14 may accelerate the progression of ICC by interfering with the abundance of monocytes and CD4 T cells.

In our study, we found new ICC characteristic gene, *MMP14*, and clarified that it might influence the infiltration pattern of immune cells in complex tumor microenvironments. It could be helpful for the clinical diagnosis and immunotherapy of ICC, and provides new ideas for the future study of the occurrence and molecular mechanism of ICC.

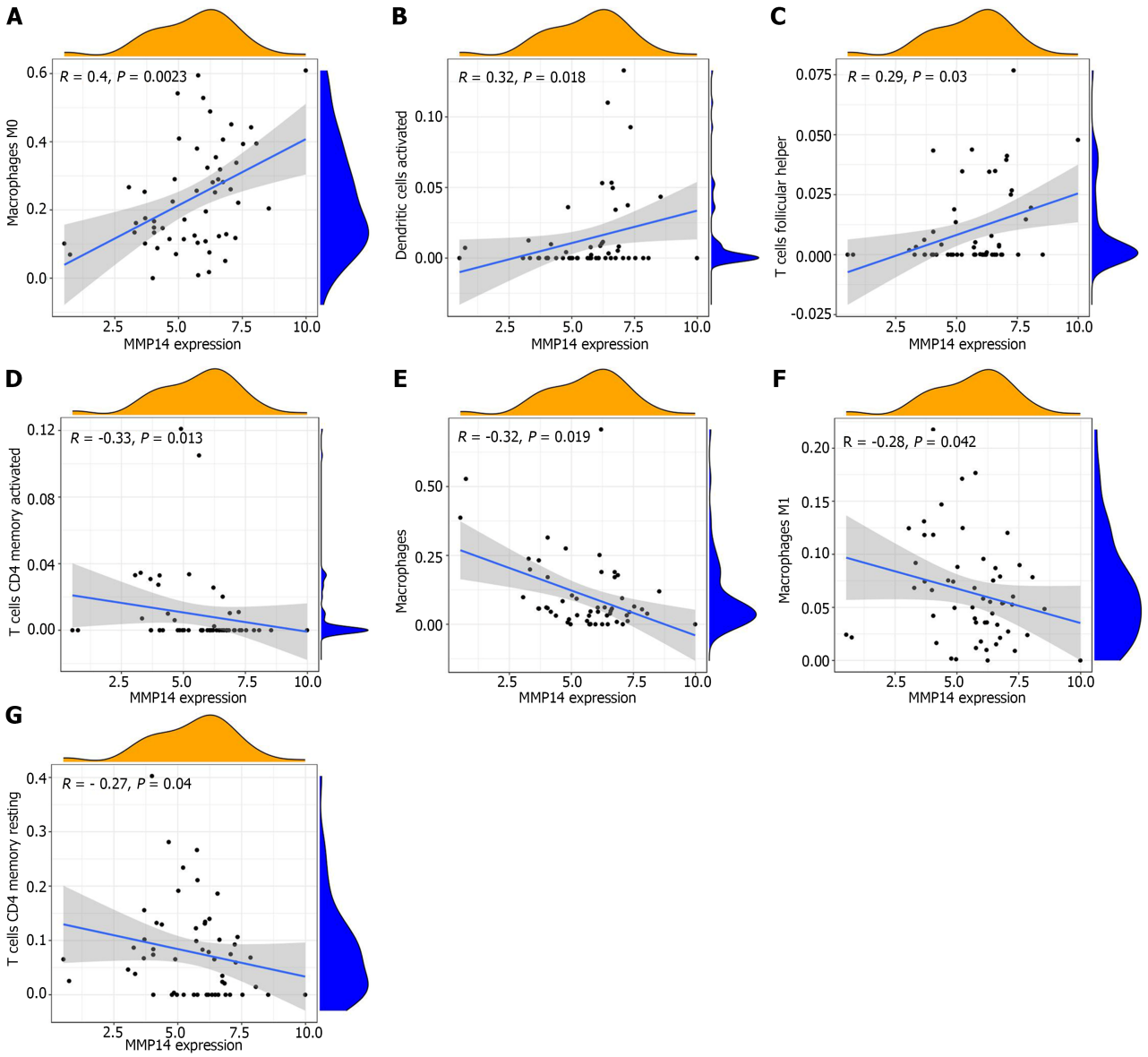

DOI: 10.3748/wjg.v29.i19.2961

Figure 7 The scatter plot of the correlation between MMP14 expression and immune cells. A: Macrophage M0; B: Dendritic cell activation; C: T cell follicular assisted cell activation; D: T cell CD4 memory activation; E: monocyte; F: Macrophage M1; G: T cell CD4 memory resting.

However, our research still had some limitations. Firstly, all data came from public databases, which could have led to inevitable errors or biases. Secondly, the expression and specific function of disease characteristic genes need to be verified by further experiments. Although bioinformatics and machine learning have been used to evaluate the diagnostic efficacy of ICC feature genes and their relationship with immune infiltration, a larger prospective study is needed to confirm our conclusions.

CONCLUSION

Here we investigated new candidate molecular markers that are important for the diagnosis of ICC, which was related to a variety of immune cell components and participated in the occurrence and development of ICC. The findings may have a beneficial impact on the diagnosis of ICC and the provision of precise immunotherapy in future clinical work.

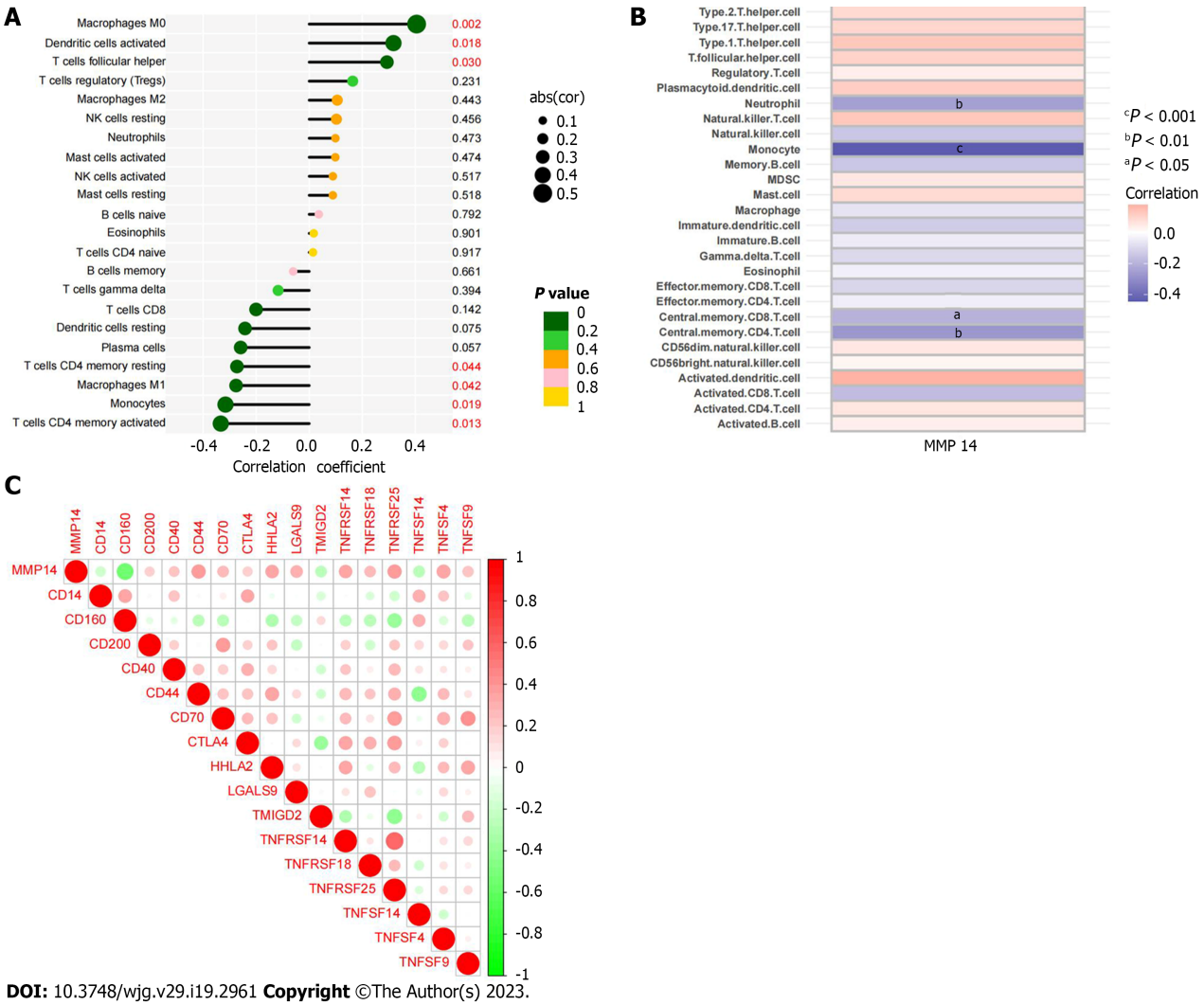

DOI: 10.3748/wjg.v29.i19.2961

Figure 8 Correlation of MMP14 with immune cell content and immune checkpoint expression. A: Correlation between MMP14 and immune cell infiltration based on CIBERSORT algorithm; B: Correlation between MMP14 and immune cell infiltration based on ssGSEA algorithm; C: The heat map of the correlation between MMP14 and immune checkpoint expression.

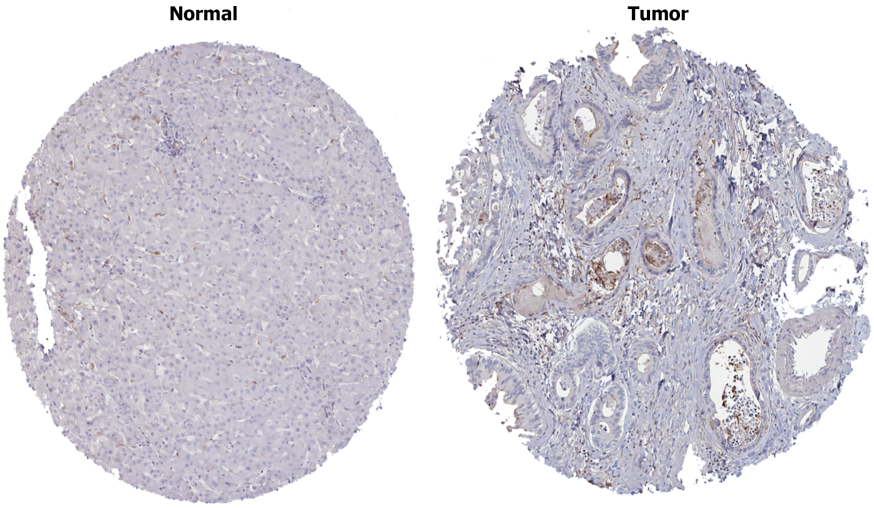

DOI: 10.3748/wjg.v29.i19.2961

Figure 9 Human Protein Atlas analysis of MMP14 protein expression levels in intrahepatic cholangiocarcinoma cancer and paracancerous tissues.

ARTICLE HIGHLIGHTS

Research background

Intrahepatic cholangiocarcinoma (ICC) has a high mortality rate. Its early diagnosis is very important.

Research motivation

At present, there are no diagnostic markers of ICC, and most patients are in the middle and late stage when the tumors are found, and the treatment options for these patients are limited, resulting in a poor prognosis.

Research objectives

It is urgent to find new biomarkers for early screening and diagnosis of ICC.

Research methods

Bioinformatics analysis and machine learning algorithm were used to screen for ICC disease characteristic genes, and the diagnostic performance of characteristic gene *MMP14* was verified by different databases. The relationship between different immune cell infiltration in MMP14 and ICC tumor microenvironment was analyzed.

Research results

We discovered for the first time a new gene *MMP14* for the diagnosis of ICC. We further analyzed the expression of *MMP14* and its significance in immune cell infiltration in ICC tumor microenvironment, indicating that *MMP14* is closely related to a variety of immune cell infiltration, which may provide a new direction for immune-related research.

Research conclusions

In this study, we found that *MMP14* can be used as a disease characteristic gene for ICC diagnosis using a variety of machine learning algorithms. There is a relationship between different immune cell infiltration in *MMP14* and ICC tumor microenvironment, which plays an important role in the occurrence and development of tumor. *MMP14* may be a potential target for ICC immunotherapy.

Research perspectives

Based on bioinformatics analysis and machine learning algorithm, *MMP14* was identified as the characteristic gene of ICC and was associated with ICC immune cell infiltration. In the future research, it will be of great significance to explore the signal pathway mediated by *MMP14* in the occurrence and development of ICC and the mechanism of immune cell infiltration.

FOOTNOTES

Author contributions: Han L conceived and directed the entire study, and should be regarded as corresponding author; Wu J and Guo Y designed the study and prepared the manuscript; Zuo ZF defined the intellectual content of the study and participated in the literature research; Wu J, Guo Y, and Zuo ZF contributed equally to this study; Zhu ZW conducted data analysis; Han L and Wu J revised the manuscript; and all authors approved to submit the manuscript.

Institutional review board statement: This study is not involved any human and animal.

Conflict-of-interest statement: The authors declare no conflict of interest.

Data sharing statement: The bioinformatic data could be downloaded from the public databases, and no additional data are available.

Country/Territory of origin: China

ORCID number: Lei Han 0000-0002-9606-7837.

S-Editor: Chen YL
L-Editor: A

P-Editor: Cai YX

REFERENCES

1 **Siegel RL**, Miller KD, Fuchs HE, Jemal A. Cancer statistics, 2022. *CA Cancer J Clin* 2022; **72**: 7-33 [PMID: 35020204 DOI: 10.3322/caac.21708]

2 **Bridgewater J**, Galle PR, Khan SA, Llovet JM, Park JW, Patel T, Pawlik TM, Gores GJ. Guidelines for the diagnosis and management of intrahepatic cholangiocarcinoma. *J Hepatol* 2014; **60**: 1268-1289 [PMID: 24681130 DOI: 10.1016/j.jhep.2014.01.021]

3 **Khan SA**, Tavolari S, Brandi G. Cholangiocarcinoma: Epidemiology and risk factors. *Liver Int* 2019; **39** Suppl 1: 19-31 [PMID: 30851228 DOI: 10.1111/liv.14095]

4 **Clements O**, Eliahoo J, Kim JU, Taylor-Robinson SD, Khan SA. Risk factors for intrahepatic and extrahepatic cholangiocarcinoma: A systematic review and meta-analysis. *J Hepatol* 2020; **72**: 95-103 [PMID: 31536748 DOI: 10.1016/j.jhep.2019.09.007]

5 **Mazzaferro V**, Gorgen A, Roayaie S, Droz Dit Busset M, Sapisochin G. Liver resection and transplantation for intrahepatic cholangiocarcinoma. *J Hepatol* 2020; **72**: 364-377 [PMID: 31954498 DOI: 10.1016/j.jhep.2019.11.020]

6 **Chen Q**, Wang H, Li Z, Li F, Liang L, Zou Y, Shen H, Li J, Xia Y, Cheng Z, Yang T, Wang K, Shen F. Circular RNA ACTN4 promotes intrahepatic cholangiocarcinoma progression by recruiting YBX1 to initiate FZD7 transcription. *J Hepatol* 2022; **76**: 135-147 [PMID: 34509526 DOI: 10.1016/j.jhep.2021.08.027]

7 **Chen C**, Wu YH, Zhang JW, Qiu YH, Wu H, Li Q, Song TQ, He Y, Mao XH, Zhai WL, Cheng ZJ, Li JD, Si SB, Cai ZQ, Geng ZM, Tang ZH. [A prognostic model of intrahepatic cholangiocarcinoma after curative intent resection based on Bayesian network]. *Zhonghua Wai Ke Za Zhi* 2021; **59**: 265-271 [PMID: 33706443 DOI: 10.3760/cma.j.cn112139-20201230-00891]

8 **Moris D**, Palta M, Kim C, Allen PJ, Morse MA, Lidsky ME. Advances in the treatment of intrahepatic cholangiocarcinoma: An overview of the current and future therapeutic landscape for clinicians. *CA Cancer J Clin* 2023; **73**: 198-222 [PMID: 36260350 DOI: 10.3322/caac.21759]

9 **Izquierdo-Sanchez L**, Lamarca A, La Casta A, Buettner S, Utpatel K, Klümpen HJ, Adeva J, Vogel A, Lleo A, Fabris L, Ponz-Sarvise M, Brustia R, Cardinale V, Braconi C, Vidili G, Jamieson NB, Macias RI, Jonas JP, Marzioni M, Hołówko W, Folseraas T, Kupčinskas J, Sparchez Z, Krawczyk M, Krupa Ł, Scripcariu V, Grazi GL, Landa-Magdalena A, Ijzermans JN, Evert K, Erdmann JI, López-López F, Saborowski A, Scheiter A, Santos-Laso A, Carpino G, Andersen JB, Marin JJ, Alvaro D, Bujanda L, Forner A, Valle JW, Koerkamp BG, Banales JM. Cholangiocarcinoma landscape in Europe: Diagnostic, prognostic and therapeutic insights from the ENSCCA Registry. *J Hepatol* 2022; **76**: 1109-1121 [PMID: 35167909 DOI: 10.1016/j.jhep.2021.12.010]

10 **Kam AE**, Masood A, Shroff RT. Current and emerging therapies for advanced biliary tract cancers. *Lancet Gastroenterol Hepatol* 2021; **6**: 956-969 [PMID: 34626563 DOI: 10.1016/S2468-1253(21)00171-0]

11 **Greener JG**, Kandathil SM, Moffat L, Jones DT. A guide to machine learning for biologists. *Nat Rev Mol Cell Biol* 2022; **23**: 40-55 [PMID: 34518686 DOI: 10.1038/s41580-021-00407-0]

12 **Handelman GS**, Kok HK, Chandra RV, Razavi AH, Lee MJ, Asadi H. eDoctor: machine learning and the future of medicine. *J Intern Med* 2018; **284**: 603-619 [PMID: 30102808 DOI: 10.1111/joim.12822]

13 **Mosele F**, Remon J, Mateo J, Westphalen CB, Barlesi F, Lolkema MP, Normanno N, Scarpa A, Robson M, Meric-Bernstam F, Wagle N, Stenzinger A, Bonastre J, Bayle A, Michiels S, Bièche I, Rouleau E, Jezdic S, Douillard JY, Reis-Filho JS, Dienstmann R, André F. Recommendations for the use of next-generation sequencing (NGS) for patients with metastatic cancers: a report from the ESMO Precision Medicine Working Group. *Ann Oncol* 2020; **31**: 1491-1505 [PMID: 32853681 DOI: 10.1016/j.annonc.2020.07.014]

14 **Nault JC**, Villanueva A. Biomarkers for Hepatobiliary Cancers. *Hepatology* 2021; **73** Suppl 1: 115-127 [PMID: 32045030 DOI: 10.1002/hep.31175]

15 **Banales JM**, Cardinale V, Carpino G, Marzioni M, Andersen JB, Invernizzi P, Lind GE, Folseraas T, Forbes SJ, Fouassier L, Geier A, Calvisi DF, Mertens JC, Trauner M, Benedetti A, Maroni L, Vaquero J, Macias RI, Raggi C, Perugorria MJ, Gaudio E, Boberg KM, Marin JJ, Alvaro D. Expert consensus document: Cholangiocarcinoma: current knowledge and future perspectives consensus statement from the European Network for the Study of Cholangiocarcinoma (ENS-CCA). *Nat Rev Gastroenterol Hepatol* 2016; **13**: 261-280 [PMID: 27095655 DOI: 10.1038/nrgastro.2016.51]

16 **Rizvi S**, Khan SA, Hallemeier CL, Kelley RK, Gores GJ. Cholangiocarcinoma - evolving concepts and therapeutic strategies. *Nat Rev Clin Oncol* 2018; **15**: 95-111 [PMID: 28994423 DOI: 10.1038/nrclinonc.2017.157]

17 **Charalampakis N**, Papageorgiou G, Tsakatikas S, Fioretzaki R, Kole C, Kykalos S, Tolia M, Schizas D. Immunotherapy for cholangiocarcinoma: a 2021 update. *Immunotherapy* 2021; **13**: 1113-1134 [PMID: 34190581 DOI: 10.2217/imt-2021-0126]

18 **Zhang Y**, Xia R, Lv M, Li Z, Jin L, Chen X, Han Y, Shi C, Jiang Y, Jin S. Machine-Learning Algorithm-Based Prediction of Diagnostic Gene Biomarkers Related to Immune Infiltration in Patients With Chronic Obstructive Pulmonary Disease. *Front Immunol* 2022; **13**: 740513 [PMID: 35350787 DOI: 10.3389/fimmu.2022.740513]

19 **Zhang X**, Tian C, Cheng J, Mao W, Li M, Chen M. LTBP2 inhibits prostate cancer progression and metastasis *via* the PI3K/AKT signaling pathway. *Exp Ther Med* 2022; **24**: 563 [PMID: 36034756 DOI: 10.3892/etm.2022.11500]

20 **Raggi C**, Taddei ML, Rae C, Braconi C, Marra F. Metabolic reprogramming in cholangiocarcinoma. *J Hepatol* 2022; **77**: 849-864 [PMID: 35594992 DOI: 10.1016/j.jhep.2022.04.038]

21 **Li H**, Long J, Xie F, Kang K, Shi Y, Xu W, Wu X, Lin J, Xu H, Du S, Xu Y, Zhao H, Zheng Y, Gu J. Transcriptomic analysis and identification of prognostic biomarkers in cholangiocarcinoma. *Oncol Rep* 2019; **42**: 1833-1842 [PMID: 31545466 DOI: 10.3892/or.2019.7318]

22 **Fan S**, Ge Y, Liu J, Liu H, Yan R, Gao T, Fan X, Xiao Z, An G. Combination of anlotinib and gemcitabine promotes the G0/G1 cell cycle arrest and apoptosis of intrahepatic cholangiocarcinoma in vitro. *J Clin Lab Anal* 2021; **35**: e23986 [PMID: 34462984 DOI: 10.1002/jcla.23986]

23 **Lin Y**, Cai Q, Chen Y, Shi T, Liu W, Mao L, Deng B, Ying Z, Gao Y, Luo H, Yang X, Huang X, Shi Y, He R. CAFs shape myeloid-derived suppressor cells to promote stemness of intrahepatic cholangiocarcinoma through 5-lipoxygenase. *Hepatology* 2022; **75**: 28-42 [PMID: 34387870 DOI: 10.1002/hep.32099]

24 **Claesson-Welsh L**. How the matrix metalloproteinase MMP14 contributes to the progression of colorectal cancer. *J Clin Invest* 2020; **130**: 1093-1095 [PMID: 32015228 DOI: 10.1172/JCI135239]

25 **Määttä M**, Soini Y, Liakka A, Autio-Harmainen H. Differential expression of matrix metalloproteinase (MMP)-2, MMP-9, and membrane type 1-MMP in hepatocellular and pancreatic adenocarcinoma: implications for tumor progression and clinical prognosis. *Clin Cancer Res* 2000; **6**: 2726-2734 [PMID: 10914717]

26 **Qiang L**, Cao H, Chen J, Weller SG, Krueger EW, Zhang L, Razidlo GL, McNiven MA. Pancreatic tumor cell metastasis is restricted by MT1-MMP binding protein MTCBP-1. *J Cell Biol* 2019; **218**: 317-332 [PMID: 30487181 DOI: 10.1083/jcb.201802032]

27 **Yu J**, He Z, He X, Luo Z, Lian L, Wu B, Lan P, Chen H. Comprehensive Analysis of the Expression and Prognosis for MMPs in Human Colorectal Cancer. *Front Oncol* 2021; **11**: 771099 [PMID: 34804973 DOI: 10.3389/fonc.2021.771099]

28 **Decotret LR**, Wadsworth BJ, Li LV, Lim CJ, Bennewith KL, Pallen CJ. Receptor-type protein tyrosine phosphatase alpha (PTPα) mediates MMP14 Localization and facilitates triple-negative breast cancer cell invasion. *Mol Biol Cell* 2021; **32**: 567-578 [PMID: 33566639 DOI: 10.1091/mbc.E20-01-0060]

29 **Jin Y**, Liang ZY, Zhou WX, Zhou L. High MMP14 expression is predictive of poor prognosis in resectable hepatocellular carcinoma. *Pathology* 2020; **52**: 359-365 [PMID: 32122646 DOI: 10.1016/j.pathol.2020.01.436]

30 **Liu H**, Hu G, Wang Z, Liu Q, Zhang J, Chen Y, Huang Y, Xue W, Xu Y, Zhai W. circPTCH1 promotes invasion and metastasis in renal cell carcinoma *via* regulating miR-485-5p/MMP14 axis. *Theranostics* 2020; **10**: 10791-10807 [PMID: 32929380 DOI: 10.7150/thno.47239]

31 **Poincloux R**, Lizárraga F, Chavrier P. Matrix invasion by tumour cells: a focus on MT1-MMP trafficking to invadopodia. *J Cell Sci* 2009; **122**: 3015-3024 [PMID: 19692588 DOI: 10.1242/jcs.034561]

32 **Gonzalez-Molina J**, Gramolelli S, Liao Z, Carlson JW, Ojala PM, Lehti K. MMP14 in Sarcoma: A Regulator of Tumor Microenvironment Communication in Connective Tissues. *Cells* 2019; **8** [PMID: 31466240 DOI: 10.3390/cells8090991]

33 **DeBerardinis RJ**. Tumor Microenvironment, Metabolism, and Immunotherapy. *N Engl J Med* 2020; **382**: 869-871 [PMID: 32101671 DOI: 10.1056/NEJMcibr1914890]

34 **Vitale I**, Manic G, Coussens LM, Kroemer G, Galluzzi L. Macrophages and Metabolism in the Tumor Microenvironment. *Cell Metab* 2019; **30**: 36-50 [PMID: 31269428 DOI: 10.1016/j.cmet.2019.06.001]

35 **Bader JE**, Voss K, Rathmell JC. Targeting Metabolism to Improve the Tumor Microenvironment for Cancer Immunotherapy. *Mol Cell* 2020; **78**: 1019-1033 [PMID: 32559423 DOI: 10.1016/j.molcel.2020.05.034]

36 **Borst J**, Ahrends T, Bąbała N, Melief CJM, Kastenmüller W. CD4(+) T cell help in cancer immunology and immunotherapy. *Nat Rev Immunol* 2018; **18**: 635-647 [PMID: 30057419 DOI: 10.1038/s41577-018-0044-0]

37 **Olingy CE**, Dinh HQ, Hedrick CC. Monocyte heterogeneity and functions in cancer. *J Leukoc Biol* 2019; **106**: 309-322 [PMID: 30776148 DOI: 10.1002/JLB.4RI0818-311R]

38 **Gordon IO**, Freedman RS. Defective antitumor function of monocyte-derived macrophages from epithelial ovarian cancer patients. *Clin Cancer Res* 2006; **12**: 1515-1524 [PMID: 16533776 DOI: 10.1158/1078-0432.CCR-05-2254]

39 **Yeap WH**, Wong KL, Shimasaki N, Teo EC, Quek JK, Yong HX, Diong CP, Bertoletti A, Linn YC, Wong SC. CD16 is indispensable for antibody-dependent cellular cytotoxicity by human monocytes. *Sci Rep* 2016; **6**: 34310 [PMID: 27670158 DOI: 10.1038/srep34310]

World Journal of Gastroenterology

Submit a Manuscript: https://www.f6publishing.com

World J Gastroenterol 2023 May 21; 29(19): 2979-2991

DOI: 10.3748/wjg.v29.i19.2979

ISSN 1007-9327 (print) ISSN 2219-2840 (online)

ORIGINAL ARTICLE

Case Control Study

Machine learning model for prediction of low anterior resection syndrome following laparoscopic anterior resection of rectal cancer: A multicenter study

Zhang Wang, Sheng-Li Shao, Lu Liu, Qi-Yi Lu, Lei Mu, Ji-Chao Qin

Specialty type: Surgery

Provenance and peer review: Unsolicited article; Externally peer reviewed.

Peer-review model: Single blind

Peer-review report's scientific quality classification

Grade A (Excellent): 0
Grade B (Very good): 0
Grade C (Good): C, C
Grade D (Fair): 0
Grade E (Poor): 0

P-Reviewer: Calabro F, Italy; Muneer A, Malaysia

Received: February 23, 2023
Peer-review started: February 23, 2023
First decision: March 23, 2023
Revised: April 2, 2023
Accepted: April 25, 2023
Article in press: April 25, 2023
Published online: May 21, 2023

Zhang Wang, Sheng-Li Shao, Lu Liu, Qi-Yi Lu, Lei Mu, Ji-Chao Qin, Department of Surgery, Tongji Hospital, Tongji Medical College, Huazhong University of Science and Technology, Wuhan 430030, Hubei Province, China

Zhang Wang, Sheng-Li Shao, Lu Liu, Qi-Yi Lu, Lei Mu, Ji-Chao Qin, Molecular Medicine Center, Tongji Hospital, Tongji Medical College, Huazhong University of Science and Technology, Wuhan 430030, Hubei Province, China

Corresponding author: Ji-Chao Qin, MD, PhD, Professor, Researcher, Surgeon, Department of Surgery, Tongji Hospital, Tongji Medical College, Huazhong University of Science and Technology, No. 1095 Jiefang Avenue, Wuhan 430030, Hubei Province, China.
jcqin@tjh.tjmu.edu.cn

Abstract

BACKGROUND

Low anterior resection syndrome (LARS) severely impairs patient postoperative quality of life, especially major LARS. However, there are few tools that can accurately predict major LARS in clinical practice.

AIM

To develop a machine learning model using preoperative and intraoperative factors for predicting major LARS following laparoscopic surgery of rectal cancer in Chinese populations.

METHODS

Clinical data and follow-up information of patients who received laparoscopic anterior resection for rectal cancer from two medical centers (one discovery cohort and one external validation cohort) were included in this retrospective study. For the discovery cohort, the machine learning prediction algorithms were developed and internally validated. In the external validation cohort, we evaluated the trained model using various performance metrics. Further, the clinical utility of the model was tested by decision curve analysis.

RESULTS

Overall, 1651 patients were included in the present study. Anastomotic height, neoadjuvant therapy, diverting stoma, body mass index, clinical stage, specimen

length, tumor size, and age were the risk factors associated with major LARS. They were used to construct the machine learning model to predict major LARS. The trained random forest (RF) model performed with an area under the curve of 0.852 and a sensitivity of 0.795 (95%CI: 0.681-0.877), a specificity of 0.758 (95%CI: 0.671-0.828), and Brier score of 0.166 in the external validation set. Compared to the previous preoperative LARS score model, the current model exhibited superior predictive performance in predicting major LARS in our cohort (accuracy of 0.772 for the RF model *vs* 0.355 for the preoperative LARS score model).

CONCLUSION

We developed and validated a robust tool for predicting major LARS. This model could potentially be used in the clinic to identify patients with a high risk of developing major LARS and then improve the quality of life.

Key Words: Machine learning; Low anterior resection syndrome; Rectal cancer; Laparoscopy; Prediction

Core Tip: We developed and externally validated a machine learning-based prediction model that integrated preoperative and intraoperative risk factors as input features and showed satisfactory predictive performance in Chinese patients. According to the decision curve analysis, patients with major low anterior resection syndrome (LARS) would have a net benefit superior to "treat all" or "treat none" with a range of threshold probabilities by using the model. This study provides a new tool for predicting major LARS, which can potentially be used for rectal cancer patients to acquire early postoperative consultation and strengthen self-management to improve their quality of life.

Citation: Wang Z, Shao SL, Liu L, Lu QY, Mu L, Qin JC. Machine learning model for prediction of low anterior resection syndrome following laparoscopic anterior resection of rectal cancer: A multicenter study. *World J Gastroenterol* 2023; 29(19): 2979-2991

URL: https://www.wjgnet.com/1007-9327/full/v29/i19/2979.htm

DOI: https://dx.doi.org/10.3748/wjg.v29.i19.2979

INTRODUCTION

With advances in surgical techniques and the introduction of a multidisciplinary approach, the sphincter-saving procedure for rectal cancer has increased[1], with up to 50%-80% of rectal cancer patients undergoing this procedure[2] compared with only 25% before the circular stapling device was widely used[3]. However, low anterior resection syndrome (LARS), a postoperative complication that seriously impairs patient quality of life, has also increased[4,5], and 70%-90% of these patients undergoing sphincter-saving procedures have developed LARS[2]. The majority of LARS may go into remission within a variable interval of 6-18 mo following surgery[6,7]. However, beyond this point further improvements may be impossible, and the complication may become irreversible. It is reported that approximately 40% of patients with major LARS remain 'toilet dependent,' which results in a low quality of life[8,9].

Early management of major LARS, such as conservative drugs, transanal or transtomal irrigation, pelvic floor rehabilitation, biofeedback, and sacral nerve stimulation, can improve LARS symptoms[10-14]. Therefore, it is important to identify the patients who are at a high risk of developing major LARS after surgery. A recent study established a model based on preoperative risk factors to predict a LARS score for improving patient preoperative education and counseling[15]. However, it failed to achieve an accurate prediction when it was applied to other populations[16]. Furthermore, certain intraoperative factors that were previously reported as important contributors to LARS were not included in this aforementioned model[17,18].

Due to better vision and less surgical trauma[19], laparoscopic surgery has improved the postoperative course in the treatment of rectal cancer and was widely applied in China. In theory, laparoscopic surgery ensures minimal surgical trauma and improves postoperative patient recovery as well as functional bowel outcome. However, there is still no tool to predict LARS in Asian patients who receive laparoscopic surgery.

Artificial intelligence (AI) is an innovative modeling technology and has produced promising results; our previous studies have shown that AI algorithms allow for good discrimination of anastomotic leakage and would be helpful in assisting surgeons' decision-making[20,21]. Therefore, the present study aimed to develop a machine learning model based on AI technology using preoperative and

intraoperative factors for predicting major LARS following laparoscopic surgery of rectal cancer in Chinese populations. This model was created to guide early postoperative management of medical intervention and improve patient postoperative consultation and quality of life.

MATERIALS AND METHODS

Data and participants

The present study included a discovery cohort and an external validation cohort. To develop the machine learning model, clinical data of 2120 patients with rectal cancer who received laparoscopic anterior resection in the Department of Gastrointestinal Surgery, Tongji Hospital, Huazhong University of Science and Technology from January 1, 2012 to December 31, 2020 were reviewed and collected. For external validation, data from 289 patients from the Central Hospital of Enshi Tujia and Miao Autonomous Prefecture affiliated to Wuhan University between January 1, 2012 and December 31, 2020 were collected with the same criteria. The present study was performed according to the guidelines of the Declaration of Helsinki and approved by the ethics committees of Tongji Hospital, Huazhong University of Science and Technology and The Central Hospital of Enshi Tujia and Miao Autonomous Prefecture. The requirement for informed consent was waived due to the retrospective nature of the study.

Inclusion and exclusion criteria

The inclusion criteria were as follows: (1) Age ≥ 18; (2) Primary rectal adenocarcinoma located 0-15 cm from the anal verge; and (3) Patients without communication difficulties. The exclusion criteria were as follows: (1) Patients who had their diverting stoma open; (2) Less than 1 year after laparoscopic anterior resection or after stoma reversal; (3) Patients with a history of abnormal bowel function, including drug-induced diarrhea, a chronic history of constipation, irritable bowel syndrome, and a history of pelvic injury; (4) Patients with local recurrence within 1 year after surgery; and (5) Missing data, death, or lost to follow-up.

Candidate variables

In order to develop the early postoperative major LARS prediction model, only the clinical preoperative and intraoperative variables of each patient were included. The variables were as following: age at surgery; sex; body mass index (BMI); hypertension; diabetes; previous abdominal surgery; neoadjuvant therapy; American Society of Anesthesiologists (ASA) classification; tumor size (cm); clinical stages; anastomotic height (cm); diverting stoma; and specimen length (cm). Two authors independently completed the collection and collation of clinical data, and conflicting data were documented and confirmed by a final discussion. Anastomotic height was defined as the distance between anastomosis and anal verge measured using digital rectal examination, computed tomography, or magnetic resonance imaging. Specimen length was defined as the length of the bowel removed during surgery.

Outcome

The Chinese version of the LARS score system was used to evaluate postoperative intestinal function [22], which is described by five questions concerning intestinal function. Each response was weighted and given a score according to the severity of the patient's symptoms. Scores of 0-20 indicated no LARS, 21-29 indicated minor LARS, and 30-42 indicated major LARS. All the participants were followed up by telephone, short message service, and outpatient or inpatient visits using a LARS score questionnaire from November 1, 2021 to May 1, 2022. LARS scores of each participant at 1 year after anterior resection or after stoma reversal were obtained. To highlight major LARS, patients were classified into two groups according to LARS score, one with major LARS and another with no or minor LARS.

Feature selection

Excessive variables could lead to adverse predictions and be inconvenient in an application. The Boruta algorithm can address the minimal optimization problem of multidimensional clinical features in feature selection[23]. Thus, feature selection was conducted using the Boruta algorithm. The algorithm can screen out all the variables associated with the ground truth. The importance of the features was quantified by repeated iterations based on shadow feature creation, and some weakly correlated features were removed. Finally, the selected features, combined with clinical experience, were used as predictors. R software and Boruta packages (7.0.0) were used for feature selection (R version 4.1.2[2021-11-01]).

Sample size

The one-in-ten rule is a generally accepted rule for estimating the minimum sample size[24]. According to at least ten events per variable, at least 325 to 667 patients were required in the discovery cohort for the 13 predictor variables, with an estimated event (major LARS) rate of 30%-50% and a lost follow-up

rate of 20%-35%.

Machine learning algorithms

In the present study, four prevailing machine learning algorithms, including logistic regression (LR), random forest (RF), support vector machine (SVM), and extreme gradient boosting (XGBoost), were employed to develop the predictive models. Machine learning algorithms based on AI can overcome the limitations of traditional linear models by combining clinical nonlinear features. The participants from Tongji Hospital were randomly divided into a training set and a testing set at a ratio of 8:2. To gain high-performance models, hyperparameter adjustment was adopted using a grid search approach. To balance sensitivity and specificity, the optimal Youden index (cutoff value) was calculated *via* maximizing the value of sensitivity + specificity - 1[25]. The area under the curve (AUC) and Brier scores, which represent the discrimination and calibration power of the prediction model, were calculated. The Brier score measures the difference between the predicted probability and the ground truth[26], and a value of the Brier Score closer to 0 indicates a better calibration. In addition, to assess the clinical utility of the prediction model, decision curve analysis was used, which can determine whether patients benefit from using predictive models in clinical practice[27]. All machine learning algorithms were implemented using Python (version 3.9.7) with the scikit-learn (version 0.24.2) package.

Statistical analyses

The continuous variables were presented as mean ± SD and categorical variables as the count (%). A one-way analysis of variance with post hoc contrasts by the student-Newman-Keuls test was used to compare the differences between the continuous variables. For categorical variables, as appropriate, χ^2 or Fisher's exact test was used. All P values were reported as two-tailed, and $P < 0.05$ was considered as statistical significance. 95%CI for the AUC, sensitivity, specificity, positive predictive value (PPV), negative predictive value (NPV), and accuracy of the four models were calculated using IBM SPSS Statistics 20.0 (IBM Corp, Armonk, NY, United States) or Vassar Stats (online tool, http://vassarstats.net/index.html).

RESULTS

Summary of demographic and clinical characteristics for training, testing, and external validation sets

Figure 1 presents the patient flow chart. A total of 1651 eligible cases were included, with 1163 subjects included in the training set, 291 subjects included in the testing set, and another 197 subjects in the external validation set. Comparisons between the training, testing, and external validation sets are presented in Table 1. The mean age of the 1163 patients in the training set was 57.6 years, and 59.7% were males. For the testing and the external validation sets, the mean age was 57.6 and 59.7 years, and 56.0% and 53.8% were males, respectively. Major LARS was observed in 37.2% of patients in the training set, 35.1% in the testing set, and 37.1% in the external validation set.

Risk factors associated with major LARS

The importance of all the included variables calculated by the Boruta algorithm was shown in Figure 2A. Boruta calculates variables that are both strongly and weakly relevant to provide the best prediction accuracy. The blue boxes were shadow features automatically generated by the algorithm and were not included in the analysis. As the data indicated that anastomotic height, neoadjuvant therapy, diverting stoma, BMI, clinical stage, specimen length, tumor size, and age were selected as significantly relevant to major LARS.

Model development in the training set

The LR, RF, SVM and XGBoost algorithms were trained using the eight strongly related variables, and the AUCs, sensitivities, specificities, PPVs, NPVs, and accuracies were calculated (Figure 2B and C). The RF model exhibited optimal diagnostic performance (AUC = 0.869), and the optimal cutoff was 0.406. Therefore, the RF model was used for subsequent analysis. The details of the predictions generated by the RF model using the optimal threshold were shown in Figure 2D. Additionally, the predicted probabilities for major LARS were significantly relevant to the ground truth in the training set ($P < 0.001$) (Figure 2E).

Performance of the RF model in the testing set

We tested the performance of the RF model in the testing set. The results demonstrated that the RF model performed with a favorable discrimination ability (AUC = 0.870, 95%CI: 0.833-0.901) (Figure 3A). The details of the predicted outcomes were presented in Figure 3B. Subsequently, the comparison of the predicted probabilities between the major LARS and no/minor LARS groups was conducted, and significant differences were observed (Figure 3C). Furthermore, a decision curve was plotted to evaluate

Table 1 Baseline characteristics of the training, testing, and external validation sets, *n* (%)

Variables	Training cohort, *n* = 1163	Testing cohort, *n* = 291	Validation cohort, *n* = 197	*P* value
Age, yr	57.60 ± 10.83	57.56 ± 11.23	59.72 ± 9.58	0.034
Male	694 (59.67)	163 (56.01)	106 (53.81)	0.206
BMI, kg/m^2	22.79 ± 2.92	22.89 ± 2.75	22.61 ± 4.02	0.382
Neoadjuvant	67 (5.76)	19 (6.53)	9 (4.57)	0.659
Hypertension	254 (21.84)	66 (22.68)	43 (21.83)	0.952
Diabetes	83 (7.14)	26 (8.93)	9 (4.57)	0.185
Previous abdominal surgery	141 (12.12)	45 (15.46)	22 (11.17)	0.250
ASA				< 0.001
1	178 (15.31)	42 (14.43)	55 (27.92)	
2	893 (76.78)	218 (74.91)	89 (45.12)	
3	90 (7.74)	30 (10.31)	50 (25.38)	
4	2 (0.17)	1 (0.34)	3 (1.52)	
Anastomotic height, cm	4.82 ± 2.37	4.57 ± 2.14	4.77 ± 2.56	0.298
Specimen length, cm	10.99 ± 3.01	10.88 ± 3.11	15.21 ± 4.49	< 0.001
Diverting ileostomy	315 (27.09)	81 (27.84)	35 (17.77)	0.017
Tumor size, cm	3.60 ± 1.29	3.53 ± 1.25	3.89 ± 1.35	0.546
Stage				< 0.001
1	354 (30.44)	91 (31.27)	31 (15.74)	
2	405 (34.82)	94 (32.30)	108 (54.82)	
3	404 (34.74)	106 (36.43)	58 (29.44)	
LARS				0.800
Minor/no	731 (62.85)	189 (64.95)	124 (62.94)	
Major	432 (37.15)	102 (35.05)	73 (37.06)	

ASA: American Society of Anesthesiologists classification; BMI: Body mass index; LARS: Low anterior resection syndrome.

whether using the RF model in the clinic would do better than harm[28]. According to the decision curve analysis, patients with major LARS would have a net benefit superior to "treat all" or "treat none" with a range of threshold probability in approximately 20%-75% (Figure 3D).

External validation of the RF model

To assess the generalization capability of the RF model, an external validation based on 197 patients from another independent center was performed. The RF model identified patients with major LARS with an AUC of 0.852 (95%CI: 0.820-0.890) (Figure 4A). The confusion matrix presented the classification results generated by the RF model for identifying major LARS in the external validation set (Figure 4B). Figure 4C showed that the probabilities generated by the RF model for major LARS were significantly higher than those of no/minor LARS, suggesting that the predicted probabilities were significantly associated with the ground truth in the external validation set. Decision curve analysis also showed that patients would derive clinical benefits in a range of threshold probabilities (Figure 4D).

Evaluation of the prediction model

To assess the performance and calibration degree of the RF model in both the testing set and the external validation set, six performance metrics such as sensitivity, specificity, PPV, NPV, accuracy, and Brier score were applied. Their results calculated based on the optimal Youden index (cutoff) were summarized in Table 2. These results suggested that the RF model was determined to be capable and reliable in predicting major LARS, with satisfactory Brier score of 0.152 and 0.166 and accuracy of 0.787 and 0.772, in both the testing set and the external validation set, respectively. In addition, to highlight the advantages of the RF model, the sensitivity, specificity, PPV, NPV, and accuracy of the preoperative LARS score (POLARS) model were calculated in both our testing set and external validation set. Taken

Table 2 Performance of the random forest model in the testing and external validation sets

Indicator (95%CI)	RF	
	Testing set, *n* = 291	Validation set, *n* = 197
Sensitivity	0.843 (0.755-0.905)	0.795 (0.681-0.877)
Specificity	0.757 (0.688-0.815)	0.758 (0.671-0.828)
PPV	0.652 (0.563-0.731)	0.659 (0.549-0.755)
NPV	0.899 (0.839-0.940)	0.862 (0.780-0.918)
Accuracy	0.787 (0.736-0.830)	0.772 (0.708-0.825)
Brier score	0.152	0.166

CI: Confidence interval; NPV: Negative predictive value; PPV: Positive predictive value; RF: Random forest.

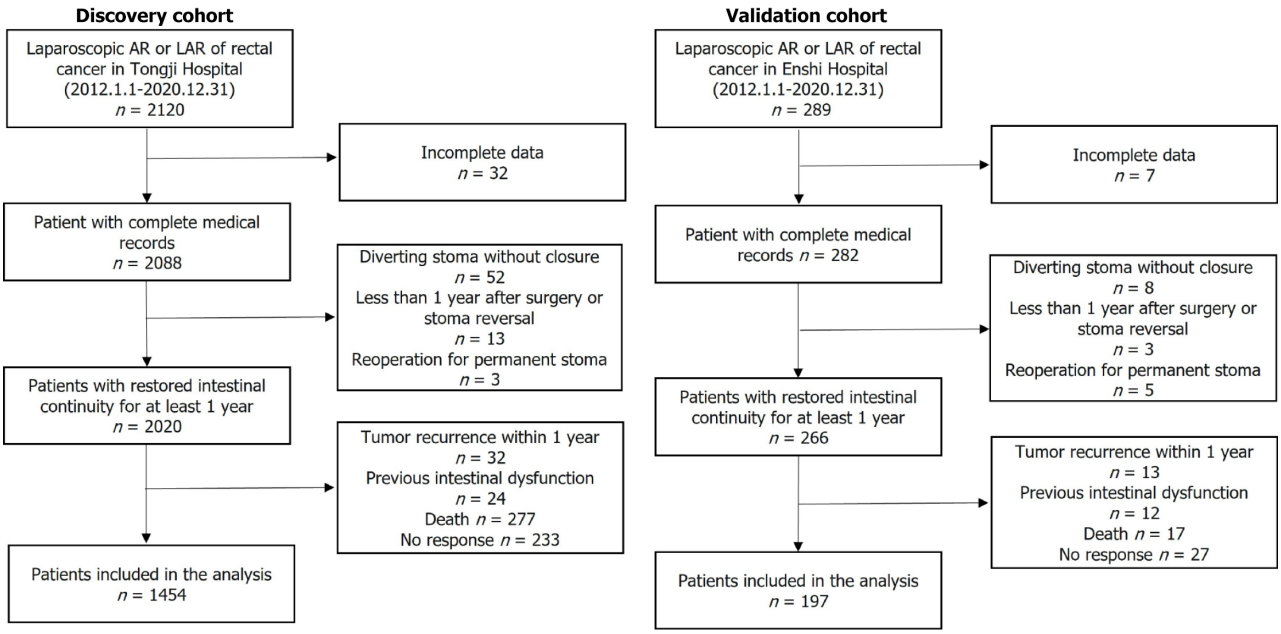

DOI: 10.3748/wjg.v29.i19.2979

Figure 1 Flow chart of the patients from two independent medical centers who were enrolled in the present study. AR: Anterior resection; LAR: Low anterior resection.

together, these values demonstrated that the performance of the RF model surpassed that of the POLARS score model, as shown in Table 3.

DISCUSSION

LARS is the most common complication following rectal cancer surgery. It is a severe complication and seriously impairs patient quality of life[1]. A meta-analysis based on 11 studies indicated that the morbidity of major LARS was as high as 41% (95%CI: 34-48)[5]. Fortunately, surgeons are now paying more and more attention to the functional consequences of cancer treatment and the quality of life[1,4]. LARS is a time-dependent syndrome, and the symptoms of some patients with LARS are relieved partly or completely 1 year or more after surgery. However, the symptoms in approximately 40% of patients remain stable and cannot be further improved[6,9,29].

Due to the variable symptom spectrum of LARS, ranging from incontinence for gas and liquid fecal matter to evacuation dysfunctions, the complex etiology, and unknown pathophysiology, there is no standard treatment available at present[30]. However, if patients with a high-risk major LARS can be treated with a conservative method (*e.g.*, pelvic floor rehabilitation, transanal irrigation), minimally invasive therapies (*e.g.*, biofeedback therapy, sacral nerve stimulation), or multimodal treatments during the period of the first year after surgery, their intestinal dysfunction may be significantly improved[9].

Table 3 Performance of the preoperative low anterior resection syndrome score model in the testing and external validation sets

Indicators (95%CI)	Testing set, *n* = 291	*P* value	Validation set, *n* = 197	*P* value
Sensitivity	0.931 (0.859-0.970)	0.046	0.836 (0.727-0.909)	0.522
Specificity	0.079 (0.047-0.130)	< 0.001	0.073 (0.036-0.137)	< 0.001
PPV	0.353 (0.297-0.414)	< 0.001	0.347 (0.278-0.422)	< 0.001
NPV	0.682 (0.451-0.853)	0.004	0.429 (0.226-0.656)	< 0.001
Accuracy	0.378 (0.323-0.437)	< 0.001	0.355 (0.289-0.427)	< 0.001

PPV: Positive predictive value; NPV: Negative predictive value.

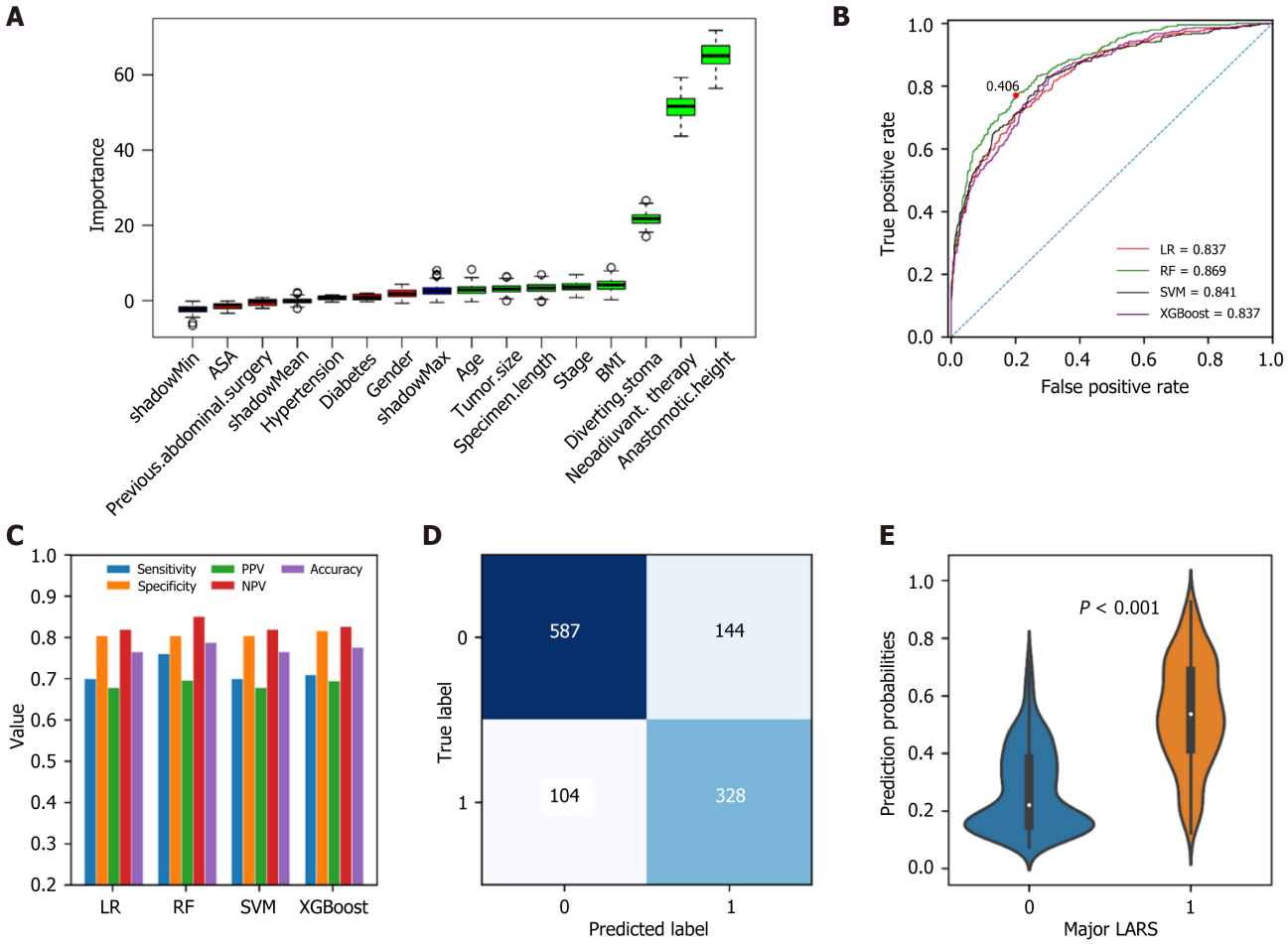

DOI: 10.3748/wjg.v29.i19.2979

Figure 2 Variable selection using the Boruta algorithm and overview of development of the models in the training set. A: The importance of all variables. The red boxes indicated the variables weakly relevant to major low anterior resection syndrome (LARS). The blue boxes were random variables automatically generated by the algorithm and were not included in the analysis. The green boxes indicated the variables strongly relevant to major LARS; B: Receiver operating characteristic curves of the four machine learning models in the training set. The red dot denotes the optimal Youden index for the random forest (RF) model; C: Performance measurements of the four machine learning models illustrated by sensitivity, specificity, positive predictive value, negative predictive value and accuracy; D: Confusion matrix of the optimization RF model; E: Comparison of predicted probabilities calculated by the RF model in patients with and without major LARS in the training set. ASA: American Society of Anesthesiologists classification; BMI: Body mass index; LR: Logistic regression; LARS: Low anterior resection syndrome; RF: Random forest; SVM: Support vector machine; XGBoost: Extreme gradient boosting; PPV: Positive predictive value; NPV: Negative predictive value.

Consequently, the negative impact of LARS on their quality of life could be minimized. In addition, since major LARS may counteract the relative benefits of anal sphincter-preserving surgery, the accurate prediction of major LARS may be helpful for patients and surgeons when deciding on temporary ileostomy, permanent colostomy, or sphincter-preserving surgery for low rectal cancer[31-33]. Therefore, it is crucial to perform risk stratification of rectal surgery cases to identify patients with a high risk of major LARS and to highlight patients who may require additional postoperative support.

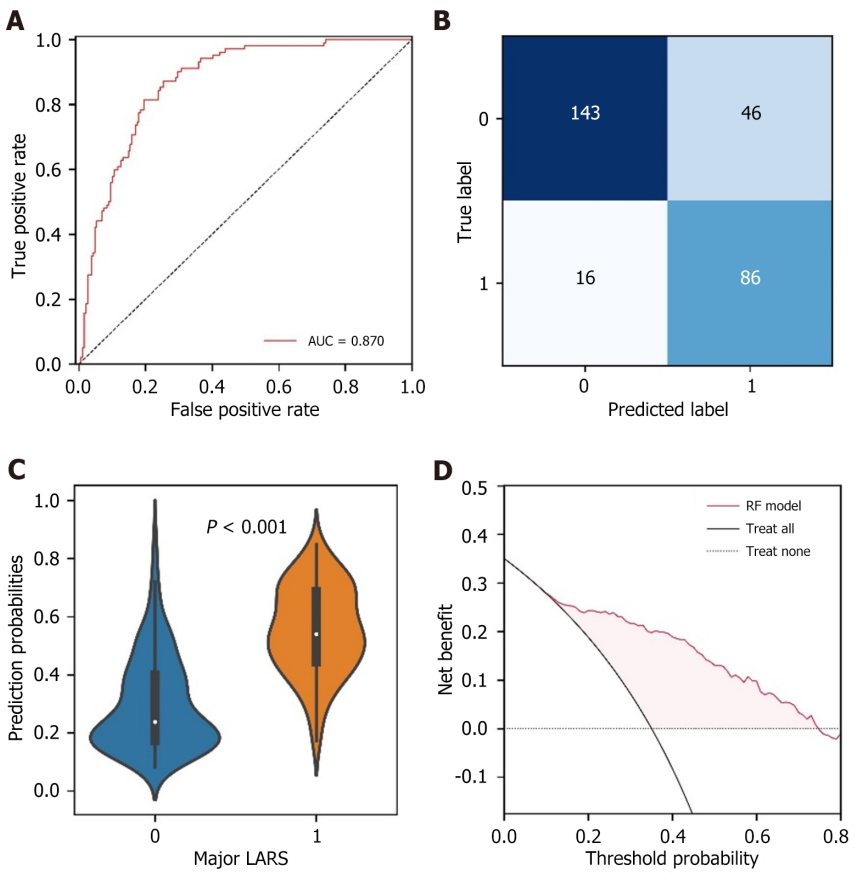

DOI: 10.3748/wjg.v29.i19.2979

Figure 3 Performance of the random forest model in the testing set. A: Receiver operating characteristic curve of the random forest (RF) model in the testing set; B: Confusion matrices showed the predicted outcomes generated by the RF model in the testing set; C: Comparison of predicted probabilities between patients with and without major low anterior resection syndrome in the testing set; D: Decision curve analysis for the RF model in the testing set. AUC: Area under the curve; LARS: Low anterior resection syndrome; RF: Random forest; ROC: Receiver operating characteristic.

Battersby *et al*[15] developed and validated the POLARS score for restorative sphincter-sparing surgery for rectal cancer to predict intestinal dysfunction. The POLARS score includes six risk factors, such as age at surgery, sex, tumor height, preoperative radiotherapy, total/partial mesorectal excision, and the presence of stoma, as predictors. The model performs with moderate discriminative accuracy with Harrell's C statistic of 0.615 and 0.625 in their two datasets. Essangri *et al*[16] reported that the POLARS score was questionable, and it failed to successfully validate the model in another population. This previous study implied that the model predictions may be dependent on patient background, including treatment strategies and physical, lifestyle, and dietary habit differences. In the present study, all participants were Chinese and underwent laparoscopic sphincter-sparing surgery for rectal cancer without splenic flexure mobilization. Several previous studies have pointed out that routine splenic flexure mobilization is not necessary for anterior resection of rectal cancer[34-36]. Instead, no splenic flexure mobilization would result in a shorter operation time and lower morbidity of postoperative complications associated with intestinal function, such as anastomotic leakage[37]. Moreover, to date, there is no machine learning model for predicting major LARS in Asian patients undergoing laparoscopic anterior resection based on a multicenter study.

In the present study, four machine learning algorithms were used to develop the machine learning model for major LARS prediction. These data suggested that the RF model performed with an optimal AUC in the training set. As expected, the RF model also achieved favorable predictions when it was tested in the testing and external validation sets. To the best of our knowledge, this is the first multicentric study to develop a machine-learning model for predicting major LARS in Asian patients undergoing laparoscopic anterior resection of rectal cancer. More importantly, the model performed with a satisfactory prediction in an independent medical center (AUC = 0.852; 95%CI: 0.820-0.890). Moreover, compared with the POLARS score, the RF model achieved superior performance in predicting major LARS in our cohort (accuracy of 0.772 for the RF model *vs* 0.355 for the POLARS score). In addition, the decision curve analysis demonstrated the net benefit (benefit minus risk) by using the model for patients diagnosed with major LARS within a range of threshold probabilities.

Although the explicit pathophysiological mechanism of LARS is still unclear, numerous studies[38-40] agree that intestinal dysfunction in patients with rectal cancer who received restorative sphincter-

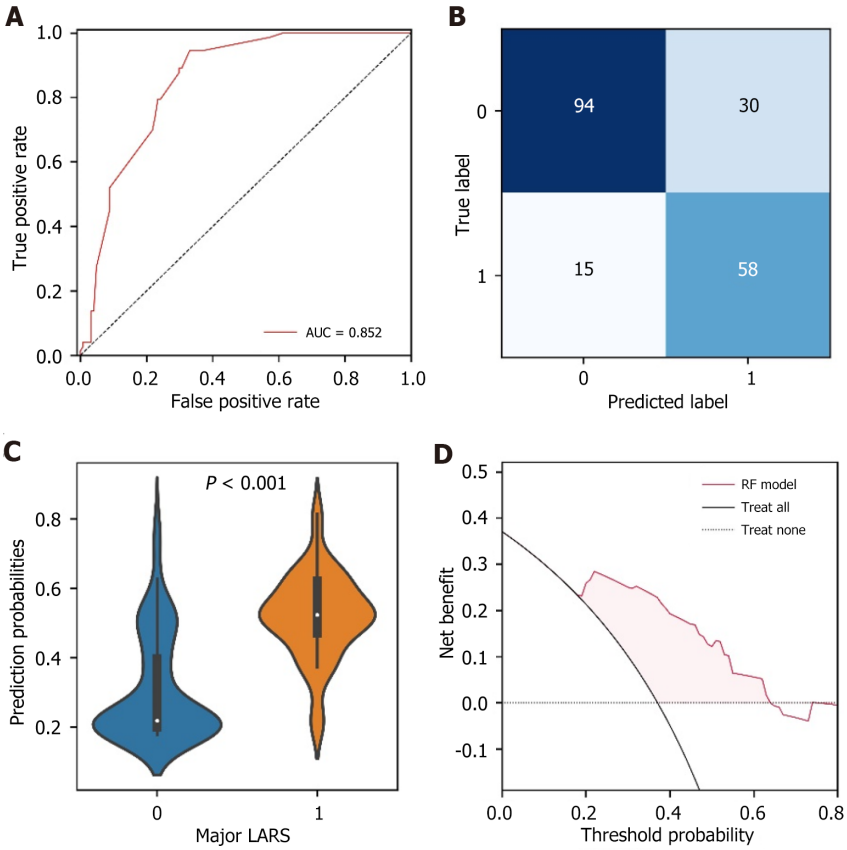

DOI: 10.3748/wjg.v29.i19.2979

Figure 4 Performance of the random forest model in the external validation set. A: Receiver operating characteristic curve of the random forest (RF) model in the external validation set; B: Confusion matrices showed the predicted outcomes generated by the RF model in the external validation set; C: Comparison of predicted probabilities between patients with and without major low anterior resection syndrome in the external validation set; D: Decision curve analysis for the RF model in the external validation set. AUC: Area under the curve; LARS: Low anterior resection syndrome; RF: Random forest.

sparing surgery is the result of a combination of multiple pathophysiological mechanisms. These include loss of rectal storage function, autonomic denervation, enhanced colonic movement, rectal-anus sensitivity reduction, anal resting pressure reduction, and diverting colitis[38]. Certain factors directly or indirectly related to these pathophysiological changes have been reported as important variables associated with LARS, such as low anastomosis, neoadjuvant therapy, postoperative chemoradiotherapy, anastomotic leakage, diverting stoma, and the time interval from the creation of diverting stoma to closure[5,18,41,42]. In order to identify major LARS in the early postoperative period, some postoperative factors were not included, such as chemoradiotherapy and the time interval from creating diverting stoma to its closure. Among the included factors, low anastomosis and neoadjuvant therapy have been unanimously considered as important predictors for major LARS[5,43]. For example, Filips *et al*[44] reported that LARS was negatively correlated with the distance from anastomosis to the anal verge (OR: -1.145, 95%CI: -2.149 to -1.141, P = 0.026). In the present study, our data also indicated that the anastomotic height was the most important factor in the development of major LARS. In addition, the specimen length was selected as a predictor for major LARS in the present study, and it may be caused by greater surgical trauma.

As with any retrospective observational study, the present study had some uncontrollable limitations. First, the model is based on the Chinese population and does not necessarily reflect the worldwide target population. Its generalizability needs to be further tested. Second, the influence of a patient's socioeconomic and cultural background, self-management ability, and social support are difficult to control. Third, the data reflecting anal sphincter injury and its severity during surgery cannot be evaluated. Finally, the LARS score may be affected by a variety of biases, such as patient selective memory, exaggeration, or understatement. To overcome these limitations, a prospective study is proposed to assess the predictive ability of the model.

CONCLUSION

In the present study, a machine learning model based on preoperative and intraoperative risk factors for

predicting LARS was developed. The model may be helpful for clinical medical staff to identify patients at an early stage with a high risk of developing major LARS within 1 year following laparoscopic surgery for rectal cancer. Moreover, it can potentially be used for patients to acquire early postoperative consultation and strengthen self-management to improve patient quality of life.

ARTICLE HIGHLIGHTS

Research background

Low anterior resection syndrome (LARS) severely impairs patient postoperative quality of life, especially major LARS. However, there are few tools that can accurately predict major LARS in clinical practice.

Research motivation

To stratify patients with LARS and predict patients at high risk of developing major LARS, improve patient counseling, and highlight patients who may need additional support after surgery.

Research objectives

The study aimed to identify the risk factors associated with major LARS and develop a prediction model that helps improve patient counseling and highlight patients who may need additional support after surgery.

Research methods

Clinical data and follow-up information of patients from two medical centers (one discovery cohort and one external validation cohort) were analyzed to identify independent factors associated with major LARS. For the discovery cohort, the machine learning prediction algorithms were developed and internally validated. In the external validation cohort, we evaluated the trained model using various performance metrics. Further, the clinical utility of the model was tested by decision curve analysis.

Research results

Eight factors, such as anastomotic height, neoadjuvant therapy, diverting stoma, body mass index, clinical stage, specimen length, tumor size, and age, were selected as significantly relevant to major LARS. A machine learning-based prediction model that integrated eight risk factors as input features was developed, externally validated, and demonstrated an acceptable predictive performance.

Research conclusions

We have developed and validated a robust tool for predicting major LARS. This model could potentially be used in the clinic to identify patients with a high risk of developing major LARS and then improve their quality of life.

Research perspectives

A prospective study including more medical centers is proposed to assess the model's predictive ability.

ACKNOWLEDGEMENTS

I would like to thank all the medical staff of the Department of Gastrointestinal Surgery in Tongji Hospital and Enshi Central Hospital for providing convenient conditions for implementing this study.

FOOTNOTES

Author contributions: Wang Z and Shao SL contributed equally to this work; Wang Z contributed to methodology, formal analysis, data extraction, follow-up, writing, reviewing, and editing; Shao SL contributed to data extraction, data curation, follow-up, formal analysis, writing, reviewing, and editing; Liu L was involved in supervision and software; Lu QY contributed to follow-up and data curation; Mu L performed data curation; Qin JC contributed to conceptualization, funding acquisition, methodology, writing, reviewing, and editing; All authors contributed to the interpretation of the study and approved the final version to be published.

Supported by the National Natural Science Foundation of China, No. 82173368 and 81903047.

Institutional review board statement: This study was supported by the Ethics Committee of Tongji Hospital, Tongji Medical College, Huazhong University of Science and Technology, and the Central Hospital of Enshi Tujia and Miao

Autonomous Prefecture.

Informed consent statement: The requirement for informed consent was waived due to the retrospective nature of the study.

Conflict-of-interest statement: All the authors report having no relevant conflicts of interest for this article.

Data sharing statement: The dataset used during the current study is available from the corresponding author on reasonable request. E-mail: jcqin@tjh.tjmu.edu.cn.

STROBE statement: The authors have read the STROBE statement-checklist of items, and the manuscript was prepared and revised according to the STROBE statement-checklist of items.

Country/Territory of origin: China

ORCID number: Sheng-Li Shao 0000-0001-8786-0051; Ji-Chao Qin 0000-0002-2961-7624.

S-Editor: Zhang H
L-Editor: Filipodia
P-Editor: Chen YX

REFERENCES

1 **Pieniowski EHA**, Palmer GJ, Juul T, Lagergren P, Johar A, Emmertsen KJ, Nordenvall C, Abraham-Nordling M. Low Anterior Resection Syndrome and Quality of Life After Sphincter-Sparing Rectal Cancer Surgery: A Long-term Longitudinal Follow-up. *Dis Colon Rectum* 2019; **62**: 14-20 [PMID: 30394987 DOI: 10.1097/DCR.0000000000001228]

2 **Bryant CL**, Lunniss PJ, Knowles CH, Thaha MA, Chan CL. Anterior resection syndrome. *Lancet Oncol* 2012; **13**: e403-e408 [PMID: 22935240 DOI: 10.1016/S1470-2045(12)70236-X]

3 **Ståhle E**, Påhlman L, Enblad P. Double stapling technique in the management of rectal tumours. *Acta Chir Scand* 1986; **152**: 743-747 [PMID: 3591203]

4 **Pieniowski EHA**, Nordenvall C, Palmer G, Johar A, Tumlin Ekelund S, Lagergren P, Abraham-Nordling M. Prevalence of low anterior resection syndrome and impact on quality of life after rectal cancer surgery: population-based study. *BJS Open* 2020; **4**: 935-942 [PMID: 32530135 DOI: 10.1002/bjs5.50312]

5 **Croese AD**, Lonie JM, Trollope AF, Vangaveti VN, Ho YH. A meta-analysis of the prevalence of Low Anterior Resection Syndrome and systematic review of risk factors. *Int J Surg* 2018; **56**: 234-241 [PMID: 29936195 DOI: 10.1016/j.ijsu.2018.06.031]

6 **Nicotera A**, Falletto E, Arezzo A, Mistrangelo M, Passera R, Morino M. Risk factors for Low Anterior Resection Syndrome (LARS) in patients undergoing laparoscopic surgery for rectal cancer. *Surg Endosc* 2022; **36**: 6059-6066 [PMID: 35137257 DOI: 10.1007/s00464-021-09002-y]

7 **Varghese C**, Wells CI, O'Grady G, Christensen P, Bissett IP, Keane C; on behalf of the Longitudinal LARS Group. The Longitudinal Course of Low-anterior Resection Syndrome: An individual Patient Meta-analysis. *Ann Surg* 2022; **276**: 46-54 [PMID: 35185131 DOI: 10.1097/SLA.0000000000005423]

8 **Juul T**, Ahlberg M, Biondo S, Espin E, Jimenez LM, Matzel KE, Palmer GJ, Sauermann A, Trenti L, Zhang W, Laurberg S, Christensen P. Low anterior resection syndrome and quality of life: an international multicenter study. *Dis Colon Rectum* 2014; **57**: 585-591 [PMID: 24819098 DOI: 10.1097/DCR.0000000000000116]

9 **Sturiale A**, Martellucci J, Zurli L, Vaccaro C, Brusciano L, Limongelli P, Docimo L, Valeri A. Long-term functional follow-up after anterior rectal resection for cancer. *Int J Colorectal Dis* 2017; **32**: 83-88 [PMID: 27695976 DOI: 10.1007/s00384-016-2659-6]

10 **van der Heijden JAG**, Kalkdijk-Dijkstra AJ, Pierie JPEN, van Westreenen HL, Broens PMA, Klarenbeek BR; FORCE trial group. Pelvic Floor Rehabilitation After Rectal Cancer Surgery: A Multicenter Randomized Clinical Trial (FORCE Trial). *Ann Surg* 2022; **276**: 38-45 [PMID: 34966064 DOI: 10.1097/SLA.0000000000005353]

11 **Li H**, Guo C, Gao J, Yao H. Effectiveness of Biofeedback Therapy in Patients with Bowel Dysfunction Following Rectal Cancer Surgery: A Systemic Review with Meta-Analysis. *Ther Clin Risk Manag* 2022; **18**: 71-93 [PMID: 35140468 DOI: 10.2147/TCRM.S344375]

12 **Embleton R**, Henderson M. Using transanal irrigation in the management of low anterior resection syndrome: a service audit. *Br J Nurs* 2021; **30**: 1226-1230 [PMID: 34839681 DOI: 10.12968/bjon.2021.30.21.1226]

13 **Itagaki R**, Koda K, Yamazaki M, Shuto K, Kosugi C, Hirano A, Arimitsu H, Shiragami R, Yoshimura Y, Suzuki M. Serotonin (5-HT3) receptor antagonists for the reduction of symptoms of low anterior resection syndrome. *Clin Exp Gastroenterol* 2014; **7**: 47-52 [PMID: 24648748 DOI: 10.2147/CEG.S55410]

14 **De Meyere C**, Nuytens F, Parmentier I, D'Hondt M. Five-year single center experience of sacral neuromodulation for isolated fecal incontinence or fecal incontinence combined with low anterior resection syndrome. *Tech Coloproctol* 2020; **24**: 947-958 [PMID: 32556866 DOI: 10.1007/s10151-020-02245-2]

15 **Battersby NJ**, Bouliotis G, Emmertsen KJ, Juul T, Glynne-Jones R, Branagan G, Christensen P, Laurberg S, Moran BJ; UK and Danish LARS Study Groups. Development and external validation of a nomogram and online tool to predict bowel dysfunction following restorative rectal cancer resection: the POLARS score. *Gut* 2018; **67**: 688-696 [PMID: 28115491 DOI: 10.1136/gutjnl-2016-312695]

16 **Essangri H**, Majbar MA, Benkabbou A, Belkhadir Z, Amrani L, Mohsine R, Souadka A. Do we have enough Foreknowledge to predict the low anterior resection syndrome (LARS) score preoperatively? *Colorectal Dis* 2020; **22**: 1445 [PMID: 32270539 DOI: 10.1111/codi.15062]

17 **Miacci FLC**, Guetter CR, Moreira PH, Sartor MC, Savio MC, Baldin Júnior A, Nóbrega NL. Predictive factors of low anterior resection syndrome following anterior resection of the rectum. *Rev Col Bras Cir* 2020; **46**: e20192361 [PMID: 32022113 DOI: 10.1590/0100-6991e-20192361]

18 **Ekkarat P**, Boonpipattanapong T, Tantiphlachiva K, Sangkhathat S. Factors determining low anterior resection syndrome after rectal cancer resection: A study in Thai patients. *Asian J Surg* 2016; **39**: 225-231 [PMID: 26340884 DOI: 10.1016/j.asjsur.2015.07.003]

19 **Lourenco T**, Murray A, Grant A, McKinley A, Krukowski Z, Vale L. Laparoscopic surgery for colorectal cancer: safe and effective? *Surg Endosc* 2008; **22**: 1146-1160 [PMID: 18071810 DOI: 10.1007/s00464-007-9686-x]

20 **Shao S**, Liu L, Zhao Y, Mu L, Lu Q, Qin J. Application of Machine Learning for Predicting Anastomotic Leakage in Patients with Gastric Adenocarcinoma Who Received Total or Proximal Gastrectomy. *J Pers Med* 2021; **11** [PMID: 34442391 DOI: 10.3390/jpm11080748]

21 **Shao S**, Zhao Y, Lu Q, Liu L, Mu L, Qin J. Artificial intelligence assists surgeons' decision-making of temporary ileostomy in patients with rectal cancer who have received anterior resection. *Eur J Surg Oncol* 2023; **49**: 433-439 [PMID: 36244844 DOI: 10.1016/j.ejso.2022.09.020]

22 **Hou XT**, Pang D, Lu Q, Yang P, Jin SL, Zhou YJ, Tian SH. Validation of the Chinese version of the low anterior resection syndrome score for measuring bowel dysfunction after sphincter-preserving surgery among rectal cancer patients. *Eur J Oncol Nurs* 2015; **19**: 495-501 [PMID: 25813530 DOI: 10.1016/j.ejon.2015.02.009]

23 **Kursa MB**, Rudnicki WR. Feature selection with the Boruta Package. *J Stat Softw* 2010; **36**: 1-13 [DOI: 10.18637/jss.v036.i11]

24 **Peduzzi P**, Concato J, Kemper E, Holford TR, Feinstein AR. A simulation study of the number of events per variable in logistic regression analysis. *J Clin Epidemiol* 1996; **49**: 1373-1379 [PMID: 8970487 DOI: 10.1016/s0895-4356(96)00236-3]

25 **Fluss R**, Faraggi D, Reiser B. Estimation of the Youden Index and its associated cutoff point. *Biom J* 2005; **47**: 458-472 [PMID: 16161804 DOI: 10.1002/bimj.200410135]

26 **Roulston MS**. Performance targets and the Brier score. *Meteorological Applications* 2007; **14**: 185-194 [DOI: 10.1002/met.21]

27 **Vickers AJ**, Elkin EB. Decision curve analysis: a novel method for evaluating prediction models. *Med Decis Making* 2006; **26**: 565-574 [PMID: 17099194 DOI: 10.1177/0272989X06295361]

28 **Vickers AJ**, van Calster B, Steyerberg EW. A simple, step-by-step guide to interpreting decision curve analysis. *Diagn Progn Res* 2019; **3**: 18 [PMID: 31592444 DOI: 10.1186/s41512-019-0064-7]

29 **Afshari K**, Smedh K, Wagner P, Chabok A, Nikberg M. Risk factors for developing anorectal dysfunction after anterior resection. *Int J Colorectal Dis* 2021; **36**: 2697-2705 [PMID: 34471965 DOI: 10.1007/s00384-021-04024-3]

30 **Dulskas A**, Smolskas E, Kildusiene I, Samalavicius NE. Treatment possibilities for low anterior resection syndrome: a review of the literature. *Int J Colorectal Dis* 2018; **33**: 251-260 [PMID: 29313107 DOI: 10.1007/s00384-017-2954-x]

31 **Pachler J**, Wille-Jørgensen P. Quality of life after rectal resection for cancer, with or without permanent colostomy. *Cochrane Database Syst Rev* 2012; **12**: CD004323 [PMID: 23235607 DOI: 10.1002/14651858.CD004323.pub4]

32 **Cornish JA**, Tilney HS, Heriot AG, Lavery IC, Fazio VW, Tekkis PP. A meta-analysis of quality of life for abdominoperineal excision of rectum versus anterior resection for rectal cancer. *Ann Surg Oncol* 2007; **14**: 2056-2068 [PMID: 17431723 DOI: 10.1245/s10434-007-9402-z]

33 **Trenti L**, Galvez A, Biondo S, Solis A, Vallribera-Valls F, Espin-Basany E, Garcia-Granero A, Kreisler E. Quality of life and anterior resection syndrome after surgery for mid to low rectal cancer: A cross-sectional study. *Eur J Surg Oncol* 2018; **44**: 1031-1039 [PMID: 29665980 DOI: 10.1016/j.ejso.2018.03.025]

34 **Park JS**, Kang SB, Kim DW, Lee KH, Kim YH. Laparoscopic versus open resection without splenic flexure mobilization for the treatment of rectum and sigmoid cancer: a study from a single institution that selectively used splenic flexure mobilization. *Surg Laparosc Endosc Percutan Tech* 2009; **19**: 62-68 [PMID: 19238070 DOI: 10.1097/SLE.0b013e318196cdb0]

35 **Kim J**, Choi DJ, Kim SH. Laparoscopic rectal resection without splenic flexure mobilization: a prospective study assessing anastomotic safety. *Hepatogastroenterology* 2009; **56**: 1354-1358 [PMID: 19950790]

36 **Tian C**, Li H, Meng WJ. Should splenic flexure be routinely mobilized during laparoscopic low anterior resection for rectal cancer? *Surg Laparosc Endosc Percutan Tech* 2014; **24**: 283-284 [PMID: 24887544 DOI: 10.1097/SLE.0b013e3182937c67]

37 **Brennan DJ**, Moynagh M, Brannigan AE, Gleeson F, Rowland M, O'Connell PR. Routine mobilization of the splenic flexure is not necessary during anterior resection for rectal cancer. *Dis Colon Rectum* 2007; **50**: 302-7; discussion 307 [PMID: 17211537 DOI: 10.1007/10350-006-0811-z]

38 **Buzatti KCLR**, Petroianu A. Pathophysiological aspects of the low anterior resection syndrome for treatment of rectal cancer. *Rev Col Bras Cir* 2017; **44**: 397-402 [PMID: 29019544 DOI: 10.1590/0100-69912017004003]

39 **Ziv Y**, Zbar A, Bar-Shavit Y, Igov I. Low anterior resection syndrome (LARS): cause and effect and reconstructive considerations. *Tech Coloproctol* 2013; **17**: 151-162 [PMID: 23076289 DOI: 10.1007/s10151-012-0909-3]

40 **van der Heijden JAG**, van Heinsbergen M, Thomas G, Caers F, Slooter GD, Maaskant-Braat AJG. Implementation of a

Postoperative Screening and Treatment Guidance for the Low Anterior Resection Syndrome: Preliminary Results. *Dis Colon Rectum* 2019; **62**: 1033-1042 [PMID: 31318775 DOI: 10.1097/DCR.0000000000001428]

41 **Hughes DL**, Cornish J, Morris C; LARRIS Trial Management Group. Functional outcome following rectal surgery-predisposing factors for low anterior resection syndrome. *Int J Colorectal Dis* 2017; **32**: 691-697 [PMID: 28130593 DOI: 10.1007/s00384-017-2765-0]

42 **Vogel I**, Reeves N, Tanis PJ, Bemelman WA, Torkington J, Hompes R, Cornish JA. Impact of a defunctioning ileostomy and time to stoma closure on bowel function after low anterior resection for rectal cancer: a systematic review and meta-analysis. *Tech Coloproctol* 2021; **25**: 751-760 [PMID: 33792822 DOI: 10.1007/s10151-021-02436-5]

43 **Battersby NJ**, Juul T, Christensen P, Janjua AZ, Branagan G, Emmertsen KJ, Norton C, Hughes R, Laurberg S, Moran BJ; United Kingdom Low Anterior Resection Syndrome Study Group. Predicting the Risk of Bowel-Related Quality-of-Life Impairment After Restorative Resection for Rectal Cancer: A Multicenter Cross-Sectional Study. *Dis Colon Rectum* 2016; **59**: 270-280 [PMID: 26953985 DOI: 10.1097/DCR.0000000000000552]

44 **Filips A**, Haltmeier T, Kohler A, Candinas D, Brügger L, Studer P. LARS is Associated with Lower Anastomoses, but not with the Transanal Approach in Patients Undergoing Rectal Cancer Resection. *World J Surg* 2021; **45**: 873-879 [PMID: 33301048 DOI: 10.1007/s00268-020-05876-6]

World Journal of Gastroenterology

Submit a Manuscript: https://www.f6publishing.com

World J Gastroenterol 2023 May 21; 29(19): 2992-3002

DOI: 10.3748/wjg.v29.i19.2992

ISSN 1007-9327 (print) ISSN 2219-2840 (online)

ORIGINAL ARTICLE

Retrospective Study

Where is the optimal plane to mobilize the anterior rectal wall in female patients undergoing total mesorectal excision?

Wei Jin, Jun Yang, Xin-Yu Li, Wei-Cheng Wang, Wen-Jian Meng, You Li, Yi-Chao Liang, Yi-Ming Zhou, Xin-Dong Yang, Yang-Yang Li, Shao-Tang Li

Specialty type: Gastroenterology and hepatology

Provenance and peer review: Unsolicited article; Externally peer reviewed.

Peer-review model: Single blind

Peer-review report's scientific quality classification
Grade A (Excellent): 0
Grade B (Very good): B, B, B
Grade C (Good): C, C, C
Grade D (Fair): 0
Grade E (Poor): 0

P-Reviewer: Bae SU, South Korea; Brisinda G, Italy; Luglio G, Italy; Martínez-Pérez A, Spain; M'Koma AE, United States; Tonelli F, Italy

Received: February 6, 2023
Peer-review started: February 6, 2023
First decision: March 20, 2023
Revised: April 3, 2023
Accepted: April 20, 2023
Article in press: April 20, 2023
Published online: May 21, 2023

Wei Jin, Jun Yang, Wei-Cheng Wang, Department of Colorectal and Anal Surgery, The First Affiliated Hospital of Wenzhou Medical University, Wenzhou 325000, Zhejiang Province, China

Xin-Yu Li, Department of Gastrointestinal Surgery, The First Hospital of Quanzhou Affiliated to Fujian Medical University, Quanzhou 362002, Fujian Province, China

Wen-Jian Meng, Department of Gastrointestinal Surgery, West China Hospital. Sichuan University, Chengdu 610041, Sichuan Province, China

You Li, Department of General Surgery, Shanghai Jiao Tong University Medical School Affiliated Ruijin, Shanghai 201800, China

Yi-Chao Liang, Department of General Surgery, Shengjing Hospital of China Medical University, Shenyang 111300, Liaoning Province, China

Yi-Ming Zhou, Department of General Surgery, Huashan Hospital Fudan University, Shanghai 201800, China

Xin-Dong Yang, School of Basic Medicine, Wenzhou Medical University, Wenzhou 325000, Zhejiang Province, China

Yang-Yang Li, Department of Pathology, the First Affiliated Hospital of Wenzhou Medical University, Wenzhou 325000, Zhejiang Province, China

Shao-Tang Li, National Key Clinical Specialty (General Surgery), The First Affiliated Hospital of Wenzhou Medical University, Wenzhou 325000, Zhejiang Province, China

Corresponding author: Shao-Tang Li, MD, PhD, Chief Doctor, Doctor, Instructor, Professor, Surgeon, National Key Clinical Specialty (General Surgery), The First Affiliated Hospital of Wenzhou Medical University, Nanbaixiang Street, Ouhai District, Wenzhou 325000, Zhejiang Province, China. lishaotang163@163.com

Abstract

BACKGROUND

Since Heald proposed the total mesorectal excision (TME) procedure, the prognosis of patients with rectal cancer has been significantly improved. But Heald did not specifically describe the anterior surgical plane in female patients.

And the surgical plane for mobilizing the anterior rectal wall during TME surgery in female patients remains controversial.

AIM
To investigate the anatomy of the female pelvis and identify the optimal plane for mobilizing the anterior rectal wall.

METHODS
We retrospectively collected surgical procedure videos and clinical data of female patients diagnosed with middle or low rectal cancer who underwent the TME procedure between January 2020 and October 2022 across six hospitals. The patients were divided into two groups based on the surgical approach used to mobilize the anterior rectal wall: The experimental group was to open the peritoneum at the lowest point of the peritonea reflection and enter the plane for mobilizing, while the control group was cut at 0.5-1 cm above the peritoneal reflection and enter another plan. Then, we compared the preoperative and postoperative information between the two groups. We also dissected and observed ten adult female pelvises to analyze the anatomic structure and compare the entry plane between the two approaches. Finally, we researched the pathological structure between the rectum and the vagina.

RESULTS
Finally, 77 cases that met the criteria were included in our study. Our observations revealed that the experimental group underwent a smooth procedure, entering the plane amidst the mesorectal fascia and adventitia of the vagina, whereas the control group entered the plane between the vaginal adventitia and muscle layers. Compared to the control group, the experimental group showed a significant decrease in intraoperative bleeding [22.5 (19.5-50) mL *vs* 17 (5-20) mL, P = 0.01], as well as a shorter duration of hospitalization [9 (7-11.25) d *vs* 7 (6-10) d, P = 0.03]. Through the examination of surgical videos and cadaveric studies, we discovered that Denonvilliers' fascia is absent in females. Additionally, pathological sections further revealed the absence of Denonvilliers' fascia in females, with only loose connective tissue present between the mesorectal fascia and adventitia of the vagina.

CONCLUSION
The plane amidst the mesorectal fascia and vaginal adventitia is the optimal surgical plane to mobilize the anterior rectal wall for female patients undergoing the TME procedure.

Key Words: Rectal cancer; Procedure; Female; Rectal surgery specialty; Fascia; Laparoscopic

Core Tip: In combination with the macroscopic and microscopic perspectives, we discovered that liberating the anterior rectal wall within a certain plane not only guarantees negative perirectal margins but also mitigates the potential for hemorrhage. This plane, situated amidst the mesorectal fascia and vaginal adventitia, proves to be the most advantageous approach for female patients undergoing total mesorectal excision.

Citation: Jin W, Yang J, Li XY, Wang WC, Meng WJ, Li Y, Liang YC, Zhou YM, Yang XD, Li YY, Li ST. Where is the optimal plane to mobilize the anterior rectal wall in female patients undergoing total mesorectal excision? *World J Gastroenterol* 2023; 29(19): 2992-3002
URL: https://www.wjgnet.com/1007-9327/full/v29/i19/2992.htm
DOI: https://dx.doi.org/10.3748/wjg.v29.i19.2992

INTRODUCTION

In 1982, Heald proposed the total mesorectal excision (TME) procedure[1], which significantly improved the prognosis of patients with rectal cancer[2]. The local recurrence of rectal cancer in 5 years decreased from 25% to 5%, as compared to the traditional operation plus radiotherapy group in the TME operation group[3]. TME soon became a classical operation method and was widely accepted by colorectal surgeons. Heald subsequently described the bloodless planes of TME surgery, known as the "holy plane," as follows: “If we cut straight on to the vesicles we find an essentially bloodless plane between

them and the fascia of Denonvilliers and we can proceed down the enemy to this until it comes forward to become somewhat should come to the state, when we must cut through it to liberate the lower third of the correction enemy"[4].

Professor Heald believes that in male patients, the anterior plane of TME should be anterior to Denonvilliers' fascia, and the anterior aspect of the specimen should include the complete Denonvilliers' fascia and peritoneal folds[3]. However, he did not specifically describe the anterior surgical plane in female patients[1], and the presence of Denonvilliers' fascia in females (rectovaginal septum[5]) remains controversial[6,7]. We also haven't found any research describing the plane of TME for female patients when the front rectal wall performs mobilization till now[8-10]. Many colorectal surgeons struggle to find an ideal plane for mobilizing the anterior rectal wall during TME, which can result in intraoperative bleeding or vaginal damage.

Therefore, we conducted this study to explore the optimal plane to mobilize the anterior rectal wall in female patients. We retrospectively analyzed rectal cancer surgery videos collected from different medical centers and studied the anatomy of the female pelvis for the accurate determination of the optimal plane to mobilize the anterior rectal wall in female patients with rectal cancer.

MATERIALS AND METHODS

Clinical data and video review

We retrospectively collected clinical data and surgical videos from six hospitals between January 2020 and October 2022. The surgeries were performed by experienced colorectal surgeons, each of whom performed more than 100 colorectal cancer operations annually. Our study initially included female patients with middle or low rectal cancer who underwent laparoscopic TME. Patients who had preoperative magnetic resonance imaging assessment indicating invasion of the anterior rectal wall, a history of rectal surgery, absence of surgical videos or relevant clinical data, and the presence of distant metastases were excluded. And they were divided into two groups based on the surgical approaches used. In the experimental group, the peritoneum was incised at the lowest point of peritoneal reflection to access the mobilization plane, while in the control group, the peritoneum was incised 0.5-1 cm above the peritoneal reflection, accessing a different plane. The surgical procedures were reviewed by two experienced colorectal surgeons separately.

The patient's pre- and postoperative data were obtained from medical records, while intraoperative bleeding was measured as the total amount of blood loss recorded in surgical records. Postoperative complications were classified into postoperative bleeding, anastomotic leakage, and other complications (such as pleural effusion, fever, *etc.*). Anastomotic leakage was defined as a communication between the intra- and extraluminal compartments due to a defect in the integrity of the intestinal wall at the anastomosis between the colon and rectum or colon and anus[11], diagnosis through computed tomography (CT) imaging. Pleural effusion was confirmed through CT imaging to establish the diagnosis. Complications were graded by the Clavien-Dindo classification[12].

Cadaver specimens

Ten female cadavers were dissected in the anatomy laboratory of Wenzhou Medical University, which had been donated to the Department of Anatomy following ethical guidelines. The cadavers underwent arterial perfusion with 8% formalin and preservation with 30% alcohol. The corpses were well-preserved, without tissue decay and structural damage. All female cadavers were sourced from young adult females without a history of pelvic diseases. After separating the pelvis from the body, the pelvises were cut in the midsagittal position to expose the rectum and vagina. The pelvises were divided into two to show the rectum and vagina. After clearly exposing the rectal and vaginal structures, a skilled colorectal surgeon and anatomist performed the subsequent operations in accordance with the two different operation procedures of TME, on the same pelvis. At first, the peritoneum was cut at the lowest point of peritoneal reflection and entered the plane to mobilize as the procedure of the experimental group. Then, the surgeon incised the peritoneum at approximately 0.5–1 cm above the peritoneal reflection and started the separation as the procedure of the control group. Photos and records were taken during the dissection.

Pathological histochemistry

A pathologist participated in and supervised the pathological research. We separated the rectovaginal tissue from the other half of the complete pelvis and preserved it in 8% formalin. Then, the remaining tissue was used for pathology and immunohistochemistry analysis. Sections were stained with hematoxylin-eosin and observed under an electron microscope with a magnification of ten times. Microscopic examination of the rectal and vaginal structures enabled us to determine the presence of Denonvilliers' fascia. Immunohistochemical and pathological studies were completed by the Pathology Department of Wenzhou Medical University.

Stastical analysis

IBM SPSS Statistics 25 software was used for the analysis of clinical data, Two-sided $P < 0.05$ indicated significance. Continuous variables with normal distribution were summarized as mean (SD) and two independent samples *t*-test was used for the statistics. For continuous variables with non-normal distribution were summarized as median (IQR) and Mann-Whitney U test were used for the statistics. Categorical variables were summarized as numbers (percentages) and analyzed using the chi-square test, while the Mann-Whitney U test was used for the Statistics of ordered classification variables. The statistical review of this study was performed by a biomedical statistician.

RESULTS

Video review and clinical data

Seventy-seven patients who met the criteria were included in our study, with 35 in the experimental group and 42 in the control group. There were no significant differences in the general information between the two groups. The patients' general information is summarized in Table 1.

In the experimental group, the peritoneum was cut at the lowest point of the peritoneal reflection to enter the anterior rectal space (as shown in Figure 1), in which the anterior rectal wall can be easily dissociated from the posterior wall of the vagina. The rectum was light yellow due to the light-yellow adipose tissue surrounded by the mesorectal fascia. Blood vessels could be seen in the mesorectum, and the mesorectum was dissected completely. It can be dissociated through blunt separation combined with sharp separation. In this process, the operation field could remain bloodless, and the vaginal structure and rectal structure were easy to distinguish from each other. The mesorectal fascia and vaginal were complete after dissection, and no Denonvilliers' fascia-like structure was present between them. In contrast, the control group cut the peritoneum at approximately 0.5–1 cm above the peritoneal reflection and freed the rectal wall between the vaginal muscular and the vaginal adventitia (as shown in Figure 2). Although a structure similar to Denonvilliers' fascia was found, it was closely connected to the vaginal muscular and could only be torn off through sharp separation. The muscular structure of the vagina was revealed after the operation, which often caused bleeding. Furthermore, the vaginal structure was no longer intact after dissection since the vaginal adventitia was separated from the muscular layer. After reviewing all the surgical procedures, finding an obvious membrane structure between the mesorectal fascia and vaginal adventitia in females was difficult. The fascial structure that we found during the operation was the vaginal adventitia, while the so-called female Denonvilliers' fascia does not exist.

Compared with the control group, the experimental group had less intraoperative bleeding [22.5 (19.5-50) mL *vs* 17 (5-20) mL; $P = 0.01$], and shorter length of hospitalization [9 (7-11.25) d *vs* 7 (6-10) d; $P = 0.03$]. Although the incidence of postoperative complications was lower than that of the control group, the results were not statistically significant. No deaths occurred in either group in the first 30 d after surgery. All Pathological specimens' Circumferential Resection Margins (CRM) were negative after the operation. Statistical result is summarized in Table 2.

Gross anatomy

As depicted in Figure 3A, the layers of the rectum and vagina were displayed, and the main structures could be distinguished. The vaginal muscular layer was brown, and the mucosal layer was gray. The mucosa of the rectum was yellowish, the submucosa was white, and the muscular layer was brown. However, distinguishing between the vaginal adventitia and the mesorectal fascia with the naked eye was difficult.

The dissociation process of the experimental group proceeded seamlessly. As depicted in Figure 3B, the mobilization plane traversed the interface between the vaginal adventitia and the fascia of the mesorectum. A discernible space between the vaginal adventitia and the mesorectal fascia was observed, which could be adroitly separated through blunt dissection. The vaginal adventitia and the mesorectal fascia were generally white without fascia-like tissues or blood vessels between them. Occasionally, blood vessels were visible beneath the vaginal adventitia. The boundary between the muscular layer and the adventitia was clear, with the muscular layer appearing dark and the adventitia appearing white.

As shown in Figure 3C, the mobilization plane entered the plane between the vaginal adventitia and the muscular layer by the procedure of the control group. When the vaginal adventitia was separated from the muscular layer, we found that the attachment between the vaginal adventitia and the muscular layer was stronger than the attachment between the vaginal adventitia and the mesorectal fascia, which could not be easily mobilized by blunt separation and can only be mobilized by sharp separation. After dissociation, the vaginal adventitia could be seen to be a single-layer fascia-like structure with a white color that was different and easy to distinguish from the dark muscle layer. No distinct or separate Denonvilliers' fascia was identified. At the same time, after the vaginal adventitia was forcibly torn off from the muscular layer, the muscular layer structure was damaged. Some residual muscle fiber tissue could be seen on the vaginal adventitia.

Table 1 General information of the patient

	Control group (*n* = 42)	Experimental group (*n* = 35)	*P* value
Height, mean (SD), cm	157.64 (6.03)	157.17 (5.29)	0.72
Weight, mean (SD), kg	57.02 (8.82)	57.37 (10.22)	0.87
BSA, mean (SD)	1.62 (0.14)	1.67 (0.15)	0.17
Age, mean (SD), y	60.50 (10.94)	63.86 (12.77)	0.22
Preoperative chemoradiotherapy	6 (14.3)	4 (11.4)	0.98

BSA: Body surface area.

Table 2 Postoperative information of the patient

	Control group (*n* = 42)	Experimental group (*n* = 35)	*P* value
Operation time, mean (SD), min	233.14 (75.12)	228.66 (80.32)	0.8
IB, median (IQR), mL	22.5 (19.5-50)	17 (5-20)	0.01
NRL, median (IQR)	13.5 (10-16.5)	15 (13-19)	0.24
Hospital stays, median (IQR), days	9 (7-11.25)	7 (6-10)	0.03
Pathology stage			0.52
I	21 (50.0)	15 (42.8)	
II	10 (23.8)	9 (25.7)	
III	11 (26.2)	11 (31.5)	
T			0.62
1	12 (28.6)	8 (22.9)	
2	12 (28.6)	12 (34.3)	
3	15 (35.7)	10 (28.6)	
4	3 (7.1)	5 (14.3)	
N			0.75
0	32 (76.2)	24 (68.6)	
1	8 (19.0)	9 (25.7)	
2	2 (4.8)	2 (5.7)	
CDC			0.84
I	8 (19.0)	3 (8.6)	
II	2 (4.8)	1 (2.9)	
Postoperative complications	10 (23.81)	4 (11.43)	0.16
Postoperative bleeding	1	0	
Anastomotic leakage	3	2	
Other complications	8	4	

CDC: Clavien-Dindo classification; IB: Intraoperative bleeding; IQR: Inter-quartile range; NRL: Number of retrieved lymph nodes.

Pathological histochemistry

As shown in Figure 4, the rectal and vaginal tissues showed clear stratification: The rectum was divided into the mucosa, submucosa, inner ring muscle layer, outer longitudinal muscle layer, mesorectum, and the mesorectal fascia surrounding the mesorectum. The vaginal wall was divided into three layers: Mucosa, muscular, and adventitia layers. The adventitia layer was composed of dense connective tissue with scattered loose connective tissue among it. A gap was present between the mesorectal fascia and the vaginal adventitia. Numerous loose connective tissue, but no obvious fascia-like structures, were

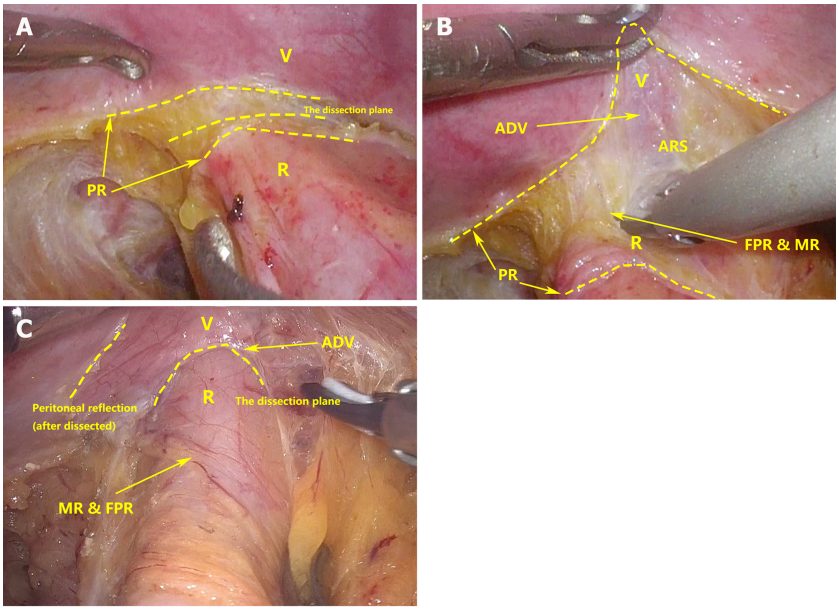

DOI: 10.3748/wjg.v29.i19.2992 **Copyright** ©The Author(s) 2023.

Figure 1 The procedure of the experimental group. A: The peritoneum was cut at the lowest point of the peritoneal reflection to enter the anterior rectal space; B: After the incision of the peritoneal reflection, a space can be seen, in which can we easily free the anterior rectal wall. This space is considered the rectovaginal space; C: No other fascial structure was present between the fascia propria of the rectum and the adventitia of the vagina, and these two fascial structures could be pushed away from each other by an ultrasonic knife through blunt separation. ADV: Adventitia of the vagina; FPR: Fascia propria of the rectum; MR: Mesorectum; PR: Peritoneal reflection; R: Rectum; V: Vagina; ARS: Anterior rectal space.

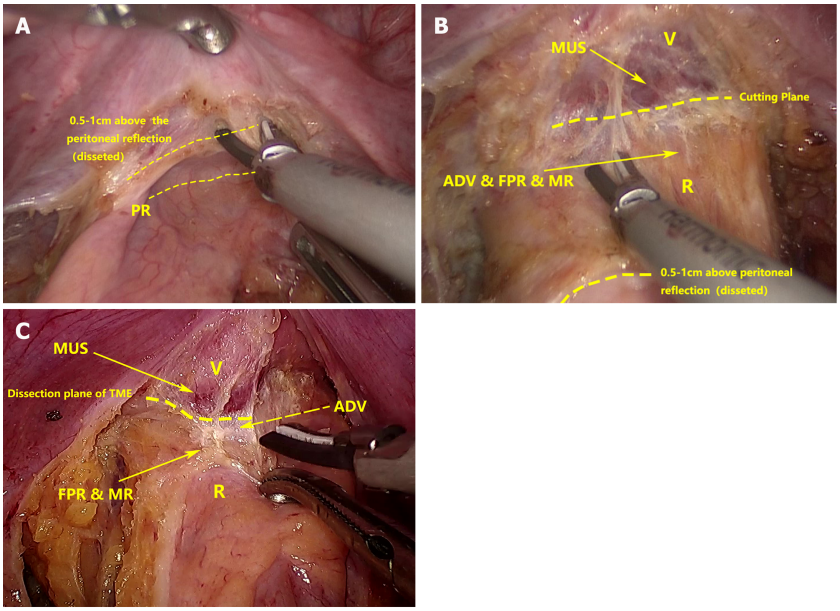

DOI: 10.3748/wjg.v29.i19.2992 **Copyright** ©The Author(s) 2023.

Figure 2 The procedure of the control group. A: The peritoneum was cut 0.5-1 cm above the peritoneal reflection. The peritoneal reflection was slightly white, and its texture was different from the texture of other structures during the operation; B: The cutting plane was between the vaginal muscle layer and the adventitia. The vaginal adventitia was closely adherent to the muscle layer; C: Bleeding occurred after stripping the vaginal adventitia from the muscle, and hemostasis was performed. ADV: Adventitia of the vagina; FPR: Fascia propria of the rectum; MR: Mesorectum; MUS: Muscle; PR: Peritoneal reflection; R: Rectum; V: Vagina.

present inside this gap. Occasionally, some scattered dense connective tissue and fragment-like fascial structure could be seen but were difficult to identify as fascial structures.

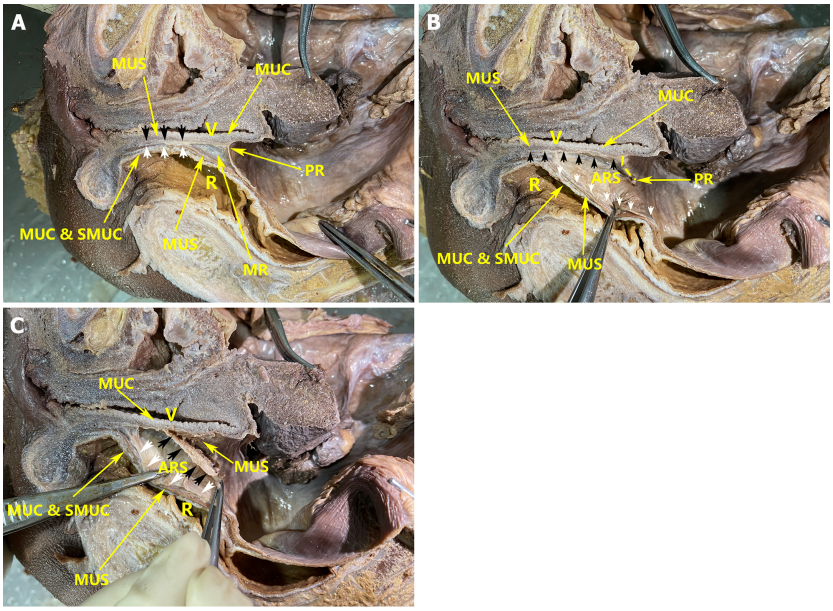

DOI: 10.3748/wjg.v29.i19.2992

Figure 3 Gross anatomy. A: Observation of the female pelvis; B: The procedure of the experimental group; C: The procedure of the control group. Black arrow: Adventitia of the vagina; white arrow: Fascia propria of the rectum. ARS: Anterior rectal space; MR: Mesorectum; MUC: Mucosa; MUS: Muscle; PR: Peritoneal reflection; R: Rectum; SMUC: Submucosa; V: Vagina; FPR: Fascia propria of the rectum; MR: Mesorectum.

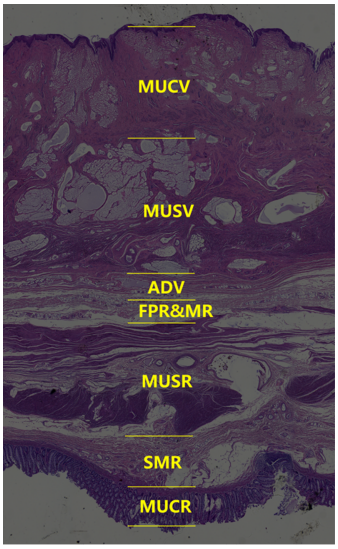

DOI: 10.3748/wjg.v29.i19.2992

Figure 4 Pathological section of the rectovaginal structure. Pathological section showing the absence of an obvious fascia-like structure between the fascia propria of the rectum and the adventitia of the vagina. ADV: Adventitia of the vagina; FPR & MR: Fascia propria of the rectum and mesorectum; MUCV: Mucosa of the vagina; MUSR: Muscle of the rectum; MUSV: Muscle of the vagina; SMR: Submucosa of the rectum; MUCR: Mucosa of the rectum.

DISCUSSION

In 1836, after observing the anatomy of the male pelvis, Denonvillier found a single-layer membrane-like structure between the rectum and prostate that he called the "prostatoperitoneal membrane"[13]. Later, in memory of Denonvillier, people called this fascial structure Denonvilliers' fascia, which is considered a structure that starts from the peritoneal reflection and ends at the perineum. The prostate and seminal vesicle glands are located in front of this structure. The rectum locates behind it, and vascular and nerve bundles are located on both sides of this structure. Undoubtedly, colorectal doctors have reached a consensus on the existence of Denonvilliers' fascia in the male pelvis. However, whether this fascia exists in females remains highly debated. Denonvillier elaborated on this structure by dissecting the male pelvis but did not mention its relevance in females. Later researchers also encountered many contradictions and disputes regarding the description of this structure.

In 1969, after dissecting 143 bodies, Milley and Nichols[14] confirmed the presence of a rectovaginal septum. They found a rectovaginal septum in 23 of 25 adult females and all dissected female infants. Despite the individual differences, the existence of this structure appears to be unaffected by age and hormones. At the same time, a close adhesion existed between this diaphragm and the fascia surrounding the vagina, they believed that this close adhesion may be a major reason why some anatomists deny the existence of the vaginal rectal septum[14].

Zhai *et al*[5] proved the existence of the female rectovaginal septum by studying the whole pelvic viscera embedded in celloidin (25 female pelvic visceral organs). He pointed out that the rectovaginal septum could be divided into two layers: Denonvilliers' fascia and the mesorectal fascia from the traditional point of view. Denonvilliers' fascia tightly surrounds the posterior and lateral walls of the vagina, and the Denonvilliers' fascia and the mesorectal fascia are not attached to the rectouterine pouch. Instead, they extend upward along the peritoneum. In this anatomy, the anterior layer integrates into the uterus, and the posterior layer gradually thins and disappears. The rectovaginal septum plays an important role in preventing the spread of malignant tumors[5].

Bertrand *et al*[6] found that Denonvilliers' fascia is an independent structure of the mesorectal fascia and the cervix as well as the vagina by studying female fetuses' anatomy[6]. However, they were likely to mistake the vaginal adventitia for Denonvilliers' fascia (rectovaginal septum). In our study on adult females, we only found loose connective tissue in the plane between the mesorectal fascia and the adventitia of the vagina. No other fascia-like structures were found between these structures. Due to the absence of other structures in this plane, we were able to easily separate the rectum and vagina without causing damage to the vaginal structure during the complete removal of the mesorectum. And the vaginal adventitia seems like Denonvilliers' fascia if it was separated from the vaginal muscle. Recognizing the adventitia of the vagina as Denonvilliers' fascia and forcefully separating it from the muscular layer could often cause bleeding.

At the same time, some people proposed the opposite opinion. Zhang *et al*[15] found only some membrane-like fascial fragments in the adipose tissue between the rectum and the vagina in the frozen sections of the corpses of three adult females aged 58–86 years old. They believed that previous studies may have regarded these fascial fragments as Denonvilliers' fascia; however, considering the age limit of their samples, their results still need further research[15]. An analysis of surgical and pathological samples from three females showed that the so-called fascia and vaginal wall had the same histological manifestations under pathology and were not distinguishable[16]. Therefore, Farrell *et al*[16] believed that the so-called fascia was an artificial surgical separation from the vagina that occurred when separating the vagina and surrounding organs[16]. In 2005, through the analysis of four female anatomical samples, Kleeman *et al*[17] also obtained a similar conclusion, that is, no fascia exists between the rectum and vagina. The rectovaginal septum used to repair the rectocele is an artificial surgical separation of tears from the vagina[17]. Meanwhile, after dissecting twenty-five female cadavers, García-Gausí *et al*[7] came to the same conclusion as Farrell *et al*[16]: That an independent rectovaginal septum could only be produced by tearing the vaginal adventitia. They found only a layer of loose connective tissue between the vagina and the rectum[7]. This is consistent with the findings of our study.

Based on the anatomy of four cadavers, Fang proposed that for surgery in early rectal cancer, mobilizing the rectum behind Denonvilliers' fascia can not only ensure the integrity of the mesorectum but also control related postoperative complications[18]. Although his viewpoint on whether Denonvilliers' fascia exists in females is different from ours, his conclusion on the female surgical approach is similar to ours. Simultaneously, some researchers have discovered that in the case of early rectal cancer, mobilizing the rectal wall behind Denonvilliers' fascia results in similar 5-year local recurrence rates as the traditional TME approach, while also reducing the incidence of complications [19]. Nevertheless, we believe that these researchers may have misidentified the vaginal adventitia as Denonvilliers' fascia in female patients.

We found that in females, the plane between the vaginal adventitia and the mesorectal fascia is suitable for rectal cancer surgery. By dissecting the rectum along the plane between the mesorectal fascia and the vaginal adventitia, not only can the risk of bleeding and damage to physiological structures be minimized, resulting in a faster recovery and shorter hospitalization, but it can also guarantee complete removal of the mesorectum and negative CRM status. Thus, this plane is the optimal plane in female patients with rectal cancer undergoing TME. Our research focused on the macro- and microlevels, combined with clinical data to explore the anatomy of the rectum and the vagina from multiple angles to obtain a highly scientific conclusion. Not only did we provide stronger evidence supporting the absence of Denonvilliers' fascia as an independent structure in females, but we also discovered that the anterior rectal space is the optimal plane to mobilize the anterior rectal wall for female patients undergoing TME.

However, as this study was retrospective and had a limited sample size, the observed differences in complication rates between the two procedures were not statistically significant. Future studies with larger sample sizes may yield more conclusive results. Additionally, due to the relatively short follow-up period since the patients' surgeries, long-term prognostic and sexual function outcomes have not been thoroughly investigated. Nonetheless, we intend to address this limitation in our subsequent studies.

CONCLUSION

In adult females, Denonvilliers' fascia is absent, we could only find loose connective tissue between the mesorectal fascia and vaginal adventitia. The vaginal adventitia is tightly adherent to the vaginal muscular layer and was difficult to separate from the muscle layer. By incising the peritoneum at the lowest point of peritoneal reflection, a plane between the mesorectal fascia and vaginal adventitia can be accessed. Mobilizing the anterior rectal wall in this plane could not only ensures the integrity of the mesorectum but also reduces intraoperative bleeding and hospital stay. Dissecting in this plane follows a natural avascular space without damaging the vaginal structure and simplifies the surgical procedure. Therefore, this is the optimal plane for mobilizing the anterior rectal wall for female patients undergoing TME procedures.

ARTICLE HIGHLIGHTS

Research background

Currently, there are no comprehensive descriptions available regarding the approach for dissecting the anterior wall of the female rectum. Many surgeons encounter intraoperative bleeding due to the lack of an appropriate dissection plane.

Research motivation

The surgical approach for mobilizing the anterior rectal wall during total mesorectal excision surgery in female patients remains controversial. However, with a more profound comprehension of the pelvic anatomy, we can identify the avascular plane, reducing intraoperative bleeding and preventing harm to physiological structures.

Research objectives

We aim to gain a better understanding of the female pelvic anatomy to identify an optimal approach for dissecting the anterior wall of the rectum. This will facilitate improved surgical outcomes for female patients with middle or low rectal cancer.

Research methods

Firstly, we retrospectively grouped patients based on different approaches after reviewing surgical videos. Clinical information was collected and pre-and post-operative data were compared, along with reviewing surgical videos to understand the anatomy and intraoperative situation. Subsequently, the female pelvic structure was studied through cadaveric dissection and histological sections.

Research results

We discovered that opening the peritoneum at the lowest point of peritoneal reflection allows access to the plane between the vaginal adventitia and mesorectal fascia. Opening the peritoneum 0.5-1 cm above the peritoneal reflection enters another plane located between the vaginal adventitia and vaginal muscle layer. The first approach has lower intraoperative bleeding and shorter hospital stay compared to the second approach. Neither cadaveric dissection nor pathological examination revealed the existence of Denonvilliers' fascia. Only loose connective tissue exists between the rectosacral fascia and the vaginal adventitia.

Research conclusions

Denonvilliers' fascia is absent in females. The plane amidst the mesorectal fascia and vaginal adventitia is the optimal surgical plane to mobilize the anterior rectal wall for female patients.

Research perspectives

In future studies, we will explore the long-term prognosis of the two approaches for women, as well as the impact on postoperative sexual and vaginal function.

ACKNOWLEDGEMENTS

Thanks to Xin-Yu Li, Yang-Yang Li, and Xin-Dong Yang's great contributions to our work.

FOOTNOTES

Author contributions: Li ST contributed to the study conceptualization and completed the dissection of cadavers; Li XY, Li Y, Liang YC, Zhou YM and Li ST provide clinical data; Li XY and Li Y reviewed the surgical videos; Jin W wrote the original draft of the manuscript and made the figures; Wang WC and Jin W finished the analysis of the data; Li XY, Zhou YM, and Yang J directly accessed and verified the underlying data; Li YY finished the pathological research; Yang XD finished the biostatistics jobs; All authors critically revised and approved the final manuscript.

Supported by Huadong Medicine Joint Funds of the Zhejiang Provincial Natura Science Foundation of China, No. LHDMY22H160002.

Institutional review board statement: The study was reviewed and approved by the Ethics Committee in Clinical Research of the First Affiliated Hospital of Wenzhou Medical University Institutional Review Board, No. KY2022-R088.

Informed consent statement: All study participants, or their legal guardian, provided informed written consent prior to study enrollment.

Conflict-of-interest statement: All the authors report no relevant conflicts of interest for this article.

Data sharing statement: Technical appendix, statistical code, and dataset available from the corresponding author at lishaotang163@163.com.

Country/Territory of origin: China

ORCID number: Wei Jin 0009-0001-0925-6016; Wen-Jian Meng 0000-0002-4578-0560; You Li 0000-0002-9560-9702; Shao-Tang Li 0000-0002-5385-2472.

S-Editor: Li L
L-Editor: A
P-Editor: Cai YX

REFERENCES

1 **Heald RJ**, Husband EM, Ryall RD. The mesorectum in rectal cancer surgery--the clue to pelvic recurrence? *Br J Surg* 1982; **69**: 613-616 [PMID: 6751457 DOI: 10.1002/bjs.1800691019]
2 **Heald RJ**, Ryall RD. Recurrence and survival after total mesorectal excision for rectal cancer. *Lancet* 1986; **1**: 1479-1482 [PMID: 2425199 DOI: 10.1016/s0140-6736(86)91510-2]
3 **MacFarlane JK**, Ryall RD, Heald RJ. Mesorectal excision for rectal cancer. *Lancet* 1993; **341**: 457-460 [PMID: 8094488 DOI: 10.1016/0140-6736(93)90207-w]
4 **Heald RJ**. The 'Holy Plane' of rectal surgery. *J R Soc Med* 1988; **81**: 503-508 [PMID: 3184105 DOI: 10.1177/014107688808100904]
5 **Zhai LD**, Liu J, Li YS, Yuan W, He L. Denonvilliers' fascia in women and its relationship with the fascia propria of the rectum examined by successive slices of celloidin-embedded pelvic viscera. *Dis Colon Rectum* 2009; **52**: 1564-1571 [PMID: 19690483 DOI: 10.1007/DCR.0b013e3181a8f75c]
6 **Bertrand MM**, Alsaid B, Droupy S, Benoit G, Prudhomme M. Biomechanical origin of the Denonvilliers' fascia. *Surg Radiol Anat* 2014; **36**: 71-78 [PMID: 23732391 DOI: 10.1007/s00276-013-1142-0]
7 **García-Gausí M**, García-Armengol J, Mulas Fernández C, Pellino G, Roig JV, García-Granero A, Pla-Marti V, Martínez-Soriano F. Surgical Anatomy of the Rectovaginal Space: Does a Standalone Rectovaginal Septum or Denonvilliers Fascia Exist in Women? *Dis Colon Rectum* 2021; **64**: 576-582 [PMID: 33939388 DOI: 10.1097/DCR.0000000000001912]
8 **Stevenson AR**, Solomon MJ, Lumley JW, Hewett P, Clouston AD, Gebski VJ, Davies L, Wilson K, Hague W, Simes J; ALaCaRT Investigators. Effect of Laparoscopic-Assisted Resection *vs* Open Resection on Pathological Outcomes in Rectal Cancer: The ALaCaRT Randomized Clinical Trial. *JAMA* 2015; **314**: 1356-1363 [PMID: 26441180 DOI: 10.1001/jama.2015.12009]
9 **Fleshman J**, Branda ME, Sargent DJ, Boller AM, George VV, Abbas MA, Peters WR Jr, Maun DC, Chang GJ, Herline A, Fichera A, Mutch MG, Wexner SD, Whiteford MH, Marks J, Birnbaum E, Margolin DA, Larson DW, Marcello PW, Posner MC, Read TE, Monson JRT, Wren SM, Pisters PWT, Nelson H. Disease-free Survival and Local Recurrence for Laparoscopic Resection Compared With Open Resection of Stage II to III Rectal Cancer: Follow-up Results of the ACOSOG Z6051 Randomized Controlled Trial. *Ann Surg* 2019; **269**: 589-595 [PMID: 30080730 DOI: 10.1097/SLA.0000000000003002]

10 **Fleshman J**, Branda M, Sargent DJ, Boller AM, George V, Abbas M, Peters WR Jr, Maun D, Chang G, Herline A, Fichera A, Mutch M, Wexner S, Whiteford M, Marks J, Birnbaum E, Margolin D, Larson D, Marcello P, Posner M, Read T, Monson J, Wren SM, Pisters PW, Nelson H. Effect of Laparoscopic-Assisted Resection *vs* Open Resection of Stage II or III Rectal Cancer on Pathologic Outcomes: The ACOSOG Z6051 Randomized Clinical Trial. *JAMA* 2015; **314**: 1346-1355 [PMID: 26441179 DOI: 10.1001/jama.2015.10529]

11 **Rahbari NN**, Weitz J, Hohenberger W, Heald RJ, Moran B, Ulrich A, Holm T, Wong WD, Tiret E, Moriya Y, Laurberg S, den Dulk M, van de Velde C, Büchler MW. Definition and grading of anastomotic leakage following anterior resection of the rectum: a proposal by the International Study Group of Rectal Cancer. *Surgery* 2010; **147**: 339-351 [PMID: 20004450 DOI: 10.1016/j.surg.2009.10.012]

12 **Dindo D**, Demartines N, Clavien PA. Classification of surgical complications: a new proposal with evaluation in a cohort of 6336 patients and results of a survey. *Ann Surg* 2004; **240**: 205-213 [PMID: 15273542 DOI: 10.1097/01.sla.0000133083.54934.ae]

13 **Denonvilliers C**. Anatomie du perinee. *Bull Soc Anat Paris* 1836; **10**: 105-107

14 **Milley PS**, Nichols DH. A correlative investigation of the human rectovaginal septum. *Anat Rec* 1969; **163**: 443-451 [PMID: 5774728 DOI: 10.1002/ar.1091630307]

15 **Zhang M**, Kaw A, Chapuis PH, Bokey L. Does Denonvilliers' fascia exist in women? *Am J Obstet Gynecol* 2016; **214**: 663-664 [PMID: 26767795 DOI: 10.1016/j.ajog.2015.12.057]

16 **Farrell SA**, Dempsey T, Geldenhuys L. Histologic examination of "fascia" used in colporrhaphy. *Obstet Gynecol* 2001; **98**: 794-798 [PMID: 11704171 DOI: 10.1016/s0029-7844(01)01533-2]

17 **Kleeman SD**, Westermann C, Karram MM. Rectoceles and the anatomy of the posteriorvaginal wall: revisited. *Am J Obstet Gynecol* 2005; **193**: 2050-2055 [PMID: 16325614 DOI: 10.1016/j.ajog.2005.07.096]

18 **Fang J**, Zheng Z, Wei H. Reconsideration of the Anterior Surgical Plane of Total Mesorectal Excision for Rectal Cancer. *Dis Colon Rectum* 2019; **62**: 639-641 [PMID: 30964796 DOI: 10.1097/DCR.0000000000001358]

19 **Killingback M**, Barron P, Dent OF. Local recurrence after curative resection of cancer of the rectum without total mesorectal excision. *Dis Colon Rectum* 2001; **44**: 473-83; discussion 483 [PMID: 11330574 DOI: 10.1007/BF02234317]

World Journal of Gastroenterology

Submit a Manuscript: https://www.f6publishing.com

World J Gastroenterol 2023 May 21; 29(19): 3003-3012

DOI: 10.3748/wjg.v29.i19.3003

ISSN 1007-9327 (print) ISSN 2219-2840 (online)

ORIGINAL ARTICLE

Retrospective Study

Association of vitamin D and polymorphisms of its receptor with antiviral therapy in pregnant women with hepatitis B

Rui Wang, Xia Zhu, Xuan Zhang, Huan Liu, Yu-Lin Ji, Yong-Hua Chen

Specialty type: Gastroenterology and hepatology

Provenance and peer review: Invited article; Externally peer reviewed.

Peer-review model: Single blind

Peer-review report's scientific quality classification

Grade A (Excellent): 0
Grade B (Very good): B, B
Grade C (Good): 0
Grade D (Fair): 0
Grade E (Poor): 0

P-Reviewer: Dabla PK, India; Shahid M, Pakistan

Received: February 17, 2023
Peer-review started: February 17, 2023
First decision: March 24, 2023
Revised: March 28, 2023
Accepted: April 24, 2023
Article in press: April 24, 2023
Published online: May 21, 2023

Rui Wang, Yong-Hua Chen, Division of Pancreatic Surgery, Department of General Surgery, West China Hospital of Sichuan University, Chengdu 610041, Sichuan Province, China

Xia Zhu, Huan Liu, Center of Infectious Diseases, West China Hospital of Sichuan University, Chengdu 610041, Sichuan Province, China

Xuan Zhang, Yu-Lin Ji, Department of Respiratory and Critical Care Medicine, West China Hospital of Sichuan University, Chengdu 610041, Sichuan Province, China

Corresponding author: Yong-Hua Chen, MD, PhD, Associate Professor, Division of Pancreatic Surgery, Department of General Surgery, West China Hospital of Sichuan University, No. 37 Guoxue Alley, Wuhou District, Chengdu 610041, Sichuan Province, China. chenyonghua2007@163.com

Abstract

BACKGROUND

The interruption of mother-to-child transmission (MTCT) is considered important to decrease the individual and population morbidity of hepatitis B virus (HBV) infection as well as the global burden of hepatitis B. Serum vitamin D (VD) is associated with hepatitis B.

AIM

To assess whether baseline VD levels and single nucleotide polymorphisms of the VD receptor gene (VDR SNPs) are associated with the efficacy of tenofovir disoproxil fumarate (TDF) in the prevention of MTCT in pregnant women with high HBV viral loads.

METHODS

Thirty-eight pregnant women who were at high risk for MTCT of HBV (those with an HBV DNA level ≥ 2×10^5 IU/mL during 12-24 wk of gestation) receiving antiviral therapy of TDF between June 1, 2019 and June 30, 2021 in Mianyang were included in this retrospective study. The women received 300 mg TDF once daily from gestational weeks 24-28 until 3 mo after delivery. To further characterize the clinical relevance of maternal serum HBV DNA levels, we stratified patients according to HBV DNA level as follows: Those with levels < 2×10^5 (full responder group) *vs* those levels ≥ 2×10^5 IU/mL (partial responder group) at delivery. Serum levels of 25-hydroxyvitamin D [25(OH)D], liver function markers, virological parameters, VDR SNPs and other clinical parameters were collected to

analyze their association with the efficacy of TDF. The Mann-Whitney *U* test or t test was used to analyze the serum levels of 25(OH)D in different groups. Multiple linear regressions were utilized to analyze the determinants of the maternal HBV DNA level at delivery. Univariate and multivariate logistic regression analyses were employed to explore the association of targeted antiviral effects with various characteristics at baseline and delivery.

RESULTS

A total of 38 pregnant women in Mianyang City at high risk for MTCT of HBV were enrolled in the study. The MTCT rate was 0%. No mother achieved hepatitis B e antigen or hepatitis B surface antigen (HBsAg) clearance at delivery. Twenty-three (60.5%) participants were full responders, and 15 (39.5%) participants were partial responders according to antiviral efficacy. The present study showed that a high percentage (76.3%) of pregnant women with high HBV viral loads had deficient (< 20 ng/mL) or insufficient (≥ 20 but < 31 ng/mL) VD levels. Serum 25(OH)D levels in partial responders appeared to be significantly lower than those in full responders both at baseline (25.44 ± 9.42 *vs* 17.66 ± 5.34 ng/mL, P = 0.006) and delivery (26.76 ± 8.59 *vs* 21.24 ± 6.88 ng/mL, P = 0.044). Serum 25(OH)D levels were negatively correlated with maternal HBV DNA levels [log(10) IU/mL] at delivery after TDF therapy (r = -0.345, P = 0.034). In a multiple linear regression analysis, maternal HBV DNA levels were associated with baseline maternal serum 25(OH)D levels (P < 0.0001, β = -0.446), BMI (P = 0.03, β = -0.245), baseline maternal log10 HBsAg levels (P = 0.05, β = 0.285) and cholesterol levels at delivery (P = 0.015, β = 0.341). Multivariate logistic regression analysis showed that baseline serum 25(OH)D levels (OR = 1.23, 95%CI: 1.04-1.44), maternal VDR Cdx2 TT (OR = 0.09, 95%CI: 0.01-0.88) and cholesterol levels at delivery (OR = 0.39, 95%CI: 0.17-0.87) were associated with targeted antiviral effects (maternal HBV DNA levels < 2×10^5 at delivery).

CONCLUSION

Maternal VD levels and VDR SNPs may be associated with the efficacy of antiviral therapy in pregnant women with high HBV viral loads. Future studies to evaluate the therapeutic value of VD and its analogs in reducing the MTCT of HBV may be justified.

Key Words: Hepatitis B virus; Vitamin D; Vitamin D receptor polymorphism; Antiviral therapy; Pregnancy; Mother-to-child transmission

Core Tip: This retrospective study investigated the influence of vitamin D (VD) levels and single nucleotide polymorphisms of the VD receptor gene (VDR SNPs) on the efficacy of tenofovir disoproxil fumarate in preventing mother-to-child transmission in 38 pregnant women with high hepatitis B viral loads. We demonstrate a significant association between low serum levels of 25-hydroxyvitamin D and high levels of hepatitis B virus replication in pregnant women with high hepatitis B viral loads, and maternal VD levels as well as VDR SNPs may be associated with the efficacy of antiviral therapy.

Citation: Wang R, Zhu X, Zhang X, Liu H, Ji YL, Chen YH. Association of vitamin D and polymorphisms of its receptor with antiviral therapy in pregnant women with hepatitis B. *World J Gastroenterol* 2023; 29(19): 3003-3012

URL: https://www.wjgnet.com/1007-9327/full/v29/i19/3003.htm

DOI: https://dx.doi.org/10.3748/wjg.v29.i19.3003

INTRODUCTION

Hepatitis B virus (HBV) infection is a serious public health problem that causes a very large medical and economic burden worldwide. Mother-to-child transmission (MTCT) is the main route of HBV transmission, accounting for 30%-50% of chronic infections in China[1]. In particular, China is a major contributor to achieving the global goal of eliminating hepatitis B as a threat to public health by 2030[2]. The interruption of MTCT is considered important to decrease the individual and population morbidity of HBV infection as well as the global burden of hepatitis B. In recent years, Chinese scholars have continuously published and updated the management algorithm for the prevention of the MTCT of HBV, which has achieved good clinical application[3,4]. To date, the use of antiviral drugs in combination with immunoprophylaxis in pregnant women has been shown to be safe and effective in

reducing the MTCT of HBV[4].

Vitamin D (VD) is a fat-soluble steroid hormone that is widely found in systemic organs and tissues, including the brain, bones, cardiac system and immune system, and has multiple effects on human health and many diseases, including infectious diseases. In fact, VD deficiency has been detected in a variety of chronic liver diseases, including chronic viral hepatitis[5-8]. Moreover, VD deficiency is common among patients with chronic hepatitis B infection and is associated with adverse clinical outcomes[9]. Similarly, VD levels are lower in pregnant women with chronic HBV infection than in healthy pregnant women[10]. Clinical and epidemiological studies support the role of VD in inhibiting HBV infection, and this antiviral effect is widely attributed to the VD receptor (VDR)[11].

Different studies have focused on single nucleotide polymorphisms of the VDR gene (VDR SNPs) and HBV. VDR ApaI has been associated with the presence of hepatitis B surface antigen (HBsAg) and viral loads at different times[12]. In addition to its effect on viruses, VD plays an important role for the mother and fetus during pregnancy and has been associated with influencing adverse perinatal events.

However, few data are available with regard to the association of VD levels and VDR SNPs with clinical parameters and treatment outcomes in pregnant women with high HBV viral loads. The aims of our present retrospective study were to study whether baseline VD levels and VDR SNPs were associated with the efficacy of tenofovir disoproxil fumarate (TDF) in the prevention of MTCT in pregnant women with high HBV viral loads.

MATERIALS AND METHODS

Study population

This was a retrospective study. As part of "The National Science & Technology Pillar Program during the 13th Five-year Plan Period", HBsAg-positive pregnant women receiving TDF were included from Mianyang between June 1, 2019 and June 30, 2021. The present study was approved by the Institutional Review Board of the West China Hospital, Sichuan University (No. 2019-151), and informed consent was obtained from all patients before recruitment.

Pregnant women screened for HBV DNA at high risk for MTCT (HBV DNA thresholds ≥ 2×10^5 IU/mL) according to WHO recommendations during 12-24 wk of gestation and completed antiviral therapy as required were included in the study. Women received 300 mg TDF once daily from gestational weeks 24-28 until 3 mo after delivery, in addition to HBV immune globulin and three doses of HBV vaccination, including a birth dose given to the neonate. The main exclusion criteria were as follows: (1) Coinfection of syphilis, *Toxoplasma gondii*, human immunodeficiency viruses, or types of viral hepatitis other than HBV; (2) major systemic disease, including heart disease, malignant neoplasm, or renal insufficiency; (3) evidence of liver cirrhosis, hepatic decompensation and other liver diseases such as drug-induced hepatitis, autoimmune liver disease, or alcoholic liver disease; (4) evidence of congenital anomalies of the fetus; (5) antiviral treatment within a short period of time prior to treatment with TDF or failure to complete TDF antiviral therapy as required; and (6) incomplete data, including basic information, VD levels before and after treatment, VDR SNPs, virological indicators, *etc.*

Data collection and definition

The basic information of the pregnant woman including age, height, weight, season of blood sample collection and other basic information was collected. Meanwhile, maternal virological indicators, including HBsAg, hepatitis B e antigen (HBeAg) and HBV DNA, were recorded before antiviral treatment and at delivery after antiviral treatment. Moreover, common clinical parameters before antiviral treatment and at delivery after antiviral treatment including peripheral blood count, liver function, kidney function and other parameters were also collected. Laboratory tests were performed according to our previous description[13,14].

Previously collected blood samples were used to assess maternal VD levels and VDR SNPs. In particular, VD was assessed at baseline and at the time of delivery by measuring serum 25-hydroxyvitamin D [25(OH)D] levels. Serum 25(OH)D was analyzed by LCMS/MS (Agilent Technologies Inc., LCMS/MS1260-6470, CA, United States) after hexane extraction with deuterated 25(OH)D as a control as previously described[15]. Levels of VD were categorized as follows: < 20 ng/mL = deficient; ≥ 20 but < 31 ng/mL = insufficient; and ≥ 31 ng/mL = normal. Genomic DNA was isolated from blood samples (MagNA Pure Compact, Roche). VDR SNPs were assessed through a real-time PCR allelic discrimination system (LightCycler 96, Roche). We investigated the following gene SNPs: VDR: rs7975232 (ApaI)C>A, rs11568820 (Cdx2)T>C, rs2228570 (FokI)A>G, rs1544410 (BsmI)C>T, rs731236 (TaqI)A>G.

The primary outcomes were the changes in the maternal viral load (HBV DNA level) at baseline and the time of delivery. A sustained virological response was defined as an HBV DNA level lower than 2×10^5 IU/mL at delivery. We aimed to determine whether the levels of VD and VD SNPs were associated with the antiviral effects of TDF in interrupting MTCT during the peripartum period.

Statistical analysis

All statistical analyses were carried out using SPSS Version 26. Categorical variables are represented as frequencies and percentages, and continuous variables are represented as medians (interquartile ranges) or mean ± SD. The outcomes were compared between the two groups using χ^2 tests or Fisher's exact test for categorical variables and the Wilcoxon signed-rank test or Student's *t* test for continuous variables. Associations between VD and each of the baseline demographic and lab values were assessed in univariate analyses using general linear models. Univariate and multivariate logistic regression analyses were employed to explore the association of targeted antiviral effects (HBV DNA levels < 2×10^5 at delivery) with various characteristics at baseline and delivery. Factors with a P value < 0.1 in univariate analysis were considered in multivariate analysis. The statistical test was 2-sided, and a P value < 0.05 was considered statistically significant.

RESULTS

Patient characteristics

The baseline characteristics, laboratory data, and VDR SNPs of the patients are presented in Table 1. No mother achieved HBeAg or HBsAg clearance at delivery. The decrease in HBV DNA levels from baseline to delivery was significant (P < 0.001). A total of 100% of the infants had negative HBsAg and undetectable HBV DNA levels at delivery; thus, the MTCT rate was 0%. To further characterize the clinical relevance of maternal serum HBV DNA levels, we stratified patients according to serum HBV DNA levels as follows: those with levels < 2×10^5 (full responder group) *vs* those with levels ≥ 2×10^5 IU/mL (partial responder group) at delivery. Mothers with serum HBV DNA viral loads below this threshold are generally considered low risk for MTCT. Twenty-three (60.5%) participants were full responders, and 15 (39.5%) participants were partial responders according to antiviral efficacy. Full and partial responders were similar in age (29.09 *vs* 28.73 years) and body mass index (BMI) (23.15 *vs* 21.42 kg/m^2).

In the virological indicators related to HBV, there was no significant difference in the HBsAg log10 and HBeAg log10 values between the two groups both at baseline and delivery. The serum HBV DNA concentration was not significantly different between the two groups at baseline, but the serum HBV DNA concentration of full responders was significantly lower than that of partial responders at delivery after antiviral treatment [log10, 3.61 (2.88, 4.46) *vs* 7.41 (5.79, 7.9), P < 0.0001].

For the laboratory test results, there were no significant differences between full and partial responders in most of the main laboratory indices before and after antiviral therapy, including hemoglobin, white blood cell count, platelets, neutrophils, lymphocytes, total bilirubin, albumin, alanine aminotransferase, triglycerides, creatinine, alkaline phosphatase, and gamma-glutamyl transferase. However, cholesterol levels were lower in complete responders than in partial responders at delivery after treatment (4.87 ± 0.79 *vs* 5.56 ± 0.96 mg/dL, P = 0.001), but there was no significant difference at baseline.

Serum 25(OH)D levels

There was no VD or multivitamin supplementation between baseline and delivery. The mean baseline serum 25(OH)D level of the entire cohort was similar to the serum 25(OH)D level at delivery, with no significant difference (22.37 ± 8.85 *vs* 24.58 ± 8.32 ng/mL, P = 0.139). Of the 38 patients in the entire cohort, 18 (47.4%), 11 (28.9%), and 9 (23.7%) had severe VD deficiency, VD insufficiency or normal serum VD levels, respectively.

In the absence of significant seasonal differences for the collected blood samples, VD deficiency and insufficiency were highly prevalent in partial responders (73.3%, 20% *vs* 30.4%, 34.8%, P = 0.021). Overall, the serum 25-hydroxyvitamin D3 [25(OH)D3] level in partial responders appeared to be significantly lower than that in full responders both at baseline (25.44 ± 9.42 *vs* 17.66 ± 5.34 ng/mL, P = 0.006) and delivery (26.76 ± 8.59 *vs* 21.24 ± 6.88 ng/mL, P = 0.044). In addition, the VDR SNP assay showed no significant difference between full and partial responders based on VDR SNPs, including VDR Cdx2, Bsm1, Fokl, Taq1 and Apa1.

Relationship between baseline serum 25(OH)D levels and virological parameters

Maternal HBsAg serum levels were not associated with serum 25(OH)D levels (data not shown). Interestingly, maternal Log10 HBV DNA levels at delivery and baseline serum 25(OH)D levels showed a significant, inverse correlation (P = 0.034, Figure 1). Therefore, we performed multiple linear regression analysis of the determinants of maternal HBV DNA levels at delivery. In both univariate and multivariate analyses, baseline maternal serum 25(OH)D levels were the strongest determinant of low maternal HBV DNA levels (P = 0.034 and < 0.0001, respectively; Table 2), together with BMI, baseline maternal log10 HBsAg levels and cholesterol levels at delivery.

We further performed univariate and multivariate regression analyses to characterize the relationship between the serum level of 25(OH)D and targeted antiviral effects. The baseline serum 25(OH)D level

Table 1 Baseline characteristics, laboratory data, and single nucleotide polymorphisms of the vitamin D receptor gene of patients included in the study

	Before treatment initiation			At delivery after treatment		
	Full responders (*n* = 23)	Partial responders (*n* = 15)	*P* value	Full responders (*n* = 23)	Partial responders (*n* = 15)	*P* value
Age, yr, mean ± SD	29.09 ± 3.55	28.73 ± 3.01	0.75	NA	NA	
BMI, kg/m^2, mean ± SD	23.15 ± 3.33	21.42 ± 3.61	0.14	NA	NA	
Season of blood draw			0.552			0.311
Winter or spring	10 (43.5%)	8 (53.3%)		16 (69.6%)	8 (53.3%)	
Summer or autumn	13 (56.5%)	7 (46.7%)		7 (30.4%)	7 (46.7%)	
HBsAg log10 IU/mL mean (IQR)	4.33 (3.73, 4.52)	4.36 (4.1, 4.72)	0.663	4.11 (2.56, 5.44)	4.33 (3.95, 4.56)	0.256
HBeAg log10 IU/mL mean (IQR)	3.16 (2.66, 3.2)	3.16 (3.12, 3.19)	0.928	3.18 (2.85, 3.19)	6.75 (6.21, 8.49)	0.510
HBV DNA, log10 mean (IQR)	8.06 (7.61, 8.44)	8.09 (7.53, 8.16)	0.56	3.61 (2.88, 4.46)	7.41 (5.79, 7.9)	< 0.0001
Vitamin D, ng/mL, mean ± SD	25.44 ± 9.42	17.66 ± 5.34	0.006	26.76 ± 8.59	21.24 ± 6.88	0.044
≥ 30	8 (34.8%)	1 (6.7%)	0.021	10 (43.5%)	2 (13.3%)	0.127
20-30	8 (34.8%)	3 (20%)		6 (26.1%)	6 (40%)	
< 20	7 (30.4%)	11 (73.3%)		7 (30.4%)	7 (46.7%)	
Hemoglobin, g/dL, mean ± SD	113.78 ± 9.29	115.47 ± 8.98	0.583	114.3 ± 12.78	118 ± 10.17	0.353
WBC count, × 10^6/μL, mean ± SD	7.83 ± 1.54	8.61 ± 2.26	0.282	7.63 ± 1.77	7.7 ± 2.17	0.918
Platelet, × 10^3/μL, mean ± SD	149.52 ± 56.73	155.6 ± 53.01	0.742	137.17 ± 53.92	149.4 ± 56.21	0.506
Neutrophil, mean ± SD	5.78 ± 1.38	6.51 ± 2.0	0.289	5.33 ± 1.62	5.53 ± 1.96	0.731
Lymphocyte, mean ± SD	1.46 ± 0.4	1.49 ± 0.49	0.823	1.63 ± 1.14	1.61 ± 0.49	0.964
Total bilirubin, mg/dL, mean ± SD	14.73 ± 3.24	13.61 ± 3.09	0.299	14.97 ± 4.15	17.13 ± 4.23	0.128
Albumin, g/dL, mean ± SD	39.21 ± 2.36	39.93 ± 2.28	0.355	26.42 ± 3.19	37.33 ± 3.68	0.698
ALT, U/L, mean (IQR)	22 (19, 28)	21 (15, 32)	0.891	22 (18, 30)	21 (17, 36)	0.893
Triglyceride, mg/dL, mean (IQR)	1.74 (1.59, 2.38)	1.58 (1.34, 1.79)	0.189	3.06 (2.41, 3.67)	2.52 (2.03, 3.21)	0.131
Cholesterol, mg/dL, mean ± SD	5.33 ± 0.85	5.7 ± 1.97	0.347	4.87 ± 0.79	5.56 ± 0.96	0.001
Creatinine, mg/dL, mean (IQR)	43 (38, 49)	43 (39, 45)	0.951	44 (37, 51)	47.5 (39.8, 55)	0.397
Alkaline phosphatase, U/L, mean (IQR)	7 (5, 10)	10 (4, 23)	0.234	48 (19, 72)	52 (47, 111)	0.199
GGT, U/L, mean ± SD	12.91 ± 8.1	13.87 ± 8.4	0.675	14.48 ± 7.57	22 ± 15.19	0.115
VDR SNPs						
Cdx2 TT	9 (39.1%)	2 (13.3%)	0.076	NA		
TC/CC	14 (30.9%)	13 (86.7%)				
Bsm1 CC	20 (87%)	13 (86.7%)	0.979	NA		
CT/TT	3 (13%)	2 (13.3%)				
FokI AA/AG	18 (78.3%)	10 (66.7%)	0.431	NA		
GG	5 (21.7%)	5 (33.3%)				

Taq1 AA	15 (65.2%)	9 (60%)	0.744	NA
AG/GG	8 (34.8%)	6 (40%)		
Apa1 CC	10 (43.5%)	7 (46.7%)	0.847	NA
CA/AA	13 (56.5%)	8 (53.3%)		

VDR SNPs: Single nucleotide polymorphisms of the vitamin D receptor gene; BMI: Body mass index; HBsAg: Hepatitis B surface antigen; HBeAg: Hepatitis B e antigen; HBV: Hepatitis B virus; WBC: White blood cell; ALT: Alanine aminotransferase; GGT: Gamma-glutamyl transferase; IQR: Interquartile range; NA: Not available.

Table 2 Factors associated with hepatitis B viral deoxyribonucleic acid serum concentration (log10 IU/mL)

Variable	*P* value, univariate	*P* value, multivariate	Standard beta, multivariate
Age (yr)	0.377		
BMI (kg/m^2)	0.049	0.03	-0.245
25(OH)D3 (ng/mL)	0.034	< 0.0001	-0.446
HBsAg (log10 IU/mL)	0.007		
HBV DNA log10	0.046		
Alkaline phosphatase	0.056		
HBeAg log10	0.025		
WBC count	0.064		
Maternal HBsAg at delivery, log10	0.003	0.05	0.285
Maternal alkaline phosphatase at delivery	0.025		
Maternal cholesterol at delivery	0.001	0.015	0.341

HBV: Hepatitis B virus; BMI: Body mass index; 25(OH)D3: 25-hydroxyvitamin D3; HBsAg: Hepatitis B surface antigen; WBC: White blood cell.

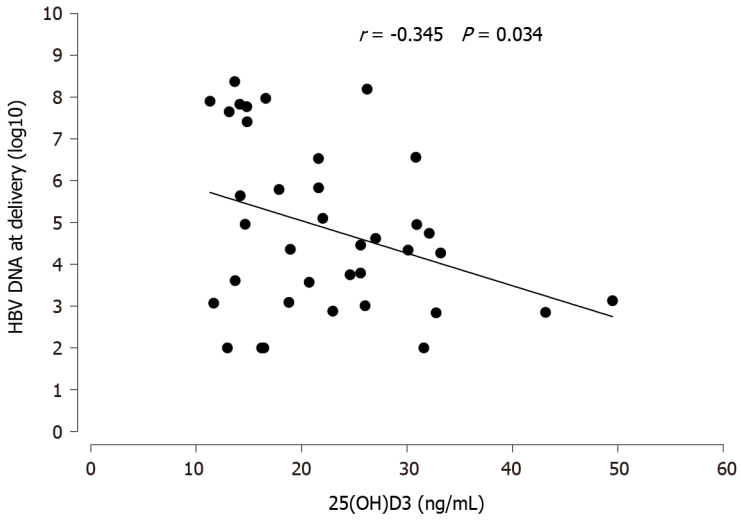

DOI: 10.3748/wjg.v29.i19.3003 **Copyright** ©The Author(s) 2023.

Figure 1 Correlation between maternal hepatitis B virus deoxyribonucleic acid levels at delivery (log10) and baseline serum 25-hydroxyvitamin D3 Levels. HBV: Hepatitis B virus; 25(OH)D3: 25-hydroxyvitamin D3.

was independently associated with targeted antiviral effects (maternal HBV DNA levels < 2 × 10^5 at delivery) in a multivariate regression model [OR 1.23 (1.04-1.44), *P* = 0.026], together with maternal VDR Cdx2 TT and cholesterol levels at delivery (Table 3).

Table 3 Factors associated with the targeted antiviral effects (hepatitis B viral deoxyribonucleic acid at delivery < 2 × 10^5)

Variable	Univariate	*P* value	Multivariate	*P* value
Age (yr, continuous)	1.034 (0.85-1.26)	0.745		0.727
BMI (kg/m^2, continuous)	1.18 (0.95-1.47)	0.146		0.071
25(OH) D3 (ng/mL, continuous)	1.16 (1.03-1.31)	0.014	1.23 (1.04-1.44)	0.026
VDR Cdx2 TT	0.2 (0.036-1.097)	0.064	0.09 (0.01-0.88)	0.039
Maternal GGT at delivery	0.94 (0.86-1.006)	0.075		0.05
Maternal VD at delivery (ng/mL, continuous)	1.1 (0.999-1.21)	0.053		0.385
Maternal alkaline phosphatase at delivery	0.98 (0.96-1.002)	0.081		0.64
Maternal cholesterol at delivery	0.47 (0.26-0.86)	0.015	0.39 (0.17-0.87)	0.021

BMI: Body mass index; 25(OH)D3: 25-hydroxyvitamin D3; VDR: Vitamin D receptor; GGT: Gamma-glutamyl transferase; VD: Vitamin D.

DISCUSSION

The present study showed that a high percentage (76.3%) of pregnant women with high HBV viral loads had deficient (< 20 ng/mL) or insufficient (≥ 20 but < 31 ng/mL) VD levels. There was a profound association between low serum 25(OH)D levels and higher levels of maternal HBV replication at delivery after TDF therapy. In a multiple linear regression analysis, maternal HBV DNA levels were associated with baseline maternal serum 25(OH)D levels, BMI, baseline maternal log10 HBsAg levels and cholesterol levels at delivery. Finally, we observed that baseline serum 25(OH)D levels, maternal VDR Cdx2 TT and cholesterol levels at delivery were associated with targeted antiviral effects (maternal HBV DNA levels < 2 × 10^5 at delivery) in a multivariate regression model.

In the human body, VD and its receptors are widely involved in a variety of life processes, regulating the nervous, immune and endocrine systems through related signaling pathways. Many studies have been conducted to reveal the association effect of VD and its receptors on HBV infection and its development. VD deficiency or declines can be detected in a variety of chronic liver diseases[5,7,16] and is associated with adverse clinical outcomes[9,16]. Abnormally low VD levels are highly prevalent among untreated patients with active chronic hepatitis B infection[6].

For a special group of people, such as pregnant females, VD is a vital nutrient that is important for both the mother and fetus in the perinatal period, and prenatal VD supplementation may reduce the risk of many adverse events and yield potential benefits. A previous study showed that pregnant women with HBV in China had lower VD levels than healthy pregnant women[10]. Our present study also showed that a high percentage (76.3%) of pregnant women with high HBV viral loads had deficient (18/38) or insufficient (11/38) VD levels, while only approximately 25.00% (9/38) had adequate VD levels. Our results suggested that abnormally low VD levels may be a common phenomenon in untreated pregnant women with high HBV viral loads in China.

Based on the evidence provided by a companion systematic review that addressed HBV DNA thresholds for identifying pregnant women at risk of MTCT, the WHO recommends administering TDF to pregnant women infected with HBV with high viral loads (≥ HBV DNA thresholds ≥ 2 × 10^5 IU/mL) from week 28 of pregnancy until at least childbirth to prevent MTCT, in addition to three doses of hepatitis B vaccination, including a birth dose given to the neonate. A recent meta-analysis showed that peripartum antiviral prophylaxis is highly effective at reducing the risk of the MTCT of HBV[17], which supports the 2020 WHO recommendation of administering antivirals during pregnancy, specifically TDF, for the prevention of the MTCT of HBV.

There is growing evidence that VD is associated with infectious diseases and immunity against infection and that VD supplementation has therapeutic potential in the treatment of infectious diseases [18,19]. Low maternal VD levels (< 32 ng/mL) were associated with a higher risk of the MTCT of HIV, and children born to women with low VD levels had a higher risk of death during follow-up[20]. Clinical and epidemiological studies support the role of VD in inhibiting HBV infection, and this antiviral effect is widely attributed to the VDR[11]. Hepatic VDR protein expression was significantly lower in patients with chronic HBV infection, and hepatic VDR expression was inversely correlated with hepatic inflammation and fibrosis[21], which could partly explain the more pronounced decrease in viral DNA in patients with higher VD levels after receiving antiviral therapy in our study.

The present study revealed a profound association between low serum 25(OH)D levels and higher levels of maternal HBV replication at delivery after TDF therapy. Consistent with our previous study, serum 25(OH)D levels were highly negatively correlated with HBV DNA levels[14]. Therefore, for HBV-infected patients, especially pregnant women, monitoring of VD levels is advocated, and increasing VD levels to a normal range in appropriate ways may be beneficial in maintaining low levels of HBV DNA.

It is expected that more in-depth studies will be performed to elucidate the mechanism of the effect of VD on HBV infection and its development, treatment and prognosis, which may offer attractive therapeutic opportunities for the treatment of chronic hepatitis B infection.

A number of studies have recently focused on the association between VDR SNPs and the disease characteristics of HBV infection. Some genotypes in VDR FokI increased the risk of HBV infection in a meta-analysis[22]. In addition, the VDR ApaI SNP was associated with viral load and the presence of HBsAg at different times, and pharmacogenetic data could help physicians identify HBV patients with a higher probability of achieving a good response[12]. In addition, VDR SNPs are correlated with HBV viral load and the severity of liver disease[23] and may be associated with occult hepatitis B infection [9]. Our results revealed that VDR Cdx2 TT was a hindering factor in achieving targeted antiviral therapeutic effects (HBV DNA levels < 2×10^5 at delivery) after TDF therapy. In pregnant women, increasing VD levels to within the normal range may help to achieve targeted antiviral treatment effects, especially in those with VDR Cdx2 TT. More basic and clinical studies are warranted for VD supplementation combined with antiviral therapy and immunoprophylaxis to block MTCT.

VD and cholesterol metabolism overlap significantly in the pathways that promote their biosynthesis and have a complex bidirectional relationship[24]. In our study, there was no significant difference in cholesterol levels between the full and partial responders before antiviral therapy, but cholesterol levels were lower in full responders after treatment. Similarly, in another study, for treatment-naive patients with chronic hepatitis B infection, total cholesterol levels showed a decreasing trend during 42 mo of TDF treatment[25]. Moreover, higher total cholesterol concentrations were associated with lower 25(OH)D concentrations[26], and VD supplementation appeared to have a beneficial effect on reducing total serum cholesterol levels[27]. In addition, VDR SNPs were associated with dyslipidemia in Chinese populations, and some variants may increase susceptibility to dyslipidemia[28]. Together, the difference in cholesterol levels after antiviral therapy may be due to differences in VD levels, VDR SNPs, and reactions to antiviral therapy.

Some limitations of the present study should be acknowledged. Most importantly, due to the type of study, the clinical correlations cannot be interpreted as causal relationships. Therefore, a suggestive functional link between VD metabolism and HBV replication remains elusive. Furthermore, the sample size included in this study was limited. Third, there are still some possible confounding factors that have not been considered. Although factors such as the season of blood collection were taken into account, other factors such as dietary habits, the duration of sunlight exposure and the ultraviolet intensity of pregnant women's living environments may also affect maternal VD levels.

CONCLUSION

In summary, we demonstrate a significant association between low serum levels of 25(OH)D and high levels of HBV replication in pregnant women with high HBV viral loads, and maternal VD levels as well as VDR SNPs may be associated with the efficacy of antiviral therapy. Future studies to evaluate the therapeutic value of VD and its analogs in reducing the MTCT of HBV may be justified.

ARTICLE HIGHLIGHTS

Research background

Mother-to-child transmission (MTCT) is the main route of hepatitis B virus (HBV) transmission, and HBV infection is associated with human vitamin D (VD) levels.

Research motivation

The role of VD and single nucleotide polymorphisms of the VD receptor gene (VDR SNPs) in blocking MTCT in pregnant women with high HBV viral load receiving antiviral therapy is unclear.

Research objectives

This study aimed to assess whether baseline VD levels and VDR SNPs are associated with the efficacy of tenofovir disoproxil fumarate (TDF) in the prevention of MTCT in pregnant women with high HBV viral loads.

Research methods

This retrospective study investigated VD levels, common clinical indicators, and virological parameters before and after antiviral therapy in 38 pregnant women with high HBV viral load, and further analyzed the effect of VD levels and VDR SNPs on the efficacy of TDF for the prevention of MTCT.

Research results

The present study showed that a high percentage (76.3%) of pregnant women with high HBV viral loads had deficient (< 20 ng/mL) or insufficient (≥ 20 but < 31 ng/mL) VD levels. There was a profound association between low serum 25-hydroxyvitamin D [25(OH)D] levels and higher levels of maternal HBV replication at delivery after TDF therapy. Multivariate logistic regression analysis showed that baseline serum 25(OH)D levels (OR = 1.23, 95%CI: 1.04-1.44), maternal VDR Cdx2 TT (OR = 0.09, 95%CI: 0.01-0.88) and cholesterol levels at delivery (OR = 0.39, 95%CI: 0.17-0.87) were associated with targeted antiviral effects (maternal HBV DNA levels < 2×10^5 at delivery).

Research conclusions

We demonstrate a significant association between low serum levels of 25(OH)D and high levels of HBV replication in pregnant women with high HBV viral loads, and maternal VD levels as well as VDR SNPs may be associated with the efficacy of antiviral therapy.

Research perspectives

Future studies to evaluate the therapeutic value of VD and its analogs in reducing the MTCT of HBV may be justified.

FOOTNOTES

Author contributions: Wang R and Zhu X contributed equally to this work; Ji YL, Zhu X and Chen YH participated in design and oversight of the study; Zhu X, Zhang X and Liu H collected and study data; Wang R, Zhu X, Zhang X, Liu H, and Chen YH analyzed the data and wrote the manuscript; Zhu X, Ji YL and Chen YH revised the manuscript for important intellectual content; all authors have read and approved the final manuscript.

Supported by the Key Research and Development Projects in Sichuan Province, No. 2021YFS0168; and the National Scientific and Technological Major Project for Infectious Diseases Control in China, No. 2018ZX10715-003.

Institutional review board statement: The study was reviewed approved by the Institutional Review Board of the West China Hospital, Sichuan University, approval No. 2019-151.

Informed consent statement: All study participants or their legal guardians provided informed written consent about personal and medical data collection prior to study enrollment.

Conflict-of-interest statement: All authors report no relevant conflict of interest for this article.

Data sharing statement: No additional data are available.

Country/Territory of origin: China

ORCID number: Rui Wang 0000-0003-0829-152X; Yong-Hua Chen 0000-0001-8485-0755.

S-Editor: Yan JP
L-Editor: A
P-Editor: Yuan YY

REFERENCES

1 **Xu Y**, Liu H, Wang Y, Hao R, Li Z, Song H. The next step in controlling HBV in China. *BMJ* 2013; **347**: f4503 [PMID: 23861426 DOI: 10.1136/bmj.f4503]
2 **Waheed Y**, Siddiq M, Jamil Z, Najmi MH. Hepatitis elimination by 2030: Progress and challenges. *World J Gastroenterol* 2018; **24**: 4959-4961 [PMID: 30510370 DOI: 10.3748/wjg.v24.i44.4959]
3 **Liu Z**, Chen Z, Cui F, Ding Y, Gao Y, Han G, Jia J, Li J, Li Z, Liu Y, Mao Q, Wang A, Wang W, Wei L, Xia J, Xie Q, Yang X, Yin X, Zhang H, Zhang L, Zhang W, Zhuang H, Dou X, Hou J. Management Algorithm for Prevention of Mother-to-child Transmission of Hepatitis B Virus (2022). *J Clin Transl Hepatol* 2022; **10**: 1004-1010 [PMID: 36304493 DOI: 10.14218/JCTH.2022.00047]
4 **Hou J**, Cui F, Ding Y, Dou X, Duan Z, Han G, Jia J, Mao Q, Li J, Li Z, Liu Z, Wei L, Xie Q, Yang X, Zhang H, Zhuang

H. Management Algorithm for Interrupting Mother-to-Child Transmission of Hepatitis B Virus. *Clin Gastroenterol Hepatol* 2019; **17**: 1929-1936.e1 [PMID: 30312789 DOI: 10.1016/j.cgh.2018.10.007]

5 **Pop TL**, Sîrbe C, Benţa G, Mititelu A, Grama A. The Role of Vitamin D and Vitamin D Binding Protein in Chronic Liver Diseases. *Int J Mol Sci* 2022; **23** [PMID: 36142636 DOI: 10.3390/ijms231810705]

6 **Chan HL**, Elkhashab M, Trinh H, Tak WY, Ma X, Chuang WL, Kim YJ, Martins EB, Lin L, Dinh P, Charuworn P, Foster GR, Marcellin P. Association of baseline vitamin D levels with clinical parameters and treatment outcomes in chronic hepatitis B. *J Hepatol* 2015; **63**: 1086-1092 [PMID: 26143444 DOI: 10.1016/j.jhep.2015.06.025]

7 **Farnik H**, Bojunga J, Berger A, Allwinn R, Waidmann O, Kronenberger B, Keppler OT, Zeuzem S, Sarrazin C, Lange CM. Low vitamin D serum concentration is associated with high levels of hepatitis B virus replication in chronically infected patients. *Hepatology* 2013; **58**: 1270-1276 [PMID: 23703797 DOI: 10.1002/hep.26488]

8 **Hoan NX**, Tong HV, Song LH, Meyer CG, Velavan TP. Vitamin D deficiency and hepatitis viruses-associated liver diseases: A literature review. *World J Gastroenterol* 2018; **24**: 445-460 [PMID: 29398866 DOI: 10.3748/wjg.v24.i4.445]

9 **Wong GL**, Chan HL, Chan HY, Tse CH, Chim AM, Lo AO, Wong VW. Adverse effects of vitamin D deficiency on outcomes of patients with chronic hepatitis B. *Clin Gastroenterol Hepatol* 2015; **13**: 783-90.e1 [PMID: 25445773 DOI: 10.1016/j.cgh.2014.09.050]

10 **Gao XR**, Wang CM, Wang WJ, Han GR, Zhang JQ. Serum 25-hydroxyvitamin D status in pregnant women with chronic hepatitis B virus infection. *J Infect Dev Ctries* 2016; **10**: 851-856 [PMID: 27580331 DOI: 10.3855/jidc.6600]

11 **Ahluwalia S**, Choudhary D, Tyagi P, Kumar V, Vivekanandan P. Vitamin D signaling inhibits HBV activity by directly targeting the HBV core promoter. *J Biol Chem* 2021; **297**: 101233 [PMID: 34562448 DOI: 10.1016/j.jbc.2021.101233]

12 **Cusato J**, Boglione L, De Nicolò A, Imbornone R, Cardellino CS, Ghisetti V, Carcieri C, Cariti G, Di Perri G, D'Avolio A. Association of vitamin D pathway SNPs and clinical response to interferon in a cohort of HBeAg-negative patients. *Pharmacogenomics* 2017; **18**: 651-661 [PMID: 28453395 DOI: 10.2217/pgs-2016-0041]

13 **Zhu X**, Wang J, Wang M, Du LY, Ji YL, Zhang X, Tang H. The positive rates of hepatitis B surface antibody in youth after booster vaccination: a 4-year follow-up study with large sample. *Biosci Rep* 2021; **41** [PMID: 34151935 DOI: 10.1042/BSR20210182]

14 **Chen EQ**, Bai L, Zhou TY, Fe M, Zhang DM, Tang H. Sustained suppression of viral replication in improving vitamin D serum concentrations in patients with chronic hepatitis B. *Sci Rep* 2015; **5**: 15441 [PMID: 26486883 DOI: 10.1038/srep15441]

15 **Lankes U**, Elder PA, Lewis JG, George P. Differential extraction of endogenous and exogenous 25-OH-vitamin D from serum makes the accurate quantification in liquid chromatography-tandem mass spectrometry assays challenging. *Ann Clin Biochem* 2015; **52**: 151-160 [PMID: 24714680 DOI: 10.1177/0004563214533316]

16 **Huang CZ**, Zhang J, Zhang L, Yu CH, Mo Y, Mo LY. Serum vitamin D and vitamin-D-binding protein levels in children with chronic hepatitis B. *World J Gastroenterol* 2021; **27**: 255-266 [PMID: 33519140 DOI: 10.3748/wjg.v27.i3.255]

17 **Funk AL**, Lu Y, Yoshida K, Zhao T, Boucheron P, van Holten J, Chou R, Bulterys M, Shimakawa Y. Efficacy and safety of antiviral prophylaxis during pregnancy to prevent mother-to-child transmission of hepatitis B virus: a systematic review and meta-analysis. *Lancet Infect Dis* 2021; **21**: 70-84 [PMID: 32805200 DOI: 10.1016/S1473-3099(20)30586-7]

18 **Ismailova A**, White JH. Vitamin D, infections and immunity. *Rev Endocr Metab Disord* 2022; **23**: 265-277 [PMID: 34322844 DOI: 10.1007/s11154-021-09679-5]

19 **White JH**. Emerging Roles of Vitamin D-Induced Antimicrobial Peptides in Antiviral Innate Immunity. *Nutrients* 2022; **14** [PMID: 35057465 DOI: 10.3390/nu14020284]

20 **Mehta S**, Hunter DJ, Mugusi FM, Spiegelman D, Manji KP, Giovannucci EL, Hertzmark E, Msamanga GI, Fawzi WW. Perinatal outcomes, including mother-to-child transmission of HIV, and child mortality and their association with maternal vitamin D status in Tanzania. *J Infect Dis* 2009; **200**: 1022-1030 [PMID: 19673647 DOI: 10.1086/605699]

21 **Yang K**, Pan Y, Zhang H, Jin L, Wang X. Hepatic vitamin D receptor expression is negatively associated with liver inflammation and fibrosis in patients with chronic HBV infection. *Clin Exp Med* 2022 [PMID: 36289101 DOI: 10.1007/s10238-022-00919-9]

22 **He Q**, Huang Y, Zhang L, Yan Y, Liu J, Song X, Chen W. Association between vitamin D receptor polymorphisms and hepatitis B virus infection susceptibility: A meta-analysis study. *Gene* 2018; **645**: 105-112 [PMID: 29248582 DOI: 10.1016/j.gene.2017.12.027]

23 **Suneetha PV**, Sarin SK, Goyal A, Kumar GT, Shukla DK, Hissar S. Association between vitamin D receptor, CCR5, TNF-alpha and TNF-beta gene polymorphisms and HBV infection and severity of liver disease. *J Hepatol* 2006; **44**: 856-863 [PMID: 16545485 DOI: 10.1016/j.jhep.2006.01.028]

24 **Warren T**, McAllister R, Morgan A, Rai TS, McGilligan V, Ennis M, Page C, Kelly C, Peace A, Corfe BM, Mc Auley M, Watterson S. The Interdependency and Co-Regulation of the Vitamin D and Cholesterol Metabolism. *Cells* 2021; **10** [PMID: 34440777 DOI: 10.3390/cells10082007]

25 **Zhang Q**, Liang J, Yin J, Jiang Y, Yu N, Liao X, Zhao S, Wu L, Fan R. Real-life impact of tenofovir disoproxil fumarate and entecavir therapy on lipid profile, glucose, and uric acid in chronic hepatitis B patients. *J Med Virol* 2022; **94**: 5465-5474 [PMID: 35794065 DOI: 10.1002/jmv.27977]

26 **Vitezova A**, Voortman T, Zillikens MC, Jansen PW, Hofman A, Uitterlinden AG, Franco OH, Kiefte-de Jong JC. Bidirectional associations between circulating vitamin D and cholesterol levels: The Rotterdam Study. *Maturitas* 2015; **82**: 411-417 [PMID: 26358932 DOI: 10.1016/j.maturitas.2015.08.005]

27 **Dibaba DT**. Effect of vitamin D supplementation on serum lipid profiles: a systematic review and meta-analysis. *Nutr Rev* 2019; **77**: 890-902 [PMID: 31407792 DOI: 10.1093/nutrit/nuz037]

28 **Jia J**, Tang Y, Shen C, Zhang N, Ding H, Zhan Y. Vitamin D receptor polymorphism rs2228570 is significantly associated with risk of dyslipidemia and serum LDL levels in Chinese Han population. *Lipids Health Dis* 2018; **17**: 193 [PMID: 30119682 DOI: 10.1186/s12944-018-0819-0]

World Journal of Gastroenterology

Submit a Manuscript: https://www.f6publishing.com

World J Gastroenterol 2023 May 21; 29(19): 3013-3026

DOI: 10.3748/wjg.v29.i19.3013

ISSN 1007-9327 (print) ISSN 2219-2840 (online)

ORIGINAL ARTICLE

Observational Study

Gastrointestinal manifestations of long-term effects after COVID-19 infection in patients with dialysis or kidney transplantation: An observational cohort study

Wiwat Chancharoenthana, Supitcha Kamolratanakul, Asada Leelahavanichkul, Wassawon Ariyanon, Sutatip Chinpraditsuk, Rattanaporn Saelim, Somratai Vadcharavivad, Weerapong Phumratanaprapin, Polrat Wilairatana

Specialty type: Gastroenterology and hepatology

Provenance and peer review: Invited article; Externally peer reviewed.

Peer-review model: Single blind

Peer-review report's scientific quality classification

Grade A (Excellent): 0
Grade B (Very good): B
Grade C (Good): C
Grade D (Fair): 0
Grade E (Poor): 0

P-Reviewer: Awad AK, Egypt; Nooripour R, Iran

Received: January 12, 2023
Peer-review started: January 12, 2023
First decision: February 4, 2023
Revised: February 13, 2023
Accepted: April 21, 2023
Article in press: April 21, 2023
Published online: May 21, 2023

Wiwat Chancharoenthana, Supitcha Kamolratanakul, Weerapong Phumratanaprapin, Polrat Wilairatana, Department of Clinical Tropical Medicine, Faculty of Tropical Medicine, Mahidol University, Bangkok 10400, Thailand

Asada Leelahavanichkul, Department of Microbiology, Faculty of Medicine, Chulalongkorn University, Bangkok 10330, Thailand

Wassawon Ariyanon, Cardiometabolic Centre, Department of Medicine, Bangkok Nursing Hospital, Bangkok 10500, Thailand

Sutatip Chinpraditsuk, Rattanaporn Saelim, Dialysis Center, Hospital for Tropical Diseases, Faculty of Tropical Medicine, Mahidol University, Bangkok 10400, Thailand

Somratai Vadcharavivad, Department of Pharmacy Practice, Faculty of Pharmaceutical Sciences, Chulalongkorn University, Bangkok 10330, Thailand

Corresponding author: Supitcha Kamolratanakul, MD, Assistant Professor, Department of Clinical Tropical Medicine, Faculty of Tropical Medicine, Mahidol University, 420/6 Ratchawithi Rd, Thung Phaya Thai, Ratchathewi, Bangkok 10400, Thailand.
supitcha.kam@mahidol.edu

Abstract

BACKGROUND

Prolonged symptoms after corona virus disease 2019 (Long-COVID) in dialysis-dependent patients and kidney transplant (KT) recipients are important as a possible risk factor for organ dysfunctions, especially gastrointestinal (GI) problems, during immunosuppressive therapy.

AIM

To identify the characteristics of GI manifestations of Long-COVID in patients with dialysis-dependent or KT status.

METHODS

This observational, prospective study included patients with COVID-19 infection,

confirmed by reverse transcription polymerase chain reaction, with the onset of symptoms between 1 January 2022 and 31 July 2022 which was explored at 3 mo after the onset, either through the out-patient follow-up or by telephone interviews.

RESULTS

The 645 eligible participants consisted of 588 cases with hemodialysis (HD), 38 patients with peritoneal dialysis (PD), and 19 KT recipients who were hospitalized with COVID-19 infection during the observation. Of these, 577 (89.5%) cases agreed to the interviews, while 64 (10.9%) patients with HD and 4 (10.5%) cases of PD were excluded. The mean age was 52 ± 11 years with 52% women. The median dialysis duration was 7 ± 3 and 5 ± 1 years for HD and PD groups, respectively, and the median time post-transplantation was 6 ± 2 years. Long-COVID was identified in 293/524 (56%) and 21/34 (62%) in HD and PD, respectively, and 7/19 (37%) KT recipients. Fatigue was the most prevalent (96%) of the non-GI tract symptoms, whereas anorexia (90.9%), loss of taste (64.4%), and abdominal pain (62.5%) were the first three common GI manifestations of Long-COVID. Notably, there were 6 cases of mesenteric panniculitis from 19 patients with GI symptoms in the KT group.

CONCLUSION

Different from patients with non-chronic kidney disease, there was a high prevalence of GI manifestations of Long-COVID in dialysis-dependent patients and KT recipients. An appropriate long-term follow-up in these vulnerable populations after COVID-19 infection is possibly necessary.

Key Words: COVID-19; Kidney transplant; Post-acute COVID-19 syndrome; Long-COVID-19; Gastrointestinal; SARS-CoV-2

Core Tip: Prolonged symptoms after coronavirus disease 2019 (COVID-19) or prolonged symptoms after COVID-19 (Long-COVID) in dialysis-dependent patients and kidney transplant (KT) recipients are important as a possible risk factor for organ dysfunctions, especially gastrointestinal (GI) problems. In this study, we observed that a GI manifestation of Long-COVID is a frequent condition in patients with dialysis-dependence and kidney-transplant recipients. Long-COVID was significantly more prevalent in peritoneal dialysis patients than in hemodialysis patient or KT cases. We also found that patients who experienced either abdominal pain or diarrhea had a longer duration of other GI manifestations of Long-COVID, suggesting a need for closer observation of these patients during COVID-19 infection.

Citation: Chancharoenthana W, Kamolratanakul S, Leelahavanichkul A, Ariyanon W, Chinpraditsuk S, Saelim R, Vadcharavivad S, Phumratanaprapin W, Wilairatana P. Gastrointestinal manifestations of long-term effects after COVID-19 infection in patients with dialysis or kidney transplantation: An observational cohort study. *World J Gastroenterol* 2023; 29(19): 3013-3026

URL: https://www.wjgnet.com/1007-9327/full/v29/i19/3013.htm

DOI: https://dx.doi.org/10.3748/wjg.v29.i19.3013

INTRODUCTION

The coronavirus disease (COVID-19) pandemic has a significant impact on the management of dialysis-dependent patients and kidney transplant (KT) recipients, while the chronic kidney disease (CKD) condition in these patients is also affecting the clinical manifestation of COVID-19 infection. The persistence of post-COVID-19 syndrome for weeks to months after the infection is a growing public health concern worldwide[1]. Currently, the definition of post-acute COVID-19 syndrome (PACS), also known as the post-acute sequelae of severe acute respiratory syndrome coronavirus 2 (PASC) or prolonged symptoms after COVID-19 (Long-COVID) syndrome, depends on the population being studied, the post-infection timing, and the assessment tools[2,3]. Moreover, the overlap in its pathophysiology between overwhelming pro-inflammatory immune responses and direct viral cytopathic effects remains inconclusive[4]. In general, PACS mainly includes fatigue, pain, headache, neurological and cognitive impairments, cardio-pulmonary symptoms, and anosmia-dysgeusia[5]. The British National Institute for Health and Care Excellence (NICE) defines Long-COVID as any signs and symptoms that develop during or after an infection consistent with COVID-19, continue for over 12 wk,

and cannot be explained by an alternative diagnosis[6]. A clinical case definition of Long-COVID by a Delphi consensus has crystallized the case definition of Long-COVID as clinical symptoms that occur in individuals with a history of probable or confirmed severe acute respiratory syndrome coronavirus 2 (SARS-CoV-2) infection, usually 3 mo from the onset of COVID-19 with symptoms, that last for at least 2 mo without an alternative explainable condition[7].

Both dialysis-dependent patients and KT recipients are classified as vulnerable populations due to their immunosuppressive status derived from their CKD condition and the high number of comorbidities[8]. Thus, a more frequent prevalence of long-term after-effects of COVID-19 infection than in the general population is possible. Accordingly, aggressive approaches, along with prompt management of acute illness, should be used in these populations, making the subject of Long-COVID even more challenging. Recent reports have revealed an incidence of post-COVID-19 syndrome in dialysis patients and KT recipients of approximately 40%-70% of those who experience a COVID-19 infection[9-13]. The Long-COVID symptoms include respiratory-related symptoms, fatigue, peripheral neuropathy, venous thromboembolism, memory impairment, and *de novo* diabetes mellitus[9-11]. Notably, 60% of dialysis patients *vs* 10% of KT recipients had residual symptoms at 6 mo post-COVID-19 infection[11,14].

Even without the gastrointestinal (GI) symptoms, the severity of COVID-19 is associated with the GI tract as the translocation of pathogen molecules from the gut into the blood circulation (leaky gut) is reported[15], possibly from a quiescent the SARS-CoV-2 infection in the intestine[16]. Indeed, the cell entry of SARS-CoV-2 virus through angiotensin-converting enzyme 2 (ACE2) receptors on the squamous and columnar epithelial cells, including enterocytes, is well-known[17]. One large study of hospitalized COVID-19 revealed that 30% of the patients reported GI symptoms, such as abdominal pain, nausea and vomiting, and diarrhea, in addition to their respiratory tract symptoms[18]. Nevertheless, the impacts of COVID-19 infection, and particularly Long-COVID-19, in the GI spectrum is not fully understood in either dialysis patients or KT patients, and data on this topic remains scarce. Of note, data from the most recent report on post-acute SARS-CoV-2 infection sub-phenotype by Zhang *et al*[19] found that GI tract-related symptoms are one of the four most common characteristics in post-acute viral symptoms.

Hence, the aim of the present study was to determine the prevalence and characteristics of Long-COVID in a cohort of these patients. We hypothesize that Long-COVID, especially in the GI symptoms, may be underestimated in these populations and may need more clarification, particularly in the post-pandemic period.

MATERIALS AND METHODS

Study populations

The study is a cohort longitudinal study performed in dialysis-dependent patients and KT recipients with COVID-19 infection under the care of three renal referral tertiary care centers. Eligible participants were those with a diagnosis of COVID-19 confirmed by an RT-PCR test from oro-nasopharyngeal swabs from January 2022 to 31 July 2022. The KT recipients with the following conditions were excluded: (1) Those who died before the follow-up interview, (2) those we were unable to contact, and (3) those without or unable to provide informed consent. The remaining dialysis-dependent patients and KT recipients who had experienced a post-COVID-19 infection for at least 3 mo were included in the study. Purposive sampling was used in order to ensure the representation of a range of characteristics and experiences of analytic relevance. Informed consent for participation in interviews was obtained either written or verbally over the phone from all participants in the study and the study was approved by the Research Ethics Commission of the Faculty of Tropical Medicine, Mahidol University, Thailand (MUTM 2022-081-01) along with adhered to STROBE guideline.

Interview conduct and data collection

An interview consisting of a set of open-ended questions regarding symptoms during COVID-19 and post-COVID-19 infection periods. Then, interviews were designed to explore the specific persistent or emerging symptoms potentially due to GI tract-associated Long COVID-19 syndrome, as previously described[20]. Participants were interviewed either in person or by telephone by trained research nurses. Participants were considered to have GI tract-associated symptoms of Long COVID-19 if they showed one of the following signs: loss of appetite, nausea, weight loss, abdominal pain, heartburn, dysphagia, diarrhea, constipation, altered bowel motility, or irritable bowel syndrome[20]. In addition, the participant's electronic medical records were used to obtain clinical data, including baseline demographics and transplant-related immunological risk, comorbidity, and data about COVID-19 admission. Although abnormal laboratory tests, such as elevated alanine aminotransferase, can present as GI tract-associated Long COVID-19 syndrome[21], only clinical signs and symptoms were explored in the present study.

Statistical analysis

Descriptive characteristics were presented as means and standard deviation (means ± SD) unless otherwise noted. The Kolmogorov-Smirnov and Levene's tests were performed to establish data distribution and homogeneity, respectively. Chi-square tests were performed to compare categorical variables, whereas Tukey-Kramer multiple comparisons were used for continuous variables. Independent risk factors were assessed by applying a backward elimination stepwise binary regression and removing the least significant variables at each step. Odds ratios (ORs) and 95% confidence intervals (CIs) were estimated. $P < 0.05$ was considered statistically significant. Data analysis was performed using the PASW 18.0.0 statistical software package (SPSS Inc., Chicago, IL, United States) and GraphPad Prism 9.3.1 software (GraphPad Software, Inc., La Jolla, CA, United States).

RESULTS

Comparison baseline characteristics among participants of hemodialysis, peritoneal dialysis, and kidney transplantation

This study enrolled 645 eligible participants with COVID-19 infection, including 588 cases with hemodialysis (HD), 38 patients with peritoneal dialysis (PD), and 19 KT recipients. Of these, 577 (89.5%) participants agreed to interviews (Figure 1). All eligible KT recipients were enrolled in the study, and none of the transplant recipients in the KT cohort died or returned to dialysis.

The mean patient age was 52 ± 11 years, 300 (52%) were women, and the median dialysis duration was 7 ± 3 and 5 ± 1 years in the HD and PD groups, respectively. Hypertension (92%) and type 2 diabetes mellitus (77%) were the two most common comorbidities among the three groups of participants. The mean post-transplantation time was 6 ± 2 years (Table 1). Most of the HD patients had three dialysis sessions per week while continuous ambulatory PD (CAPD) was the most treatment modality used in PD patients. The three most common initial symptoms detected in both the dialysis and KT cohorts were fever (98%), coryza (96%), and cough (94%). Of note, the PD patients had a significant predominance of all symptoms compared to the HD and KT groups (P <0.0001); this could be because the highest comorbidities and uttermost severity of COVID-19 were observed in the PD group. For this reason, the combination therapy of Remdesivir (88.2%) and tocilizumab (63.1%) was prescribed significantly more frequently in this group with also correspondent the highest mean levels of both high-sensitivity C-reactive protein and D-dimer compared with HD and KT groups ($P < 0.0001$) (Table 1).

Different prevalence of GI manifestations of Long-COVID among the dialysis-dependent and KT populations

The Thai national guidelines for COVID-19 management in high-risk patients (during this study period) stipulate that all patients with CKD or CKD-equivalent disorders must be hospitalized for intensive care and monitoring during acute COVID-19 infection. As such, all participants in the study were hospitalized. During the early post-COVID-19 infection period, Long-COVID was identified in 293/524 (56%) of the HD, 21/34 (62%) of the PD, and 7/19 (37%) of the KT groups. Fatigue was the most prevalent symptom (96%) of the non-GI tract symptoms and was accompanied by loss of appetite or anorexia (81%), loss of taste (63%), hoarse voice (28%), unusual muscle pains (23%), hair loss (22%), a persistent cough (22%), headache (11%), and impaired cognitive and memory function (9%). Among the GI manifestations of Long-COVID, anorexia was the most prevalent symptom (525 cases, 90.9% from all groups), followed by loss of taste (372 cases, 64% from all groups), and abdominal pain (367 cases, 62.5% from all groups) (Figure 2A). Although anorexia and loss of taste were common in all three groups, they were more predominant in dialysis patients, but most cases showed much improvement by two months after the onset of COVID-19 infection. Abdominal pain and diarrhea were the symptoms that persisted for over 3 mo (Figure 2B).

Notably, our investigation of the causes of abdominal pain, which was reported by 87% of the patients, revealed that non-specific abdominal pain or probably acute gastritis was the main etiology in dialysis-dependent patients, whereas mesenteric panniculitis was the main etiology of abdominal pain (6 from 19 cases) in the KT group with a good response to oral corticosteroids (20 mg prednisolone), which were slowly tapered off in 8 wk. All six cases of mesenteric panniculitis had complete resolution, as indicated by the follow-up abdominal computer tomography.

Figure 2C shows the factors associated with the GI manifestation of Long-COVID. We found that COVID-19 patients who were older than 65 years (ORs 2.00, 95%CIs 1.2-2.8), who had chronic lung disease (ORs 2.10, 95%CIs 1.1-4.2), who were on PD (ORs 1.80, 95%CIs 1.4-2.5), or who had high levels of both C-reactive protein (CRP) and D-dimer at the onset (ORs 4.40, 95%CIs 1.4-8.8) were significantly likely to have GI manifestations of Long-COVID.

Table 1 Baseline characteristics and clinical presentation of corona virus disease 2019 in participants with or without gastrointestinal tract symptoms related to prolonged symptoms after corona virus disease 2019 at enrollment

Variables	Hemodialysis (*n* = 524)	Peritoneal dialysis (*n* = 34)	Kidney Transplantation (*n* = 19)	*P* value
Age, yr, mean ± SD	48 ± 9	71 ± 12	44 ± 12	< 0.001[a,b]
Female sex, *n* (%)	278 (53.1)	14 (41.2)	8 (42.1)	NS
Body mass index, kg/m2, mean ± SD	26 ± 4	23 ± 2	24 ± 4	< 0.001[a]
Comorbidities, *n* (%)				
Hypertension	487 (92.9)	34 (100)	12 (63.2)	< 0.0001[b], 0.0002[c]
Diabetes	408 (77.9)	30 (88.2)	6 (31.6)	< 0.0001[b,c]
Cardiovascular disease	450 (85.9)	28 (82.4)	9 (47.4)	< 0.0001[b], 0.008[c]
Pulmonary disease	52 (9.9)	5 (14.7)	1 (5.3)	NS
Hepatic disease	14 (2.7)	4 (11.8)	0 (0)	0.004[a]
Renal replacement therapy				
Dialysis vintage, years	7 ± 3	5 ± 1	6 ± 2	< 0.001[a]
Frequency, 2× per week, *n* (%)	84 (16.0)	N/A	N/A	
Frequency, 3× per week, *n* (%)	440 (84.0)	N/A	N/A	
CAPD, *n* (%)	N/A	32 (94.1)	N/A	
APD, *n* (%)	N/A	2 (5.9)	N/A	
Deceased donor transplant, *n* (%)	N/A	N/A	11 (57.9)	
Time from transplant, yr, mean ± SD	N/A	N/A	6 ± 2	< 0.001[b,c]
Maintenance immunosuppressive regimen by drug, *n* (%)				
Calcineurin inhibitors				
TAC	N/A	N/A	11 (57.9)	
CsA	N/A	N/A	8 (42.1)	
Prednisolone	N/A	N/A	19 (100)	
Antimetabolites				
MPA	N/A	N/A	16 (84.2)	
Azathioprine	N/A	N/A	0 (0)	
mTOR inhibitors	N/A	N/A	3 (15.8)	
Baseline creatinine, mean ± SD	8 ± 2	11 ± 2	2.5 ± 0.8	< 0.001[a,b,c]
Baseline creatinine > 1.5 mg/dL, *n* (%)[1]	N/A	N/A	7 (36.8)	
Day(s) of illness, mean ± SD	4 ± 2	3 ± 1	3 ± 1	< 0.001[a]
Initial symptoms, *n* (%)				
Fever or chills	511 (97.5)	34 (100)	19 (100)	NS
Cough	488 (93.1)	34 (100)	18 (94.7)	NS
Dyspnea	321 (61.3)	30 (88.2)	16 (84.2)	0.002[a], 0.043[b]
Chest pain	152 (29.0)	11 (32.4)	8 (42.1)	NS
Coryza	501 (95.6)	34 (100)	19 (100)	NS
Headache	161 (30.7)	5 (14.7)	6 (31.6)	0.048[a]
Nasal congestion	359 (68.5)	9 (26.5)	11 (57.9)	< 0.0001[a], 0.025[c]
Fatigue	209 (40.0)	34 (100)	9 (47.4)	< 0.0001[a], < 0.0001[c]
Myalgia	386 (73.7)	31 (91.2)	12 (63.2)	0.023[a], 0.013[c]

Nausea or vomiting	137 (26.1)	30 (88.2)	4 (21.1)	< 0.0001[a,c]
Diarrhea	83 (15.8)	25 (73.5)	3 (15.8)	< 0.0001[a,c]
Anosmia	66 (12.6)	7 (20.6)	1 (5.3)	NS
Ageusia	25 (4.8)	6 (17.6)	2 (10.5)	0.002[a]
Number of symptoms, mean ± SD	7 ± 2	9 ± 1	4 ± 2	< 0.0001[a,b,c]
COVID-19 severity, *n* (%)				
Mild	252 (48.1)	2 (5.9)	0 (0)	< 0.0001[a,b]
Moderate	137 (26.1)	7 (20.6)	4 (21.1)	NS
Severe	135 (25.8)	25 (73.5)	0 (0)	< 0.0001[a,c], 0.011[b]
High-sensitivity C-reactive protein (mg/L)	32 ± 14	59 ± 11	17 ± 9	< 0.0001[a,b,c]
D-dimer (ng/mL)	2749 ± 578	5339 ± 786	1699 ± 175	< 0.0001[a,b,c]
Treatments, *n* (%)				
Remdesivir	352 (67.2)	30 (88.2)	8 (42.1)	0.011[a], 0.023[b], 0.0004[c]
Favipiravir	172 (32.8)	4 (11.8)	11 (57.9)	0.011[a], 0.023[b], < 0.001[c]
Tocilizumab	39 (7.4)	12 (63.1)	0 (0)	< 0.0001[a,c]
Corticosteroids	429 (81.9)	34 (100)	19 (100)	0.007[a], 0.041[b]
Low-molecular weight heparin	482 (92.0)	32 (94.1)	7 (36.8)	< 0.0001[b,c]
Outcomes during the acute phase, *n* (%)				
Hospitalization	524 (100)	34 (100)	19 (100)	-
Intensive care unit	204 (38.9)	27 (79.4)	4 (21.1)	< 0.0001[a,c]
Oxygen therapy	272 (51.9)	32 (94.1)	4 (21.1)	< 0.0001[a,c], 0.008[b]
Invasive mechanical ventilation	104 (19.8)	23 (67.6)	0 (0)	< 0.0001[a,c], 0.031[b]
Increased dialysis frequency	178 (34.0)	0 (0)	N/A	< 0.0001[a]
Immunosuppression suspended except for steroids[1]	N/A	N/A	2 (10.5)	

[1]Only kidney transplant recipient group.
Only the comparisons between following groups with statistical significance are shown.
[a]Hemodialysis *vs* peritoneal dialysis group.
[b]Hemodialysis *vs* kidney transplantation group.
[c]Peritoneal dialysis *vs* kidney transplantation group.
APD: Automated peritoneal dialysis; COVID-19: Coronavirus disease 2019; CAPD: Continuous ambulatory peritoneal dialysis; CsA: Cyclosporin A; MPA: Mycophenolate; mTORi: Mammalian target of rapamycin inhibitors; TAC: Tacrolimus; N/A: Not applicable; NS: Non-significant.

DISCUSSION

In this study, we observed that a GI manifestation of Long-COVID is a frequent condition in patients with dialysis dependence and KT recipients. Long-COVID was significantly more prevalent in PD patients than in HD or KT cases. Notably, patients who experienced either abdominal pain or diarrhea had a longer duration of other GI manifestations of Long-COVID, suggesting a need for closer observation of these patients during COVID-19 infection.

COVID-19 has brought forth a multitude of challenges to healthcare systems across the globe. Apart from the significant morbidity and mortality associated with COVID-19 during its initial phase, recognition and concern are growing regarding the long-term consequences of COVID-19[2,3,22]. Dialysis-dependent patients and KT recipients are clearly high-risk groups associated with higher numbers of comorbidities and immunosuppressive issues and require more aggressive courses of COVID-19 treatment in terms of acute and chronic complications[8,23,24]. Although the most visible manifestation of Long-COVID in the general population is asthenia, or brain fog[22,25], we found that anorexia was the most common GI manifestation of Long-COVID in both dialysis-dependent patients and KT recipients, followed by abdominal pain and loss of taste (Figure 2A).

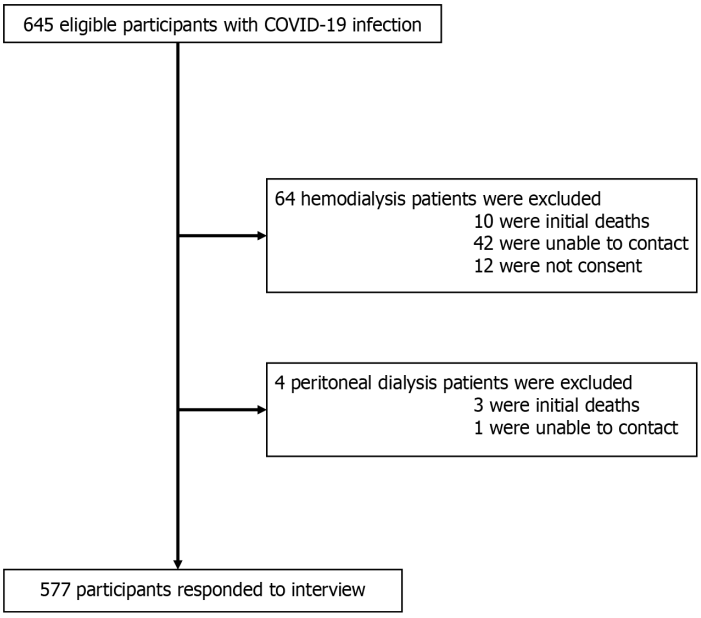

DOI: 10.3748/wjg.v29.i19.3013

Figure 1 Flow chart showing the number of eligible participants and the final cases enrolled in the study. COVID-19: Coronavirus disease 2019.

The prevalence and characteristics of Long-COVID in the present cohort seem to differ from its manifestations in other populations, in which diarrhea was the most persistently encountered GI symptom[26-31]. This difference could be explained by the combination of pre-existing uremic toxins in dialysis-dependent patients, as well as a delayed clearance of inflammatory cytokines[32] and enhanced oxidative stress associated with end-stage renal disease (ESRD)[33]. As such, restoration of renal function in KT recipients resulted in a decrease in the incidence of GI manifestations of Long-COVID compared with ESRD patients (Figure 2A). However, kidney transplantation does not entirely reverse T cell functions[34], and the underlying mechanisms of epigenetic changes induced by any combination of inflammation and oxidative stress associated with uremia are not easily reversible[35]. For these reasons, KT recipients with COVID-19 infection still have a persistently increased risk for Long-COVID.

As shown in Figure 2B, most of the participants experienced much improvement in the manifestations of Long-COVID after 4 wk and nearly complete resolution by three months. However, the differential diagnosis between the functional limitation during the COVID rehabilitation phase *vs* the Long-COVID syndrome may be difficult. Accordingly, the need for a robust clarification of the sequelae after COVID-19 infection is another concern in the post-pandemic era. The British NICE suggests that the term PASC must refer to any clinical signs and symptoms that develop during or after an infection consistent with COVID-19, that continue for more than 12 wk, and that cannot be explained by any other conditions[6]. Similarly, the World Health Organization (WHO) defines the PASC syndrome as any symptoms without an alternative diagnosis from three months onwards and that last for at least 2 mo[7]. Based on our findings, we found a significant difference in the clinical spectrum between patients with a symptom duration longer than 3 mo *vs* less than 3 mo post-COVID-19 infection (Figure 2B), in agreement with the COVID Symptom Study[36]. One explanation for the persistence of clinical signs and symptoms following COVID-19 infection may involve the underlying biological factors, such as an aberrant immune response[37], diverse functional autoantibodies[38], or gut dysbiosis[39], that drive other virus-initiated chronic syndromes.

We support using the 12-week cut-off duration as recommended by NICE and WHO for the diagnosis of PASC, and we propose an additional revision of the specific nomenclature for early and late Long-COVID syndrome. We propose using the term "post-acute COVID-19 syndrome (PACS)" for the clinical syndrome that develops three months from post-COVID-19 infection and using "chronic COVID-19 syndrome" thereafter (Figure 3). We further recommend reserving the term "Long-COVID syndrome" for the clinical syndrome that develops beyond three months post-COVID-19 infection and lasts for at least six months, because Long-COVID syndrome may be another post-viral illness spectrum, like myalgic encephalomyelitis/chronic fatigue syndrome[40].

The mechanisms underlying the GI manifestations of Long-COVID are not completely understood. One plausible explanation might be that an impairment of gut homeostasis is explained by disruption of gut-lung communication[41]. The manifestations during acute COVID-19 are believed to be related to an increased expression of ACE2 on the small bowel mucosa[17], endotoxemia[16,42], leaky gut[16], and alterations in hepatic blood flow due to sinusoidal thrombi[43], all triggered by an increased proinflammatory state and intestinal dysbiosis. Undoubtedly, the greater severity of COVID-19 infection in the elderly (high C-reactive protein > 5 mg/L, high D-dimer > 500 ng/mL with > 65 years old), as shown in

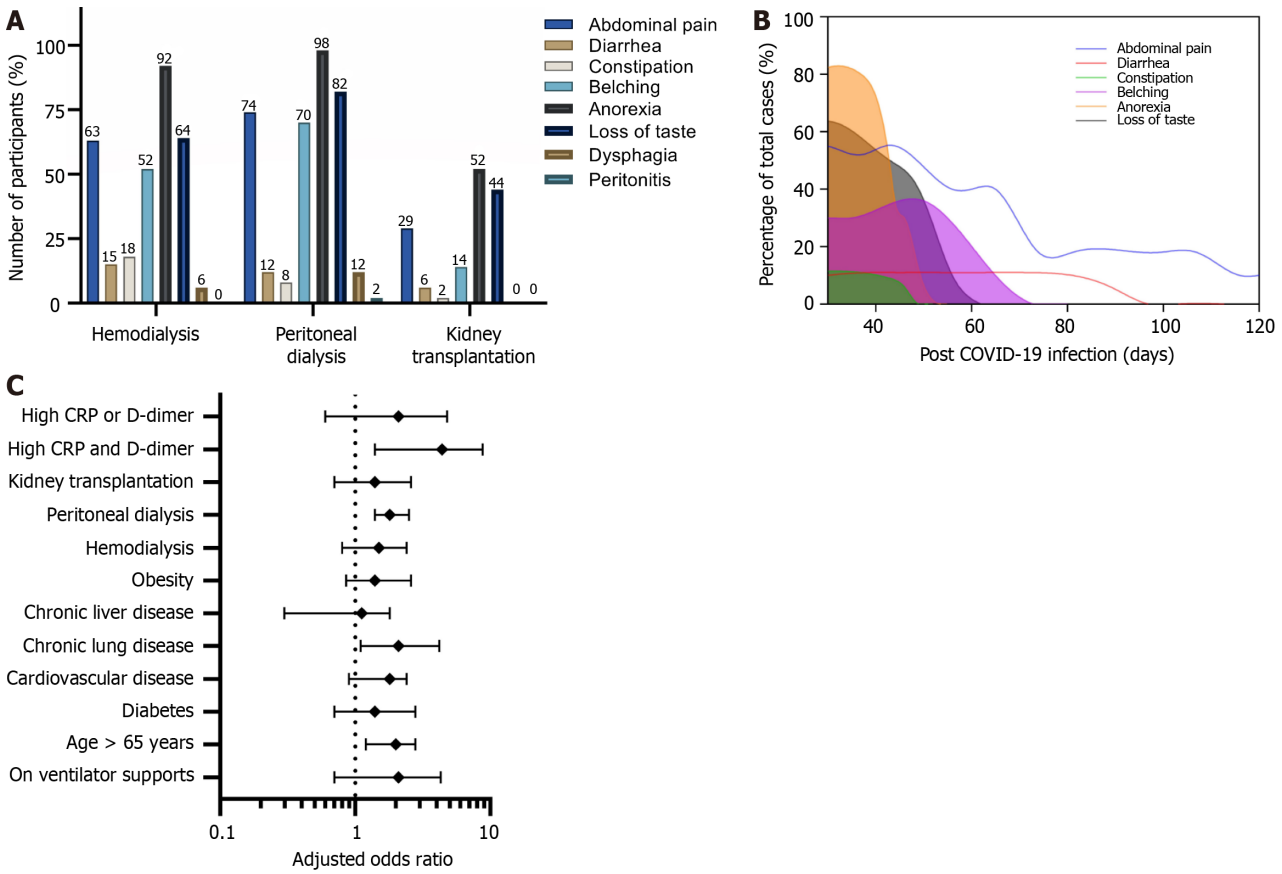

DOI: 10.3748/wjg.v29.i19.3013

Figure 2 The burden of gastrointestinal manifestations of prolonged symptoms after corona virus disease 2019. Post-acute sequelae were followed from 30 d after infection until the end of follow-up. A: Comparison of the prevalence and characteristics of prolonged symptoms after corona virus disease 2019 (Long-COVID) among dialysis-dependent (HD, *n* = 293; PD, *n* = 21) and kidney transplant recipients (*n* = 7); B: Time course of individual Long-COVID syndrome and resolution of symptoms. The color shading indicates Long-COVID syndrome that resolved within 90 d; C: Risk factors for gastrointestinal manifestations of Long-COVID. Long-COVID: Prolonged symptoms after corona virus disease 2019; CRP: C-reactive protein (high CRP > 5 mg/L, D-dimer > 500 ng/mL).

Figure 2C, also leads to a greater risk of GI manifestations of Long-COVID[44]. Although COVID-19 outcomes are comparable between PD and HD patients[45], the findings of the present study demonstrated that PD patients have a greater risk of developing GI manifestations of Long-COVID. Being elderly and having more symptoms (Table 1) may constitute key risk factors for developing Long-COVID in PD patients[46].

Irritable bowel syndrome, a condition with diverse symptoms, including diarrhea, constipation, and mixed bowel habits according to the Rome criteria[47], has been recently proposed as a possible consequence of COVID-19 infection due to disruption of the diversity and stability of the gut microbiota [48]. For this reason, evaluation of whether diarrhea and indigestion manifestations of Long-COVID alter the gut microbiome would be worth investigating[49]. This possibility also suggests that the use of specific probiotics and prebiotics in COVID-19 clinical treatment may help KT recipients with COVID-19 infections to rebalance their gut and lung microbial ecology, thereby boosting their immune responses against the virus in response to a new metabolic milieu[50].

Moreover, little is known about the pathophysiology of the abdominal pain manifestation of Long-COVID-19. Prolonged shedding of SARS-CoV-2 from the GI tract has been observed and could be responsible for some of the GI manifestations of Long-COVID[51]. Interestingly, we found that over one-third of our KT recipients had been diagnosed with mesenteric panniculitis-related Long-COVID. Although this is a rare condition, concern is growing regarding the conditional pain associated with COVID-19[52,53]. Notably, all of our recipients with mesenteric panniculitis fully recovered after corticosteroid administration, suggesting that systemic inflammation is the process involved here[54]. Although renal allograft dysfunction and graft loss following COVID-19 infection are possibly resulted from direct toxicity of SARS-CoV-2, cytokine storm-induced tubular injury, reduced immunosuppressive drugs during infection and decreased renal allograft blood flow from multiple organ failure[55-57], there was no reported case of acute kidney injury in the cohort.

The strengths of the present study are that we compiled the data available on the prevalence, symptomatology, and specific treatment of the particular GI manifestations of Long-COVID symptoms; this

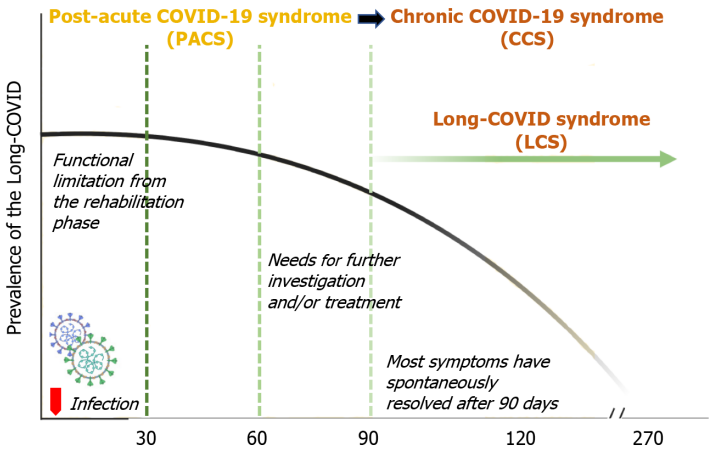

DOI: 10.3748/wjg.v29.i19.3013 **Copyright** ©The Author(s) 2023.

Figure 3 Illustration of the proposed new nomenclature for clinical syndromes following post-corona virus disease 2019 infection. We propose that the term post-acute-corona virus disease 2019 (COVID-19) syndrome should describe illness occurring within 90 d from the onset of COVID-19 infection. Chronic COVID-19 syndrome (CCS) would then be a modified classification that refers to the clinical syndrome thereafter. By contrast, the term Long-COVID syndrome should be reserved for patients showing CCS lasting for at least six months. In the case of severe symptoms, the investigation and corresponding treatments should be addressed at 60 d to prevent serious CCS. Long-COVID: Prolonged symptoms after corona virus disease 2019.

will help to guide clinicians in dealing with the pandemic. The identification of GI manifestations of Long-COVID in KT recipients could also help to define the contours of this new SARS-CoV-2 virus. Some limitations of the present study should also be acknowledged. This was a renal referral center study with a limited diversity of patient characteristics. No non-COVID-19 patients were included in the study, and the small number of participants made the study underpowered for investigating the risk factors associated with GI symptoms. Thus, the results need confirmation with larger cohorts that can apply the structural equation modeling for analysis, which has greater statistical power in terms of the probability of rejecting of a false null hypothesis than multiple regression analysis does[58]. In addition, the influence of different SARS-CoV-2 variants on GI manifestations of Long-COVID in dialysis-dependent and KT patients was not clarified, nor was the vaccination status against different variants addressed in our cohorts. However, based on the timing of the pandemic, the main strain circulating at the time of our study was the Delta (B.1.617) strain, accompanied by an early wave of the Omicron (B.1.1.529) variants[59,60]. Accordingly, an in-depth analysis of confounders should also be performed in larger, multinational cohorts. It is also challenging to find unrecovered pathophysiology of the long-term GI effects of COVID-19. Future research should not overlook other organ interactions to GI manifestations of Long-COVID, for instance, mental health symptoms (*e.g.*, depression and anxiety symptoms) nor additional post-infectious symptoms that were not assessed in the present study (*e.g.*, cardiovascular disease), as depression[61-63], gut-brain axis[64] or cardiovascular diseases[65] are the main etiology of long-term comorbidity of COVID-19[5], especially in HD patients[66]. In addition to lack of appetite, ESRD is recognized as a high risk of pre-existing undernutrition (malnutrition), including micronutrient deficiencies from malnutrition-inflammation-cachexia complex[67], which has been linked to increased mortality in patients with COVID-19[68]. Thus, nutrition support could be another critical intervention during COVID-19 infection in ESRD that robust research is needed for clarification as, vice versa, reduced long-term GI sequelae is probably part of the overall benefit from nutritional support.

CONCLUSION

In conclusion, at 3 mo after infection with SARS-CoV-2, renal replacement therapy patients and KT recipients with COVID-19 show high rates of GI manifestations of Long-COVID after discharge following their initial episode. These data point to optimized management as a potential line of research for decreasing Long-COVID syndrome in these populations.

ARTICLE HIGHLIGHTS

Research background

The characteristics of persistent coronavirus disease 2019 (COVID-19) symptoms or Long-COVID in

dialysis-dependent patients and kidney transplant (KT) is remain underestimate and urgent needs for investigation to prevent long-term complication in these vulnerable population.

Research motivation

End stage renal disease is a well-known condition for high mortality risk following COVID-19 infection. Thus, it is essential to explore the Long-COVID in these population as an early preventive strategy for preventing further morbidity and mortality.

Research objectives

To identify the characteristics of gastrointestinal (GI) manifestations of Long-COVID in patients with dialysis-dependent or KT status.

Research methods

A prospective, observational study was conducted during January 2022 to July 2022 in patients with COVID-19 infection to explore the Long-COVID symptoms in 3-months after the onset by interviewing.

Research results

As of 577 cases agreed to the interviews, the mean age was 52±11 years with 52% women. Long-COVID was identified in 56%, 62% and 37% in hemodialysis, peritoneal dialysis, and KT respectively. While fatigue was the most prevalent (96%) of the non-GI tract symptoms, anorexia (90.9%), loss of taste (64.4%), and abdominal pain (62.5%) were the first three common GI manifestations of Long-COVID. Of note, there were 6 cases of mesenteric panniculitis from 19 patients with GI symptoms in the KT group.

Research conclusions

Renal replacement therapy patients and KT recipients with COVID-19 show high rates of GI manifestations of Long-COVID after discharge following their initial episode.

Research perspectives

Further study should aim to explore the pathophysiology of the long-term GI effects of COVID-19 in renal replacement therapy and KT patients, which may have different immune response to Long-COVID symptoms compared to those with immunocompetent.

FOOTNOTES

Author contributions: Chancharoenthana W and Kamolratanakul S designed the research study; Chancharoenthana W, Kamolratanakul S, Ariyanon W, Chinpraditsuk S, and Saelim R performed the research and collected data; Chancharoenthana W, Kamolratanakul S, Ariyanon W, and Chinpraditsuk S analysed the data; Chancharoenthana W and Kamolratanakul drafted the manuscript. Chancharoenthana W, Kamolratanakul S, Leelahavanichkul A, Vadcharavivad S, Phumratanaprapin W, and Wilairatana P edited the manuscript; all authors have read and approve the final manuscript.

Institutional review board statement: The study was approved by the Human Research Ethics Committee of Faculty of Tropical Medicine, Mahidol University, Thailand (MUTM 2022-081-01).

Informed consent statement: Informed consent for participation in interviews was obtained either written or verbally over the phone from all participants in the study.

Conflict-of-interest statement: There are no conflicts of interest to disclose.

Data sharing statement: The data underlying this article will be shared on reasonable request to the corresponding author.

STROBE statement: The authors have read the STROBE Statement—checklist of items, and the manuscript was prepared and revised according to the STROBE Statement—checklist of items.

Country/Territory of origin: Thailand

ORCID number: Wiwat Chancharoenthana 0000-0002-2965-146X; Supitcha Kamolratanakul 0000-0002-0428-2354; Asada Leelahavanichkul 0000-0002-5566-6403; Somratai Vadcharavivad 0000-0001-5080-7070; Weerapong Phumratanaprapin 0000-

0001-5896-1961.

S-Editor: Chang KL
L-Editor: A
P-Editor: Zhao S

REFERENCES

1 **Marshall M**. The lasting misery of coronavirus long-haulers. *Nature* 2020; **585**: 339-341 [PMID: 32929257 DOI: 10.1038/d41586-020-02598-6]

2 **Nalbandian A**, Sehgal K, Gupta A, Madhavan MV, McGroder C, Stevens JS, Cook JR, Nordvig AS, Shalev D, Sehrawat TS, Ahluwalia N, Bikdeli B, Dietz D, Der-Nigoghossian C, Liyanage-Don N, Rosner GF, Bernstein EJ, Mohan S, Beckley AA, Seres DS, Choueiri TK, Uriel N, Ausiello JC, Accili D, Freedberg DE, Baldwin M, Schwartz A, Brodie D, Garcia CK, Elkind MSV, Connors JM, Bilezikian JP, Landry DW, Wan EY. Post-acute COVID-19 syndrome. *Nat Med* 2021; **27**: 601-615 [PMID: 33753937 DOI: 10.1038/s41591-021-01283-z]

3 **Raveendran AV**, Jayadevan R, Sashidharan S. Long COVID: An overview. *Diabetes Metab Syndr* 2021; **15**: 869-875 [PMID: 33892403 DOI: 10.1016/j.dsx.2021.04.007]

4 **Maltezou HC**, Pavli A, Tsakris A. Post-COVID Syndrome: An Insight on Its Pathogenesis. *Vaccines (Basel)* 2021; **9** [PMID: 34066007 DOI: 10.3390/vaccines9050497]

5 **Visco V**, Vitale C, Rispoli A, Izzo C, Virtuoso N, Ferruzzi GJ, Santopietro M, Melfi A, Rusciano MR, Maglio A, Di Pietro P, Carrizzo A, Galasso G, Vatrella A, Vecchione C, Ciccarelli M. Post-COVID-19 Syndrome: Involvement and Interactions between Respiratory, Cardiovascular and Nervous Systems. *J Clin Med* 2022; **11** [PMID: 35159974 DOI: 10.3390/jcm11030524]

6 National Institute for Health and Care Excellence: Clinical Guidelines. COVID-19 rapid guideline: managing the long-term effects of COVID-19. London: National Institute for Health and Care Excellence (NICE), 2020

7 **Soriano JB**, Murthy S, Marshall JC, Relan P, Diaz JV; WHO Clinical Case Definition Working Group on Post-COVID-19 Condition. A clinical case definition of post-COVID-19 condition by a Delphi consensus. *Lancet Infect Dis* 2022; **22**: e102-e107 [PMID: 34951953 DOI: 10.1016/S1473-3099(21)00703-9]

8 **Modelli de Andrade LG**, de Sandes-Freitas TV, Requião-Moura LR, Viana LA, Cristelli MP, Garcia VD, Alcântara ALC, Esmeraldo RM, Abbud Filho M, Pacheco-Silva A, de Lima Carneiro ECR, Manfro RC, Costa KMAH, Simão DR, de Sousa MV, Santana VBBM, Noronha IL, Romão EA, Zanocco JA, Arimatea GGQ, De Boni Monteiro de Carvalho D, Tedesco-Silva H, Medina-Pestana J; COVID-19-KT Brazil. Development and validation of a simple web-based tool for early prediction of COVID-19-associated death in kidney transplant recipients. *Am J Transplant* 2022; **22**: 610-625 [PMID: 34416075 DOI: 10.1111/ajt.16807]

9 **Basic-Jukic N**, Juric I, Furic-Cunko V, Katalinic L, Radic J, Bosnjak Z, Jelakovic B, Kastelan Z. Follow-up of renal transplant recipients after acute COVID-19-A prospective cohort single-center study. *Immun Inflamm Dis* 2021; **9**: 1563-1572 [PMID: 34414665 DOI: 10.1002/iid3.509]

10 **Malinowska A**, Muchlado M, Ślizień Z, Biedunkiewicz B, Heleniak Z, Dębska-Ślizień A, Tylicki L. Post-COVID-19 Sydrome and Decrease in Health-Related Quality of Life in Kidney Transplant Recipients after SARS-COV-2 Infection-A Cohort Longitudinal Study from the North of Poland. *J Clin Med* 2021; **10** [PMID: 34768725 DOI: 10.3390/jcm10215205]

11 **Chauhan S**, Meshram HS, Kute V, Patel H, Desai S, Dave R. Long-term follow-up of SARS-CoV-2 recovered renal transplant recipients: A single-center experience from India. *Transpl Infect Dis* 2021; **23**: e13735 [PMID: 34547156 DOI: 10.1111/tid.13735]

12 **Amorim CEN**, Gomes VLT, Cristelli MP, Viana LA, de Luca Correa H, Lima GBB, de Sousa Silva FS, de Castro Lima GS, Rosa TDS, Nakamura MR, Quintino PM, Tedesco-Silva H, Medina-Pestana J. High Prevalence of Long-COVID Among Kidney Transplant Recipients: A Longitudinal Cohort Study. *Transplantation* 2022; **106**: 2408-2415 [PMID: 36228200 DOI: 10.1097/TP.0000000000004359]

13 **Och A**, Tylicki P, Polewska K, Puchalska-Reglińska E, Parczewska A, Szabat K, Biedunkiewicz B, Dębska-Ślizień A, Tylicki L. Persistent Post-COVID-19 Syndrome in Hemodialyzed Patients-A Longitudinal Cohort Study from the North of Poland. *J Clin Med* 2021; **10** [PMID: 34640471 DOI: 10.3390/jcm10194451]

14 **Demiray A**, Kanbay A, Kanbay M. Long-term effect of COVID-19 infection on hemodialysis patients: Should we follow hemodialysis patients more closely? *Clin Kidney J* 2022; **15**: 369-371 [PMID: 35198153 DOI: 10.1093/ckj/sfab265]

15 **Zuo T**, Liu Q, Zhang F, Lui GC, Tso EY, Yeoh YK, Chen Z, Boon SS, Chan FK, Chan PK, Ng SC. Depicting SARS-CoV-2 faecal viral activity in association with gut microbiota composition in patients with COVID-19. *Gut* 2021; **70**: 276-284 [PMID: 32690600 DOI: 10.1136/gutjnl-2020-322294]

16 **Saithong S**, Worasilchai N, Saisorn W, Udompornpitak K, Bhunyakarnjanarat T, Chindamporn A, Tovichayathamrong P, Torvorapanit P, Chiewchengchol D, Chancharoenthana W, Leelahavanichkul A. Neutrophil Extracellular Traps in Severe SARS-CoV-2 Infection: A Possible Impact of LPS and (1→3)-β-D-glucan in Blood from Gut Translocation. *Cells* 2022; **11** [PMID: 35406667 DOI: 10.3390/cells11071103]

17 **Hoffmann M**, Kleine-Weber H, Schroeder S, Krüger N, Herrler T, Erichsen S, Schiergens TS, Herrler G, Wu NH, Nitsche A, Müller MA, Drosten C, Pöhlmann S. SARS-CoV-2 Cell Entry Depends on ACE2 and TMPRSS2 and Is Blocked by a Clinically Proven Protease Inhibitor. *Cell* 2020; **181**: 271-280.e8 [PMID: 32142651 DOI: 10.1016/j.cell.2020.02.052]

18 **Docherty AB**, Harrison EM, Green CA, Hardwick HE, Pius R, Norman L, Holden KA, Read JM, Dondelinger F, Carson G, Merson L, Lee J, Plotkin D, Sigfrid L, Halpin S, Jackson C, Gamble C, Horby PW, Nguyen-Van-Tam JS, Ho A, Russell CD, Dunning J, Openshaw PJ, Baillie JK, Semple MG; ISARIC4C investigators. Features of 20 133 UK patients

in hospital with covid-19 using the ISARIC WHO Clinical Characterisation Protocol: prospective observational cohort study. *BMJ* 2020; **369**: m1985 [PMID: 32444460 DOI: 10.1136/bmj.m1985]

19 **Zhang H**, Zang C, Xu Z, Zhang Y, Xu J, Bian J, Morozyuk D, Khullar D, Nordvig AS, Schenck EJ, Shenkman EA, Rothman RL, Block JP, Lyman K, Weiner MG, Carton TW, Wang F, Kaushal R. Data-driven identification of post-acute SARS-CoV-2 infection subphenotypes. *Nat Med* 2023; **29**: 226-235 [PMID: 36456834 DOI: 10.1038/s41591-022-02116-3]

20 **Meringer H**, Mehandru S. Gastrointestinal post-acute COVID-19 syndrome. *Nat Rev Gastroenterol Hepatol* 2022; **19**: 345-346 [PMID: 35383321 DOI: 10.1038/s41575-022-00611-z]

21 **Al-Aly Z**, Xie Y, Bowe B. High-dimensional characterization of post-acute sequelae of COVID-19. *Nature* 2021; **594**: 259-264 [PMID: 33887749 DOI: 10.1038/s41586-021-03553-9]

22 **Burke MJ**, Del Rio C. Long COVID has exposed medicine's blind-spot. *Lancet Infect Dis* 2021; **21**: 1062-1064 [PMID: 34153235 DOI: 10.1016/S1473-3099(21)00333-9]

23 **Requião-Moura LR**, Sandes-Freitas TV, Viana LA, Cristelli MP, Andrade LGM, Garcia VD, Oliveira CMC, Esmeraldo RM, Abbud Filho M, Pacheco-Silva A, Sousa KC, Vicari AR, Costa KMAH, Simão DR, Sousa MV, Campos JB, Almeida RAMB, Deboni LM, Neto MM, Zanocco JA, Tedesco-Silva H, Medina-Pestana J; COVID-19-KT Brazil. High mortality among kidney transplant recipients diagnosed with coronavirus disease 2019: Results from the Brazilian multicenter cohort study. *PLoS One* 2021; **16**: e0254822 [PMID: 34320005 DOI: 10.1371/journal.pone.0254822]

24 **Medina-Pestana J**, Cristelli MP, Foresto RD, Tedesco-Silva H, Requião-Moura LR. The Higher COVID-19 Fatality Rate Among Kidney Transplant Recipients Calls for Further Action. *Transplantation* 2022; **106**: 908-910 [PMID: 35250005 DOI: 10.1097/TP.0000000000004086]

25 **Amin-Chowdhury Z**, Ladhani SN. Causation or confounding: why controls are critical for characterizing long COVID. *Nat Med* 2021; **27**: 1129-1130 [PMID: 34140704 DOI: 10.1038/s41591-021-01402-w]

26 **Romero-Duarte Á**, Rivera-Izquierdo M, Guerrero-Fernández de Alba I, Pérez-Contreras M, Fernández-Martínez NF, Ruiz-Montero R, Serrano-Ortiz Á, González-Serna RO, Salcedo-Leal I, Jiménez-Mejías E, Cárdenas-Cruz A. Sequelae, persistent symptomatology and outcomes after COVID-19 hospitalization: the ANCOHVID multicentre 6-month follow-up study. *BMC Med* 2021; **19**: 129 [PMID: 34011359 DOI: 10.1186/s12916-021-02003-7]

27 **Dennis A**, Wamil M, Alberts J, Oben J, Cuthbertson DJ, Wootton D, Crooks M, Gabbay M, Brady M, Hishmeh L, Attree E, Heightman M, Banerjee R, Banerjee A; COVERSCAN study investigators. Multiorgan impairment in low-risk individuals with post-COVID-19 syndrome: a prospective, community-based study. *BMJ Open* 2021; **11**: e048391 [PMID: 33785495 DOI: 10.1136/bmjopen-2020-048391]

28 **Blackett JW**, Wainberg M, Elkind MSV, Freedberg DE. Potential Long Coronavirus Disease 2019 Gastrointestinal Symptoms 6 Months After Coronavirus Infection Are Associated With Mental Health Symptoms. *Gastroenterology* 2022; **162**: 648-650.e2 [PMID: 34728186 DOI: 10.1053/j.gastro.2021.10.040]

29 **Carfì A**, Bernabei R, Landi F; Gemelli Against COVID-19 Post-Acute Care Study Group. Persistent Symptoms in Patients After Acute COVID-19. *JAMA* 2020; **324**: 603-605 [PMID: 32644129 DOI: 10.1001/jama.2020.12603]

30 **Moreno-Pérez O**, Merino E, Leon-Ramirez JM, Andres M, Ramos JM, Arenas-Jiménez J, Asensio S, Sanchez R, Ruiz-Torregrosa P, Galan I, Scholz A, Amo A, González-delaAleja P, Boix V, Gil J; COVID19-ALC research group. Post-acute COVID-19 syndrome. Incidence and risk factors: A Mediterranean cohort study. *J Infect* 2021; **82**: 378-383 [PMID: 33450302 DOI: 10.1016/j.jinf.2021.01.004]

31 **Carvalho-Schneider C**, Laurent E, Lemaignen A, Beaufils E, Bourbao-Tournois C, Laribi S, Flament T, Ferreira-Maldent N, Bruyère F, Stefic K, Gaudy-Graffin C, Grammatico-Guillon L, Bernard L. Follow-up of adults with noncritical COVID-19 two months after symptom onset. *Clin Microbiol Infect* 2021; **27**: 258-263 [PMID: 33031948 DOI: 10.1016/j.cmi.2020.09.052]

32 **Caso JR**, MacDowell KS, Soto M, Ruiz-Guerrero F, Carrasco-Díaz Á, Leza JC, Carrasco JL, Díaz-Marsá M. Dysfunction of Inflammatory Pathways and Their Relationship With Psychological Factors in Adult Female Patients With Eating Disorders. *Front Pharmacol* 2022; **13**: 846172 [PMID: 35517819 DOI: 10.3389/fphar.2022.846172]

33 **Chancharoenthana W**, Udompronpitak K, Manochantr Y, Kantagowit P, Kaewkanha P, Issara-Amphorn J, Leelahavanichkul A. Repurposing of High-Dose Erythropoietin as a Potential Drug Attenuates Sepsis in Preconditioning Renal Injury. *Cells* 2021; **10** [PMID: 34831360 DOI: 10.3390/cells10113133]

34 **Meijers RW**, Litjens NH, de Wit EA, Langerak AW, Baan CC, Betjes MG. Uremia-associated immunological aging is stably imprinted in the T-cell system and not reversed by kidney transplantation. *Transpl Int* 2014; **27**: 1272-1284 [PMID: 25082296 DOI: 10.1111/tri.12416]

35 **Betjes MG**. Immune cell dysfunction and inflammation in end-stage renal disease. *Nat Rev Nephrol* 2013; **9**: 255-265 [PMID: 23507826 DOI: 10.1038/nrneph.2013.44]

36 **Sudre CH**, Murray B, Varsavsky T, Graham MS, Penfold RS, Bowyer RC, Pujol JC, Klaser K, Antonelli M, Canas LS, Molteni E, Modat M, Jorge Cardoso M, May A, Ganesh S, Davies R, Nguyen LH, Drew DA, Astley CM, Joshi AD, Merino J, Tsereteli N, Fall T, Gomez MF, Duncan EL, Menni C, Williams FMK, Franks PW, Chan AT, Wolf J, Ourselin S, Spector T, Steves CJ. Author Correction: Attributes and predictors of long COVID. *Nat Med* 2021; **27**: 1116 [PMID: 34045738 DOI: 10.1038/s41591-021-01361-2]

37 **Vibholm LK**, Nielsen SSF, Pahus MH, Frattari GS, Olesen R, Andersen R, Monrad I, Andersen AHF, Thomsen MM, Konrad CV, Andersen SD, Højen JF, Gunst JD, Østergaard L, Søgaard OS, Schleimann MH, Tolstrup M. SARS-CoV-2 persistence is associated with antigen-specific CD8 T-cell responses. *EBioMedicine* 2021; **64**: 103230 [PMID: 33530000 DOI: 10.1016/j.ebiom.2021.103230]

38 **Wang EY**, Mao T, Klein J, Dai Y, Huck JD, Liu F, Zheng NS, Zhou T, Israelow B, Wong P, Lucas C, Silva J, Oh JE, Song E, Perotti ES, Fischer S, Campbell M, Fournier JB, Wyllie AL, Vogels CBF, Ott IM, Kalinich CC, Petrone ME, Watkins AE; Yale IMPACT Team, Cruz CD, Farhadian SF, Schulz WL, Grubaugh ND, Ko AI, Iwasaki A, Ring AM. Diverse Functional Autoantibodies in Patients with COVID-19. *medRxiv* 2021 [PMID: 33330894 DOI: 10.1101/2020.12.10.20247205]

39 **Thomas RM**, Jobin C. Microbiota in pancreatic health and disease: the next frontier in microbiome research. *Nat Rev*

Gastroenterol Hepatol 2020; **17**: 53-64 [PMID: 31811279 DOI: 10.1038/s41575-019-0242-7]

40 **Astin R**, Banerjee A, Baker MR, Dani M, Ford E, Hull JH, Lim PB, McNarry M, Morten K, O'Sullivan O, Pretorius E, Raman B, Soteropoulos DS, Taquet M, Hall CN. Long COVID: mechanisms, risk factors and recovery. *Exp Physiol* 2023; **108**: 12-27 [PMID: 36412084 DOI: 10.1113/EP090802]

41 **Enaud R**, Prevel R, Ciarlo E, Beaufils F, Wieërs G, Guery B, Delhaes L. The Gut-Lung Axis in Health and Respiratory Diseases: A Place for Inter-Organ and Inter-Kingdom Crosstalks. *Front Cell Infect Microbiol* 2020; **10**: 9 [PMID: 32140452 DOI: 10.3389/fcimb.2020.00009]

42 **Sirivongrangson P**, Kulvichit W, Payungporn S, Pisitkun T, Chindamporn A, Peerapornratana S, Pisitkun P, Chitcharoen S, Sawaswong V, Worasilchai N, Kampunya S, Putcharoen O, Thawitsri T, Leelayuwatanakul N, Kongpolprom N, Phoophiboon V, Sriprasart T, Samransamruajkit R, Tungsanga S, Tiankanon K, Lumlertgul N, Leelahavanichkul A, Sriphojanart T, Tantawichien T, Thisyakorn U, Chirathaworn C, Praditpornsilpa K, Tungsanga K, Eiam-Ong S, Sitprija V, Kellum JA, Srisawat N. Endotoxemia and circulating bacteriome in severe COVID-19 patients. *Intensive Care Med Exp* 2020; **8**: 72 [PMID: 33284413 DOI: 10.1186/s40635-020-00362-8]

43 **Cichoż-Lach H**, Michalak A. Liver injury in the era of COVID-19. *World J Gastroenterol* 2021; **27**: 377-390 [PMID: 33584070 DOI: 10.3748/wjg.v27.i5.377]

44 **Mandal S**, Barnett J, Brill SE, Brown JS, Denneny EK, Hare SS, Heightman M, Hillman TE, Jacob J, Jarvis HC, Lipman MCI, Naidu SB, Nair A, Porter JC, Tomlinson GS, Hurst JR; ARC Study Group. 'Long-COVID': a cross-sectional study of persisting symptoms, biomarker and imaging abnormalities following hospitalisation for COVID-19. *Thorax* 2021; **76**: 396-398 [PMID: 33172844 DOI: 10.1136/thoraxjnl-2020-215818]

45 **Ghonimi TAL**, Alkad MM, Abuhelaiqa EA, Othman MM, Elgaali MA, Ibrahim RAM, Joseph SM, Al-Malki HA, Hamad AI. Mortality and associated risk factors of COVID-19 infection in dialysis patients in Qatar: A nationwide cohort study. *PLoS One* 2021; **16**: e0254246 [PMID: 34293004 DOI: 10.1371/journal.pone.0254246]

46 **Robineau O**, Zins M, Touvier M, Wiernik E, Lemogne C, de Lamballerie X, Blanché H, Deleuze JF, Saba Villarroel PM, Dorival C, Nicol J, Gomes-Rima R, Correia E, Coeuret-Pellicer M, Druesne-Pecollo N, Esseddik Y, Ribet C, Goldberg M, Severi G, Carrat F; Santé, Pratiques, Relations et Inégalités Sociales en Population Générale Pendant la Crise COVID-19–Sérologie (SAPRIS-SERO) Study Group. Long-lasting Symptoms After an Acute COVID-19 Infection and Factors Associated With Their Resolution. *JAMA Netw Open* 2022; **5**: e2240985 [PMID: 36350653 DOI: 10.1001/jamanetworkopen.2022.40985]

47 **Drossman DA**, Hasler WL. Rome IV-Functional GI Disorders: Disorders of Gut-Brain Interaction. *Gastroenterology* 2016; **150**: 1257-1261 [PMID: 27147121 DOI: 10.1053/j.gastro.2016.03.035]

48 **Settanni CR**, Ianiro G, Ponziani FR, Bibbò S, Segal JP, Cammarota G, Gasbarrini A. COVID-19 as a trigger of irritable bowel syndrome: A review of potential mechanisms. *World J Gastroenterol* 2021; **27**: 7433-7445 [PMID: 34887641 DOI: 10.3748/wjg.v27.i43.7433]

49 **Liu Q**, Mak JWY, Su Q, Yeoh YK, Lui GC, Ng SSS, Zhang F, Li AYL, Lu W, Hui DS, Chan PK, Chan FKL, Ng SC. Gut microbiota dynamics in a prospective cohort of patients with post-acute COVID-19 syndrome. *Gut* 2022; **71**: 544-552 [PMID: 35082169 DOI: 10.1136/gutjnl-2021-325989]

50 **Tungsanga S**, Panpetch W, Bhunyakarnjanarat T, Udompornpitak K, Katavetin P, Chancharoenthana W, Chatthanathon P, Somboonna N, Tungsanga K, Tumwasorn S, Leelahavanichkul A. Uremia-Induced Gut Barrier Defect in 5/6 Nephrectomized Mice Is Worsened by Candida Administration through a Synergy of Uremic Toxin, Lipopolysaccharide, and (1→3)-β-D-Glucan, but Is Attenuated by Lacticaseibacillus rhamnosus L34. *Int J Mol Sci* 2022; **23** [PMID: 35269654 DOI: 10.3390/ijms23052511]

51 **Wu Y**, Guo C, Tang L, Hong Z, Zhou J, Dong X, Yin H, Xiao Q, Tang Y, Qu X, Kuang L, Fang X, Mishra N, Lu J, Shan H, Jiang G, Huang X. Prolonged presence of SARS-CoV-2 viral RNA in faecal samples. *Lancet Gastroenterol Hepatol* 2020; **5**: 434-435 [PMID: 32199469 DOI: 10.1016/S2468-1253(20)30083-2]

52 **Mandala S**, Kodati R, Tadepalli A, Reddy C, Kalyan S. An Unusual Cause of Acute Abdominal Pain in Coronavirus Disease (COVID-19): Report of Two Cases. *Indian J Crit Care Med* 2022; **26**: 1045-1048 [PMID: 36213717 DOI: 10.5005/jp-journals-10071-24310]

53 **Alyousef IA**, Alsaileek ZA, Alabdulsalam MA, Almohanna MA, Alshaqhaa NA, Alqahtani MM, Al Alyany AA, Alzahrani MA, Fallatah HA, Alqadhib JI, Alhawsawi AM, Alsuhaymi AD, Alasmari AM, Alshareef AJ, Al-Hawaj F. Mesenteric Panniculitis and COVID-19: A Rare Association. *Cureus* 2022; **14**: e21314 [PMID: 35186573 DOI: 10.7759/cureus.21314]

54 **Jiang QW**, Wang FD, Wang WZ, Wu X, Shu HJ, Li JN, Yang AM, Qian JM, Wu D. [An analysis of clinical characteristics of twelve cases of mesenteric panniculitis]. *Zhonghua Nei Ke Za Zhi* 2017; **56**: 112-115 [PMID: 28162180 DOI: 10.3760/cma.j.issn.0578-1426.2017.02.006]

55 **Cravedi P**, Mothi SS, Azzi Y, Haverly M, Farouk SS, Pérez-Sáez MJ, Redondo-Pachón MD, Murphy B, Florman S, Cyrino LG, Grafals M, Venkataraman S, Cheng XS, Wang AX, Zaza G, Ranghino A, Furian L, Manrique J, Maggiore U, Gandolfini I, Agrawal N, Patel H, Akalin E, Riella LV. COVID-19 and kidney transplantation: Results from the TANGO International Transplant Consortium. *Am J Transplant* 2020; **20**: 3140-3148 [PMID: 32649791 DOI: 10.1111/ajt.16185]

56 **Mohamed IH**, Chowdary PB, Shetty S, Sammartino C, Sivaprakasam R, Lindsey B, Thuraisingham R, Yaqoob MM, Khurram MA. Outcomes of Renal Transplant Recipients With SARS-CoV-2 Infection in the Eye of the Storm: A Comparative Study With Waitlisted Patients. *Transplantation* 2021; **105**: 115-120 [PMID: 33350626 DOI: 10.1097/TP.0000000000003406]

57 **Hadi YB**, Naqvi SFZ, Kupec JT, Sofka S, Sarwari A. Outcomes of COVID-19 in Solid Organ Transplant Recipients: A Propensity-matched Analysis of a Large Research Network. *Transplantation* 2021; **105**: 1365-1371 [PMID: 33988341 DOI: 10.1097/TP.0000000000003670]

58 **Beran TN**, Violato C. Structural equation modeling in medical research: a primer. *BMC Res Notes* 2010; **3**: 267 [PMID: 20969789 DOI: 10.1186/1756-0500-3-267]

59 **Chantasrisawad N**, Puthanakit T, Kornsitthikul K, Jaru-Ampornpan P, Tawan M, Matapituk P, Sophonphan J, Anugulruengkitt S, Tangsathapornpong A, Katanyutanon A; KIDSBOOST study team. Immunogenicity to SARS-CoV-2

Omicron variant among school-aged children with 2-dose of inactivated SARS-CoV-2 vaccines followed by BNT162b2 booster. *Vaccine X* 2022; **12**: 100221 [PMID: 36213592 DOI: 10.1016/j.jvacx.2022.100221]

60 **Chancharoenthana W**, Leelahavanichkul A, Chinpraditsuk S, Pongpirul K, Kamolratanakul S, Phumratanaprapin W, Wilairatana P, Pitisuttithum P. Social restriction versus herd immunity policies in the early phase of the SARS-CoV-2 pandemic: A mathematical modelling study. *Asian Pac J Allergy Immunol* 2021 [PMID: 33386788 DOI: 10.12932/AP-140720-0914]

61 **Nooripour R**, Ghanbari N, Radwin LE, Hosseinian S, Hassani-Abharian P. Development and validation of COVID-19 Stress Scale (CSS) in an Iranian non-clinical population. *Zahedan J Res Med Sci* 2022; **24**: e118719 [DOI: 10.5812/zjrms-118719]

62 **Nooripour R**, Hosseinian S, Farmani F, Abtahi Foroshani N, Ghanbari N, Farkhojasteh VS. Relationship Between Hardiness and Stress of COVID-19 Through the Mediating Role of Mindfulness in Iranian Students. *PCP* 2022; **10**: 193-202 [DOI: 10.32598/jpcp.10.3.288.7]

63 **Nooripour R**, Hosseinian S, Hussain AJ, Annabestani M, Maadal A, Radwin LE, Hassani-Abharian P, Pirkashani NG, Khoshkonesh A. How Resiliency and Hope Can Predict Stress of Covid-19 by Mediating Role of Spiritual Well-being Based on Machine Learning. *J Relig Health* 2021; **60**: 2306-2321 [PMID: 33398655 DOI: 10.1007/s10943-020-01151-z]

64 **Chen J**, Vitetta L. Gut-brain axis in the neurological comorbidity of COVID-19. *Brain Commun* 2021; **3**: fcab118 [PMID: 34169281 DOI: 10.1093/braincomms/fcab118]

65 **Elseidy SA**, Awad AK, Vorla M, Fatima A, Elbadawy MA, Mandal D, Mohamad T. Cardiovascular complications in the Post-Acute COVID-19 syndrome (PACS). *Int J Cardiol Heart Vasc* 2022; **40**: 101012 [PMID: 35355927 DOI: 10.1016/j.ijcha.2022.101012]

66 **Carriazo S**, Mas-Fontao S, Seghers C, Cano J, Goma E, Avello A, Ortiz A, Gonzalez-Parra E. Increased 1-year mortality in haemodialysis patients with COVID-19: a prospective, observational study. *Clin Kidney J* 2022; **15**: 432-441 [PMID: 35198156 DOI: 10.1093/ckj/sfab248]

67 **Kilpatrick RD**, McAllister CJ, Kovesdy CP, Derose SF, Kopple JD, Kalantar-Zadeh K. Association between serum lipids and survival in hemodialysis patients and impact of race. *J Am Soc Nephrol* 2007; **18**: 293-303 [PMID: 17167113 DOI: 10.1681/ASN.2006070795]

68 **Barazzoni R**, Breda J, Cuerda C, Schneider S, Deutz NE, Wickramasinghe K; COVID-19 Call Editorial Board. COVID-19: Lessons on malnutrition, nutritional care and public health from the ESPEN-WHO Europe call for papers. *Clin Nutr* 2022; **41**: 2858-2868 [PMID: 36075815 DOI: 10.1016/j.clnu.2022.07.033]

World Journal of Gastroenterology

Submit a Manuscript: https://www.f6publishing.com

World J Gastroenterol 2023 May 21; 29(19): 3027-3039

DOI: 10.3748/wjg.v29.i19.3027

ISSN 1007-9327 (print) ISSN 2219-2840 (online)

META-ANALYSIS

Short *vs* long-course antibiotic therapy in adults with acute cholangitis: A systematic review, meta-analysis, and evidence quality assessment

Karampet Kasparian, Chrysanthos D Christou, Konstantinos Petidis, Michail Doumas, Olga Giouleme

Specialty type: Gastroenterology and hepatology

Provenance and peer review: Unsolicited article; Externally peer reviewed.

Peer-review model: Single blind

Peer-review report's scientific quality classification

Grade A (Excellent): A, A
Grade B (Very good): 0
Grade C (Good): 0
Grade D (Fair): 0
Grade E (Poor): 0

P-Reviewer: Jain N, Latvia; Kimura Y, Japan

Received: March 4, 2023
Peer-review started: March 4, 2023
First decision: April 10, 2023
Revised: April 11, 2023
Accepted: April 23, 2023
Article in press: April 23, 2023
Published online: May 21, 2023

Karampet Kasparian, Clinic of Oncology, Gastroenterology and Hematology, Alfried Krupp Hospital, Essen 45131, Germany

Karampet Kasparian, Konstantinos Petidis, Michail Doumas, Olga Giouleme, Second Propedeutic Department of Internal Medicine, Hippokration General Hospital, Aristotle University of Thessaloniki, Thessaloniki 54642, Greece

Chrysanthos D Christou, Department of Transplantation Surgery, Hippokration General Hospital, Aristotle University of Thessaloniki, Thessaloniki 54642, Greece

Corresponding author: Karampet Kasparian, MD, MSc, Doctor, Clinic of Oncology, Gastroenterology and Hematology, Alfried Krupp Hospital, Alfried-Krupp-Strasse 21, Essen 45131, Germany. kar.kasparian@gmail.com

Abstract

BACKGROUND

Acute cholangitis (AC) constitutes an infection with increased mortality rates in the past. Due to new diagnostic tools and therapeutic methods, the mortality of AC has been significantly reduced nowadays. The initial antibiotic treatment of AC has been oriented to the most common pathogens connected to this infection. However, the optimal duration of the antibiotic treatment of AC is still debatable.

AIM

To investigate if shorter-course antibiotic treatments could be similarly effective to long-course treatments in adults with AC.

METHODS

This study constitutes a systematic review and meta-analysis of the existing literature concerning the duration of antibiotic therapy of AC and an assessment of the quality of the evidence. The study was conducted in accordance with the recommendations of the Preferred Reporting Items for Systematic Review and Meta-Analyses. Fifteen studies were included in the systematic review, and eight were eligible for meta-analysis. Due to heterogeneous duration cutoffs, three study-analysis groups were formed, with a cutoff of 2-3, 6-7, and 14 d.

RESULTS

A total of 2763 patients were included in the systematic review, and 1313 were

accounted for the meta-analysis. The mean age was 73.66 ± 14.67 years, and the male and female ratio was 1:08. No significant differences were observed in the mortality rates of antibiotic treatment of 2-3 d, compared to longer treatments (odds ratio = 0.78, 95% confidence interval: 0.23-2.67, *I2* = 9%) and the recurrence rates and hospitalization length were also not different in all study groups.

CONCLUSION

Short- and long-course antibiotic treatments may be similarly effective concerning the mortality and recurrence rates of AC. Safe conclusions cannot be extracted concerning the hospitalization duration.

Key Words: Acute cholangitis; Antibiotic; Short-course; Long-course; Antimicrobial; Treatment duration

Core Tip: The exact duration of antibiotic therapy for acute cholangitis in adult patients remains a controversial subject in the field of gastroenterology. A total antibiotic treatment of 4-7 d is recommended by the Tokyo Guidelines of 2018. However, recent studies present that schemata of shorter-course therapies could promise similar efficacy and safety. In our study, we systematically reviewed the existing literature in order to compare the death and recurrence rates and the length of hospitalization between patients with antibiotic treatments of shorter and longer durations. Our findings showed no significant differences between the study groups in all outcomes.

Citation: Kasparian K, Christou CD, Petidis K, Doumas M, Giouleme O. Short *vs* long-course antibiotic therapy in adults with acute cholangitis: A systematic review, meta-analysis, and evidence quality assessment. *World J Gastroenterol* 2023; 29(19): 3027-3039

URL: https://www.wjgnet.com/1007-9327/full/v29/i19/3027.htm

DOI: https://dx.doi.org/10.3748/wjg.v29.i19.3027

INTRODUCTION

The mortality rates of acute cholangitis (AC) have significantly decreased by comparing patients' data before 1980 and after 2000, from 10%-30% to 2.7%-10%[1]. Multiple factors, such as the development of modern diagnostic techniques, therapeutic methods for bile duct decompression, and new antibiotics adapted to microbiological studies, have significantly contributed to this improvement in the prognosis of AC[2].

The bacterial species commonly detected in AC differ in relationship with the severity of AC[1,3]. Because of this fact, the empirical antibiotic therapy provided should be oriented to the severity grade as defined in the Tokyo Guidelines (TG)[4]. Previous operations, the origin of the infection, possible allergies, pharmacodynamics, pharmacokinetics, local antibiogram and liver or renal dysfunction should also determine the choice of antimicrobial therapy in patients with AC[5].

A major issue concerning the therapy of AC is the exact duration of the definite antibiotic treatment. The TG 2018 (TG18) suggest that the antimicrobial therapy should last 4-7 d, and if gram-positive cocci are present, a minimum therapy of two weeks should be administrated[5]. This interval between the recommended treatment days is relatively wide, and the recommendation provided is not based on a high level of evidence (level C). Recent studies suggest that even a therapy of two or three days could be equally effective and safe, and it could reduce the length of in-hospital stay of patients, with a consequent reduction in the economic burden on the health systems[6-8]. A randomized controlled trial also showed similar clinical outcomes for patients with intraabdominal infections who received antibiotic therapy for two days after the resolution of fever, compared to those who received therapy for a maximum of 10 d[9].

Our purpose in conducting this systematic review and meta-analysis is to collect all available data existing in the current bibliography in order to ascertain if short-course antibiotic therapies could promise lower mortality, lower rates of recurrent AC, and shorter hospitalizations in adults with AC, compared to long-course antibiotic therapies and, if possible, to attempt to clarify the optimal duration of the antimicrobial treatment of the AC.

MATERIALS AND METHODS

Review protocol

Our systematic review was conducted according to the guidelines of the Preferred Reporting Items for Systematic reviews and Meta-Analyses (PRISMA)[10]. Two independent reviewers (Kasparian K and Christou CD) performed research in Medline-PubMed and Cochrane databases by applying a predefined research algorithm. The last search date was the 5th of October, 2022. The studies were initially controlled according to their title and abstract and followingly according to their full texts and the extractability of their content. We included studies concerning adults who received antibiotic therapy against AC, and whose therapy duration or mean/median duration was documented. We included only original studies in our systematic review (observational studies and randomized controlled trials). The exclusion criteria for the articles in our review, were studies concerning infantile population, animal studies, non-English studies, case reports or case series, comments or editorials, book chapters, studies with non-extractable data, abstract publications, protocols of incomplete clinical trials, irrelevant articles, surveys, and articles whose full-texts could not be retrieved. Conflicts during the eligibility process were resolved after a discussion between the two reviewers.

From the 1380 articles retrieved from the research, 50 were removed as duplicates and 1150 were excluded according to their titles and abstracts. From the 177 remaining studies, 15 were included in our systematic review[6,8,11-23], and the quantitative analysis of our research question was based on eight studies[8,11,12,16,17,21-23]. Forty-five papers contained data that was not extractable for our review, one study concerned a population of non-adult patients, 49 studies were irrelevant to our research questions, and the remaining excluded papers concerned non-original studies. One of the final papers constitutes a randomized-controlled trial, while the other fourteen concern retrospective observational studies. The details of the reasons for the exclusion of the papers are summarized in the PRISMA flowchart in Figure 1.

Data extraction

The two reviewers (Kasparian K and Christou CD) collected and tabulated independently the data of the final papers chosen for this review. Each reviewer gathered data concerning the study protocol, the baseline characteristics of the participants, and data concerning the outcomes and their definitions. The baseline characteristics to be collected for our review were predefined: Mean age and standard deviations (SD), gender, comorbidities, severity grade of AC, antibiotic therapy, and biliary drainage method. Heterogenous numerical data were transformed into the same predefined measurement units for statistical analysis. The two reviewers compared the data that each one collected, and conflicts were resolved between them.

Outcomes

The primary outcome of our study was the mortality of the patients. Secondary outcomes were the recurrence rate and the length of hospitalization of AC, measured with days. All outcomes were predefined. As mortality, we define the total, all-cause mortality of the participants until the end of the follow-up period of each study. In-hospital mortality due to AC was not examined.

Due to the heterogeneity in the time cutoff points between the intervention groups in each study, our quantitative analysis was divided into three subgroups. More specifically, an analysis was conducted among the studies which compared a therapy of 2-3 d to longer antibiotic treatments[6,8,11,21], studies with a cutoff of 6-7 d were separately analyzed[22,23], and the two papers which assessed clinical outcomes in AC-patients who received antibiotic treatment of for 14 d or less were summarized together [12,16].

Statistical analysis

All continuous variables are presented with the means and SD. For numerical variables which were not normally distributed and for which their medians and interquartile ranges or ranges were provided, we used the Hozo equation to calculate their means and SD[24]. For the data synthesis of the numerical variables, standardized mean differences (SMD) and 95% confidence intervals (95%CI) were calculated, with the use of Hedge´s method, for bias to be minimized[25]. For the categorical variables, we collected the absolute values and calculated the odds ratios (OR) and their 95%CIs. The data synthesis of the qualitative variables was based on the random effects model. In cases where no events were presented concerning a qualitative variable in a study group, the proper changes were conducted, in order for the statistical analysis to be feasible[26]. For the evaluation of the study heterogeneity, the I^2 value was calculated for each outcome. We presume $I^2 > 70\%$ as an indicator of heterogeneity among the studies. For all other measurements, we selected a P value of 0.05 as the cutoff point for the presence of statistical significance. All calculations and Forest plots were conducted through the program R Studio, version 1.4.1103.

Quality assessment

To assess the quality of the observational studies included in our systematic review and meta-analysis,

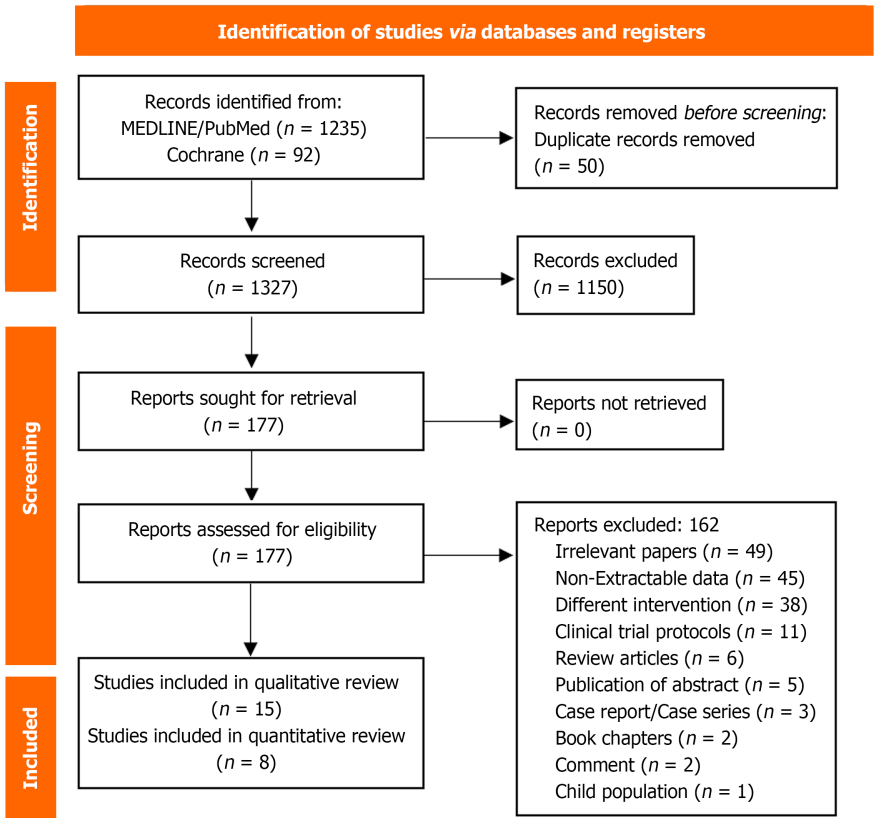

Figure 1 The Preferred Reporting Items for Systematic Review and Meta-Analyses flow chart of the systematic review and meta-analysis.

the Newcastle-Ottawa Scale was used[27]. The randomized clinical trials were evaluated for quality according to the Risk-of-Bias tool version 2 (RoB 2) provided by Cochrane[28]. Two reviewers (Kasparian K and Christou CD) independently assessed the final studies using the methods mentioned above, and possible conflicts were resolved afterward.

RESULTS

Baseline characteristics

As mentioned, 15 studies were included in our systematic review, and eight were considered eligible for the meta-analysis. The included studies were primarily conducted in Japan (8/15), two in the Netherlands, and the remaining studies originated from medical centers in France, Germany, Pakistan, South Korea, and Thailand. In 11/15 studies, the diagnosis of AC was based on the TG18/TG13 guidelines[6,8,12-14,16-18,20,21,23], two studies defined AC, depending on the TG07[15,19], Doi *et al*[22] controlled the presence the proper code of the 10th Edition of the International Classification of Diseases in hospital registries and positive bile or blood cultures for the selection of the patients, while van Lent *et al*[11] based the diagnosis of cholangitis on clinical, laboratory and imaging criteria.

The overall number of patients included in the systematic review was n = 2763, which corresponded to 2812 cases of AC. In the eight studies selected for the quantitative analysis, a total of 1219 patients and 1313 cases received antibiotic treatment against AC. The pooled mean age of the participants in the meta-analysis was 73.66 ± 14.67 years, and 721 (54.9%) of them were males, with a male to female ratio of 1:0.8. According to the TG18 severity grading system, 400/972 (41.1%) patients were classified as grade I, 525/972 (54.1%) as grade II while 45/972 (4.6%) of the patients suffered from grade III AC. Positive blood culture was detected in 383/742 (51.6%) participants. *Escherichia coli* (188/383, 49.1%) and *Klebsiella spp.* (75/383, 19.6%) were the most frequently identified pathogens, while 26/278 (9.3%) patients presented infection with gram-positive bacteria. A total of 244/1155 (21.1%) patients suffered from diabetes mellitus, 126/779 (16.2%) had a history of chronic kidney disease, and 107/779 (13.7%) participants presented a cardiac comorbidity, either chronic heart failure or coronary artery disease. Most patients received Cephalosporines (229/540, 42.4%) as antibiotic treatment and based on the available data, 275/326 (84.3%) patients underwent papillotomy during endoscopic retrograde cholangiopancreatography. For the last characteristic, only two studies included available data. Details for the baseline characteristics of the studies are summarized in Table 1.

Table 1 Baseline characteristics of the studies

Ref.	Country	Study period	Study design	Definition of AC	Population	Intervention	Outcomes
Ferstl *et al* [23], 2022	Germany	2008-2019	Retrospective observational study	TG18/TG13	Grade I and grade II AC after ERCP	Antibiotic therapy of 6 d	Recurrent cholangitis within 28 d
Kihara and Yokomizo [20], 2022	Japan	January 2009 to August 2018	Retrospective observational study	TG18/TG13	Postoperative cholangitis after pancreaticoduodenectomy	Antibiotic therapy and pancreaticoduoedenectomy	Clinical characteristics and outcomes in patients with acute cholangitis
Masuda *et al* [6], 2022	Japan	January 2018 to July 2020	Retrospective observational study	TG18/TG13	Grade I and grade II AC after successful ERCP	Antibiotic therapy of 3 d	30-d-mortality, recurrent cholangitis within 3 mo, length of hospitalization, in-hospital mortality
Sokal *et al*[14], 2022	France	2016-2018	Retrospective observational study	TG18/TG13	Patients with AC with and without malignant etiology	Cancer-associated AC	Duration of antibiotic therapy, 28-d-mortality, liver abscess
Masuda *et al* [17], 2021	Japan	April 2018 to March 2020	Retrospective observational study	TG18/TG13	AC patients with positive blood or bile culture and early ERCP	AC due to antibiotic resistant bacteria	Duration of antibiotic therapy, duration of hospitalization, in-hospital mortality, increased disease severity
Akhtar *et al* [18], 2020	Pakistan	June 2012 to June 2017	Cross-sectional observational study	TG18/TG13	AC patients without liver metastases or other reason for deranged liver function test. 70% of patients received ERCP	3-mo-mortality	Duration of antibiotic therapy, clinical severity, bacteremia
Haal *et al*[21], 2020	Netherlands	January 2012 to January 2017	Retrospective observational study	TG18/TG13	AC only due to stone in the common bile duct, without prior antibiotic therapy after ERCP	Antibiotic therapy of ≤ 3 d	3-mo-mortality, length of hospitalization, recurrent cholangitis, other complications
Satake *et al*[8], 2020	Japan	April 2014 to March 2019	Retrospective observational study	TG18/TG13	Grade I and grade II AC only due to choledocholithiasis who underwent ERCP	Antibiotic therapy of ≤ 3 d	30-d-mortality, length of hospitalization, recurrent cholangitis within 3 mo
Netinatsunton *et al*[16], 2019	Thailand	August 2017 to August 2018	Randomized controlled trial	TG18/TG13	AC only due to choledocholithiasis without presence of the Reynold´s pentad. Time to ERCP same between the study groups	Antibiotic therapy of ≤ 14 d	Recurrent cholangitis, length of hospitalization
Doi *et al*[22], 2018	Japan	January 2012 to February 2017	Retrospective observational study	ICD-10 and positive blood culture	AC and positive blood culture	Antibiotic therapy of ≤ 7 d	30-d-mortality, recurrent cholangitis within 3 mo (recurrence of symptoms)
Tagashira *et al* [13], 2017	Japan	January 2009 to December 2015	Retrospective observational study	TG18/TG13	Bacteriemic AC and ERCP where indicated	Adequate initial antibiotic therapy	Duration of antibiotic treatment, 30-d mortality
Uno *et al*[12], 2017	Japan	July 2012 to March 2014	Retrospective observational study	TG18/TG13	AC patients with gram-negative bacteriemia and after ERCP	Antibiotic therapy of ≤ 14 d	30-d mortality, recurrent cholangitis within 3 mo,

							antimicrobial treatment duration
Park *et al*[15], 2014	South Korea	September 2010 to November 2012	Randomized controlled trial	TG07	AC with bacteremia and ERCP within 24 h after admission	Intravenous antibiotic therapy of 6 d plus 8 d oral antibiotic therapy	30-d mortality, length of hospitalization, eradication of bacteria after 30 d
Kogure *et al* [19], 2011	Japan	September 2007 to August 2009	Retrospective observational study	TG07	Moderate and severe AC with ERCP	Antibiotic therapy of 3 d	Recurrent cholangitis
Van Lent *et al* [11], 2002	Netherlands	February 1999 to September 1999	Retrospective observational study	Fever > 38 °C and elevated bilirubin levels or bile duct dilatation in ultrasound	AC after successful ERCP. Exclusion of patients with primary sclerosing cholangitis, liver transplant recipients, bile duct atresia, inflammatory bowel disease	Antibiotic therapy of ≤ 3 d	6-mo mortality and recurrent cholangitis

AC: Acute cholangitis; TG18: Tokyo Guidelines 2018; TG13: Tokyo Guidelines 2013; TG07: Tokyo Guidelines 2007; ICD-10: The 10th Edition of the International Classification of Diseases; ERCP: Endoscopic retrograde cholangiopancreatography.

Mortality

Among the eight studies which were included in the quantitative analysis, six of them included mortality as an outcome[6,8,11,12,21,22], while five of the studies that were not suitable for the meta-analysis provided information for the participants' death[13-15,17,18]. Six studies calculated a 30-d mortality rate[6,8,12,13,15,22], Sokal *et al*[14] presented data concerning 28-d mortality, and Haal *et al* [21] conducted a follow-up of 3 mo concerning the death rates of the participants. Van Lent *et al*[11] observed the mortality of the patients for the following six months after the intervention.

After summarizing the data of the four studies with a duration of 2-3 of antibiotic treatment as cutoff point[6,8,11,21], no significant difference in the mortality between the two patient groups is present (OR = 0.78, 95%CI: 0.23-2.67, I^2 = 9%) (Figure 2A). No heterogeneity among these studies concerning our primary outcome is noted (I^2 = 9%).

In the study of Doi *et al*[22], patients who received an antibiotic treatment of fewer than seven days presented similar death rates compared to those with longer therapeutic schemata (OR = 0.82, 95%CI: 0.18-2.95, I^2 = 9%). The 30-d mortality rates of AC patients did not seem to differ between antibiotic therapies, of 14 d or shorter, according to Uno *et al*[12] (2 *vs* 0, P = 0.79, Fisher´s exact test).

Similar findings are also observable in the rest of the studies, which were not included in the meta-analysis. Sokal *et al*[14] presented that although patients with cancer-related-AC took an antibiotic treatment of mean duration with no significant difference compared to those that suffered from non-cancer-related-AC (10.6 ± 9.7 *vs* 7.8 ± 7.5 d, P = 0.13), the patients who belonged in the first group had significantly higher mortality rates (17 *vs* 0 deaths, P = 0.0002). In the rest of the studies, no differences concerning mortality were to be noted[13,15,17,18].

Recurrent cholangitis

Five of the included papers calculated a recurrence rate up to a follow-up period of 3 mo[6,8,12,21,22], van Lent *et al*[11] estimated a 28-d recurrence rate, Ferstl *et al*[23] recorded the shortest follow-up period among the studies (28 d) and two studies did not clarify the exact duration of follow-up for this outcome[16,19].

According to the studies retrieved from our review, a two to three-day antibiotic therapy was not associated with a significantly more frequent appearance of recurrent cholangitis (OR = 0.89, 95%CI: 0.49-1.60) (Figure 2B)[6,8,11,21]. No differences were also noted in the rates of recurrent AC neither in the 6-7-d-cutoff (OR = 1.11, 95%CI: 0.45-2.75) nor the 14-d-cutoff study groups (OR = 0.15, 95%CI: 0.02-1.35) (Figures 3 and 4A respectively). In all these comparisons, no significant study heterogeneity was observed (I^2 = 38%, 0%, and 0%, respectively). In the study of Kogure *et al*[19], no recurrent cholangitis was observed in both study groups, with and without withdrawal of the antibiotic therapy on the third day of treatment.

Length of hospitalization

Although in the studies of Masuda *et al*[6] and Haal *et al*[21], the patients who belong to the two-day and three-day antibiotic therapy have a significantly shorter hospitalization duration, the SMD of all three studies with a cutoff of 2-3 d is not significantly lower in the short-term antibiotic group (SMD = -0.53, 95%CI: -1.88 to 0.82, I^2 = 91%) (Figure 2C). Similarly, no difference was found between the short-

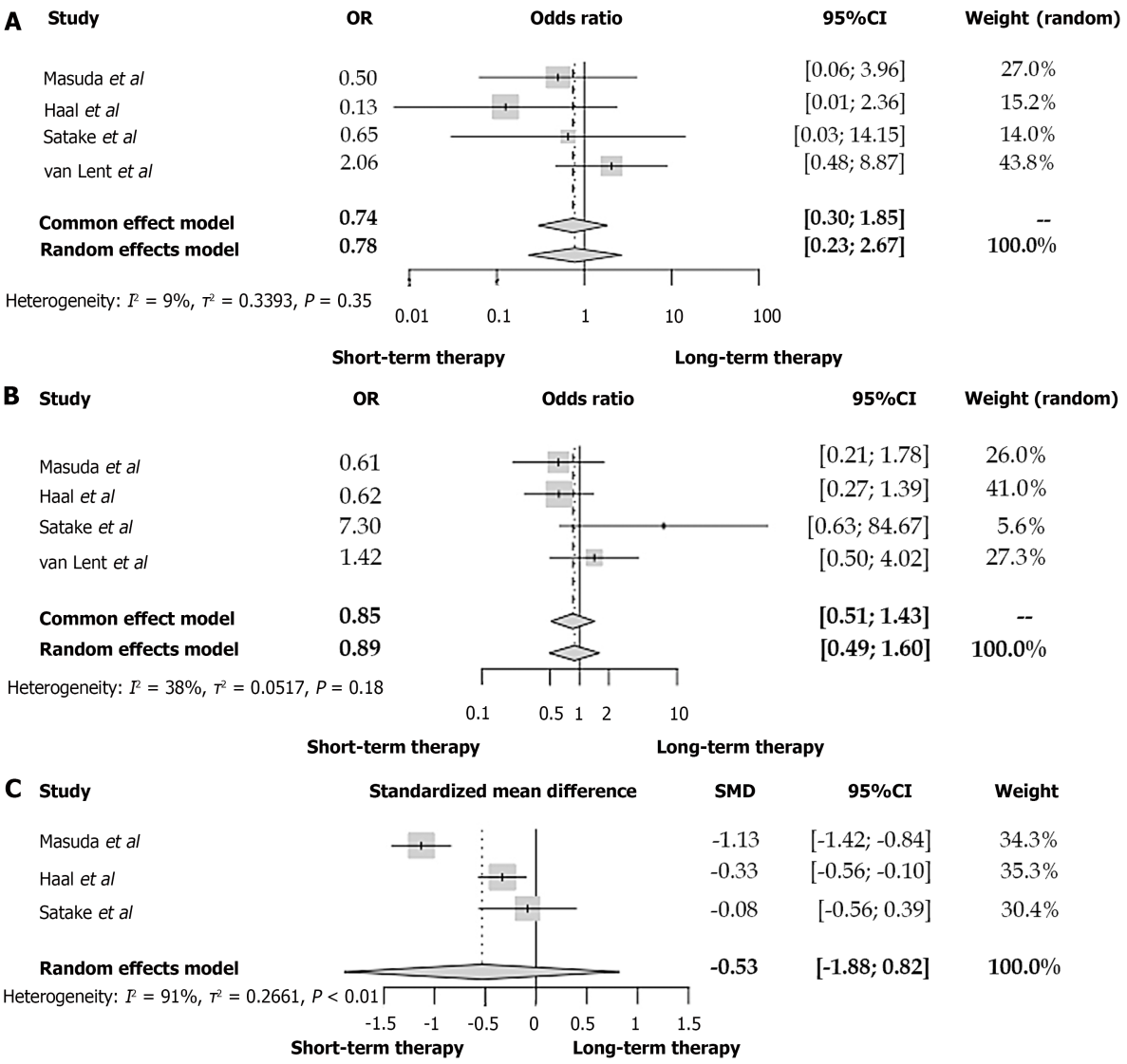

Figure 2 Forest plot between patients with acute cholangitis who received an antibiotic therapy of 2-3 d and acute cholangitis-patients with longer antibiotic treatment. A: Mortality; B: Recurrent cholangitis; C: Duration of hospitalization. OR: Odds ratio; CI: Confidence interval; SMD: Standardized mean difference.

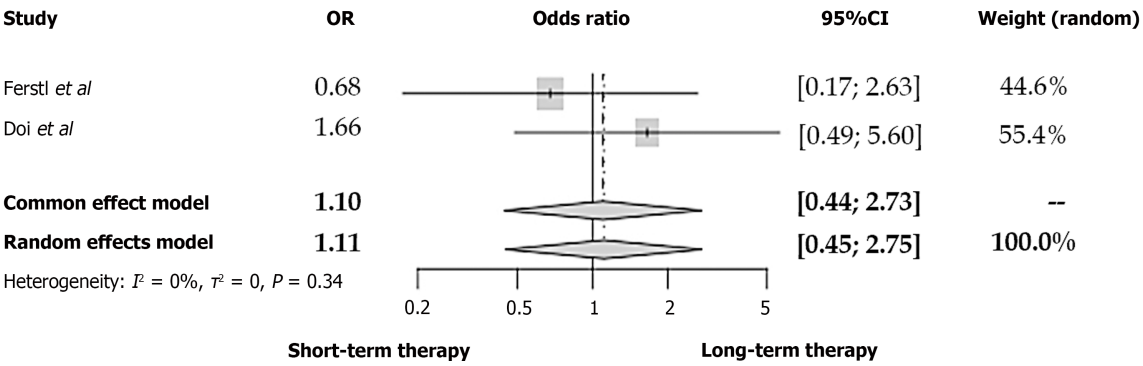

Figure 3 Forest plot of recurrent cholangitis between patients with acute cholangitis who received an antibiotic therapy of 6-7 d and acute cholangitis-patients with longer antibiotic treatment. OR: Odds ratio; CI: Confidence interval.

and long-term treatment groups concerning the length of in-hospital stay (SMD = -1.30, 95%CI: -14.43 to 11.84, I^2 = 95%) (Figure 4B). However, the considerable study heterogeneity (I^2 = 91% and 95%, respectively) does not allow us to extract strong conclusions. On the contrary, Park *et al*[15] estimated that a switch from intravenous to oral antibiotic therapy after six days from the treatment initiation led

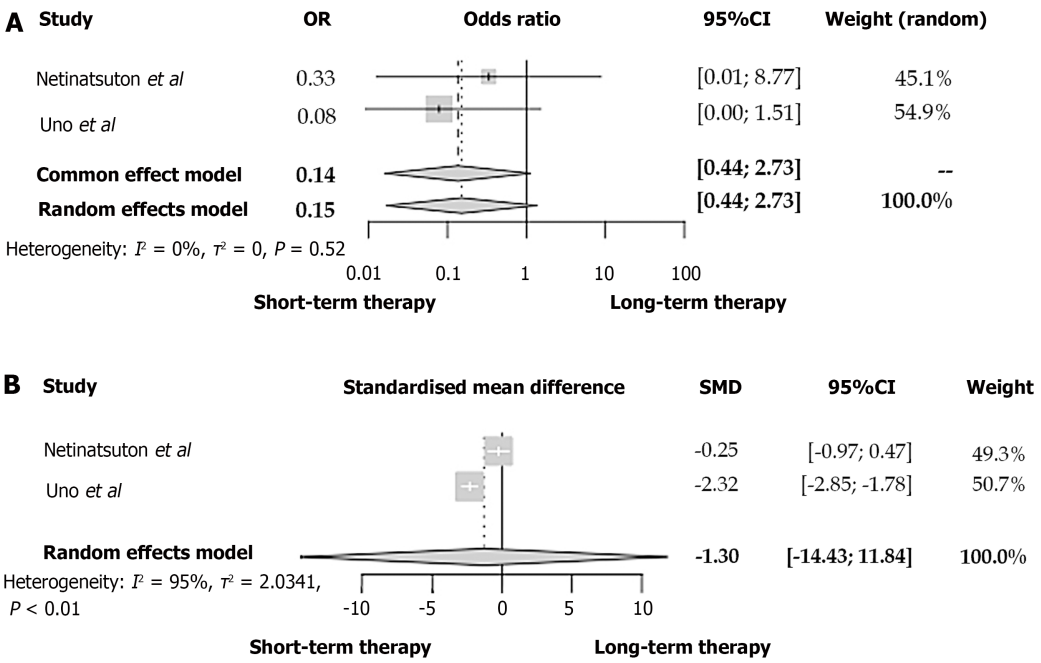

Figure 4 Forest plot between patients with acute cholangitis who received an antibiotic therapy of 14 d and acute cholangitis-patients with shorter antibiotic treatment. A: Recurrent cholangitis; B: Duration of hospitalization. OR: Odds ratio; CI: Confidence interval; SMD: Standardized mean difference.

to a significantly lower length of hospitalization in comparison with a switch at ten days of treatment.

Quality assessment

Based on the Newcastlte-Ottawa Scale, six of the observational studies included in the systematic review were considered of good quality[6,8,13,17,21,23], while the remaining seven were graded as low-quality studies, concerning our outcomes of interest, mostly due to lack of comparability between the cohort participants[11,13,14,18-20,22] (Table 2). In the study of Netinatsunton *et al*[16], as far as the randomization process is concerned, although the patients were randomized with the use of a computer-generated process and the baseline characteristics of the patients did not significantly differ, the results of the randomization were stated to be concealed in envelopes. However, the status and the accessibility of the envelopes are not provided, which raises concerns regarding the absolute transparency of the randomization. Additionally, no information is provided to manage the patients who did not adhere to the trial. Furthermore, the fact that no more information is provided concerning the construction of the study, as the trial protocol is provided neither in the clinicaltrials.gov website nor in the text in its complete form, leads us to the conclusion that the risk of bias in this study is high.

The trial of Park *et al*[15] has been based on a computer-generated block randomization model. However, no allocation concealment was possible due to the different application ways of the different interventions (oral *vs* intravenous). The authors followed an intention-to-treat model, but the lack of blinding may have led to a bias in measuring the outcome. Due to these facts, we conclude that the trial of Park *et al*[15] may also be connected to a high risk of bias.

DISCUSSION

To our knowledge, this is the first complete meta-analysis examining the duration of antibiotic therapy against the AC. In previously conducted systematic reviews with similar thematology, the limited data and the heterogenous outcomes and populations did not allow the authors to perform a meta-analysis [7,29]. Our data synthesis showed that antibiotic treatment of less than 2 or 3 d is not associated with significantly higher mortality rates, according to the random effects model (OR = 0.82, 95%CI: 0.18-2.95, I^2 = 9%). Our findings agree with the conclusions of the systematic review of Haal *et al*[7]. The fact that van Lent *et al*[11] did not base their diagnosis on the TG07 or TG18/13, possibly because the study was conducted before the establishment of the diagnostic criteria, may weaken the weight of this outcome. Although the combination of the diagnostic criteria of van Lent (fever > 38°C + elevated bilirubin levels or dilated bile duct by ultrasound) theoretically covers the criteria needed for the diagnosis of AC[30], the authors did not provide the exact cutoff, above which the bilirubin levels are considered elevated and the sensitivity of ultrasound on the diagnosis of AC is limited[31,32]. This could lead to a false

Table 2 Quality assessment of the observational studies

	Ferstl *et al* [23], *n* = 115	Kihara and Yokomizo [20], *n* = 112	Masuda *et al* [6], *n* = 11	Sokal *et al* [14], *n* = 107	Masuda *et al* [17], *n* = 110	Akhtar *et al* [18], *n* = 55	Haal *et al* [21], *n* = 113	Satake *et al* [8], *n* = 101	Doi *et al* [22], *n* = 114	Tagashira *et al*[13], *n* = 106	Uno *et al* [12], *n* = 105	Kogure *et al* [19], *n* = 111	Van Lent *et al*[11], *n* = 104
Selection													
Representativeness of exposed cohort	*	-	*	-	*	*	*	*	*	*	*	*	*
Selection of non-exposed cohort	*	*	*	*	*	*	*	*	*	*	*	*	*
Ascertainment of exposure	*	*	*	*	*	*	*	*	*	*	*	*	*
Demonstration that outcome of interest was not present at start of study	*	*	*	*	*	*	*	*	*	*	*	*	*
Comparability													
Comparability of the cohorts	**	-	**	-	**	-	**	**	-	-	**	-	-
Outcome													
Assessment of outcome	*	*	*	*	*	*	*	*	*	*	*	*	*
Was follow-up long enough for outcomes to occur?	*	*	*	*	*	*	*	*	*	*	*	*	*
Adequacy of follow-up cohorts	*	*	*	*	*	*	*	*	*	*	*	*	*
Overall	**Good**	**Low**	**Good**	**Low**	**Good**	**Low**	**Good**	**Good**	**Low**	**Low**	**Good**	**Low**	**Low**

*Represents study meets a criterion in each section of the Newcastle-Ottawa scale; -Represents study meets no criterion in each section of the Newcastle-Ottawa scale.

estimation of the actual patients suffering from AC. In the studies of Doi *et al*[22] and Uno *et al*[12], who set higher cutoffs for the definition of short- and long-term treatments, significance in the OR of the mortality rates was also not reached[12,22]. The findings of Sokal *et al*[33] that cancer-related AC patients presented a higher 28-d mortality compared to patients with AC not related to malignancies, in combination with the fact that the patients in the two groups received an antibiotic therapy of no different duration, may imply that the antibiotic therapy in cancer-related AC-patients should be longer. This study alone can provide no evidence for this assumption.

Concerning the rates of recurrent cholangitis, no significant differences were found between the study groups in all three duration cutoffs we set for our analysis. Although Uno *et al*[12] estimated a slightly higher recurrence rate in the group with > 14 d of antibiotic treatment, our synthesis with the study of Netinatsunton *et al*[16] resulted in no significantly different rates compared with the longer-course group. Haal *et al*[7] and Tinusz *et al*[29] enforce our results that the duration of antibiotic treatment of AC does not seem to affect the possibility of the appearance of cholangitis recurrence. The increasing resistance of the usual bacteria causing AC, such as *Escherichia coli*, the higher rates of gram-positive pathogens in recurrent cholangitis, and the possible lack of coverage against those bacteria in the initial empiric scheme provided against AC may constitute the major factors for the appearance of episodes of cholangitis recurrence[3,34,35]. As Tagashira *et al*[13] stated, inadequate initial antibiotic treatment could increase mortality and adverse events in bacteremic patients with AC.

Among the studies with a cutoff of 2-3 d of antibiotic treatment, Masuda *et al*[6] and Haal *et al*[21] presented a significantly shorter in-hospital stay for patients receiving short-term treatment compared to the control group of the study. However, when summarizing those two studies with the observational study of Satake *et al*[8], the SMD in the length of hospitalization was not significant (SMD = -0.6, 95%CI: -2.27 to 1.07, I^2 = 0%). Antibiotic treatment of less than 14 did also not seem to lead to a shorter hospitalization of patients compared to the control group, according to our study (SMD = -1.3, 95%CI: -14.49 to 11.89, I^2 = 96%), even though the short-course antibiotic treatment in Uno *et al*[12], presented a significantly lower hospitalization duration. However, the high heterogeneity of the studies included in these tests concerning this outcome (I^2 = 91% and 96%, respectively) may have affected our results. Park *et al*[15] reinforced the claim that shorter antibiotic treatment may benefit the patients concerning their length of stay in the hospital, as no mortality cases were recorded. In every case, more studies examining the hospitalization length should be conducted, as the extraction of evidence that proves that a short-course antibiotic treatment leads to shorter hospitalizations would protect patients from exposure to several dangers, such as thromboembolic episodes and unwanted infections[36,37].

Our study presents several limitations which should be accounted for. First of all, as many studies were conducted before 2013, the choice of the participants as patients suffering from AC was not based on the updated TG18/13, especially in the study of van Lent *et al*[11]. This may alter the actual population we wish to study. The difference in patients' inclusion and exclusion criteria and the variable severity grades of the patients included in the studies also constitute an important limitation. Additionally, small discrepancies are also noticed in the follow-up periods concerning the mortality and recurrent cholangitis in each study. These inequalities in the follow-up of the patients may lead to lost data which may have altered our results. Finally, significant statistical heterogeneity was detected among the studies selected for the quantitative analysis of the length of hospitalizations, which may lead to invalid conclusions.

CONCLUSION

Depending on our findings, the duration of antibiotic therapy may not significantly affect the mortality rate, the rate of recurrent cholangitis, and the length of hospitalization of patients suffering from AC. More specifically, a 2 to 3-d antibiotic treatment could be similarly effective in preventing mortality and recurrent cholangitis, as the 4 to 7-d therapy proposed by the TG18. However, these results are based on a small number of heterogeneous studies. It is vital that more primary and secondary studies are conducted for new recommendations with high-level evidence to be established.

ARTICLE HIGHLIGHTS

Research background

The mortality rates of acute cholangitis (AC) have significantly decreased in the last decades. The development of new diagnostic and therapeutic tools has contributed to this result.

Research motivation

The Tokyo Guidelines of 2018 suggest an antibiotic treatment of four to seven days in AC cases without gram-positive cocci. This interval between the recommended treatment days is relatively wide, and the recommendation provided is not based on a high level of evidence (level C).

Research objectives

The aim of this study is to investigate if shorter-course antibiotic treatments could be similarly effective to long-course treatments in adults with AC.

Research methods

We conducted a systematic review and meta-analysis of the existing literature based on the recommendations of the Preferred Reporting Items for Systematic Review and Meta-Analyses. Two reviewers (Kasparian K and Christou CD) conducted the literature research, study selection, and data collection. The inclusion and exclusion criteria were predefined. The data synthesis, statistical analysis, and Forest plot creation were conducted through the program R Studio version 1.4.1103.

Research results

Fifteen studies were included in the systematic review and eight in the final meta-analysis. Most of the patients were classified as Grade I (41,1%) or Grade II (54,1%), while only 4,6% of the participants suffered from Grade III AC. No significant differences were observed between patients receiving a 2-3 d antibiotic therapy and those who were treated with longer antibiotic schemata concerning the mortality (odds ratio = 0.78, 95% confidence interval: 0.23-2.67, I^2 = 9%). In all calculations conducted, no differences could be detected among patients receiving shorter and longer antibiotic treatments concerning the rates of recurrent AC and the length of hospitalization.

Research conclusions

Short- and long-course antibiotic treatments may be similarly effective concerning the mortality and recurrence rates of AC.

Research perspectives

This study could constitute the occasion for the conduction of more primary and secondary studies for new robust recommendations with a high level of evidence to be established.

FOOTNOTES

Author contributions: Kasparian K, Christou CD, Petidis K, Doumas M, and Giouleme O designed the research study; Kasparian K and Christou CD performed the research; Kasparian K analyzed the data and wrote the manuscript; and all authors have read and approved the final manuscript.

Conflict-of-interest statement: All the authors report no relevant conflicts of interest for this article.

PRISMA 2009 Checklist statement: The authors have read the PRISMA 2009 Checklist, and the manuscript was prepared and revised according to the PRISMA 2009 Checklist.

Country/Territory of origin: Greece

ORCID number: Karampet Kasparian 0000-0002-5443-0749; Chrysanthos D Christou 0000-0002-5417-8686; Olga Giouleme 0000-0003-0176-3598.

S-Editor: Wang JJ
L-Editor: A
P-Editor: Cai YX

REFERENCES

1 **Kimura Y**, Takada T, Strasberg SM, Pitt HA, Gouma DJ, Garden OJ, Büchler MW, Windsor JA, Mayumi T, Yoshida M, Miura F, Higuchi R, Gabata T, Hata J, Gomi H, Dervenis C, Lau WY, Belli G, Kim MH, Hilvano SC, Yamashita Y. TG13 current terminology, etiology, and epidemiology of acute cholangitis and cholecystitis. *J Hepatobiliary Pancreat Sci* 2013; **20**: 8-23 [PMID: 23307004 DOI: 10.1007/s00534-012-0564-0]

2 **Zimmer V**, Lammert F. Acute Bacterial Cholangitis. *Viszeralmedizin* 2015; **31**: 166-172 [PMID: 26468310 DOI: 10.1159/000430965]

3 **Gomi H**, Takada T, Hwang TL, Akazawa K, Mori R, Endo I, Miura F, Kiriyama S, Matsunaga N, Itoi T, Yokoe M, Chen MF, Jan YY, Ker CG, Wang HP, Wada K, Yamaue H, Miyazaki M, Yamamoto M. Updated comprehensive epidemiology, microbiology, and outcomes among patients with acute cholangitis. *J Hepatobiliary Pancreat Sci* 2017; **24**: 310-318 [PMID: 28371094 DOI: 10.1002/jhbp.452]

4 **Kiriyama S**, Kozaka K, Takada T, Strasberg SM, Pitt HA, Gabata T, Hata J, Liau KH, Miura F, Horiguchi A, Liu KH, Su

CH, Wada K, Jagannath P, Itoi T, Gouma DJ, Mori Y, Mukai S, Giménez ME, Huang WS, Kim MH, Okamoto K, Belli G, Dervenis C, Chan ACW, Lau WY, Endo I, Gomi H, Yoshida M, Mayumi T, Baron TH, de Santibañes E, Teoh AYB, Hwang TL, Ker CG, Chen MF, Han HS, Yoon YS, Choi IS, Yoon DS, Higuchi R, Kitano S, Inomata M, Deziel DJ, Jonas E, Hirata K, Sumiyama Y, Inui K, Yamamoto M. Tokyo Guidelines 2018: diagnostic criteria and severity grading of acute cholangitis (with videos). *J Hepatobiliary Pancreat Sci* 2018; **25**: 17-30 [PMID: 29032610 DOI: 10.1002/jhbp.512]

5 **Gomi H**, Solomkin JS, Schlossberg D, Okamoto K, Takada T, Strasberg SM, Ukai T, Endo I, Iwashita Y, Hibi T, Pitt HA, Matsunaga N, Takamori Y, Umezawa A, Asai K, Suzuki K, Han HS, Hwang TL, Mori Y, Yoon YS, Huang WS, Belli G, Dervenis C, Yokoe M, Kiriyama S, Itoi T, Jagannath P, Garden OJ, Miura F, de Santibañes E, Shikata S, Noguchi Y, Wada K, Honda G, Supe AN, Yoshida M, Mayumi T, Gouma DJ, Deziel DJ, Liau KH, Chen MF, Liu KH, Su CH, Chan ACW, Yoon DS, Choi IS, Jonas E, Chen XP, Fan ST, Ker CG, Giménez ME, Kitano S, Inomata M, Mukai S, Higuchi R, Hirata K, Inui K, Sumiyama Y, Yamamoto M. Tokyo Guidelines 2018: antimicrobial therapy for acute cholangitis and cholecystitis. *J Hepatobiliary Pancreat Sci* 2018; **25**: 3-16 [PMID: 29090866 DOI: 10.1002/jhbp.518]

6 **Masuda S**, Koizumi K, Makazu M, Uojima H, Kubota J, Kimura K, Nishino T, Sumida C, Ichita C, Sasaki A, Shionoya K. Antibiotic Administration within Two Days after Successful Endoscopic Retrograde Cholangiopancreatography Is Sufficient for Mild and Moderate Acute Cholangitis. *J Clin Med* 2022; **11** [PMID: 35628824 DOI: 10.3390/jcm11102697]

7 **Haal S**, Wielenga MCB, Fockens P, Leseman CA, Ponsioen CY, van Soest EJ, van Wanrooij RLJ, Sieswerda E, Voermans RP. Antibiotic Therapy of 3 Days May Be Sufficient After Biliary Drainage for Acute Cholangitis: A Systematic Review. *Dig Dis Sci* 2021; **66**: 4128-4139 [PMID: 33462749 DOI: 10.1007/s10620-020-06820-3]

8 **Satake M**, Yamaguchi Y. Three-day antibiotic treatment for acute cholangitis due to choledocholithiasis with successful biliary duct drainage: A single-center retrospective cohort study. *Int J Infect Dis* 2020; **96**: 343-347 [PMID: 32376307 DOI: 10.1016/j.ijid.2020.04.074]

9 **Sawyer RG**, Claridge JA, Nathens AB, Rotstein OD, Duane TM, Evans HL, Cook CH, O'Neill PJ, Mazuski JE, Askari R, Wilson MA, Napolitano LM, Namias N, Miller PR, Dellinger EP, Watson CM, Coimbra R, Dent DL, Lowry SF, Cocanour CS, West MA, Banton KL, Cheadle WG, Lipsett PA, Guidry CA, Popovsky K; STOP-IT Trial Investigators. Trial of short-course antimicrobial therapy for intraabdominal infection. *N Engl J Med* 2015; **372**: 1996-2005 [PMID: 25992746 DOI: 10.1056/NEJMoa1411162]

10 **Page MJ**, McKenzie JE, Bossuyt PM, Boutron I, Hoffmann TC, Mulrow CD, Shamseer L, Tetzlaff JM, Akl EA, Brennan SE, Chou R, Glanville J, Grimshaw JM, Hróbjartsson A, Lalu MM, Li T, Loder EW, Mayo-Wilson E, McDonald S, McGuinness LA, Stewart LA, Thomas J, Tricco AC, Welch VA, Whiting P, Moher D. The PRISMA 2020 statement: an updated guideline for reporting systematic reviews. *BMJ* 2021; **372**: n71 [PMID: 33782057 DOI: 10.1136/bmj.n71]

11 **van Lent AU**, Bartelsman JF, Tytgat GN, Speelman P, Prins JM. Duration of antibiotic therapy for cholangitis after successful endoscopic drainage of the biliary tract. *Gastrointest Endosc* 2002; **55**: 518-522 [PMID: 11923764 DOI: 10.1067/mge.2002.122334]

12 **Uno S**, Hase R, Kobayashi M, Shiratori T, Nakaji S, Hirata N, Hosokawa N. Short-course antimicrobial treatment for acute cholangitis with Gram-negative bacillary bacteremia. *Int J Infect Dis* 2017; **55**: 81-85 [PMID: 28027992 DOI: 10.1016/j.ijid.2016.12.018]

13 **Tagashira Y**, Sakamoto N, Isogai T, Hikone M, Kosaka A, Chino R, Higuchi M, Uehara Y, Honda H. Impact of inadequate initial antimicrobial therapy on mortality in patients with bacteraemic cholangitis: a retrospective cohort study. *Clin Microbiol Infect* 2017; **23**: 740-747 [PMID: 28254686 DOI: 10.1016/j.cmi.2017.02.027]

14 **Sokal A**, Chawki S, Nguyen Y, Sauvanet A, Ponsot P, Maire F, Fantin B, de Lastours V. Specificities of acute cholangitis in patients with cancer: a retrospective comparative study of 130 episodes. *Eur J Clin Microbiol Infect Dis* 2022; **41**: 143-146 [PMID: 34415466 DOI: 10.1007/s10096-021-04289-0]

15 **Park TY**, Choi JS, Song TJ, Do JH, Choi SH, Oh HC. Early oral antibiotic switch compared with conventional intravenous antibiotic therapy for acute cholangitis with bacteremia. *Dig Dis Sci* 2014; **59**: 2790-2796 [PMID: 24898101 DOI: 10.1007/s10620-014-3233-0]

16 **Netinatsunton N**, Limmathurotsakul D, Attasaranya S, Sottisuporn J, Pattarapuntakul T, Ovartlarnporn B. Short Duration versus 14-day Antibiotic Treatment in Acute Cholangitis due to Bile Duct Stone: A randomized study. *J Gastroenterol Hepatol Res* 2019; **8**: 3020-3024

17 **Masuda S**, Koizumi K, Uojima H, Kimura K, Nishino T, Tasaki J, Ichita C, Sasaki A. Effect of Antibiotic Resistance of Pathogens on Initial Antibiotic Therapy for Patients With Cholangitis. *Cureus* 2021; **13**: e18449 [PMID: 34650837 DOI: 10.7759/cureus.18449]

18 **Akhtar F**, Siddique MZ, Raza A, Mehmood S, Yusuf MA, Sultan F. Microbiology and clinical characteristics of acute cholangitis with their impact on mortality; a retrospective cross sectional study. *J Pak Med Assoc* 2020; **70**: 607-612 [PMID: 32296203 DOI: 10.5455/JPMA.29747]

19 **Kogure H**, Tsujino T, Yamamoto K, Mizuno S, Yashima Y, Yagioka H, Kawakubo K, Sasaki T, Nakai Y, Hirano K, Sasahira N, Isayama H, Tada M, Kawabe T, Omata M, Harada S, Ota Y, Koike K. Fever-based antibiotic therapy for acute cholangitis following successful endoscopic biliary drainage. *J Gastroenterol* 2011; **46**: 1411-1417 [PMID: 21842232 DOI: 10.1007/s00535-011-0451-5]

20 **Kihara Y**, Yokomizo H. The clinical features of late postoperative cholangitis following pancreaticoduodenectomy brought on by conditions other than cancer recurrence: a single-center retrospective study. *BMC Surg* 2022; **22**: 301 [PMID: 35932000 DOI: 10.1186/s12893-022-01752-3]

21 **Haal S**, Ten Böhmer B, Balkema S, Depla AC, Fockens P, Jansen JM, Kuiken SD, Liberov BI, van Soest E, van Hooft JE, Sieswerda E, Voermans RP. Antimicrobial therapy of 3 days or less is sufficient after successful ERCP for acute cholangitis. *United European Gastroenterol J* 2020; **8**: 481-488 [PMID: 32213042 DOI: 10.1177/2050640620915016]

22 **Doi A**, Morimoto T, Iwata K. Shorter duration of antibiotic treatment for acute bacteraemic cholangitis with successful biliary drainage: a retrospective cohort study. *Clin Microbiol Infect* 2018; **24**: 1184-1189 [PMID: 29408612 DOI: 10.1016/j.cmi.2018.01.021]

23 **Ferstl PG**, Queck A, Bremer K, Filmann N, Weiler N, Welker MW, Waidmann O, Knabe M, Bechstein WO, Hogardt M, Kempf VAJ, Zeuzem S, Trebicka J, Friedrich-Rust M, Walter D. Comparison of short-course antibiotic therapy of 6 or less

days with a longer treatment in patients with cholangitis after liver transplantation. *Transpl Infect Dis* 2022; **24**: e13868 [PMID: 35598281 DOI: 10.1111/tid.13868]

24 **Hozo SP**, Djulbegovic B, Hozo I. Estimating the mean and variance from the median, range, and the size of a sample. *BMC Med Res Methodol* 2005; **5**: 13 [PMID: 15840177 DOI: 10.1186/1471-2288-5-13]

25 **Lin L**, Aloe AM. Evaluation of various estimators for standardized mean difference in meta-analysis. *Stat Med* 2021; **40**: 403-426 [PMID: 33180373 DOI: 10.1002/sim.8781]

26 **Sweeting MJ**, Sutton AJ, Lambert PC. What to add to nothing? *Stat Med* 2004; **23**: 1351-1375 [PMID: 15116347 DOI: 10.1002/sim.1761]

27 **Cook DA**, Reed DA. Appraising the quality of medical education research methods: the Medical Education Research Study Quality Instrument and the Newcastle-Ottawa Scale-Education. *Acad Med* 2015; **90**: 1067-1076 [PMID: 26107881 DOI: 10.1097/ACM.0000000000000786]

28 **Higgins JPT**, Savović J, Page MJ, Elbers RG, Sterne JAC. Chapter 8: Assessing risk of bias in a randomized trial. In: Cochrane Handbook for Systematic Reviews of Interventions, Version 6.3, 2022. British: Cochrane Collaboration, 2022

29 **Tinusz B**, Szapáry L, Paládi B, Tenk J, Rumbus Z, Pécsi D, Szakács Z, Varga G, Rakonczay Z Jr, Szepes Z, Czimmer J, Vincze Á, Hegyi P, Erőss B. Short-Course Antibiotic Treatment Is Not Inferior to a Long-Course One in Acute Cholangitis: A Systematic Review. *Dig Dis Sci* 2019; **64**: 307-315 [PMID: 30368681 DOI: 10.1007/s10620-018-5327-6]

30 **Kiriyama S**, Takada T, Strasberg SM, Solomkin JS, Mayumi T, Pitt HA, Gouma DJ, Garden OJ, Büchler MW, Yokoe M, Kimura Y, Tsuyuguchi T, Itoi T, Yoshida M, Miura F, Yamashita Y, Okamoto K, Gabata T, Hata J, Higuchi R, Windsor JA, Bornman PC, Fan ST, Singh H, de Santibanes E, Gomi H, Kusachi S, Murata A, Chen XP, Jagannath P, Lee S, Padbury R, Chen MF; Tokyo Guidelines Revision Committee. New diagnostic criteria and severity assessment of acute cholangitis in revised Tokyo Guidelines. *J Hepatobiliary Pancreat Sci* 2012; **19**: 548-556 [PMID: 22825491 DOI: 10.1007/s00534-012-0537-3]

31 **Walas MK**, Skoczylas K, Gierbliński I. Errors and mistakes in the ultrasound diagnostics of the liver, gallbladder and bile ducts. *J Ultrason* 2012; **12**: 446-462 [PMID: 26673428 DOI: 10.15557/JoU.2012.0032]

32 **Majeed AW**, Ross B, Johnson AG, Reed MW. Common duct diameter as an independent predictor of choledocholithiasis: is it useful? *Clin Radiol* 1999; **54**: 170-172 [PMID: 10201865 DOI: 10.1016/s0009-9260(99)91008-5]

33 **Sokal A**, Sauvanet A, Fantin B, de Lastours V. Acute cholangitis: Diagnosis and management. *J Visc Surg* 2019; **156**: 515-525 [PMID: 31248783 DOI: 10.1016/j.jviscsurg.2019.05.007]

34 **Hara T**, Taniguchi M, Hattori C, Sakai H, Oka K, Iwai N, Tsuji T, Harada T, Okuda T, Komaki T, Sakagami J, Kagawa K. Microbiological analysis of patients with first and recurrent episodes of acute cholangitis in a middle-sized hospital: A single-center retrospective study in rural North Kyoto, Japan. *J Infect Chemother* 2022; **28**: 413-419 [PMID: 34973874 DOI: 10.1016/j.jiac.2021.11.025]

35 **van den Hazel SJ**, Speelman P, Tytgat GN, Dankert J, van Leeuwen DJ. Role of antibiotics in the treatment and prevention of acute and recurrent cholangitis. *Clin Infect Dis* 1994; **19**: 279-286 [PMID: 7986900 DOI: 10.1093/clinids/19.2.279]

36 **Welch C**, K Hassan-Smith Z, A Greig C, M Lord J, A Jackson T. Acute Sarcopenia Secondary to Hospitalisation - An Emerging Condition Affecting Older Adults. *Aging Dis* 2018; **9**: 151-164 [PMID: 29392090 DOI: 10.14336/AD.2017.0315]

37 **Heit JA**, Melton LJ 3rd, Lohse CM, Petterson TM, Silverstein MD, Mohr DN, O'Fallon WM. Incidence of venous thromboembolism in hospitalized patients *vs* community residents. *Mayo Clin Proc* 2001; **76**: 1102-1110 [PMID: 11702898 DOI: 10.4065/76.11.1102]

World Journal of Gastroenterology

Submit a Manuscript: https://www.f6publishing.com

World J Gastroenterol 2023 May 21; 29(19): 3040-3047

DOI: 10.3748/wjg.v29.i19.3040

ISSN 1007-9327 (print) ISSN 2219-2840 (online)

CASE REPORT

Pulmonary hypertension, nephrotic syndrome, and polymyositis due to hepatitis C virus infection: A case report

Ya-Nan Zhao, Guo-Hui Liu, Chang Wang, Yi-Xuan Zhang, Ping Yang, Ming Yu

Specialty type: Gastroenterology and hepatology

Provenance and peer review: Unsolicited article; Externally peer reviewed.

Peer-review model: Single blind

Peer-review report's scientific quality classification

Grade A (Excellent): 0
Grade B (Very good): B
Grade C (Good): C, C
Grade D (Fair): 0
Grade E (Poor): 0

P-Reviewer: Beenet L, United States; Rodrigues AT, Brazil; Salvadori M, Italy

Received: March 14, 2023
Peer-review started: March 14, 2023
First decision: April 10, 2023
Revised: April 17, 2023
Accepted: April 25, 2023
Article in press: April 25, 2023
Published online: May 21, 2023

Ya-Nan Zhao, Guo-Hui Liu, Chang Wang, Yi-Xuan Zhang, Ping Yang, Ming Yu, Department of Cardiology, China-Japan Union Hospital of Jilin University, Changchun 130033, Jilin Province, China

Corresponding author: Ming Yu, Doctor, Department of Cardiology, China-Japan Union Hospital of Jilin University, No. 126 Xian-tai Street, Changchun 130033, Jilin Province, China. yuming2019@jlu.edu.cn

Abstract

BACKGROUND

Hepatitis C infection not only damages the liver but also often accompanies many extrahepatic manifestations. Incidences of pulmonary hypertension (PH) caused by hepatitis C are rare, and incidences of concurrent nephrotic syndrome and polymyositis are even rarer.

CASE SUMMARY

Herein we describe the case of a 57-year-old woman who was admitted to our department for intermittent chest tightness upon exertion for 5 years, aggravated with dyspnea for 10 d. After relevant examinations she was diagnosed with PH, nephrotic syndrome, and polymyositis due to chronic hepatitis C infection. A multi-disciplinary recommendation was that the patient should be treated with sildenafil and macitentan in combination and methylprednisolone. During treatment autoimmune symptoms, liver function, hepatitis C RNA levels, and cardiac parameters of right heart catheterization were monitored closely. The patient showed significant improvement in 6-min walking distance from 100 to 300 m at 3-mo follow-up and pulmonary artery pressure drops to 50 mmHg. Long-term follow-up is needed to confirm further efficacy and safety.

CONCLUSION

Increasing evidence supports a relationship between hepatitis C infection and diverse extrahepatic manifestations, but it is very rare to have PH, nephrotic syndrome, and polymyositis in a single patient. We conducted a literature review on the management of several specific extrahepatic manifestations of hepatitis C.

Key Words: Hepatitis C; Nephrotic syndrome; Polymyositis; Pulmonary hypertension; Case report

Core Tip: Hepatitis C virus (HCV) infection should be considered a systemic disease which is often associated with many extrahepatic manifestations, but it is very rare to have multiple different extrahepatic manifestations in a single patient. In this article, we report a case of pulmonary hypertension (PH), nephrotic syndrome, and polymyositis due to HCV infection. The optimal treatment strategy for hepatitis C-related extrahepatic manifestations remains to be determined. Our case confirms sildenafil and macitentan as effective treatment option for patients suffering from PH due to hepatitis C infection. However, randomized, controlled trials are warranted to confirm the present results.

Citation: Zhao YN, Liu GH, Wang C, Zhang YX, Yang P, Yu M. Pulmonary hypertension, nephrotic syndrome, and polymyositis due to hepatitis C virus infection: A case report. *World J Gastroenterol* 2023; 29(19): 3040-3047
URL: https://www.wjgnet.com/1007-9327/full/v29/i19/3040.htm
DOI: https://dx.doi.org/10.3748/wjg.v29.i19.3040

INTRODUCTION

Hepatitis C virus (HCV) is a sporadic and a common cause of chronic hepatitis after blood transfusion. In recent years various authors have described associations between hepatitis C infection and a heterogeneous group of non-hepatic diseases such as cryoglobulinemia, rheumatoid arthritis, Sjogren's syndrome, and glomerulonephritis, which are seen as extrahepatic manifestations of chronic hepatitis C infection[1].

Pulmonary hypertension (PH) is defined as a mean pulmonary arterial pressure (mPAP) ≥ 20 mmHg at rest with right heart catheterization[2]. PH affects approximately 1% of the global population, up to 10% of individuals aged ≥ 65 years, and at least 50% of patients with heart failure[3]. PH has several different causes with different management and outcomes. However, PH due to hepatitis C has rarely been reported. Herein we describe a case of PH, nephrotic syndrome, and polymyositis following chronic hepatitis C infection in a 57-year-old woman.

CASE PRESENTATION

Chief complaints

A 57-year-old Chinese woman presenting with untreated chest tightness, shortness of breath, and fatigue for 5 years and with dyspnea for 10 d was admitted to the China-Japan Union Hospital of Jilin University.

History of present illness

She had no precordial pain, orthopnea, or palpitation. She had no joint pain, dental ulcers, or rash.

History of past illness

Forty years previously she had received an intravenous blood transfusion for a right ovariectomy. Sixteen years previously she was diagnosed with hepatitis C, nephrotic syndrome, and hypertension, but did not receive standard treatment. Five years previously she developed mild PH with pulmonary arterial pressure of 54 mmHg measured by transthoracic echocardiography, which was not treated further. Three years previously she developed severe myopathy. She was diagnosed with polymyositis and administered methylprednisolone 40 mg once a day (QD) and cyclophosphamide 50 mg QD. She lapsed into intermittent coma due to hyperemic ammonia however, thus cyclophosphamide was discontinued, and methylprednisolone 20 mg QD was initiated and has been maintained to date.

Personal and family history

She had no family history of genetically related diseases, but her daughter had hepatitis C and had been treated with interferon.

Physical examination

Physical examination revealed no fever, heart rate 70 bpm, blood pressure 140/90 mmHg, O_2 saturation 94% on room air, second heart sound accentuation, and moderate edema in both lower limbs.

Laboratory examinations

Primary laboratory data on admission are shown in Table 1. The 6-min walking distance was 100 m.

Table 1 The patient's laboratory data at admission and at 1-mo follow-up

Parameter	Value (admission)	Value (month 1)	References value	Unit
N-terminal-pro B-type natriuretic peptide	590		0-125	pg/mL
Urea	10.02	11.6	2.5-6.1	mmol/L
Creatinine	123.4	124.9	46-92	μmol/L
Troponin	< 0.01		0-0.04	ng/mL
Myoglobin	208.1		0-120	ng/mL
Creatine kinase	576.24	98.6	30-135	U/L
Creatine kinase MB isoenzyme	42.1	50.2	0-16	U/L
Lactic dehydrogenase	378.88	777.2	120-246	U/L
D-dimer	1.28		0-0.5	μg/mL
White blood cell	9.10	14.05	4-10	10^9/L
Platelet	140	111	125-350	10^9/L
Hemoglobin	119	152	110-150	g/L
Alanine aminotransferase	18.28	41.4	5-40	IU/L
Aspartate aminotransferase	15.44	16.1	8-40	IU/L
Total bilirubin	16.48	30.10	5-21	μmol/L
Direct bilirubin	3.36	7.40	0-3.4	μmol/L
Indirect bilirubin	13.12	22.70	1.6-21	μmol/L
Albumin	22.73	25.65	35-52	g/L
Total cholesterol	7.67		3.0-5.7	mmol/L
Low density lipoprotein cholesterol	3.65		< 4.13	mmol/L
High density lipoprotein cholesterol	2.86		1.29-1.55	mmol/L
Fasting blood glucose	4.44		3.9-6.1	Mmol/L
Urinary protein	4+		negative	-
24-h proteinuria	416.01		0-150	mg/d
Hepatitis B surface antigen	0		< 0.05	IU/mL
Antibody to hepatitis C	6.04		< 1	S/CO
Immunodeficiency virus antigen and antibody	0.09		< 1	S/CO
Antibody to treponema pallidum	0.07		< 1	S/CO
Hepatitis C virus RNA	0		0	IU/mL
Anti-nuclear antibodies	negative		negative	-
Anti-cyclic citrullinated peptide antibody	13.89		< 25	RU/mL
Anti-cardiolipin antibody	2.23		0-12	RU/mL
Immunoglobulin G	4.92		7.51-15.60	g/L
Immunoglobulin A	2.82		0.82-4.53	g/L
Immunoglobulin M	1.81		0.46-3.04	g/L
C3	0.58		0.79-1.52	g/L
C4	0.14		0.16-0.38	g/L
Blood ammonia	56		9-30	μmol/L
Erythrocyte sedimentation rate	22	6	0-20	mm/h

Imaging examinations

Muscle biopsy showed striated muscle atrophy with inflammatory cell infiltration (Figure 1A). Electrocardiography indicated a normal sinus rhythm (Figure 1B). Transthoracic echocardiography showed enlargement of the left atrium (43.7 × 45.2 × 60.0), right atrium (59.8 × 39.4), and right ventricle (49.3), normal left ventricular ejection fraction (71.3%), elevated pulmonary artery pressure (61 mmHg), and reduced diastolic function (Figure 1C-F). Chest computed tomography (CT) depicted pulmonary arterial hypertension, right atrium and right ventricle enlargement, and no parenchymal lung disease (Figure 2A-C). Pulmonary ventilation/perfusion scanning indicated no evidence of typical signs of thromboembolic disease (Figure 2D). Abdominal CT suggested normal liver size with a hepato-renal shunt and a spleno-renal shunt (Figure 2E and F). Right heart catheterization showed that mPAP was 55.33, pulmonary artery wedge pressure (PAWP) was 24, and pulmonary vascular resistance (PVR) was 5.13 Woods units (WU) (Table 2).

FINAL DIAGNOSIS

Based on the medical history, symptoms, and auxiliary examinations, a diagnosis of moderate PH, nephrotic syndrome, polymyositis, hypertension, and hepatitis C was determined.

TREATMENT

The patient was treated with sildenafil 20 mg QD, macitentan 10 mg QD, irbesartan and hydrochlorothiazide 150 mg QD, furosemide 20 mg QD, and methylprednisolone 80 mg QD with the dose gradually reduced to 20 mg QD. Due to suspected hepatitis C-induced multiple organ injury the patient was referred to the gastroenterology department for further assessment of liver disease. There was no evidence of a liver tumor. Liver stiffness as evaluated by transient elastography was 8.3 kPa. Hepatitis C antibody was 6.8 S/CO, but serum tests were negative for HCV RNA. Therefore, she was not prescribed antiviral therapy.

OUTCOME AND FOLLOW-UP

At the 3-mo follow up the patient's dyspnea was dramatically improved and the 6-min walking distance was 300 m and pulmonary artery pressure drops to 50 mmHg.

DISCUSSION

HCV infection should be considered a systemic disease which is often associated with many extrahepatic manifestations. According to different studies, 40%-80% of patients infected with HCV develop at least one extrahepatic manifestation[4]. However, PH associated with HCV is relatively rare.

PH is divided into five clinical subgroups; pulmonary arterial hypertension (PAH), PH associated with left heart disease, PH associated with chronic lung disease and/or hypoxia, chronic thromboembolic, and PH with unclear and/or multifactorial mechanisms. Pre-capillary PH is hemodynamically defined as mPAP > 20 mmHg, PAWP ≤ 15 mmHg, and PVR > 2 WU. PAWP > 15 mmHg is the threshold of post-capillary PH. PVR is used to distinguish patients with post-capillary PH who have significant components of pre-capillary PH (PVR > 2 WU, combined with post-capillary and pre-capillary PH; CpcPH) from those who do not (PVR ≤ 2 WU, isolated post-capillary PH)[5]. The current patient had no relevant family history to support a heritable cause of PH. Valvular/congenital heart diseases, lung diseases, chronic pulmonary artery obstruction, and human immunodeficiency virus infection were systemically eliminated *via* relevant tests. Drugs were also unlikely to have caused her PH. The onset of PH predated the polymyositis, and connective tissue disease could also be excluded as a cause of PH. Thus, the possibility remained that PH associated with portal hypertension was due to chronic hepatitis C.

Portal PH (PoPH) is a well-known serious complication of portal hypertension in chronic liver disease. According to statistics, PoPH occurs in 1%–2% of patients with liver disease and portal hypertension[6]. The incidence of PoPH is higher in patients with HCV-related cirrhosis. In PAH registry studies, PoPH patients accounted for 5%–15% of PAH patients[7-9]. Hemodynamically, patients with PoPH had significantly higher cardiac output and lower systemic and PVR than patients with idiopathic PH[10]. The diagnosis of PoPH is based on the presence of otherwise unexplained pre-capillary PH in patients with portal hypertension or a portosystemic shunt[5]. In patients with an established diagnosis of PoPH, treatment should follow the same general principles as in other patients

Table 2 Results of right heart catheterization

Parameter	Value	Unit
Heart rate	76	bpm
Pulmonary arterial pressure	90/38/55.33	mmHg
Right atrium pressure	12.17	mmHg
Pulmonary artery wedge pressure	34/19/24	mmHg
Pulmonary vascular resistance	5.13	Wood units
Pulmonary vascular resistance	410.23	dyne s/cm
Cardiac output	9.53	L/min
Cardiac index	4.51	L/min/m^2

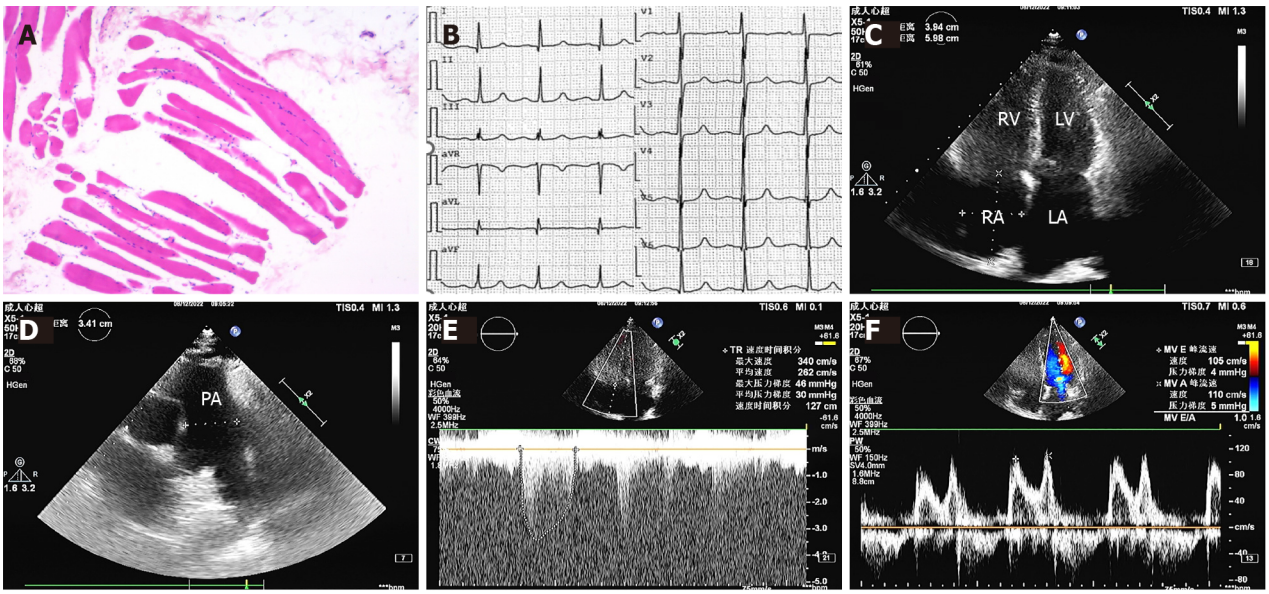

DOI: 10.3748/wjg.v29.i19.3040

Figure 1 Pathological image of muscle, electrocardiogram, and Echocardiography upon admission. A: Muscle biopsy with hematoxylin and eosin staining (× 100) showed inflammatory cell infiltration; B: Electrocardiography indicated a normal sinus rhythm; C: A four-chamber view showed an enlarged right atrium, right ventricle, and left atrium; D: A long axis view of the pulmonary artery indicated widening of that artery; E: Doppler echocardiography showed that the peak tricuspid regurgitation velocity was 3.4 m/s, and the tricuspid regurgitation pressure gradient was 46 mmHg; F: Bicuspid valve doppler indicated reduced diastolic function. RV: Right ventricular; LV: Left ventricle; RA: Right atrium; LA: Left atrium; PA: Pulmonary artery.

with PAH. PAH medications can affect gas exchange, which may deteriorate with vasodilators in patients with PoPH[11]. Various case series support the use of approved PAH medication in patients with PoPH. The survival and prognostic factors in PoPH remain controversial and are still poorly studied in the current era of PH management[7,12,13]. The current patient had a history of HCV infection, mild liver fibrosis, and hepato-renal shunt, thus the diagnosis of PoPH was considered. The results of right heart catheterization in the present patient were consistent with CpcPH, considering that there may have been other factors involved in PH, not only PoPH. The patient had a history of hypertension with left atrium and right atrium enlargement, and the N-terminal-pro B-type natriuretic peptide was elevated. Therefore, heart failure with preserved ejection fraction was involved in PH. Sildenafil, macitentan, diuretics, and angiotensin receptor blocker were prescribed. Short-term follow-up indicated improvement in respiratory status and increased activity tolerance. Confirmation of further efficacy requires long-term follow-up.

What is intriguing in the current case is the coexistence of PH, nephrotic syndrome, and polymyositis in a chronic hepatitis C patient, which is reported herein for the first time to our knowledge. Increasing epidemiological evidence indicates an association between HCV infection and renal disease, with membranoproliferative glomerulonephritis and membranous nephropathy being the most common [14]. The main clinical manifestations of nephrotic syndrome in HCV-infected patients are proteinuria and hypoalbuminemia, with or without a reduced glomerular filtration rate. Treatments include antiviral and nonspecific immunosuppressive therapy[15], but their efficacy and safety are contro-

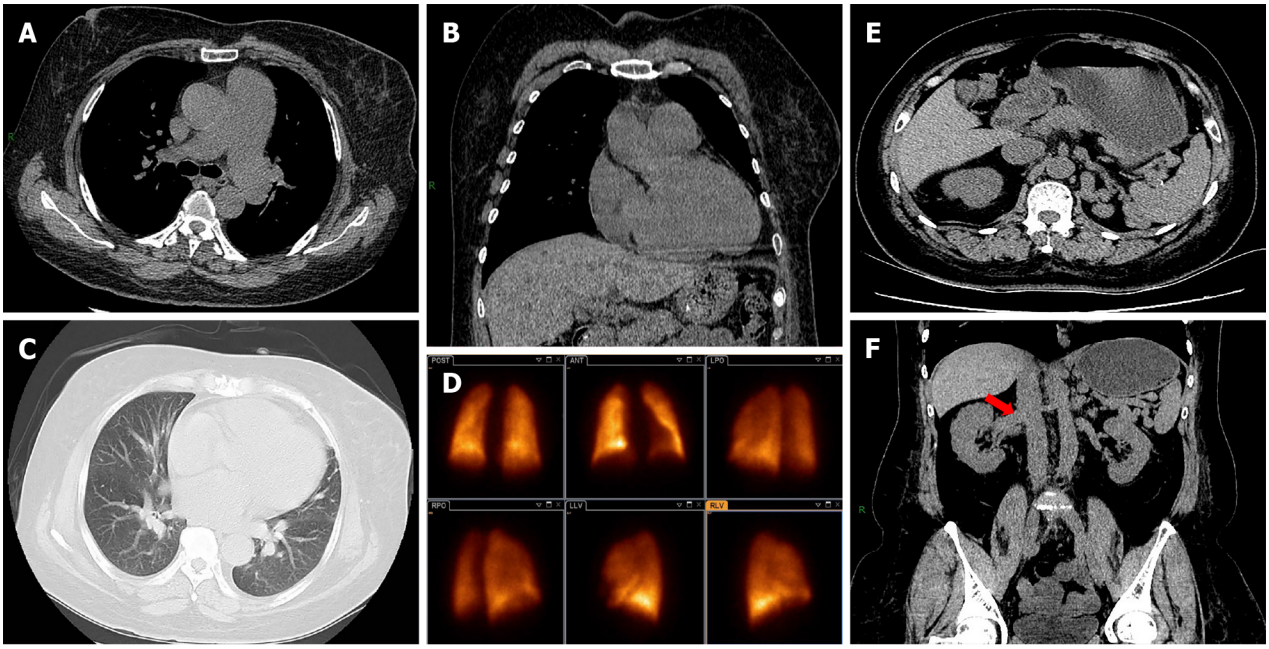

DOI: 10.3748/wjg.v29.i19.3040 **Copyright** ©The Author(s) 2023.

Figure 2 Computed tomography images and pulmonary ventilation/perfusion scan. A: Axial chest computed tomography (CT) depicted widening of the pulmonary artery; B: Coronal chest CT depicted right atrial and right ventricle enlargement; C: The pulmonary window showed no significant parenchymal pulmonary disease; D: A pulmonary ventilation/perfusion scan indicated normal perfusion function; E: An axial abdominal CT showed normal liver size, slight spleen enlargement, and multiple venous tortuosity; F: A coronal abdominal CT showed thickened venous shunt between the portal vein, splenic vein and left renal vein (red arrow).

versial. HCV infection is often associated with autoimmune diseases such as cryoglobulinemia, rheumatoid arthritis, Sjogren's syndrome, systemic lupus erythematosus, dermatomyositis, and polymyositis[1,16-18]. Most of these diseases appear to be related to virus-induced non-specific activation of the immune system, including autoantibody production, cryoglobulinemia, autoimmune thyroid disorders, and B cell lymphomas[19]. Although most data are based on small series and case reports, the association between chronic HCV infection and systemic autoimmune disease has received increasing attention. The exact etiology is unknown, but interaction between viral infection and autoimmune responses is thought to be one of the mechanisms involved. Chronic HCV infection should be considered as the cause of polymyositis if no other etiology is found. The diagnosis and treatment of HCV-associated autoimmune features has become a clinical challenge in patients with HCV infection. There are few reports on the outcome of corticosteroid treatment in patients with chronic HCV infection. Several studies have described rapid progression of liver disease after immunosuppression therapy in patients with chronic HCV infection[20]. The current patient's nephrotic syndrome and polymyositis may have been caused by chronic HCV infection *via* an autoimmune mechanism. The patient was initially treated with methylprednisolone and cyclophosphamide at the time of her polymyositis diagnosis. However, cyclophosphamide was discontinued and methylprednisolone was reduced because of her repeated episodes of abnormal behavior and coma due to hyperammonemia.

The optimal treatment strategy for hepatitis C-related extrahepatic manifestations remains to be determined. Due to the limited data available, more information is needed before definitive therapeutic recommendations can be established. The guidelines for treatment of HCV-related extrahepatic manifestations should be based on clinical features rather than underlying pathogenic mechanisms. Because of the poor prognosis and high mortality associated with these manifestations, the establishment of a safe and effective regimen for the therapy of HCV-related extrahepatic features requires further investigation.

CONCLUSION

Herein we have described a case of chronic hepatitis C with coexisting PoPH, nephrotic syndrome, and polymyositis. Increasing evidence supports a relationship between hepatitis C infection and diverse extrahepatic manifestations, but it is very rare to have multiple different extrahepatic manifestations in a single patient. To our knowledge, this is the first reported case. The exact mechanism by which hepatitis C mediated the development of diverse extrahepatic manifestations remains unclear. Further research on the specific mechanism involved is needed, to facilitated the development of safer and more effective

treatment plans.

FOOTNOTES

Author contributions: Zhao YN and Liu GH were the patient's physicians; Yu M reviewed the literature and contributed to manuscript drafting; Wang C and Zhang YX performed the contributed to data collection; Yu M and Yang P were responsible for the revision of the manuscript for important intellectual content; All authors issued final approval for the version to be submitted.

Informed consent statement: Written informed consent was obtained from the patient for publication of this report and any accompanying images.

Conflict-of-interest statement: All the authors report no relevant conflicts of interest for this article.

CARE Checklist (2016) statement: The authors have read CARE Checklist (2016), and the manuscript was prepared and revised according to CARE Checklist (2016).

Country/Territory of origin: China

ORCID number: Ya-Nan Zhao 0000-0002-4611-9678; Guo-Hui Liu 0000-0001-5342-1018; Ping Yang 0000-0001-7960-6248; Ming Yu 0000-0003-4264-5811.

S-Editor: Li L
L-Editor: A
P-Editor: Fan JR

REFERENCES

1 **Ramos-Casals M**, Trejo O, García-Carrasco M, Font J. Therapeutic management of extrahepatic manifestations in patients with chronic hepatitis C virus infection. *Rheumatology (Oxford)* 2003; **42**: 818-828 [PMID: 12730523 DOI: 10.1093/rheumatology/keg299]

2 **Simonneau G**, Montani D, Celermajer DS, Denton CP, Gatzoulis MA, Krowka M, Williams PG, Souza R. Haemodynamic definitions and updated clinical classification of pulmonary hypertension. *Eur Respir J* 2019; **53** [PMID: 30545968 DOI: 10.1183/13993003.01913-2018]

3 **Hoeper MM**, Humbert M, Souza R, Idrees M, Kawut SM, Sliwa-Hahnle K, Jing ZC, Gibbs JS. A global view of pulmonary hypertension. *Lancet Respir Med* 2016; **4**: 306-322 [PMID: 26975810 DOI: 10.1016/S2213-2600(15)00543-3]

4 **Böckle BC**, Sepp NT. Hepatitis C virus and autoimmunity. *Auto Immun Highlights* 2010; **1**: 23-35 [PMID: 26000104 DOI: 10.1007/s13317-010-0005-5]

5 **Humbert M**, Kovacs G, Hoeper MM, Badagliacca R, Berger RMF, Brida M, Carlsen J, Coats AJS, Escribano-Subias P, Ferrari P, Ferreira DS, Ghofrani HA, Giannakoulas G, Kiely DG, Mayer E, Meszaros G, Nagavci B, Olsson KM, Pepke-Zaba J, Quint JK, Rådegran G, Simonneau G, Sitbon O, Tonia T, Toshner M, Vachiery JL, Vonk Noordegraaf A, Delcroix M, Rosenkranz S; ESC/ERS Scientific Document Group. 2022 ESC/ERS Guidelines for the diagnosis and treatment of pulmonary hypertension. *Eur Respir J* 2023; **61** [PMID: 36028254 DOI: 10.1183/13993003.00879-2022]

6 **Mancuso L**, Scordato F, Pieri M, Valerio E, Mancuso A. Management of portopulmonary hypertension: new perspectives. *World J Gastroenterol* 2013; **19**: 8252-8257 [PMID: 24363516 DOI: 10.3748/wjg.v19.i45.8252]

7 **Krowka MJ**, Miller DP, Barst RJ, Taichman D, Dweik RA, Badesch DB, McGoon MD. Portopulmonary hypertension: a report from the US-based REVEAL Registry. *Chest* 2012; **141**: 906-915 [PMID: 21778257 DOI: 10.1378/chest.11-0160]

8 **Lazaro Salvador M**, Quezada Loaiza CA, Rodríguez Padial L, Barberá JA, López-Meseguer M, López-Reyes R, Sala-Llinas E, Alcolea S, Blanco I, Escribano-Subías P; REHAP Investigators. Portopulmonary hypertension: prognosis and management in the current treatment era - results from the REHAP registry. *Intern Med J* 2021; **51**: 355-365 [PMID: 31943676 DOI: 10.1111/imj.14751]

9 **Savale L**, Guimas M, Ebstein N, Fertin M, Jevnikar M, Renard S, Horeau-Langlard D, Tromeur C, Chabanne C, Prevot G, Chaouat A, Moceri P, Artaud-Macari É, Degano B, Tresorier R, Boissin C, Bouvaist H, Simon AC, Riou M, Favrolt N, Palat S, Bourlier D, Magro P, Cottin V, Bergot E, Lamblin N, Jaïs X, Coilly A, Durand F, Francoz C, Conti F, Hervé P, Simonneau G, Montani D, Duclos-Vallée JC, Samuel D, Humbert M, De Groote P, Sitbon O. Portopulmonary hypertension in the current era of pulmonary hypertension management. *J Hepatol* 2020; **73**: 130-139 [PMID: 32145258 DOI: 10.1016/j.jhep.2020.02.021]

10 **Galiè N**, Torbicki A, Barst R, Dartevelle P, Haworth S, Higenbottam T, Olschewski H, Peacock A, Pietra G, Rubin LJ, Simonneau G; Grupo de Trabajo sobre el diagnóstico y tratamiento de la Hipertensión Arterial Pulmonar de la Sociedad

Europea de Cardiología. [Guidelines on diagnosis and treatment of pulmonary arterial hypertension]. *Rev Esp Cardiol* 2005; **58**: 523-566 [PMID: 15899198 DOI: 10.1157/13074846]

11 **Olsson KM**, Meyer K, Berliner D, Hoeper MM. Development of hepatopulmonary syndrome during combination therapy for portopulmonary hypertension. *Eur Respir J* 2019; **53** [PMID: 30655448 DOI: 10.1183/13993003.01880-2018]

12 **Le Pavec J**, Souza R, Herve P, Lebrec D, Savale L, Tcherakian C, Jaïs X, Yaïci A, Humbert M, Simonneau G, Sitbon O. Portopulmonary hypertension: survival and prognostic factors. *Am J Respir Crit Care Med* 2008; **178**: 637-643 [PMID: 18617641 DOI: 10.1164/rccm.200804-613OC]

13 **Sithamparanathan S**, Nair A, Thirugnanasothy L, Coghlan JG, Condliffe R, Dimopoulos K, Elliot CA, Fisher AJ, Gaine S, Gibbs JSR, Gatzoulis MA, E Handler C, Howard LS, Johnson M, Kiely DG, Lordan JL, Peacock AJ, Pepke-Zaba J, Schreiber BE, Sheares KKK, Wort SJ, Corris PA; National Pulmonary Hypertension Service Research Collaboration of the United Kingdom and Ireland. Survival in portopulmonary hypertension: Outcomes of the United Kingdom National Pulmonary Arterial Hypertension Registry. *J Heart Lung Transplant* 2017; **36**: 770-779 [PMID: 28190786 DOI: 10.1016/j.healun.2016.12.014]

14 **Sabry AA**, Sobh MA, Sheaashaa HA, Kudesia G, Wild G, Fox S, Wagner BE, Irving WL, Grabowska A, El-Nahas AM. Effect of combination therapy (ribavirin and interferon) in HCV-related glomerulopathy. *Nephrol Dial Transplant* 2002; **17**: 1924-1930 [PMID: 12401848 DOI: 10.1093/ndt/17.11.1924]

15 **Fabrizi F**, Martin P, Cacoub P, Messa P, Donato FM. Treatment of hepatitis C-related kidney disease. *Expert Opin Pharmacother* 2015; **16**: 1815-1827 [PMID: 26161511 DOI: 10.1517/14656566.2015.1066333]

16 **Arrais de Castro R**, Vilas P, Borges-Costa J, Tato Marinho R. Hepatitis C virus infection: 'beyond the liver'. *BMJ Case Rep* 2018; **2018** [PMID: 30049677 DOI: 10.1136/bcr-2018-225817]

17 **Uruha A**, Noguchi S, Hayashi YK, Tsuburaya RS, Yonekawa T, Nonaka I, Nishino I. Hepatitis C virus infection in inclusion body myositis: A case-control study. *Neurology* 2016; **86**: 211-217 [PMID: 26683644 DOI: 10.1212/WNL.0000000000002291]

18 **Aisa Y**, Yokomori H, Kashiwagi K, Nagata S, Yanagisawa R, Takahashi M, Hasegawa H, Tochikubo Y. Polymyositis, pulmonary fibrosis and malignant lymphoma associated with hepatitis C virus infection. *Intern Med* 2001; **40**: 1109-1112 [PMID: 11757765 DOI: 10.2169/internalmedicine.40.1109]

19 **Bianchi FB**, Muratori P, Granito A, Pappas G, Ferri S, Muratori L. Hepatitis C and autoreactivity. *Dig Liver Dis* 2007; **39** Suppl 1: S22-S24 [PMID: 17936218 DOI: 10.1016/s1590-8658(07)80006-5]

20 **Rockstroh JK**, Spengler U, Sudhop T, Ewig S, Theisen A, Hammerstein U, Bierhoff E, Fischer HP, Oldenburg J, Brackmann HH, Sauerbruch T. Immunosuppression may lead to progression of hepatitis C virus-associated liver disease in hemophiliacs coinfected with HIV. *Am J Gastroenterol* 1996; **91**: 2563-2568 [PMID: 8946987]

Published by **Baishideng Publishing Group Inc**
7041 Koll Center Parkway, Suite 160, Pleasanton, CA 94566, USA
Telephone: +1-925-3991568
E-mail: bpgoffice@wjgnet.com
Help Desk: https://www.f6publishing.com/helpdesk
https://www.wjgnet.com